Keck Adaptive Optics Note 860

Near-Infrared Tip-Tilt Sensor Preliminary Design Manual

Version 2.0
March 28, 2011

Authors:
Peter Wizinowich

Contributors:
Randy Bartos, Andrew Cooper, John Cromer, Richard Dekany, David Hale, Mike Hess, Ean James, Shui Kwok, Sudha LaVen, Jim Lyke, Chris Neyman, Roger Smith, Thomas Stalcup, Marcos van Dam, Ed Wetherell

Document Revision History

Revision Number	Revision Date	Summary of Changes	Author
1.0	11/24/2010	SDR version	P. Wizinowich
2.0	3/28/2011	PDR version	P. Wizinowich

Table of Contents

Acronyms

AO	Adaptive Optics
API	Application Programming Interface
ARC	Astronomical Research Cameras (AKA Leach)
ATI	Advanced Technologies and Instrumentation
DAR	Differential Atmospheric Refraction
DIMM	Differential Image Motion Monitor
DTT	Downlink Tip-Tilt
EE	Ensquared Energy
EPICS	Experimental Physics and Industrial Control System
FITS	Flexible Image Transport System
FWHM	Full Width at Half Maximum
GUI	Graphical User Interface
IFU	Integral Field Unit
IRSA	InfraRed Science Archive
KAON	Keck Adaptive Optics Note
KTL	Keck Task Library
LBWFS	Low Bandwidth WaveFront Sensor
LGS	Laser Guide Star
MAGIQ	Multifunction Acquisition, Guiding, and Image Quality
MASS	Multi-Aperture Scintillation Sensor
NGAO	Next Generation Adaptive Optics
NGS	Natural Guide Star
NGWFC	Next Generation Wave Front Controller
NIR	Near InfraRed
NSF	National Science Foundation
OBS	Optics Bench Subsystem
OSIRIS	Oh-Suppression near InfraRed Integral field Spectrograph
PCC	Polycold Compact Cryocooler
PSF	Point Spread Function
RMS	Root Mean Square
RPC	Remote Procedure Call
RTC	Real-Time Control
SC	Supervisory Controller
SDM	System Design Manual
SDR	System Design Requirements
SOW	Statement of Work
SR	Strehl Ratio
SR	System Requirement
STRAP	System for Tip-tilt Removal with Avalanche Photodiodes
TRICK	Tip-tilt Removal with Ir Compensation at Keck
TRS	Telemetry Recorder / Server
TSS	Tip-tilt Sensor Stage
TT	Tip-Tilt
TTM	Tip-Tilt Mirror
TTS	Tip-Tilt Sensor
WCP	Wavefront Command Processor
WFP	WaveFront Processor
WFS	WaveFront Sensor
WIF	Wavefront controller InterFace
WMKO	W. M. Keck Observatory

Introduction

This preliminary design manual (PDM) is written in support of the NSF ATI-funded near-infrared (NIR) tip-tilt sensor (TTS) project; the proposal is documented in KAON 777. The purpose of the PDM is to document the preliminary level design for the NIR TTS system.

The PDM is a key document for the preliminary design review. The other key documents include:

- KAON 823. System Requirements Document (SRD).
- KAON 859. Observing Operations Concept Document (OOCD).
- KAON 855. Acceptance, Integration, Test and Commissioning Plan (AIT).
- KAON 861. Systems Engineering Management Plan (SEMP).

The requirements and interfaces are contained in four configuration controlled documents:

- KAON 824. Microgate Statement of Work (SOW).
- KAON 835. System and Functional Requirements Spreadsheet.
- KAON 836. Camera to AO Interface Control Document (ICD).
- KAON 857. Keyword Interface Spreadsheet.

The Real-time Control (RTC) preliminary design is separately documented in KAON 862. This KAON is a revision of the existing as built RTC document.

1. Overview

1.1 Design Concept

The NIR TTS system will provide high bandwidth (up to 1 kHz) tip-tilt (TT) information from one to three stars in a ~120" diameter field to the laser guide star (LGS) adaptive optics (AO) wavefront controller. The TTS system will be added to the existing LGS AO control system as shown schematically in Figure 1. The TT information could be used instead of or in addition to the TT information from the existing visible TT sensor (STRAP, Bonaccini et al., 1997) to drive the tip-tilt mirror (TTM).

The TTS will be implemented with Keck I LGS AO. The Keck I system was chosen since it has a higher power, center launched laser and hence higher Strehl performance. The major elements of the TTS include the following:

- Dichroic beamsplitters to send the appropriate wavelength light to the TTS while transmitting the science light to the Keck I science instrument, OSIRIS.
- Relay optics to relay the required field to the TTS camera with the right magnification. These optics include a field lens and fold mirror (outside the camera dewar), a dewar window, some reimaging optics, a pupil stop and a filter.
- A NIR camera dewar which will house an H2RG detector and some optics.
- Camera control and readout electronics.
- Real-time controller modifications to accept and process the NIR camera data.
- Real-time telemetry modifications to accept, store, and access the new real-time control system data.
- Motion control (total of 3 degrees of freedom) for the dichroic exchanger to move between 4 positions, a focus stage for the relay optics and camera assembly, and a filter wheel to change between two filters and a blocked position.
- Device control to control the camera.
- Operations software modifications to calibrate and operate the system for science.

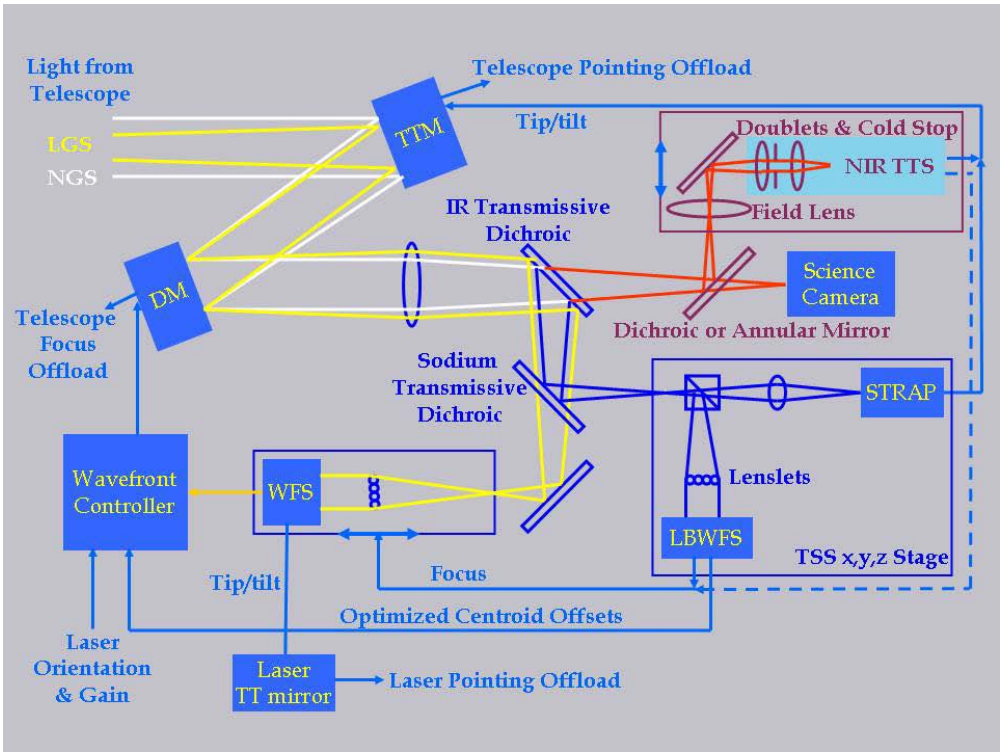

Figure 1: LGS AO control schematic with the new NIR TTS system added (upper right). *A fold located just in front of the science camera reflects light to the NIR TTS assembly mounted on a focus stage. The TTS output is processed to provide TT control of the Tip-Tilt Mirror (TTM) as an alternative to the existing visible TTS (STRAP) or in combination. Focus information, if available, could be used to control the wavefront sensor (WFS) focus.*

These elements have been divided into the five major subsystems shown in Figure 2. The Operations Software, Controls and Real-Time Control are modifications to existing AO systems. The Camera System is a new system. The opto-mechanical system and the near-IR camera portion of the Camera System represent additions to the existing AO bench.

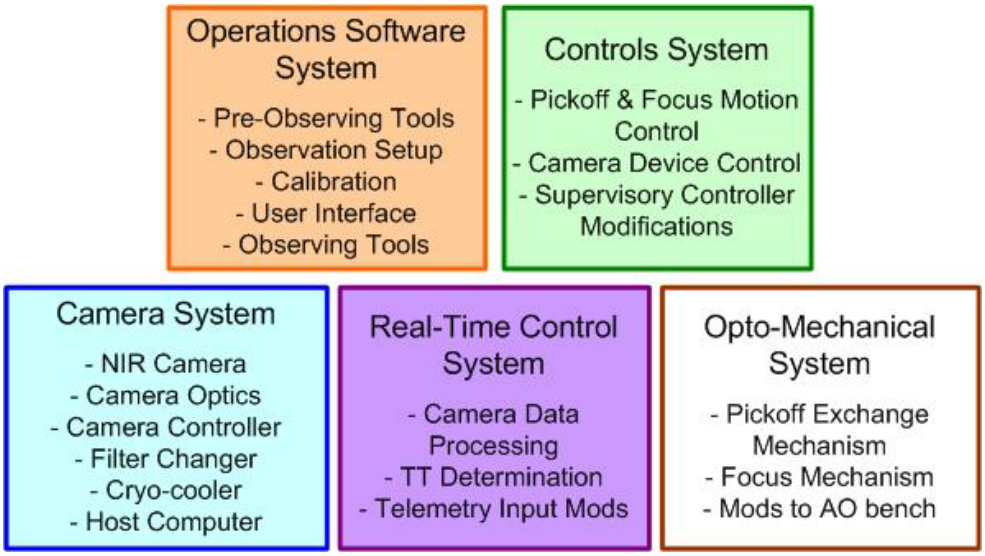

Figure 2: NIR TTS major subsystems

1.2 Potential Performance Benefits

The NSF ATI proposal for the NIR TTS identified three limitations of Keck LGS AO that this proposal was intended to alleviate:

- Improve the sky coverage for intrinsically rare science objects.
- Allow LGS AO science in heavily dust obscured regions such as star forming regions.
- Improve the astrometric precision and spatial resolution currently limited by residual tip-tilt errors.

The NIR TTS will allow the performance to be improved in several ways:

- Using AO-corrected tip-tilt stars improves the level of tip-tilt correction.
- Using AO-corrected tip-tilt stars allows fainter stars to be used thereby increasing sky coverage.
- Using NIR tip-tilt stars allows objects that were previously dust obscured to be observed with LGS AO.
- Using NIR tip-tilt stars will allow some red science objects to be used for tip-tilt sensing (previously off-axis tip-tilt stars bright enough in the visible were required) thereby reducing tip-tilt anisoplanatism.
- Using multiple NIR tip-tilt stars may reduce the tip-tilt anisoplanatism error (goal).
- Using simultaneous NIR and visible tip-tilt stars could improve tip-tilt correction for some science targets (goal).

If the NIR sensor also provided focus information then performance would be further improved:

- Using a higher bandwidth focus measurement would reduce the error due to sodium layer altitude changes. Currently focus corrections are provided by the low bandwidth wavefront sensor (LBWFS) which must integrate for periods of at least a few seconds.
- Using a higher bandwidth focus measurement would require less time to start science observations for observations with faint tip-tilt stars. The current LBWFS used to sense focus can take several minutes to converge on focus for faint guide stars.

Our baseline design does not provide focus information from the NIR sensor. However, we will design the system so that this is a future option.

1.3 System Requirements and Design Choices

The system requirements document (KAON 823) includes a list of the areas that directly impact the science and the system requirements. We use these science area categories here to provide a design overview in relationship to the requirements. For each category we indicate whether the system level design meets the requirement or allows the requirement to be achieved:

- Sky coverage - requirements met by design.
    - The NIR TTS optics have been designed to pass a 120" diameter field of view
    - The NIR TTS detector provides a 100"x100" field on the sky. The corners are vignetted by the 120" diameter field of view of the optics.
    - The NIR TTS can be used for acquisition.
- Tip-tilt residuals – requirements achievable by design.
    - Differential atmospheric refraction correction is provided between the science and TT sensing wavelengths by changing the requested star(s) centroid positions on the TTS.
- Science and tip-tilt sensing wavelengths - requirements met by design.
    - Two pickoff options are offered. A dichroic that reflects Ks to the NIR TTS while transmitting shorter wavelengths. Another dichroic that reflects H while transmitting K. A 3rd position will either remove the pickoff (initial implementation) or allow a future pickoff option (nominally an annular mirror).
    - A filter in the TTS camera dewar allows either H or Ks-band light to be used.
- Throughput and emissivity – requirements met by design.
    - The dichroics have good reflection and transmission performance.
    - The NIR TTS optics are optimized for H and Ks-band.
    - The H2RG has high sensitivity at both H and Ks-band.

    - A cold pupil stop and cold baffles are located in the TTS camera dewar.
- Science field of view – requirements met by design.
    - The entire science field of view is transmitted by the dichroics.
    - A future annular mirror option only transmits the IFU field.
- Observing modes – requirements met by design.
    - The TTS camera and re-imaging optics are mounted on a focus stage to stay parfocal to the OSIRIS focal plane.
    - Dithering, nodding and offsetting are all supported. The tip-tilt stars can be located anywhere on the detector (assuming good pixels); they do not have to be centered at the intersection of four pixels.
    - Non-sidereal tracking is only a goal, however the current design would support this mode.
    - Non-point sources can be used with reduced performance. The largest allowable region for centroiding is 0.8"x0.8" versus the goal of 1" diameter objects.
- Positioning accuracy and repeatability – requirements achievable by design.
- Observing efficiency – requirements achievable by design.
    - Observing efficiency budget to be designed during the detailed design.
- Higher bandwidth focus measurements
    - This is a goal only. The real-time control system will provide focus. A choice was made not to incorporate astigmatism into the current optical design. The system is designed to support experiments to measure the benefits of focus sensing.
- Performance monitoring – requirements achievable by design.
    - Related tools designed during the preliminary design.
- Observation planning – requirements achievable by design.
    - Tool designed during the preliminary design.

The system requirements are maintained in a configuration controlled excel spreadsheet (KAON 835). The system requirements have been flowed down into functional requirements for each of the five major subsystems shown in Figure 2. KAON 835 contains a sheet for the functional requirements for each of these five systems. Compliance matrices for the system and functional requirements are provided in sections 12 and 13, respectively.

2. Design Considerations

This section begins with some design constraints imposed by the existing OSIRIS science instrument (section 2.1), AO bench (2.2) and the NIR TTS detector (2.3), which has already been procured. In section 2.4 the impact of differential atmospheric refraction is considered, which will move the tip-tilt star away from the center of a quad cell. The impact and performance of not operating in quad cell mode is then evaluated in section 2.5. Measuring focus requires the tip-tilt star to be at the center of a quad cell as reviewed in section 2.6. A single star could be maintained at the center of a quad cell with a tip-tilt mirror as discussed in 2.7; we have decided to proceed without this additional complexity given that it would only work for 1 tip-tilt star.

2.1 OSIRIS Science Instrument

Since the NIR TTS will be used with OSIRIS it is important to understand some features of this instrument. Much of the following data is from the OSIRIS Users' Manual version 2.2 (dated April 1, 2008).

OSIRIS provides four spatial scales to choose from (0.020, 0.035, 0.050 and 0.100 arcsec per lenslet). The pupil mask size for each of these plate scales is shown in Figure 3. The 0.020 arcsec scale is optimized for image quality and has a slightly oversized pupil that is circumscribed around the 10.94 m outer edges of the Keck primary mirror. It therefore has an elevated thermal background (K=11.2 mag/sq arcsec). The 0.035 and 0.050 arcsec scales are optimized for maximum sensitivity at thermal wavelengths (K=11.8 mag/sq arcsec). They both have circular pupils equivalent to a 10 m telescope. The 0.1 arcsec scale has an oversized pupil allowing a great deal of excess background (K=10.6 mag/sq arcsec). For this reason a duplicate K-band filter is installed with a smaller, 9 m diameter effective pupil.

The filters, scales and fields of view for the spectrograph are provided in Table 1.

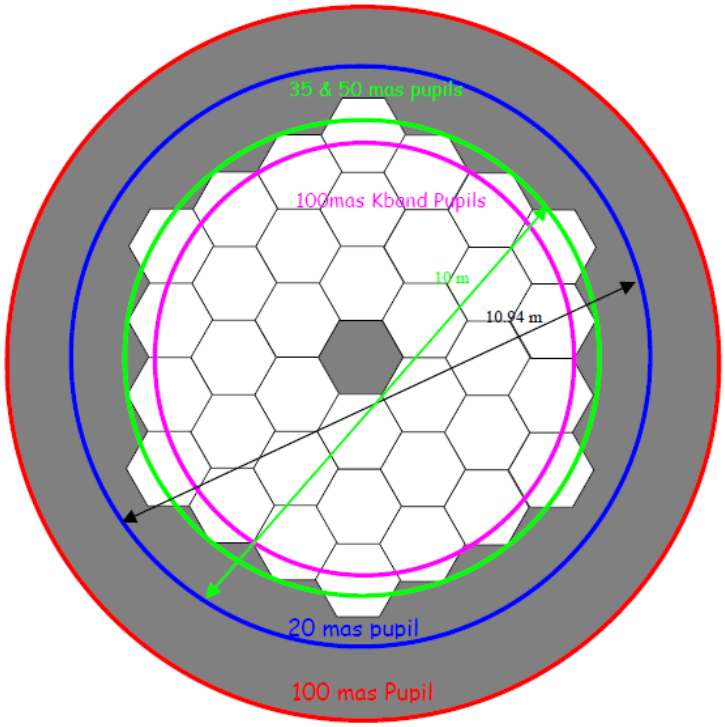

Figure 3: Scale drawing of the pupils for each of the four plate scales.

Filter	Shortest Wavelength Extracted(nm)	Longest Wavelength Extracted(nm)	Number of Spectral Channels	Number of Complete Spectra	Approx. Lenslet Geometry	FOV for 0.020"	FOV for 0.035"	FOV for 0.050"	FOV for 0.100"
Zbb	999*	1176*	1476	1019	16x64	0.32x1.28	0.56x2.24	0.8 x 3.2	1.6 x 6.4
Jbb	1180	1416*	1574	1019	16x64	0.32x1.28	0.56x2.24	0.8 x 3.2	1.6 x 6.4
Hbb	1473	1803	1651	1019	16x64	0.32x1.28	0.56x2.24	0.8 x 3.2	1.6 x 6.4
Kbb*	1965	2381	1665	1019	16x64	0.32x1.28	0.56x2.24	0.8 x 3.2	1.6 x 6.4
Zn4	1103	1158	459	2038	32x64	0.64x1.28	1.12x2.24	1.6 x 3.2	3.2 x 6.4
Jn1	1174	1232	388	2038	32x64	0.64x1.28	1.12x2.24	1.6 x 3.2	3.2 x 6.4
Jn2	1228	1289	408	2678	42x64	0.84x1.28	1.47x2.24	2.1 x 3.2	4.2 x 6.4
Jn3	1275	1339	428	3063	48x64	0.96x1.28	1.68x2.24	2.4 x 3.2	4.8 x 6.4
Jn4	1323	1389	441	2678	42x64	0.84x1.28	1.47x2.24	2.1 x 3.2	4.2 x 6.4
Hn1	1466	1541	376	2292	36x64	0.72x1.28	1.26x2.24	1.8 x 3.2	3.6 x 6.4
Hn2	1532	1610	391	2868	45x64	0.90x1.28	1.58x2.24	2.25x3.2	4.5 x 6.4
Hn3	1594	1676	411	3063	48x64	0.96x1.28	1.68x2.24	2.4 x 3.2	4.8 x 6.4
Hn4	1652	1737	426	2671	42x64	0.84x1.28	1.47x2.24	2.1 x 3.2	4.2 x 6.4
Hn5	1721	1808	436	2038	32x64	0.64x1.28	1.12x2.24	1.6 x 3.2	3.2 x 6.4
Kn1	1955	2055	401	2292	36x64	0.72x1.28	1.26x2.24	1.8 x 3.2	3.6 x 6.4
Kn2	2036	2141	421	2868	45x64	0.90x1.28	1.58x2.24	2.25x3.2	4.5 x 6.4
Kn3*	2121	2229	433	3063	48x64	0.96x1.28	1.68x2.24	2.4 x 3.2	4.8 x 6.4
Kn4*	2208	2320	449	2671	42x64	0.84x1.28	1.47x2.24	2.1 x 3.2	4.2 x 6.4
Kn5	2292	2408	465	2038	32x64	0.64x1.28	1.12x2.24	1.6 x 3.2	3.2 x 6.4

Table 1: OSIRIS spectrograph filters, scales and fields of view

The imager uses a Rockwell Scientific Hawaii-1 detector with 1024x1024 pixels and a plate scale of 0.020 arcsec/pixel. For most cases the imager will be sky background limited since the cold pupil is oversized (since the pupil is poorly formed). The imager zero point (defined as Mag = -2.5 log(flux in DN/sec) + Mag (zero point)) is 27.8, 28.1 and 27.6 mag at J, H and K, respectively. The imager background is 16.2, 14.6 and 10.6 mag/sq arcsec at J, H and K, respectively. The spectrograph zero points are 23.5, 24.3 and 23.7 mag at J, H and K, respectively.

Jim Lyke reports that we do not currently adjust the AO focus for OSIRIS between filters. Between pixel scales there is a ± 2 mm difference between the two most extreme scales.

The relative locations of the imager and spectrograph are shown in Figure 4. On Keck II the AO optical axis is located partway between the spectrograph and imager fields. OSIRIS will be moved to Keck I in August 2011. Prior to that time we will need to decide on the optimal location of the AO optical axis to be used in aligning OSIRIS; a recommendation will be made as part of the NIR TTS preliminary design.

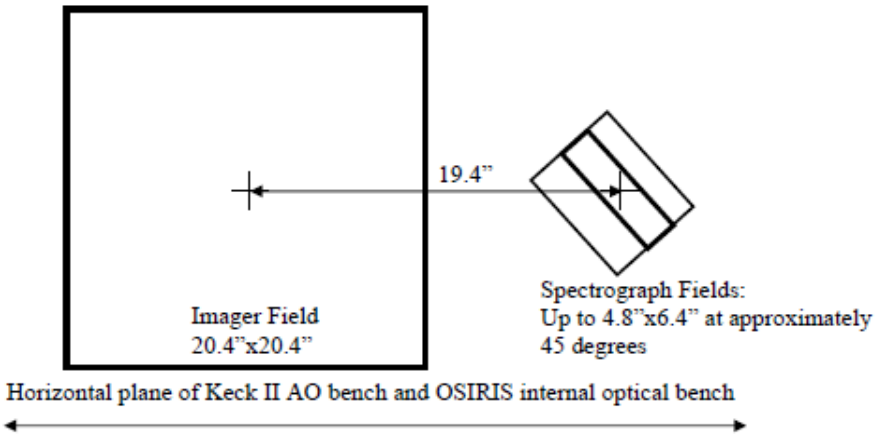

Figure 4: Relative locations of the imager and spectrograph focal planes. The perspective of this image is from OSIRIS looking toward the AO system. On Keck II the AO rotator axis is located partway between the spectrograph and imager fields.

Figure 5 (provided by Jason Chin) shows the layout of OSIRIS with respect to the AO bench. Based on this drawing the OSIRIS focal plane is estimated to be 393 mm from the edge of the AO bench. Note that center line of OSIRIS is offset by 53 mm with respect to the AO optical axis.

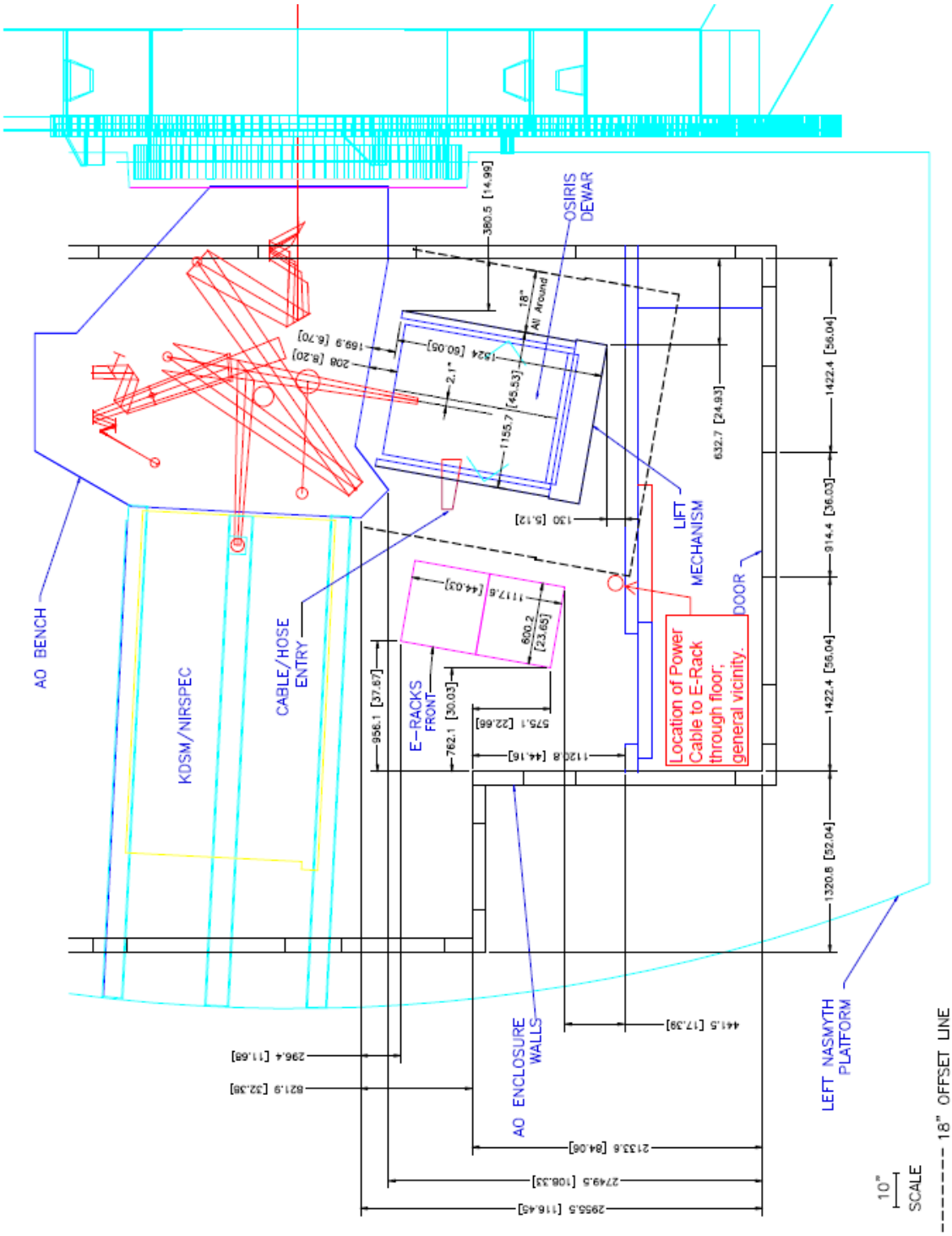

Figure 5: OSIRIS layout in Keck 1 AO (Rev A 2009-03-05)

2.2 AO Bench

A schematic of the AO bench is shown in Figure 6. The portion of the bench where the NIR TTS will need to be located is shown in Figure 7. The optical axis is at a height of 305 mm from the surface of the AO bench. The pupil simulator, item 23 in Figure 6 could be repackaged if necessary to provide additional space for the NIR TTS; however that is not required.

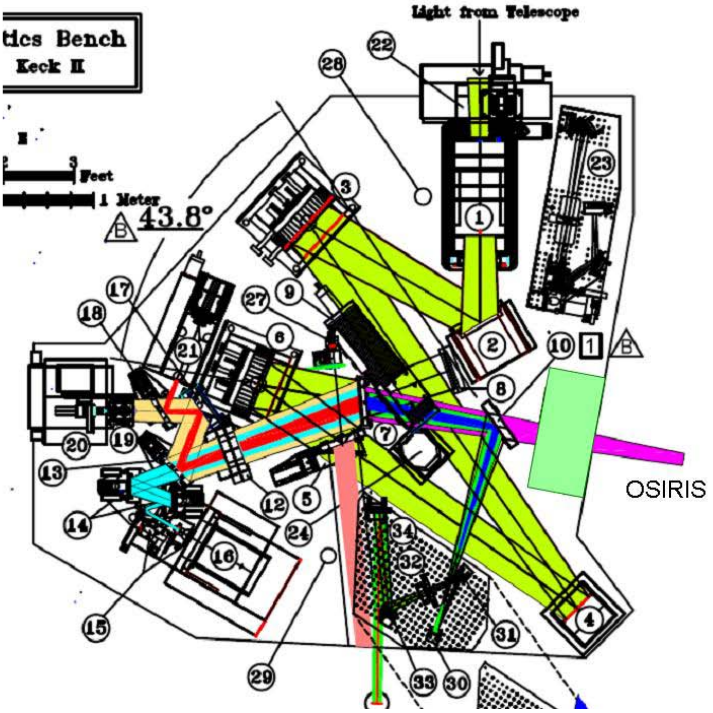

Figure 6: AO bench schematic. *The light green area is where the pickoff to feed the NIR TTS will be located. Item 2 is the fast tip-tilt mirror, item 7 is the IR transmissive dichroic, item 10 is the interferometer fold mirror and item 23 is the pupil simulator.*

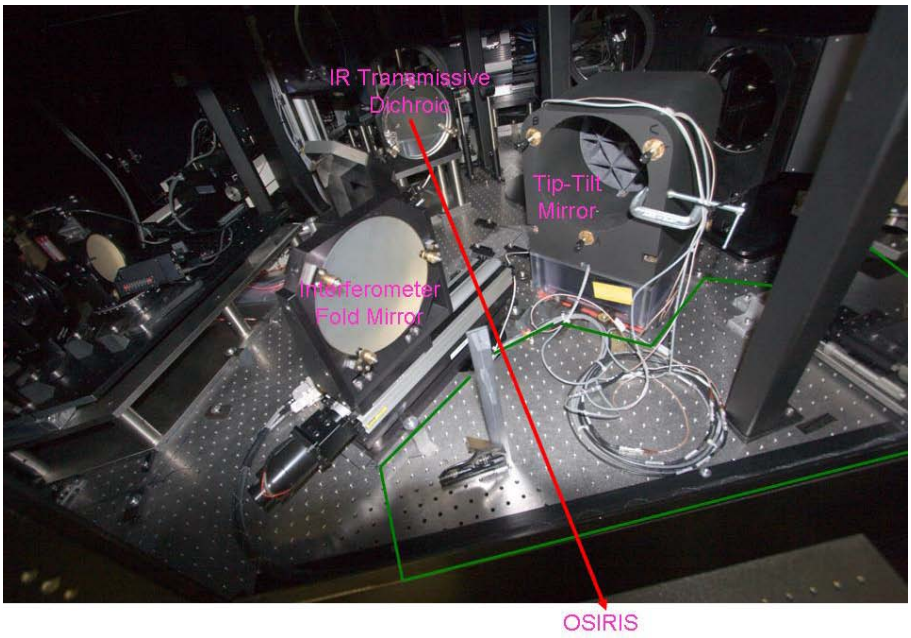

Figure 7: The Keck I AO bench. The red line shows the light path to OSIRIS. The green bordered area is roughly where the NIR TTS and its pickoff will need to be located.

The risers that sit on the AO bench and hold the AO bench cover are 711 mm (28 inches) tall. The AO bench cover has two 0.8 mm (0.032 inch) thick aluminum facesheets sandwiching a 50.8 mm (2 inch) thick aluminum core with a 6.4 mm (0.25 inch) thick aluminum edge finish. The estimated weight of the cover is 91 kg (200 lbs).

2.3 Tip-Tilt Sensor Detector

The H2RG detector has been procured. The pixel quantum efficiency plot produced by Teledyne at 2.0 μm is shown in Figure 8 for the received detector. The median QE is ~ 84% at this wavelength with 95% of the pixels having a QE > 58% at this wavelength; 97.7% of the pixels are operable with the inoperable pixels mostly concentrated in two areas at the bottom of the chip. According to Teledyne the feature at the bottom of the chip is due to some chemical re-flow on the edge during substrate removal; this feature is not expected to propagate. At 1.23 μm the median QE is 65% with 95% of the pixels having a QE > 38%; 95.3% of the pixels are operable.

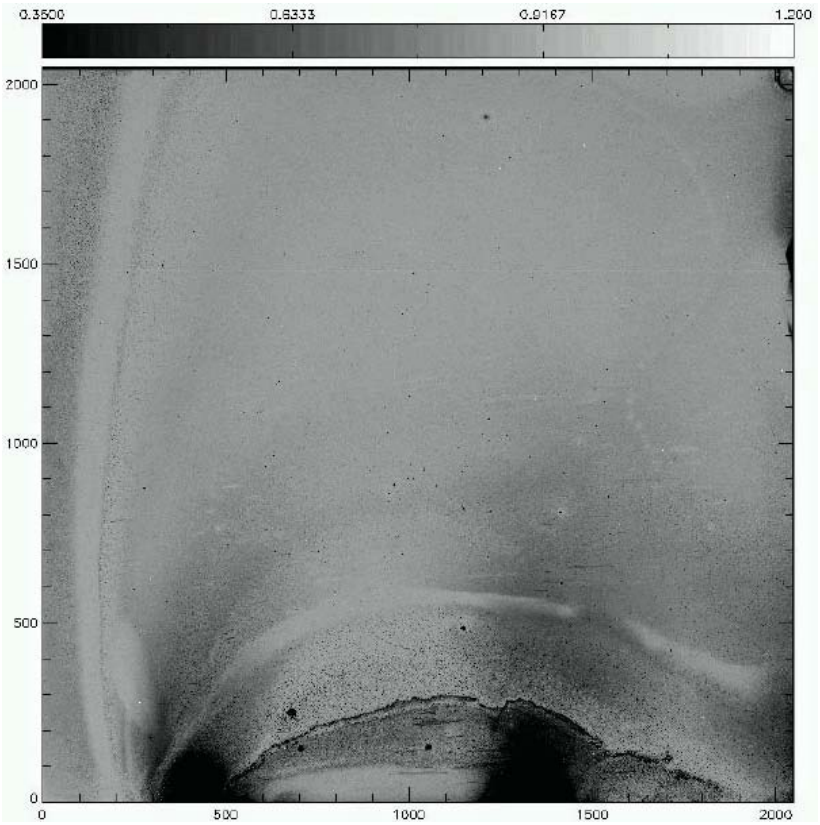

Figure 8: Pixel quantum efficiency at 2.0 μm

2.4 Differential Atmospheric Refraction

Differential atmospheric refraction (DAR) will cause the science image to move with respect to the tip-tilt star image if these two observations are made at different wavelengths and/or with stars of different colors.

The relevant system requirement is "The NIR TTS system shall support differential atmospheric refraction corrections between the TTS and the science instrument for a ≤ 20 minute (TBC) science exposure for zenith angles ≤ 60°."

As an example, the DAR term between a science observation in J-band (center wavelength of 1.25 μm) and K-band tip-tilt sensing (center wavelength of 2.2 μm) is 86 mas * tan z, where z is the zenith angle (as derived in atmdisp$.xls from KAON 134). Over the course of a 20 minute integration the zenith angle can change from 45° to 50° resulting in a DAR change of 16 mas. This is large compared to the stability requirement of 5 mas over a 1 hour exposure. A strategy is therefore needed to maintain the science object position to better than 5 mas while the tip-tilt star image moves on the NIR TTS.

The DAR mechanism used in the existing AO system is for the wavefront sensor or STRAP to use centroid offsets during a science exposure. The sensor is then physically moved between science exposures to zero the centroid offsets. Physically moving the NIR TTS would require a 2-axis translation stage or a tip-tilt

mirror in the path to this sensor (this would not work for more than one star). An atmospheric dispersion corrector could be another possible alternative however we have not chosen this option due to its additional complexity and cost. Assuming neither of these options it will be necessary to allow the tip-tilt star to be located at an arbitrary location with respect to the intersection of 4 pixels or at least to work within a significant fraction of a pixel from this intersection.

2.5 Tip-Tilt Measurement Analysis and Simulations

The impacts of pixel scale and star positioning on tip-tilt measurement accuracy have been evaluated. The results are summarized and discussed in this section.

Differential atmospheric refraction and the need to accurately position the science object on the science instrument, plus the goal of non-sidereal tracking, make it difficult to position a single TT star at the intersection of 4 pixels. Maintaining the star at a 4 pixel intersection could be accomplished with a tracking device such as a tip-tilt mirror in the TTS path. However, once you have three TT stars then it becomes impractical to have all 3 stars at the intersections of 4 pixels. We have therefore taken the route of determining how best to work with stars that are at arbitrary locations on the TTS. A fallback, which doesn't appear necessary, would be to only work with one star and to have a tip-tilt mirror in the TTS path. You could also constrain your TT star selection to be near pixel intersections, to maximize performance, but again this does not seem to be necessary.

Two analyses were performed. In the first approach, discussed in the next section, a simple excel spreadsheet was used to understand the impact of pixel scale and decentration from the 4 pixel intersection. This was useful for developing a physical understanding. A more sophisticated analysis, summarized in section 2.5.2, was performed by Marcos van Dam to quantify the performance impact.

The conclusions from these analyses are:

(1) Use 50 mas pixels.
(2) Implement a correlation algorithm (better performance than centroiding).
(3) Implement a 4x4 centroiding algorithm (simpler + may work better for far off-axis stars).
(4) Implement some level of seeing disk background subtraction. Alternatively implement an approach to measuring gain or Strehl.
(5) The region of interest (ROI) will need to change to be best centered on each star.
(6) Multiple stars do improve the performance.

2.5.1 Pixel Scale and Positioning Error – Simple Analysis

Figure 9 is a schematic representation of three star images on the NIR TTS detector. The image of star A is ideally located at the intersection of four pixels to allow for optimal tip-tilt correction (since it is null seeking). The performance might be expected to degrade as the star position moved off the intersection to position B or worse of all to position C.

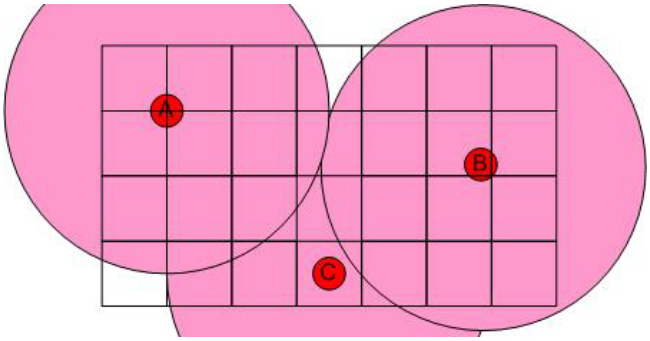

Figure 9: Positioning stars on the NIR TTS detector.
The grid represents the boundaries of individual pixels. The red and pink circles represent the approximate full-width-at-half-maximum diffraction-limited core and seeing limited halo, respectively, of star images. This is roughly to scale assuming 100 mas pixels, a 50 mas core and 0.5 arcsec seeing.

A simple quantitative analysis was performed with an MS Excel tool. The seeing limited halo and the diffraction-limited core were both assumed to be Gaussian with a full-width-at-half maximum (FWHM) of λ/D and λ/r_0, respectively; λ is the NIR TTS operating wavelength, D is the telescope diameter and r_0 is the spatial scale of the turbulence (Fried's parameter). Figure 10 is a cut through a star image, with a Strehl of 0.41 at 2.2 μm, on the NIR TTS that is offset from the intersection of 4 pixels by 0.03". The measured tilt for this and other offsets of the image from the center of 4 pixels is shown in Figure 11. The measured tilt is seen to be a linear function of the actual tilt only for a small range of decenter from the pixel intersection, less than ~ 20 mas. The measured tilt is also a strong function of the Strehl of the image. This is due to the contribution of the seeing limited disk. If the seeing limited disk were perfectly subtracted then all of the curves in Figure 11 would overlap the SR = 1 curve (albeit with lower SNR for lower SR). In the absence of good seeing disk subtraction it will be important to know the Strehl of the image if the image is not kept centered near the intersection of 4 pixels. Even when it is kept centered without good seeing disk subtraction it will be important to know the Strehl in order to set the optimal gain. A potential method to measure the seeing disk background is briefly discussed in section 8.5.6; seeing disk subtraction will require more attention during the preliminary design (this is not critical to the use of the correlation approach discussed in the next section).

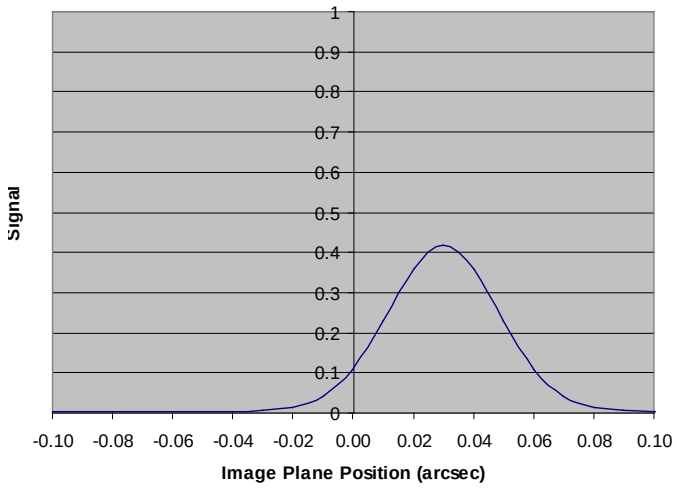

Figure 10: A cut through a NIR TTS image with an offset of 30 mas.
λ = 2.2 μm, rms wavefront error = 329 nm, $r_0(\lambda=0.5\mu)$ = 0.16 m, off-axis distance = 0", isokinetic angle = 44", zenith angle = 30° and pixel size = 0.10".

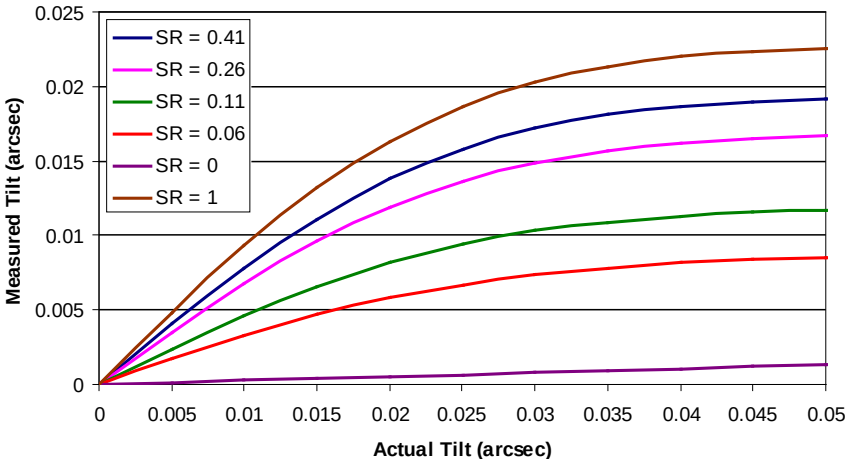

Figure 11: Tilt measured by the NIR TTS for 100 mas pixels and 2x2 pixel centroiding.
The measured tilt is a function of Strehl ratio and is only linear for a small range of decenters from the intersection of 4 pixels. For the parameters used to produce Figure 6, the SR of 0.41 corresponds to an off-

axis distance of 0" which falls to SR = 0.26, 0.11 and 0.06 for off-axis distances of 30", 50" and 60", respectively.

We can make the system more linear by using smaller pixels and more pixels to determine a centroid; unfortunately at the expense of reduced field of view for acquisition and increased readout and dark noise. This is seen in Figure 12 where the pixel size has been reduced to 50 mas and 4x4 pixels were used for centroiding. The performance is now essentially linear for all image decenters. Knowing the Strehl is still critical to setting the proper gain if the seeing disk cannot be adequately subtracted. Note that Figure 12 only extends to 25 mas or ½ of a pixel since it is assumed that the ROI will be shifted by 1 pixel for larger offsets.

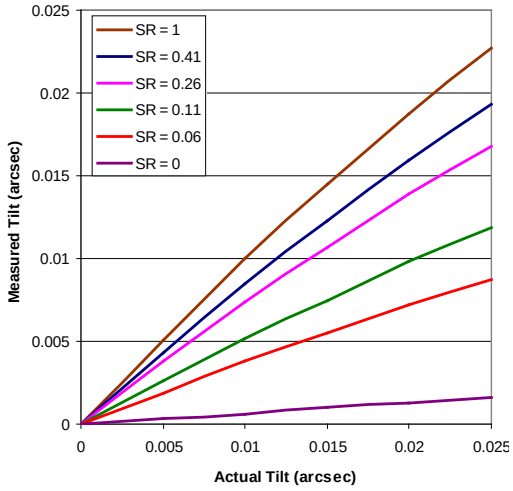

Figure 12: Tilt measured by the NIR TTS for 50 mas pixels and 4x4 pixel centroiding.
Note that once the actual tilt exceeds 25 mas that you would switch to a different 4x4 pixel area for centroiding.

An analysis needs to be performed during the preliminary design of how well the seeing disk needs to be subtracted in order to be able to use the SR = 1 curve in Figure 12. We will also need to determine how well we can determine the seeing disk (see section 8.5.4).

2.5.2 Pixel Scale and Positioning Error – Simulation Results

The results of Marcos van Dam's analysis of the TTS performance are documented in KAON 826 which is summarized here. Three cases were evaluated: 100 mas and 50 mas pixels using a centroiding algorithm and 50 mas pixels using a correlation algorithm. All were done with 4x4 pixels. The difference between the actual tilt and the measured (or specified) tilt is shown in Figure 13 for K = 14^{th} and 16^{th} magnitude stars. Similar to the results in Figure 11 and Figure 12 the measured tilt drops as the Strehl is reduced (e.g. the star gets fainter). The correlation algorithm, with 50 mas pixels, produces the most accurate and linear tilt measurement and the result is quite insensitive to the stellar magnitude (at least for stars ≤ 16^{th} magnitude). The Strehl stability versus offset for the correlation algorithm can also be seen in Figure 14. The Strehl for the centroid algorithm, also shown in Figure 14, can be seen to fall versus offset as fainter stars are used.

KAON 826 also examines the case of multiple (3) guide stars in an equilateral triangle at a specified radius; the Strehl for the 30" and 60" radius cases are also plotted in Figure 14.

A matched filter could potentially be considered as an alternative to a correlation algorithm, but we have not explored this option.

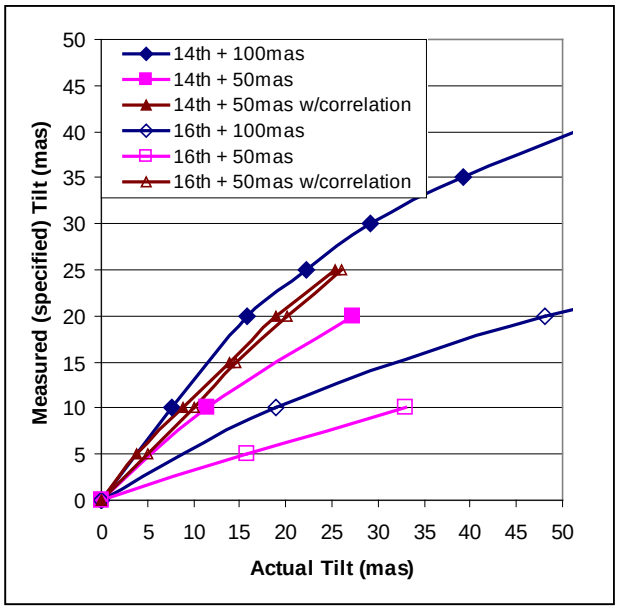

Figure 13: Simulation results for measured versus actual tilt

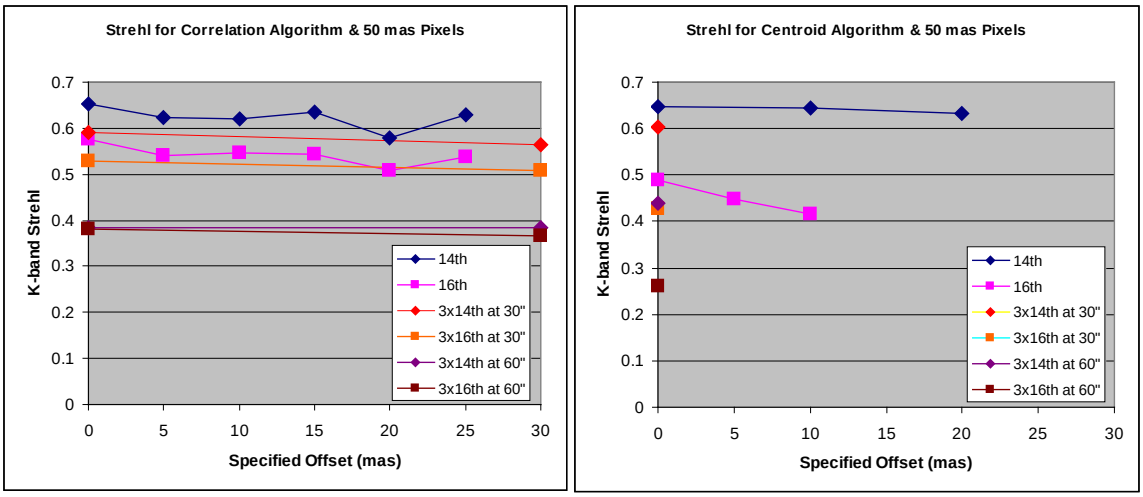

Figure 14: K-band Strehl for the correlation (left) and centroid (right) algorithms versus specified offset for the case of 50 mas pixels

2.5.3 Performance versus Off-Axis Distance – Simulation Results

Sandler et al. (JOSA A, 1994) pointed out the advantage of AO sharpening of a NIR TT star but also noted that this advantage can break down as multiple speckles appear as you move off-axis. When the breakdown occurs is highly dependent on the Cn2 profile. This is illustrated in Figure 15. Under low altitude dominated seeing conditions (θ_0 = 3" at 0.5 μm wavelength) the image continues to have a dominate core far off-axis. While under conditions with higher altitude turbulence (θ_0 = 1.3") the core breaks into two speckles even at 20" off-axis. Note that the median Mauna Kea isoplanatic angle is 2.7".

An additional set of simulations were performed by van Dam (KAON 858) during the preliminary design focusing on the impact of guide star image degradation far off-axis. The typically lower Strehl and multiple peaked structure is seen in Figure 16.

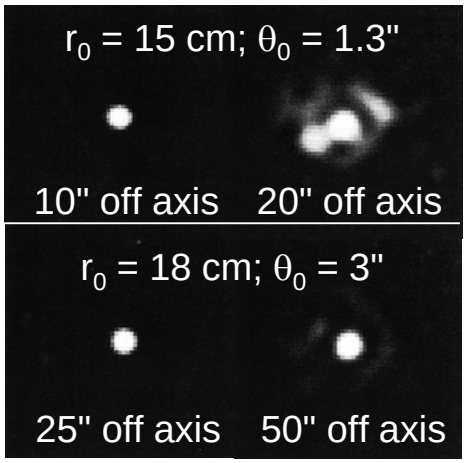

Figure 15: 1.45 μm AO corrected image as a function of seeing conditions and off-axis distance (Sandler et al., 1994)

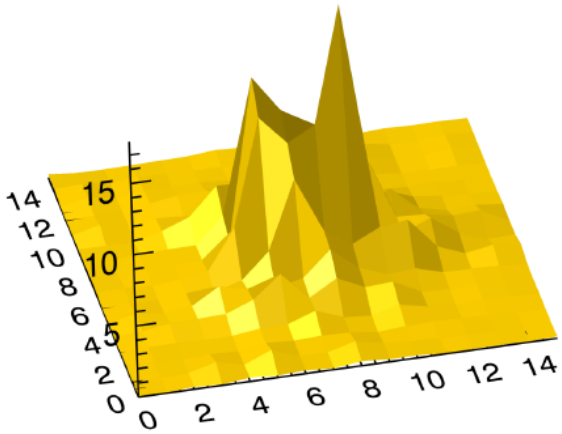

Figure 16: Typical K-band image at 60" off-axis. Two large peaks and three smaller peaks can be seen over a 6x6 pixel region.

The on-axis Strehl degradation versus off-axis distance for a bright tip-tilt star is shown in Figure 17 (note that since this simulation does not include all error terms the absolute Strehl is higher than we expect with Keck AO). The mean slope curve shows the degradation simply due to anisoplanatism. The performance with H and K-band tip-tilt stars further degrades due to the image structure seen in Figure 16. In particular much of the energy in the central core extends outside the area sampled in 4x4 pixel centroiding. One could increase the number of pixels used for centroiding at the expense of increased noise (background, readout and photon).

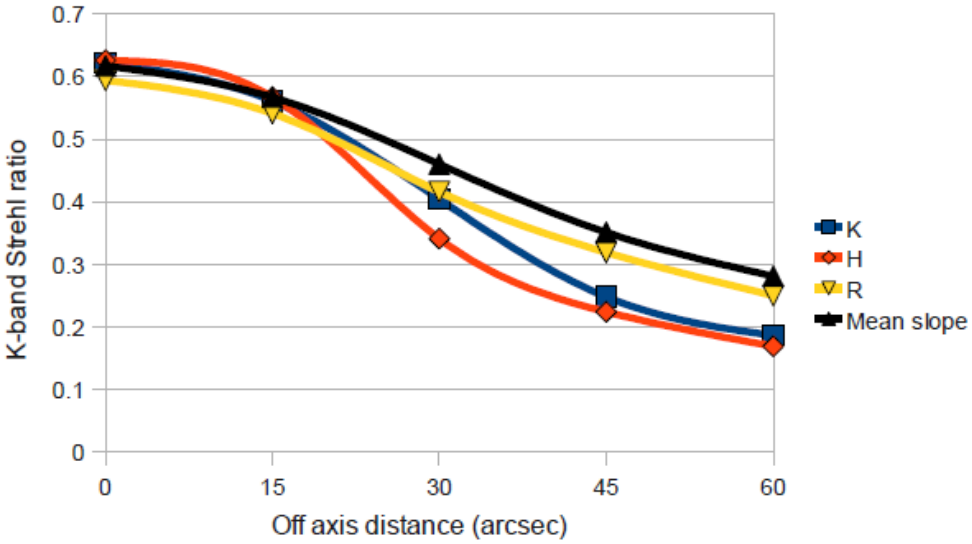

Figure 17: On-axis K-band Strehl degradation as a function of tip-tilt star off-axis distance for a 14th magnitude tip-tilt star at three different tip-tilt sensing wavelengths. H and K-band using a 4x4 centroider with 50 mas pixels. R-band using a quad cell with 500 mas pixels.

The performance improvement with K-band tip-tilt sensing is seen as we go to fainter tip-tilt stars, as shown in Figure 18. However, the performance drop off due to K-band tip-tilt image structure as a function of off-axis distance results in better performance with STRAP toward the edge of the field.

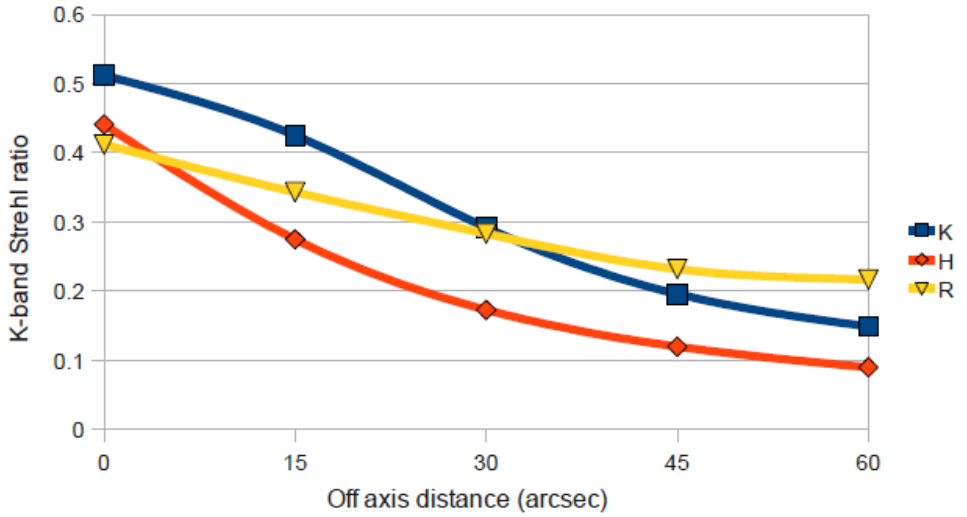

Figure 18: On-axis K-band Strehl as a function of tip-tilt star off-axis distance for a M0 guide star (R=18.5, H=16.5 and K=16). H and K-band using a 4x4 centroider with 50 mas pixels. R-band using a quad cell with 900 mas pixels.

In the bright tip-tilt star case and the 60" off-axis case not much performance difference was seen in the simulations between using a 4x4 pixel centroiding or correlation algorithm. The correlation algorithm performance does not improve with more pixels since in this case the algorithm is only trying to track the brightest peak. In the absence of noise the centroid algorithm performance does improve but this gain would be quickly lost when noise was included.

A question that was asked was whether the multiple speckles persist long enough for previously recorded and averaged images to be used as reference correlation images in subsequent tip-tilt estimates. The image

decorrelates too quickly to be useful in a practical correlation algorithm, especially if faint guide stars are used. The image does not decorrelate fast enough to reduce the tip-tilt star image with longer integrations.

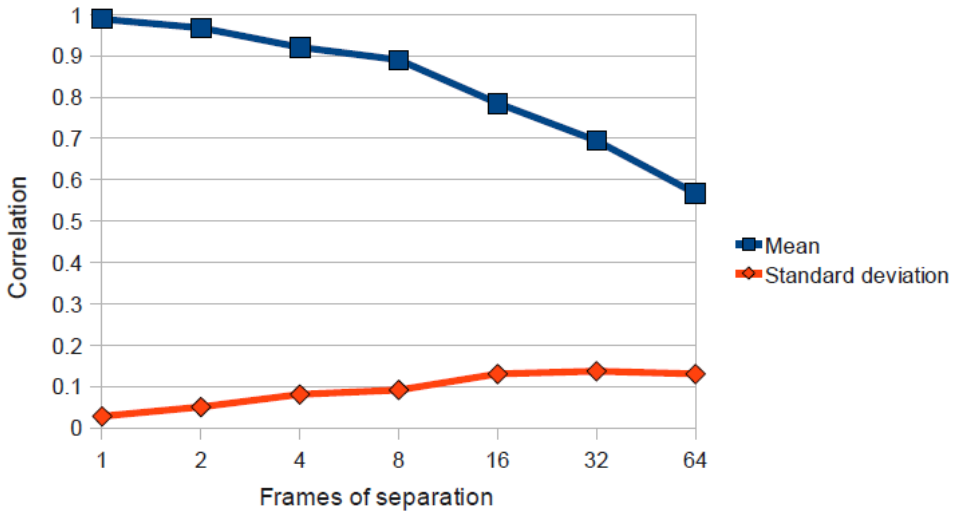

Figure 19: Tip-tilt image decorrelation as a function of the number of frames of separation at a frame rate of 500 Hz for a K-band star 60" off-axis.

The effect of multiple tip-tilt stars was studied by van Dam in a note titled "Tip-tilt tomography using covariance matrices" (FWN 17). Figure 20 from this note shows the reduction in the rms wavefront error, from anisokinetic and tomographic error, as two stars are used at 180° or three stars at 120°, all at the same radius. The performance improvement in going from one to two stars is significant, and only a modest improvement is made when a 3rd star is added. From this analysis the rms wavefront error improvement in going to two stars depends linearly on the angular separation between the two stars, with the maximum at 180°.

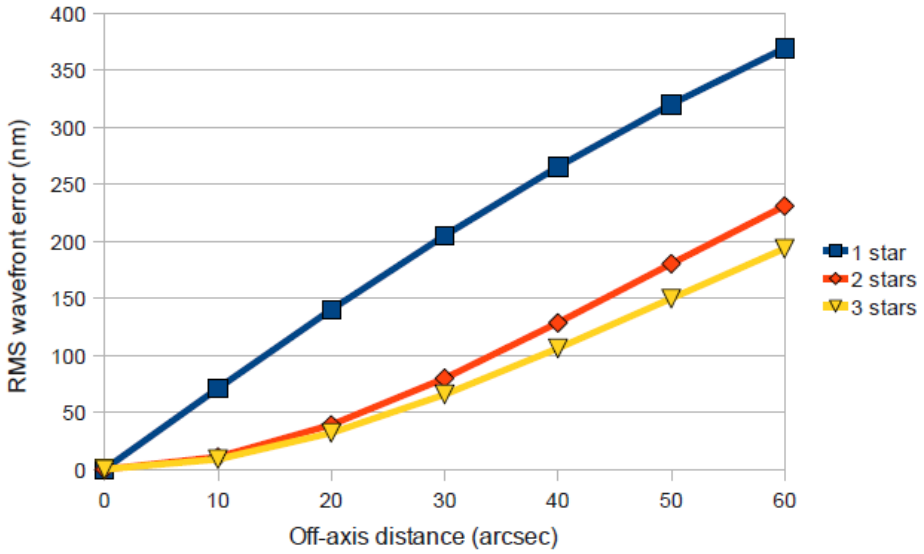

Figure 20: Tip-tilt anisoplanatism RMS wavefront error as a function of tip-tilt star off-axis distance (using the Mauna Kea turbulence profile, a 10 m circular telescope and 2 stars at 180° or 3 stars at 120°).

2.6 Measuring Focus

In principle, the NIR TTS could measure focus aberrations if astigmatism was added to the NIR TTS optical path. The advantage of this technique is that it offers a higher bandwidth measurement of the true

focus than the LBWFS, and hence higher bandwidth measurements of changes in the sodium layer altitude when used in conjunction with the LGS WFS focus measurements. This could significantly improve the observing efficiency since currently significant time is lost waiting for the low bandwidth wavefront sensor (LBWFS) to settle after each dither or offset. The required amount of astigmatism is a function of how accurately the focus needs to be measured. A measurement with 50 to 100 nm rms focus error would likely be sufficient. The downside of adding astigmatism is that it will broaden the TT star image and therefore impact the centroiding accuracy.

The results of Marcos van Dam's analysis of measuring focus with the NIR TTS are documented in KAON 827 which is summarized here. The concept is to add astigmatism to the NIR TTS optical path as a means of measuring defocus using a quad cell as illustrated in Figure 21.

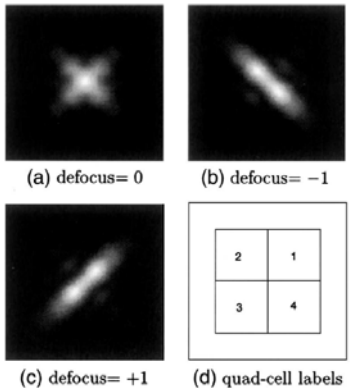

Figure 21: Focal plane images obtained when the beam has 45° astigmatism
(from Patterson & Dainty, Optics Letters 25, 1687 (2000))

It was found that the focus can easily be sensed by the tip-tilt sensor without causing a reduction in Strehl due to aberrations in the tip-tilt sensing spot. In the case of using a bright guide star, the accuracy of the signal is limited by what appears to be contamination from very high-order spherically symmetric aberrations. These aberrations, particularly spherical aberration, should be measured with the LBWFS and corrected. However, the impact of these aberrations on the focus measurement error can be kept below 20 nm if the sensor runs at 1 Hz. If the tip-tilt sensor is operating under noisy conditions, the individual focus measurements are extremely noisy, but a time average of the measurements can still be used to yield a focus estimate. The gain of the signal is significantly reduced, so needs to be calculated from the control loop, in the same way that the centroid gain of an NGS AO system changes. Operating the tip-tilt sensor off-axis also causes a reduction in the sensitivity of the focus measurement.

The above focus analysis assumed that the star image was centered on a quad cell. Van Dam separately noted that measuring focus with the star offset from the quad cell would only be possible if you had a good way to calibrate the zero point and concluded that it would not really be possible to have accurate focus calibrations especially since the offset would be dynamically changing. A potential solution would be to keep one star nulled on a quad cell with a TTM in the path to the NIR TTS. You would then need to combine this TTM position information with the centroid residual to determine the science path TT error.

2.7 Tip-Tilt Mirror

A tip-tilt mirror (TTM) in the path to the NIR TTS could be used to reposition the tip-tilt star(s) without impacting the science field. If it had sufficient range it could also allow for a larger field in which to find a tip-tilt star. It could be used to deal with DAR either as a tracking device or as a positioning device between science exposures. It could allow for focus measurements on a single star as discussed in section 2.6. If necessary, a TTM could be used to dither to measure the centroid gain.

In the absence of a TTM you either need to be able to do tip-tilt sensing at an arbitrary location (including the middle of a pixel) or to be restricted to only be able to position the science object to locations sufficiently close to the intersection of 4 pixels.

The cons of implementing a TTM include cost, and additional development and operations complexity. Unless the TTM has a very modest stroke the TTM would need to be located at a pupil plane which requires an intermediate pupil plane, which would be strongly preferred to be outside of the dewar.

Our current baseline is not to include a TTM in the path to the NIR TTS given that good TT performance can be achieved without it and because of the cons listed above.

3. Opto-Mechanical Design

This section covers the optical design for the entire NIR TTS, including the optical pickoff and the reimaging optics between the optical pickoff and the NIR TTS detector. This section only covers the mechanical design for hardware outside of the NIR TTS camera assembly. The camera assembly mechanical design, discussed in section 4.1, includes the mounting of the reimaging optics. We begin with the mechanical design concept to provide the reader with an initial overall perspective on the opto-mechanical system (section 3.1), even though later sections will need to be read to understand the components. We then discuss the plate scale (3.2), the optical pickoff (3.3) and the optical design for the re-imaging optics (3.4) before finishing with the optical alignment concept (0).

3.1 Mechanical Design

In this section we will describe the mechanical design of the optical pickoff that feeds the camera, the focus stage on which the camera is mounted, and the mechanical modifications to the AO bench and enclosure to support the camera. The NIR TTS camera is shown in this section as part of the overall SolidWorks model, although it's mechanical design will not be described until section 4.1.

As discussed in section 2.2 the NIR TTS is located on the edge of the AO bench close to OSIRIS. An exchange mechanism will be used to switch between optical pickoff options. A vertical translation stage approach has been selected. As discussed in section 3.3.2 only a 3 position device, including open, is needed if the optical pickoff mechanism must be located on the AO bench (i.e. > 400 mm from the focal plane). A three or four position device to accommodate three optics (H reflective dichroic, K reflective dichroic, annular mirror) is desirable if the optical pickoff mechanism can be located between the AO bench and OSIRIS (i.e., ≤ 300 mm from the focal plane). We have gone with the four position device shown in Figure 24 to insert one of the three optical pickoff options (plus an open position) into the science path. With the reflective surface of the pickoff located 300 mm from the focal plane the exchange mechanism does not interfere with the AO bench or its cover; the top and bottom positions for the optical pickoffs extend above and below the AO bench. The advantage of having the optical pickoff closer to the focal plane is that it allows the annular mirror option and it also means that the NIR TTS can be closer to the optical pickoff mechanism therefore requiring less real-estate on the AO bench. Its disadvantage is the need for an enclosure extending off the AO bench.

The tall box on which the translation stage is mounted is hollow so that vibration damping material can be added if necessary. The translation stage is a Parker Daedal 402600XR1. The optical pickoff holder is mounted with a flexure to the translation stage. The vertical bar to the right of the optical pickoff holders provides a guide roller track to ensure positioning repeatability and to reduce susceptibility to vibrations. The co-alignment and repeatability of the fold optics must be good enough to ensure that a re-acquisition is not required when switching between fold optics.

Each optic is 140 mm in diameter and 15 mm thick. Each optic is held by three pads on either side in a similar fashion to existing AO bench vertical stages. The pad on the reflective surface of the optic will be a hard point while the pad on the non-reflective side will be spring loaded.

The Figure 23 top view of the pickoff assembly shows the light transmitted to OSIRIS and reflected to the NIR TTS camera. The angle of incidence on the pickoff is 30°. Although a smaller angle of incidence would have been preferred this angle was chosen to prevent interference with another existing component on the AO bench (the fast tip-tilt mirror).

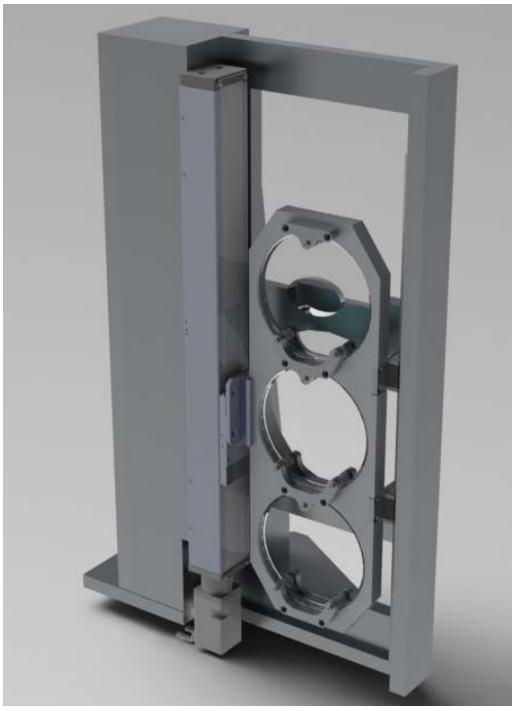

Figure 22: Optical pickoff stage

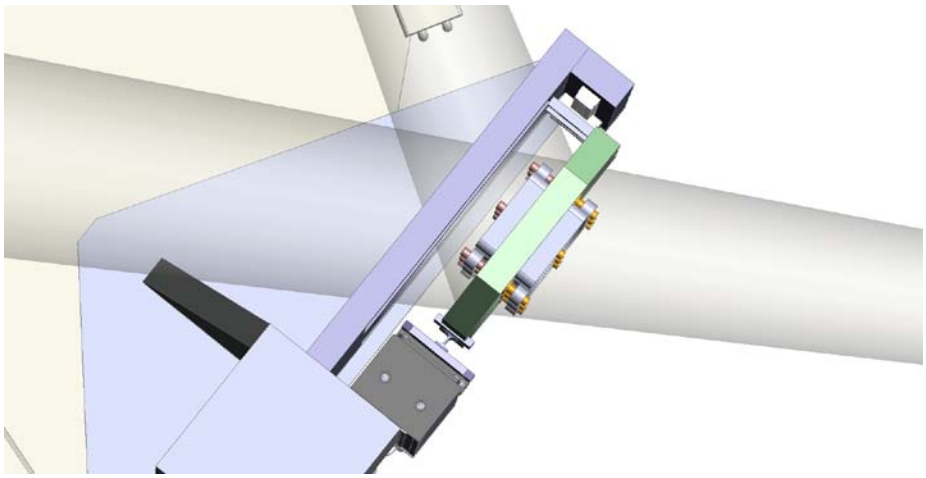

Figure 23: Top view of the pickoff assembly. The gray beam entering from the left is transmitted through the pickoff to OSIRIS while part of the light is reflected to the NIR TTS camera.

The optical pickoff assembly and NIR TTS camera are shown on the AO bench in Figure 24. Note that a hole must be cut in the AO bench top cover to accommodate the camera which extends above this cover. Since the reflective surface of the optical pickoff is 300 mm from the OSIRIS focal plane, the pickoff translation stage is located partially off the existing AO bench on an extension plate. As a result a new AO bench side panel assembly (transparent green in Figure 24) must also be provided. In addition one of the existing AO bench top cover supports must be removed to make space for the camera and this is replaced with new supports at either edge of the new side panel assembly. Connectors for the cables to the two new stages will be located on the bottom surface of the new side panel assembly.

The focus of the AO system is adjusted to maintain focus on the science instrument. The NIR TTS camera must be adjusted in focus to stay conjugate to the science instrument focus. The camera assembly, which includes the reimaging optics, is therefore mounted on a focus stage (a Parker Daedal 808CTE06). The

camera mounts to this focus translation stage via a kinematic interface plate (supplied with the camera). The focus stage is mounted on a riser to center the camera optics on the AO optical axis (305 mm above the AO bench). The riser is of the same type as used elsewhere on the table; two stainless steel plates separated by four 1.5 inch diameter stainless steel Thorlabs posts. Note that the camera assembly does not interfere with the existing pupil simulator (seen on the right of Figure 24).

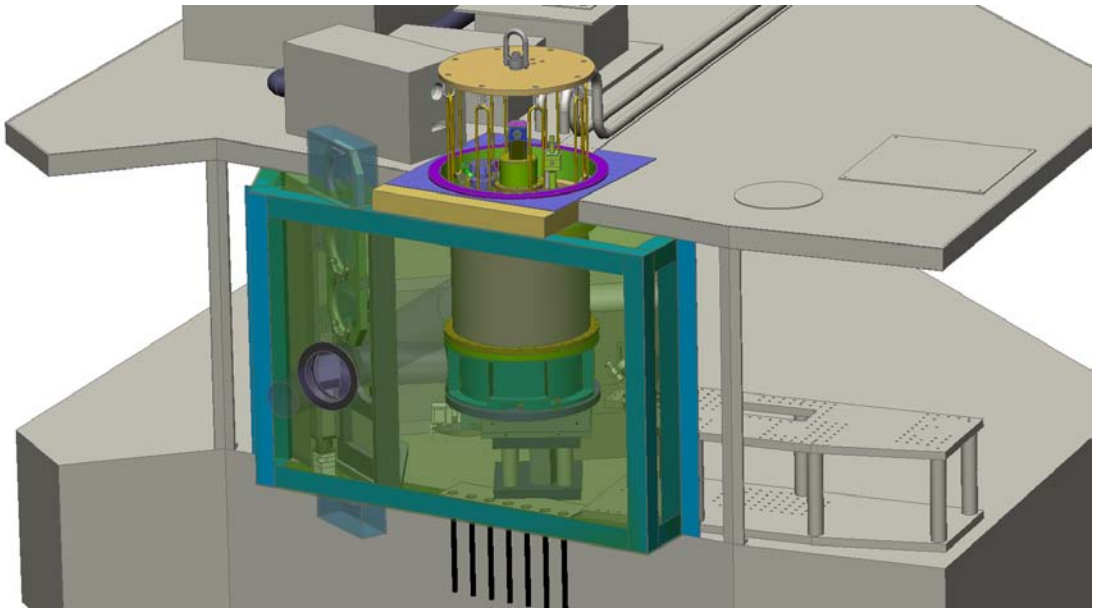

Figure 24: Optical pickoff stage and the NIR TTS camera mounted on a focus stage. The gray box on the AO bench top cover just to the left of the top of the camera is a thermally insulated box for the camera electronics.

The new mechanical components associated with the NIR TTS (only) are shown in Figure 25. These include the camera and optical pickoff at lower right and the cryocooler compressor (see section 4.4) at upper left. The compressor sits on a platform suspended from the ceiling. Vibration isolation material is installed between the suspended platform and the compressor.

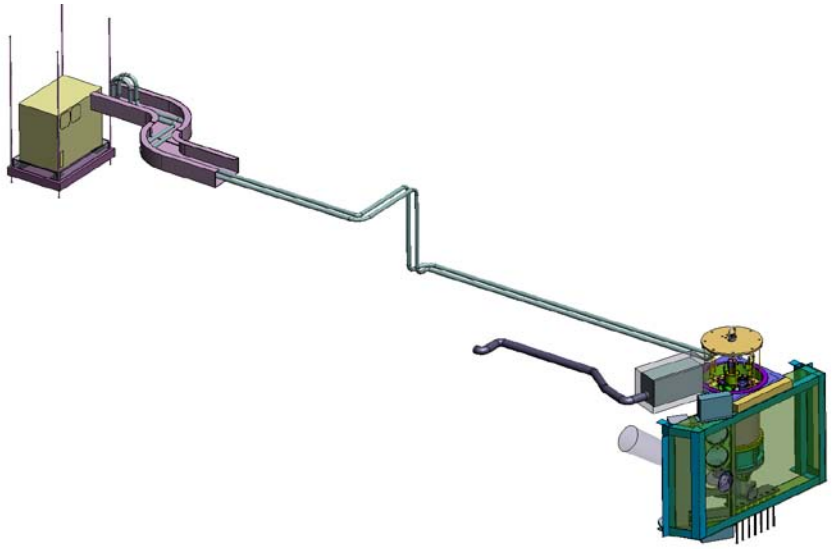

Figure 25: New mechanical components associated with the NIR TTS. At bottom right is the camera and optical pickoff. At top left is the cryocooler compressor.

The compressor lines are flexible. Two hoses must be run from the compressor to the top (back end) of the camera dewar.

The new mechanical components associated with the NIR TTS are shown within the context of the existing AO system in Figure 26; there is only a small gap between the new side panels and OSIRIS.

Figure 26 also shows a temporary frame with a hoist straddling the AO bench that would be used for installing the camera. This installation system is discussed in the assembly, integration, test and commissioning plan document (KAON 855).

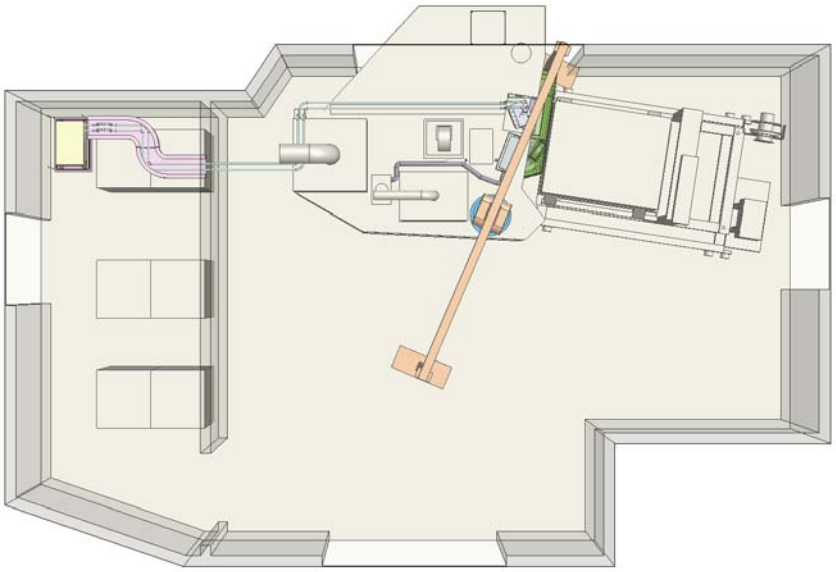

Figure 26: Top view of the NIR TTS components with respect to the existing AO system and OSIRIS science instrument.

3.2 Plate Scale

Choosing the optimal plate scale is a balance between field of view and centroiding performance. For reference, note that the diffraction-limited core diameter at Ks (2.15 μm wavelength) is 44 mas and the optimal field of view is 120" diameter.

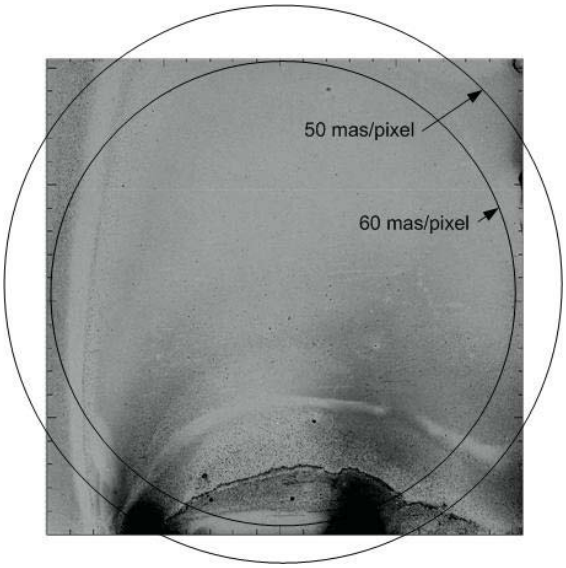

Figure 27: 120" diameter field of view, for 2 different plate scales, superposed on the H2RG detector
The field of view has been displaced slightly upward with respect to the detector.

A plate scale of ~0.05"/pixel or less would be desirable from the analysis in section 2.5. This plate scale would give a field of 102"x102", and a diagonal of 145", on the procured H2RG detector. This case and the case of a 0.06"/pixel plate scale are shown against the detector in Figure 27. Given the quality of the detector we do not need to consider plate scales larger than 60 mas/pixel. A somewhat smaller plate scale would improve the centroiding. We have selected 50 mas/pixel as the plate scale. This plate scale meets the requirement of a minimum field of view of 100" diameter.

A plate scale of 0.05"/pixel, or 0.360 mm/" given the 18 μm pixels, requires a demagnification of 0.727/0.36 = 2.0 corresponding to a final f/# of 6.8 (versus the f/13.66 AO focal ratio).

3.3 Optical Pickoff

3.3.1 Fields of View

The position and size of the three detectors are shown with respect to each other in the focal plane in Figure 28. The OSIRIS imager and integral field unit (IFU) size and position are from Figure 4. It is possible to decenter the OSIRIS imager and IFU together with respect to the optical axis (defined by the AO rotator axis) during the initial alignment of OSIRIS to the Keck I AO system. The NIR TTS is shown with a small decenter down to be consistent with Figure 27.

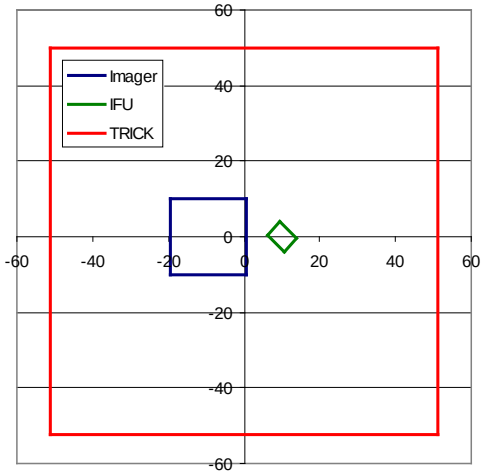

Figure 28: The OSIRIS imager and integral field unit (IFU), and the NIR TTS detector (TRICK), in the focal plane (units are arcsec). *(0,0) represents the AO optical axis. The largest IFU field is shown.*

3.3.2 Size

A fold mirror and/or dichroic will be used to reflect the required light to the NIR TTS and pass the science field to the science camera, OSIRIS. If we assume that the fold is on the AO bench then it must be located > 393 mm from the focal plane (from section 2.1). If we allow it to extend into the space between OSIRIS and the AO bench then the fold must still be located > 185 mm from the focal plane.

The NIR fold should be located as close to the OSIRIS image plane as possible in order to minimize vignetting and the required size of the fold. The required major axis diameter of the fold or dichroic

$$d = (fov * ps + t / f\#) / \cos\theta ,$$

depends on the field of view (fov) of the TTS sensor, the plate scale (ps = 0.727 mm/arcscec) at the focal plane, the distance (t) of this fold from the focal plane, the focal ratio (f# = 13.66) of the beam and the angle of incidence (θ) on the fold mirror. Assuming fov = 120", t = 300 mm and θ = 45° then D = 154 mm. If the distance of the fold from the focal plane were increased to t = 500 mm then the fold diameter is increased to d = 175 mm.

A very similar equation can be used to calculate the major axis diameter of the hole in a fold mirror required to transmit the fov to the science instrument. In order to transmit the maximum IFU size of

4.8"x6.4" the mirror would need a hole of 41 mm in height and 58 mm in width if t = 500 mm and θ = 45°. For the smallest IFU size of 0.32"x1.28" the hole could only be reduced to 38 mm x 53 mm.

The hole in a fold mirror would vignette a field of diameter

$$fov = (d * \cos\theta + t / f\#) / ps.$$

The vignetted field of view would be 62" for the smallest IFU size and 67" for the largest IFU size, assuming t = 300 mm. The vignetted field would be 102" for the smallest IFU size and 107" for the largest IFU size, assuming t = 500 mm. This implies that an annular mirror concept is only valid for t ≤ 300 mm.

The field at the dichroic, for t = 500 mm and 300 mm, is represented in Figure 29 by circles showing the size of the expanding f/13.66 beam for multiple image points at the dichroic. The circle size is 36.6 mm for t = 500 mm and this reduces linearly with the distance to the focal plane, t. This figure provides a check on the required outer diameter of the dichroic. The height of the dichroic need only be ~110 mm for t = 500 mm. Assuming a dichroic at 30° incidence angle the dichroic could be 127 mm if it were a circular optic.

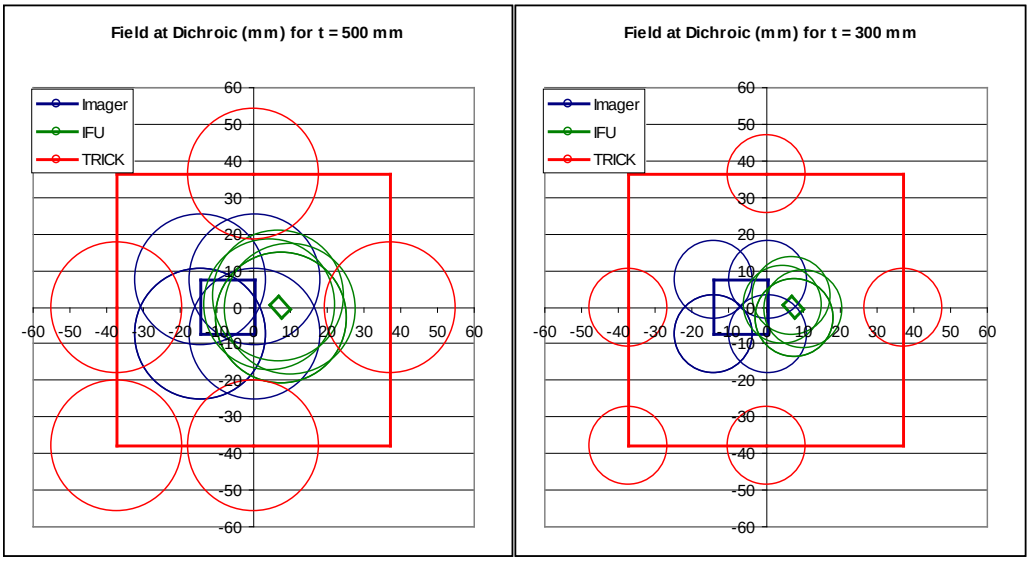

Figure 29: The OSIRIS and NIR TTS fields of view projected onto the dichroic.
The distance of the dichroic from the focal plane is 500 mm (left) and 300 mm (right). The circles represent the size of the expanding f/13.66 beam on the dichroic for points in the focal plane at the corners of the imager and IFU fields and at the sides of the imager field. Units are mm.

3.3.3 Optical Pickoff Options

The fold options that have been considered are listed in Table 2. Case 1 is with no fold in the beam. Case 2 is an annular mirror, the IFU field is transmitted through the hole in the mirror, and the mirror reflects an annular field to the TTS. Case 3 is a K-band reflective dichroic that transmits the shorter wavelength bands to OSIRIS. Case 4 is a H-band reflective dichroic that transmits K-band to OSIRIS. Case 5 and 6 are for IFU science only and consists of an annular mirror with an H-band reflective dichroic at its center. This allows you to do H-band TT sensing with stars in the IFU field or K-band TT sensing with stars in the outer reflected annulus. We did consider a partially K-band reflective dichroic but for emissivity and throughput reasons we discarded this option.

The K-band dichroic (case 3) would always be the best choice for J & H-band science. The H-band dichroic (case 4) is the only option listed for K-band imaging science. The annular mirror (case 2) would be a better option for K-band IFU science if there were tip-tilt stars in the outer annulus (where they are most likely to be). The annular mirror with an H-band dichroic (case 5 and 6) at its center offers a compromise between cases 2 and 4, and therefore the option of only requiring two dichroics, at the expense of lower throughput to the IFU and no K-band imaging, respectively.

Case	Science λ	IFU	Imager	NGS location	Tip-tilt λ	NIR fold
1	JHK	Yes	Yes	0-60" off-axis	Vis	n/a
2	JHK	Yes	No	35-60" off-axis	K (or H)	annular mirror
3	JH	Yes	Yes	0-60" off-axis	K	K-dichroic
4	K	Yes	Yes	0-60" off-axis	H	H-dichroic
5	K	Yes	No	<35" off-axis	H	H annular mirr
6	K	Yes	No	35-60" off-axis	K (or H)	H annular mirr

Table 2: Configuration options for tip-tilt sensing

To provide broad user applicability at least a 3 position exchange mechanism should be provided. We could start with the K-band and H-band dichroics in this mechanism and later add the annular mirror in the open position assuming the performance predictions have been achieved. Imaging science with STRAP would be impacted because either the H-band or K-band dichroic would need to be in the science path however, there would be no impact on IFU science with STRAP since the annular mirror could be used.

3.3.4 Dichroic Optical Impact on Science Path

A tilted plane parallel plate inserted into the science path will introduce a variety of aberrations including lateral chromatic, longitudinal chromatic, astigmatism, coma and spherical. The AO deformable mirror could be used to remove the non-chromatic aberrations in the science path, which will put these aberrations instead in the NIR TTS optical path and also in the wavefront sensor path.

The third-order wavefront aberrations for a tilted plate are

$$\Delta W_{spherical} = -[t/(f/\#)^4][(n^2-1)/(128n^3)] = -1 \text{ nm}$$

$$\Delta W_{coma} = -[(t\sin\alpha)/(f/\#)^3][(n^2-1)/(16n^3)] = -50 \text{ nm}$$

$$\Delta W_{astig} = -[(t\sin^2\alpha)/(f/\#)^2][(n^2-1)/(8n^3)] = -749 \text{ nm} ,$$

where we have used the current design parameters of thickness t = 15 mm, angle of incidence $\alpha = 30°$, f/# = 15 and fused silica index n = 1.44.

The lateral and longitudinal displacement as a function of wavelength are given by

$$\Delta y(\lambda) = t\{\sin\alpha - \cos\alpha \tan[\sin^{-1}(\sin\alpha/n(\lambda))]\} .$$

$$\Delta z(\lambda) = [(n-1)/n]t .$$

Across the J-band (1.05 to 1.45 μm) the index of fused silica varies from 1.4498 to 1.4452 resulting in a lateral chromatic aberration of 17.3 μm and a longitudinal chromatic aberration image blur of $\Delta(\Delta z)/(2f/\#) = 1.1$ μm.

The impact of these aberrations was evaluated in Zemax by adding this new dichroic, located 300 mm from the focal plane, to the existing Zemax model of the telescope and AO system. The resulting RMS wavefront error versus field position is shown in Figure 30.

Non-chromatic aberrations to the science instrument can be measured with image sharpening and corrected with the deformable mirror by using centroid offsets on the wavefront sensor. However, this would result in putting these aberrations into the NIR TTS path. A similar plane parallel plate, tilted by the same amount in the orthogonal direction, in the science or NIR TTS path could be used to remove the astigmatism in that path at the expense of doubling the lateral and longitudinal color and coma.

The compensation approach we have settled on for the system design is to add a Zernike surface and wedge to the 2nd surface of the dichroic. The Zernike surface compensates for astigmatism and the wedge corrects for lateral chromatic. The resultant greatly improved wavefront error is shown in Figure 31 and the resultant spot diagrams in Figure 32. This solution results in the best compensation of the science, NIR TTS and wavefront sensor paths. It is in fact an improvement over the current situation since the correction added to the 2nd surface of this dichroic is also used to compensate for astigmatism from the existing dichroic. The existing IR transmissive dichroic does have a wedge so we have existing experience with procuring such dichroics, however the additional very low power cylinder is a new requirement.

Note that leaving a small amount of non-common path astigmatism between the science and NIR TTS paths would facilitate focus sensing with the NIR TTS.

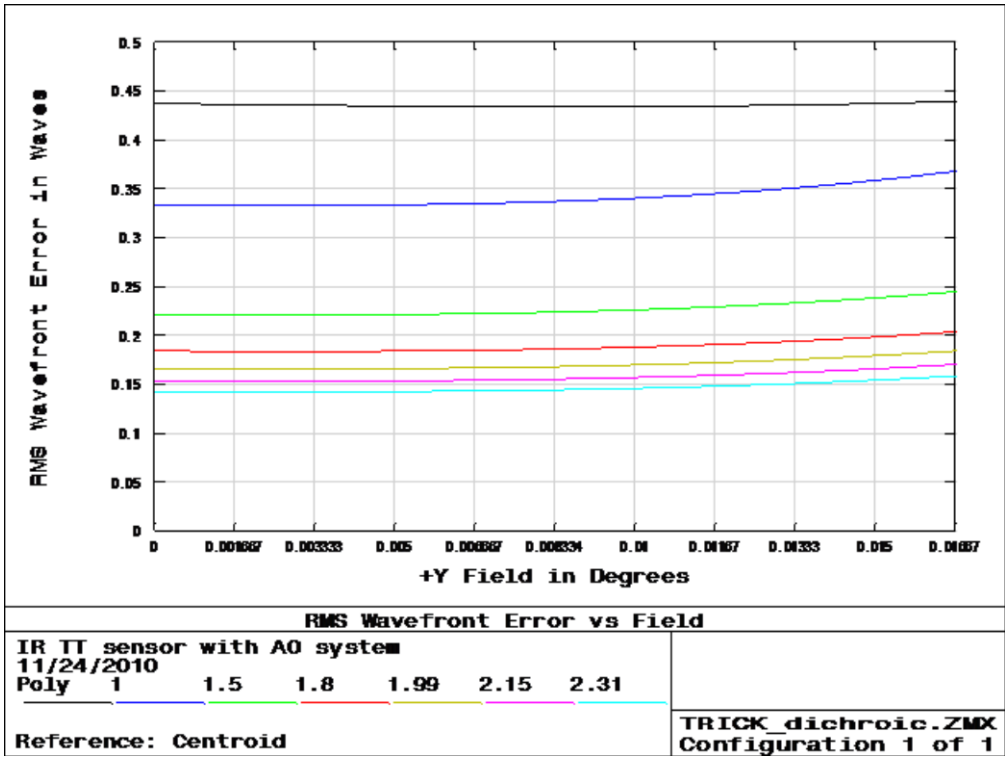

Figure 30: RMS wavefront error for a 15 mm thick fused silica dichroic at 30° angle of incidence

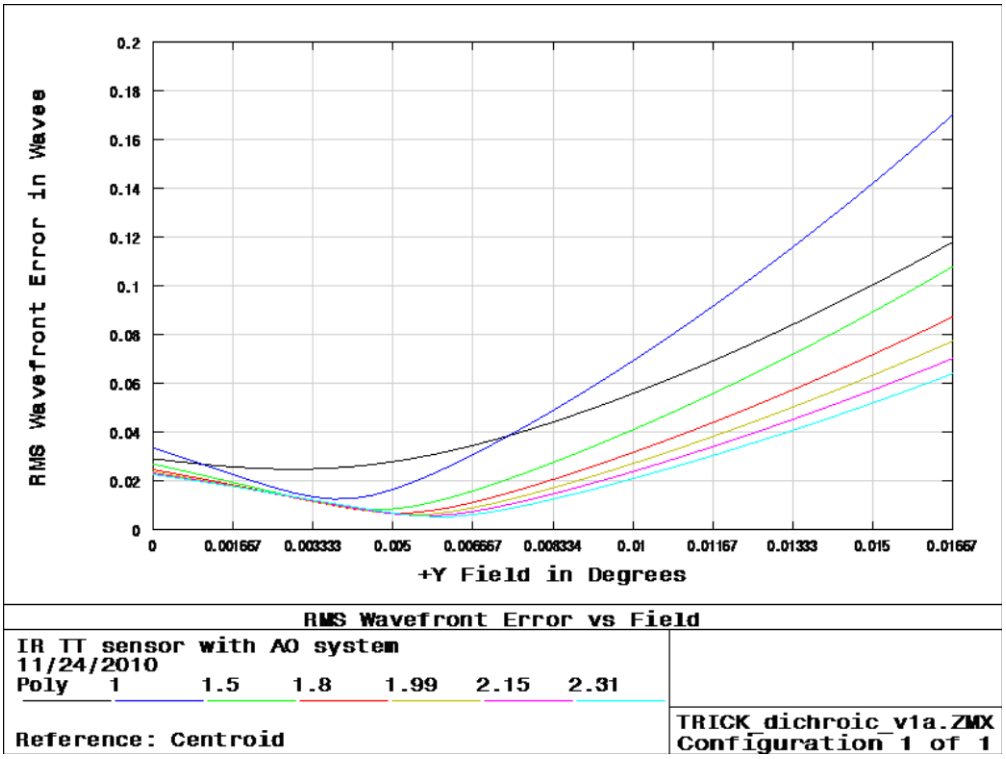

Figure 31: RMS wavefront error for a 15 mm thick fused silica dichroic at 30° angle of incidence, with a 0.55° wedge and a 19.343 m radius cylinder

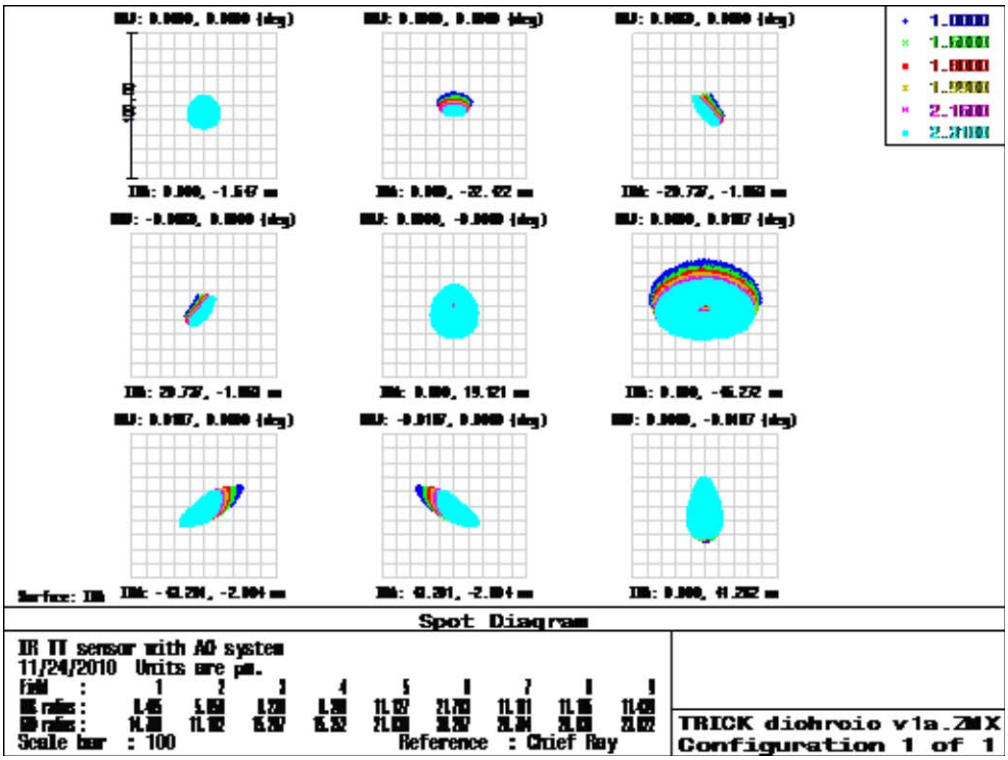

Figure 32: Spot diagrams for the case shown in Figure 31

3.3.5 Dichroic Requirements

The dichroic specifications are summarized in Table 3. The current Keck AO IR transmissive / visible reflecting dichroics were obtained, using a similar specification table, from Custom Scientific. Previous versions were obtained from Barr Associates. We will pursue quotes from both of these vendors.

3.3.6 Emissivity

The K-band reflective dichroic will add background in K-band to the NIR TTS to the extent that it is not 100% K-band reflective. This dichroic will not add significant background to the JH science being done with OSIRIS.

The H-band reflective dichroic will add background to K-band science with OSIRIS to the extent that it is not 100% K-band transmissive. This dichroic will not add significant background to the H-band tip-tilt sensing.

The annular mirror, used for K-band IFU science, would add significant thermal background to the central part of the NIR TTS field and the outer part of the OSIRIS field. If the annular mirror was at a focal plane then the pupil stop in OSIRIS would prevent the thermal background from this mirror from reaching the IFU. Similarly, the pupil stop in the TTS would prevent thermal background from the hole in the mirror from reaching the outer radius of the TTS field; the part of the field used for TT sensing with the annular mirror. The extent to which this background will contaminate the field depends on how far the annular mirror is from the focal plane. For the 300 to 500 mm distance at which the dichroic is expected to be from the focal plane the additional thermal background should have no impact on the IFU and little impact on the minimum radius at which TT stars can be used. This statement will be checked with the optical model.

In order to remove this background either a narcissus mirror could be installed on the opposite side of the dichroic from the NIR TTS so that the NIR TTS would be looking at its cold reflection in the narcissus mirror or something cold could be placed at this location. Our baseline plan is to procure high reflectivity/transmission dichroics in order to minimize the increase in background. A narcissus mirror or cold surface could be a future upgrade if necessary. This topic will be further assessed during the detailed design.

Table 3: Dichroic specifications

Category	Specification	
Name	**H-band reflective**	**K-band reflective**
Quantity	1	1
Diameter	140 ± 0.5 mm	
Thickness	15 ± 0.5 mm	
Clear aperture (CA)	≥ 135 mm of central diameter	
Wedge angle	TBD to minimize lateral dispersion	
Cylinder radius	TBD to minimize astigmatism	
Edges	chamfered edges, bevel = 2 mm at 45° on both surfaces	
Substrate material	Infrasil (vendor supplied)	
Environmental conditions	temperature: -5 to +25°C; pressure: 450 to 760 mm-Hg; relative humidity: 0 to 100%	
Reflectance (1st surface)	≥ 96% average, ≥ 93% min. for 1.45 ≤ λ ≤ 1.8 μm	≥ 97% average, ≥ 95% min. for 1.95 ≤ λ ≤ 2.4 μm
Anti-reflectance (2nd surface)	≤ 0.5% for 0.975 ≤ λ ≤ 2.4 μm	
Transmittance (through optic)	≥ 96% average, ≥ 93% min. for 0.975 ≤ λ ≤ 1.40 μm & ≥ 97.5% average, ≥ 95% min. for 1.95 ≤ λ ≤ 2.4 mm	≥ 96% average, ≥ 93% min. for 0.975 ≤ λ ≤ 1.81 μm
Polarization	the optics shall be non-polarizing (i.e. ≤ 0.1% polarizing)	
Angle of incidence	30° ± 0.1° (TBC)	
Wavefront rms (focus removed)	≤ 20 nm rms in reflection & transmission	
Wavefront rms (with focus)	≤ 450 nm rms in reflection & transmission	
Smoothness	≤ 10 nm rms for any 2 points separated by ≤ 25 mm	
Surface quality	60/40 scratch/dig for both surfaces (MIL-F-48616, section 4.6.7.2)	
Adhesion durability	Tape test per MIL-F-48616, section 4.6.8.1	
Abrasion durability	Cheesecloth test per MIL-F-48616, section 4.6.8.3	
Cleanability	Solvents test per MIL-F-48616, section 4.6.9.2	
Performance tests required	Spectrophotometer curves over the CA at the nominal incidence angle. Interferometric scans in reflection & transmission over the CA. Adhesion, abrasion & solubility test results from a witness sample from the same coating run. Certification that each requirement has been met.	

3.4 Reimaging Optic

Reimaging optics will be required to achieve the desired 0.05"/pixel plate scale. A pupil location is required for a cold pupil stop to reduce thermal background. Two filter options will be used: a Ks (1.99 to 2.30 μm) filter (chosen to block the steepest part of the thermal background) and an H filter. The pupil stop will be placed on the filters.

A reflective optical design was briefly considered due to the broad range of operating wavelengths, but was quickly discarded due to the small space envelope available and the need for an accessible real pupil image. The refractive optical design that has been developed is described in the following section.

3.4.1 Optical Design

The reimaging optics were first designed using a paraxial model of the telescope. These were then tested and optimized behind the full model of the telescope and AO system including the optical pickoff dichroic that feeds the NIR TTS camera (see Figure 33).

To ensure that the results were accurate, the calibration method for the AO system was taken into account. The science path light does have some astigmatism due primarily to the existing dichroic that reflects the visible light to the wavefront sensor. This is normally corrected by placing a static shape on the DM that is determined using phase diversity measurements. This was simulated by adding Zernike terms, mostly astigmatism, to the DM surface in the Zemax model to optimize the science path wavefront.

The NIR TTS optical pickoff dichroic also adds astigmatism to the science path that must be compensated for in some manner. If a static shape is placed on the DM to correct for the TRICK dichroic, the NIR TTS camera will see a resulting wavefront error. This limits the Strehl to about 65% or so and is not acceptable.

Therefore, two different methods were evaluated to compensate for this. One is to polish a long radius cylinder term into the backside of the NIR TTS dichroic. This produces good results, but there are some concerns about the manufacturability of the 40 m radius cylinder that is required. As an alternative to the cylinder term, a tilted plate can be added to the path to the NIR TTS camera; 18.5° in the orthogonal direction to the pickoff dichroic tilt. In the current model this plate is added inside the cryogenic dewar to minimize the number of warm surfaces.

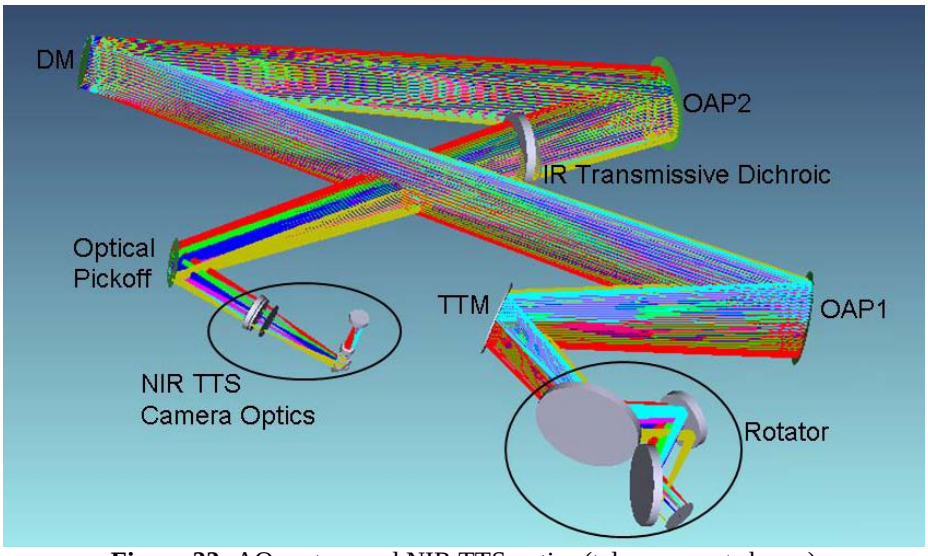

Figure 33: AO system and NIR TTS optics (telescope not shown)

The performance of the plate and the cylinder options are virtually identical. Since the tilted plate compensates for aberrations introduced by a dichroic in the science beam it is not the right solution if an annular mirror is instead used for the optical pickoff. To address the annular mirror case either it would have been better to have added the compensating cylinder term to the dichroic so that a second plate was not required or to have the tilted plate be removable. A removable plate would be much easier outside the dewar. The cylinder term is therefore our preferred option as we proceed into the detailed design, and this is the option presented in the remainder of this section.

The current design based on refractive optics has all spherical surfaces and is shown in Figure 34.

The first element group is a field lens to create a real pupil image. Due to the large wavelength range it is a doublet to control chromatic aberration of the pupil image. It was moved before the image plane to both shorten the overall camera length and to reduce the problem of reimaging dust and defects present on its surface. A fold mirror is incorporated to fold the beam up into the camera dewar. In order to keep the dewar at a reasonable size, the field lens and fold mirror will be warm while the remaining optics are located inside the dewar. The design has the components outside the dewar at 0.6 atmospheres and 0 °C and the components inside the dewar at vacuum and 73 K. Testing showed that it is easy to re-optimize for different temperatures such as 123 K. A minor note is that model currently uses an approximation for the cryogenic index of sapphire.

The next portion of the camera optics was initially modeled as a pair of doublets surrounding the pupil image similar to a double Gauss lens. As the system was optimized these were driven to the current configuration. A flat piece of glass is included at the pupil location to represent the H or K-band filter. A mask will be deposited directly on the second surface of the filter to function as the cold stop.

The final element is a meniscus with a small net power which functions as a field flattener and provides some aberration compensation.

The system prescription is shown below in Table 4. Note that these dimensions are slightly different than the dimensions in the current SolidWorks model (the SolidWorks and Zemax models will be made consistent).

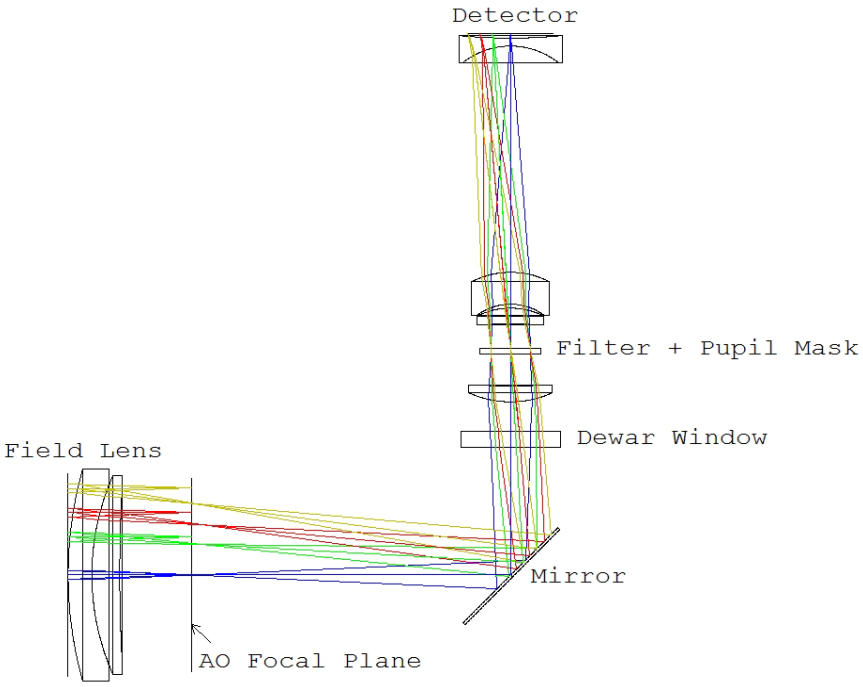

Figure 34: Reimaging optics layout

Table 4: Reimaging optics system prescription (all units are mm)

#	Comment	Radius	Thickness	Glass	Semi-Diameter
4	Focal Plane	--	-62.300		
5	Field Lens 1	165.55	12.000	SILICON	50.7
6	Field Lens 1	111.63	2.72		47.7
7	Field Lens 2	116.42	14.000	ZNSE	48.5
8	Field Lens 2	469.48	224.95		47.6
10	Mirror at 45°	--	-35.00	MIRROR	30.5
12	Window	--	-8.00	F_SILICA	21.6
13	Window	--	-15.00	Vacuum	21.1
14	Collimator 1	-48.24	-8.00	BAF2	19.7
15	Collimator 1	-482.99	-16.00	Vacuum	18.7
16	Filter	--	-3.00	F_SILICA	15.2
17	Pupil	--	-12.00	Vacuum	14.8
18	Collimator 2	-146.97	-8.00	BAF2	15.8
19	Collimator 2	33.95	-2.09	Vacuum	16.4
20	Collimator 2	25.99	-15.90	SAPPHIRE	16.4
21	Collimator 2	39.70	-114.88	Vacuum	19.4
22	Field Flattener	43.69	-4.00	BAF2	25.2
23	Field Flattener	-321.25	-4.80	Vacuum	27.1
IMA	Detector	--	0.00		23.4

All of the following performance results, except for the pupil image, are for a circular 10.95 m diameter primary mirror aperture.

The performance of the current design is quite good. The Ks-band PSF at 60" off-axis is shown in Figure 35. The H and Ks-band Strehls range from 95 to 97% over the entire 120" diameter field. The rms wavefront error versus off-axis distance in the +Y direction is shown in Figure 36 for Ks-band and in Figure 37 for H-band; other field directions look similar. The Ks-band ensquared energy plot is provided in Figure 38; the ensquared energy performance is also seen to be quite uniform over the field.

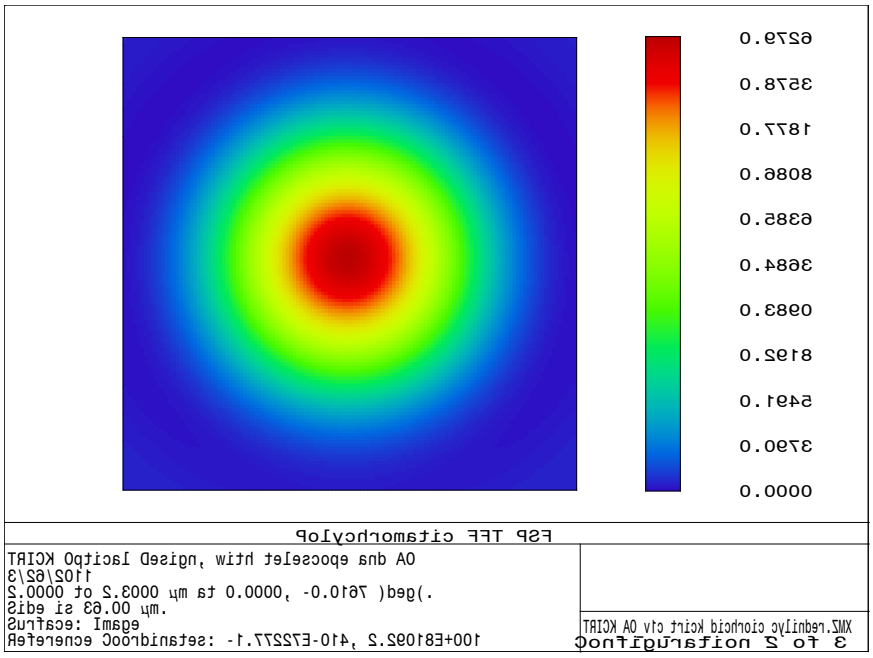

Figure 35: Ks-band PSF at 60" off-axis. The Strehl is 97%. A 2x2 pixel (36x36 μm) image is shown.

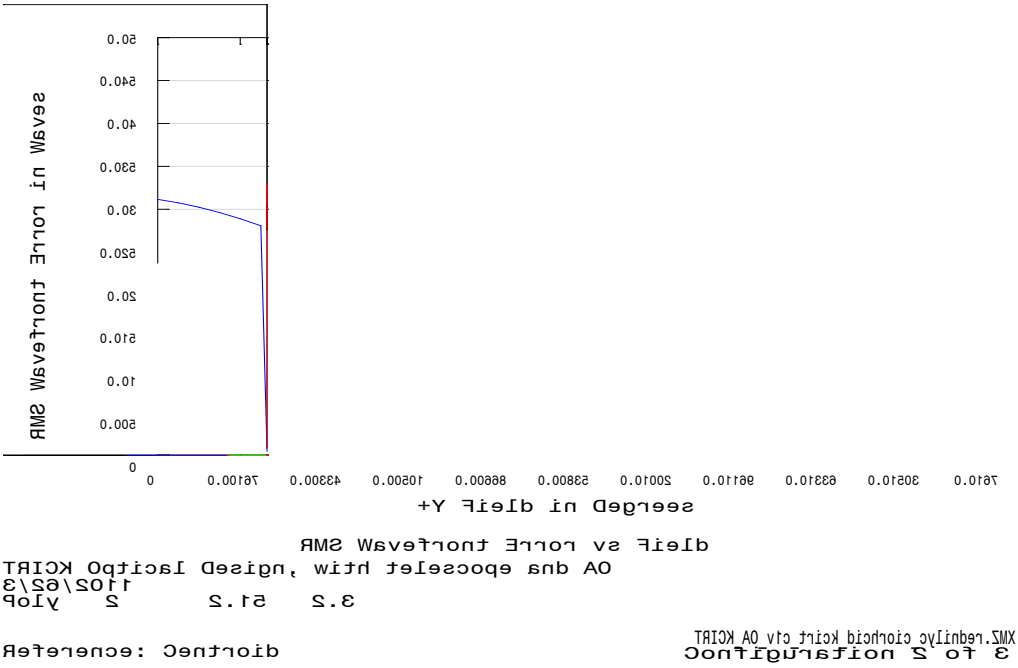

Figure 36: Ks-band rms wavefront error versus field to 60" off-axis

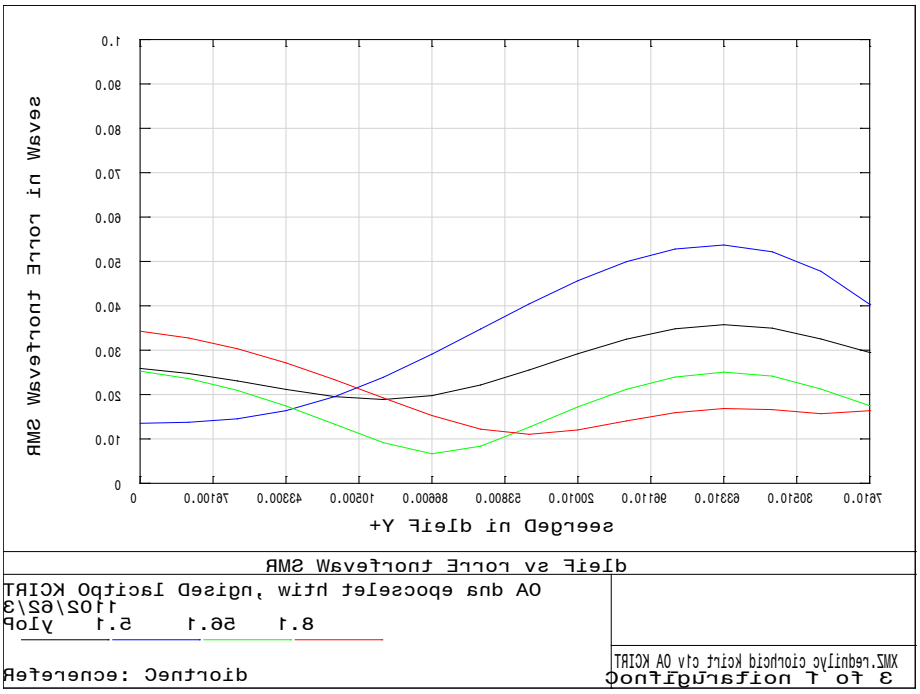

Figure 37: H-band rms wavefront error versus field to 60" off-axis

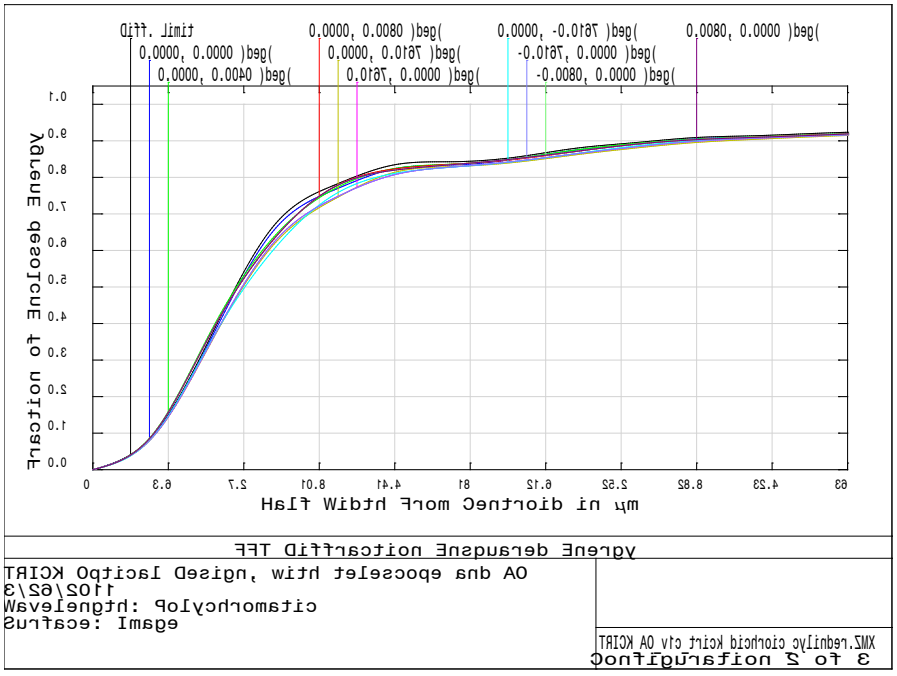

Figure 38: Ks-band ensquared energy (18 μm is 1 pixel)

The field curvature and distortion for Ks-band are shown in Figure 39. The field is quite flat. The maximum amount of grid distortion (pincushion), from the grid distortion plot, is 5.1%.

The telescope pupil footprint at the pupil mask location on the filter, for all field points, is shown in Figure 40.

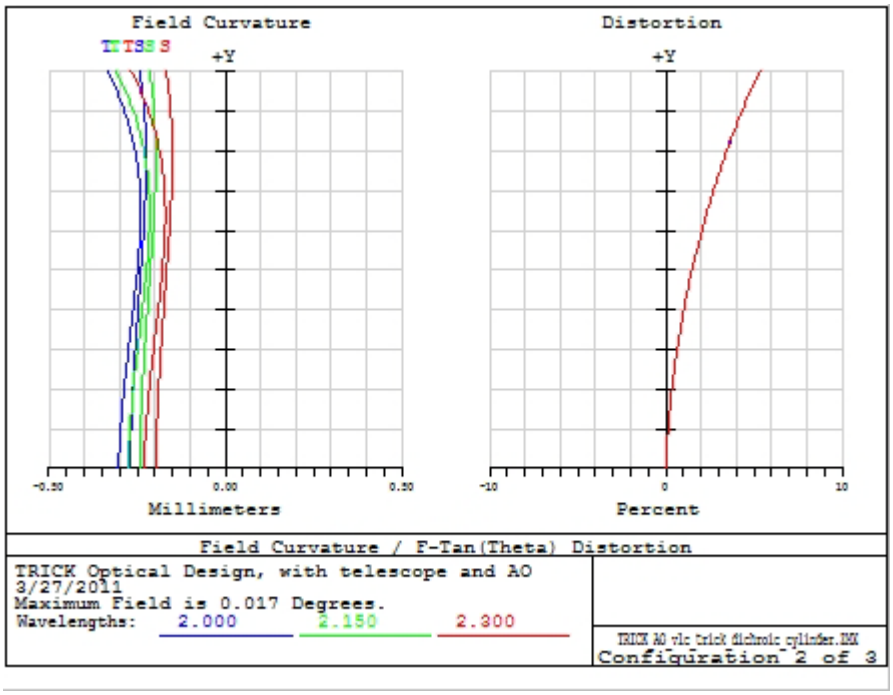

Figure 39: Ks-band field curvature and distortion

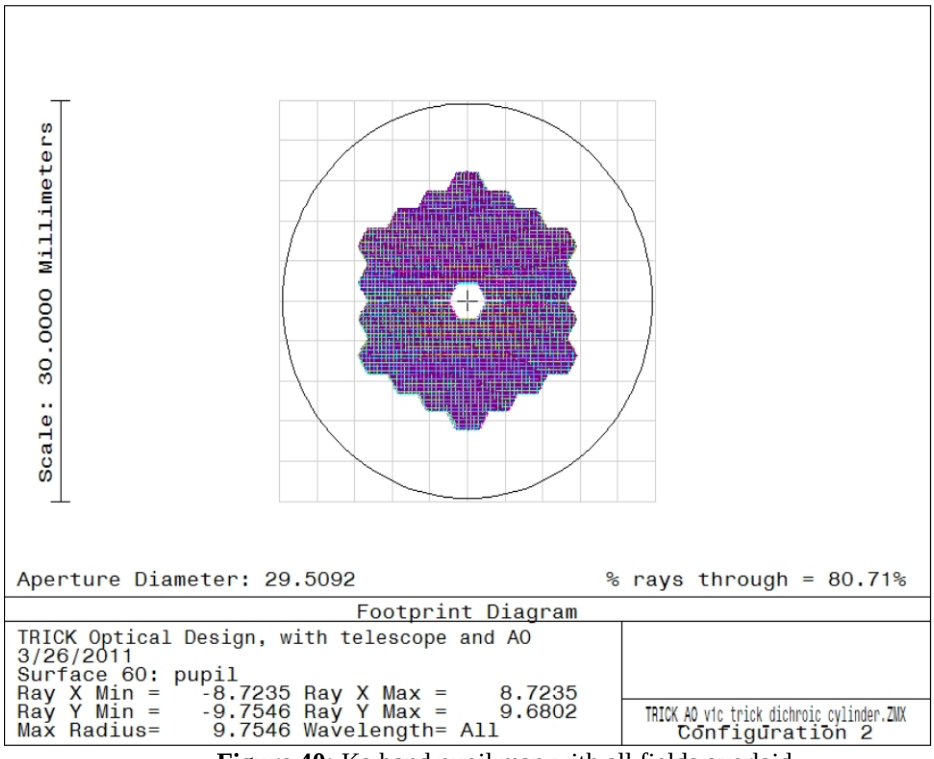

Figure 40: Ks-band pupil map with all fields overlaid

Note that for AO-correction of the TT star we would want to include a MEMS deformable mirror at a pupil location; however we have declined to pursue this option for the NIR TTS. Similarly if we wanted to include a TTM in the path the best location would be at a pupil; however, again we have declined to pursue this option. There is a mirror between the field lens and the next optic that might have little impact on pupil motion if it were used for small TT adjustments.

3.4.2 Optical Tolerance Analysis

A preliminary tolerance analysis has been performed, with only focus being used as a compensation term. The tolerancing will be investigated further during the detailed design and other compensators will be examined. For example, if the surface radii are measured accurately during lens production, the nominal spacing between lenses may be adjusted to compensate for errors in lens radius of curvature.

The tolerances listed in Table 5 were chosen for the tolerance analysis. The thickness and radii tolerances for the lenses follow the Precision Quality and High Precision Quality guidelines from Optimax: http://www.optimaxsi.com/Resources/ManufacturingChart.php. L2 and L3 were given the toughest tolerances for both fabrication and installation.

Table 5: Tolerances used for analysis

Element	Radius (%)	Thickness (mm)	Decenter (mm)	Tilt (deg)
Field Lens 1	0.10	0.050	0.250	0.1
Field Lens 2	0.10	0.150	0.250	0.1
L1	0.05	0.150	0.075	0.1
Filter		0.150		
L2	0.05	0.025	0.075	0.1
L3	0.05	0.050	0.050	0.1
L4	0.10	0.150	0.100	0.1
Field lens spacing		0.100		
L1 – filter		0.200		
L2-L3		0.025		
L3-L4		0.050		

A Monte Carlo analysis was done for 100 systems according to the Table 5 tolerances with the following results:

- 90% were better than 72% Strehl
- 80% were better than 75% Strehl
- 50% were better than 84% Strehl
- 20% were better than 90% Strehl
- 10% were better than 93% Strehl

3.4.3 Cold Baffling and Stray Light Analysis

In addition to the cold pupil stop, a light-tight cold baffle must surround the light path within the dewar to block the considerable thermal radiation emitted by surrounding surfaces. In K-band reimaging systems the cold baffle normally extends as far forward as the field lens which usually serves as the dewar window; but we have found that a shorter cold baffle will suffice such that the fold mirror can remain outside the dewar where it is readily adjusted or replaced by a tip-tilt mirror.

A stray light analysis was performed to investigate if cold baffles were needed close to the field lens. The camera design was set up as a non-sequential file, where the H2RG was made a source and a hemispherical detector construct was placed around the camera. Randomly distributed rays were then traced in this "backward" direction to determine if the detector was exposed to any stray light from the surrounding warm AO bench. Also included in the design were cold stops at each lens. These, coupled with the overall length of the system, ensure that only rays coming through the field lens make it to the H2RG detector.

In Figure 41 only rays that make it out of the camera dewar are shown. 1 million rays were traced for this image, however the same results were obtained for 10 million rays. The conclusion is that cold baffles inside a dewar that does not include the field lens or fold mirror are sufficient to prevent thermal background from outside the telescope pupil from making it to the detector.

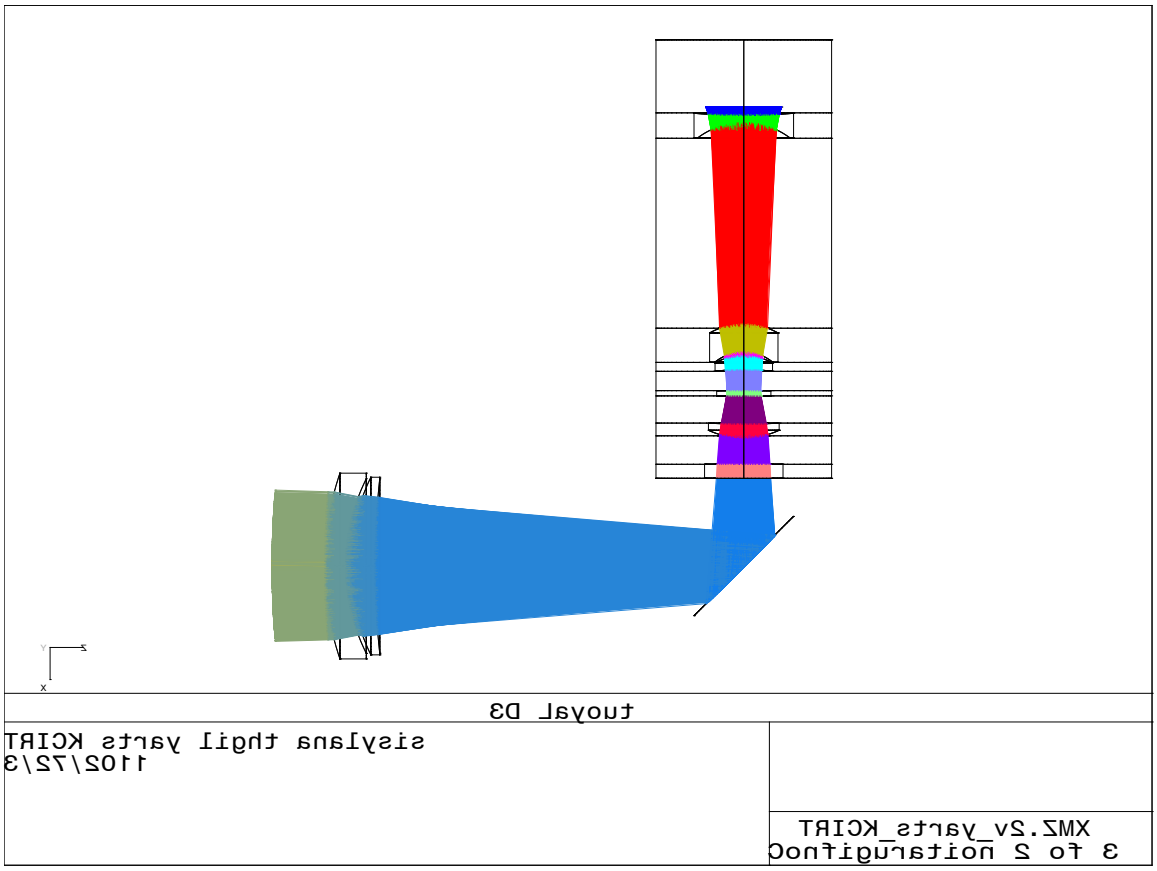

Figure 41: Stray light analysis. Cold stops are placed at each lens.

3.5 Optical Alignment

Access will be limited to the Keck I AO bench with OSIRIS in the beam. Much of the optical alignment will therefore be done prior to installation on the AO bench. Only alignment to the AO rotator axis should be required once the system is installed on the AO bench. The AO rotator axis can be defined by placing the pupil simulator on the rotator axis. The image position on the rotator axis can be defined with an input fiber through the pupil simulator of by placing the AO input fiber on the rotator axis.

For access reasons it will probably be necessary to install the NIR TTS assembly on the AO bench prior to installing the dichroic fold mechanism. Both should be initially aligned to the positions and orientations in the mechanical model.

3.5.1 Optical Pickoff Alignment

The vertical translation stage is aligned off the telescope to insure that the stage moves vertically, the reflective optical surfaces are perpendicular to vertical and each optic is centered at a height of 305 mm from the AO bench mounting surface when it is in its in-beam position.

The vertical translation stage will initially be populated with mirrors in each of the dichroic positions. A paper target should be able to be supported at the mirror face. The defining points for the reflective surface face toward the AO input so that once these are aligned the mirrors can be replaced with dichroic fold optics without affecting the alignment.

The fold optics should be centered on the optical axis of the AO rotator. A visual horizontal centering should be sufficient, preferably by moving the optic in the plane of its surface. A laser source can be input to a multimode fiber either at the AO input or in the pupil simulator. The laser source should provide

sufficient light even through the IR transmissive dichroic to center the dichroic fold optics. A mask can be put in front of the deformable mirror if necessary to stop down the beam.

After centering the beam the paper targets can be removed. The defining points for each mirror could be adjusted if necessary to insure that the reflected beam remains parallel to the AO bench (at a height of 305 mm). The entire assembly can be rotated about a vertical axis, and/or translated along the optical axis, until the reflected beam is centered on the NIR TTS field lens and dewar entrance window.

The mirrors can be replaced with the dichroics once the alignment is at a satisfactory point. It will be important that a re-acquisition will not be required when switching between dichroics. A small known offset may be acceptable but it must be repeatable.

3.5.2 NIR TTS Assembly Alignment

The NIR TTS assembly consists of the field lens, a fold mirror, and camera dewar mounted on a focus translation stage.

The optical system from the field lens to the detector will be pre-aligned off the telescope such that the optics and detector are centered on an optical axis parallel to the focus translation stages axis and at a height of 305 mm above the AO bench mounting surface.

The alignment procedure and how to test the image quality will be determined during the detailed design.

The field lens positioning is not critical. It should be sufficient to center the field lens at the required position mechanically. Its tilt could be checked by placing a laser beam at a height of 305 mm, aligning the focus translation stage to be parallel to this, and making sure that the field lens reflects the laser beam back on itself. This procedure could also be used to ensure that the dewar entrance window surface is centered and orthogonal to the focus direction (prior to installing the field lens).

After installation on the AO bench the remaining step is to align the NIR TTS assembly to the AO rotator axis. The field lens should be centered on the rotator axis and the fiber image should be in focus at the required position with respect to the field lens. Images of the fiber can then be taken with the camera. The backend of the assembly will be moved to center the image on the camera while maintaining the rotator axis centered on the field lens.

The pupil alignment can be checked during the day with the AO fiber source and a mask, with 4 symmetric off-axis holes near the edge of the pupil, placed in front of the deformable mirror. The fiber can be moved out of focus so that the 4 images are separated on the NIR TTS. The relative flux of the 4 images on the NIR TTS is a measure of the pupil alignment or misalignment. This approach is used to check and adjust the NIRSPEC pupil mask alignment when NIRSPEC is installed with the AO system.

3.6 Alignment Adjusters and Motion Control

3.6.1 Optical Pickoff Motion Control

The optical pickoff must move between 3 pickoff choices and an open position. Given the existing mechanical design with a center-to-center distance of 150 mm between optical pickoffs the full required range of motion control is 3 * 150 mm = 450 mm. A few extra mm of travel range are appropriate for initial alignment purposes.

The beam size at the pickoff for a single star is 300 / 13.66 = 22 mm. A 1 mm error in positioning is acceptable so the positioning requirement is quite loose.

The stage that we have selected for translation is a 402XR Parker linear stage. This stage has a positioning accuracy of 50 μm (standard grade) for travel ranges up to 600 mm and can accept an axial load of up to 38 kg. The 600 mm unit has a unit weight of 4.8 kg.

For initial alignment purposes the adjustment knobs should be able to co-align the images from the various pickoffs to within < 1 pixel (50 mas or 36 μm). The center of the three mounting pads lie on a 126 mm

diameter circle. Since the focal plane is 300 mm from the pickoffs, the required tilt precision is 63 mm * 0.036 / 300 = 8 μm.

3.6.2 Focus Motion Control

The nominal AO focal plane is located 300 mm from the front surface of the optical pickoff. When a 15 mm thick fused silica dichroic is inserted into the beam the focus will be shifted out by ~(n-1)/n*t = (1.5-1)/1.5 * 15 mm = 5 mm toward OSIRIS. The telescope focus will need to be pulled in by 5 mm to refocus on OSIRIS which will require that the NIR TTS camera move 5 mm closer to the dichroic. In addition, as discussed in section 2.1, a ±2 mm focus adjustment is required between the OSIRIS plate scales. We would also like some focus range for image sharpening (out of focus images) and initial installation offset. So, an overall range of 15 to 20 mm should be sufficient.

From the Zemax model a 50 μm focus error produces a noticeable but negligible change in the rms spot size radius, so the positioning tolerance is fairly loose.

The stage that we have selected for focus translation is an 800CTE06 series Parker Daedal stage (see Figure 42. These stages have a minimum travel range of 100 mm and a minimum load capacity of 90 kg. The repeatable positioning accuracy, depending on the precision grade, is between 1.3 and 12 μm.

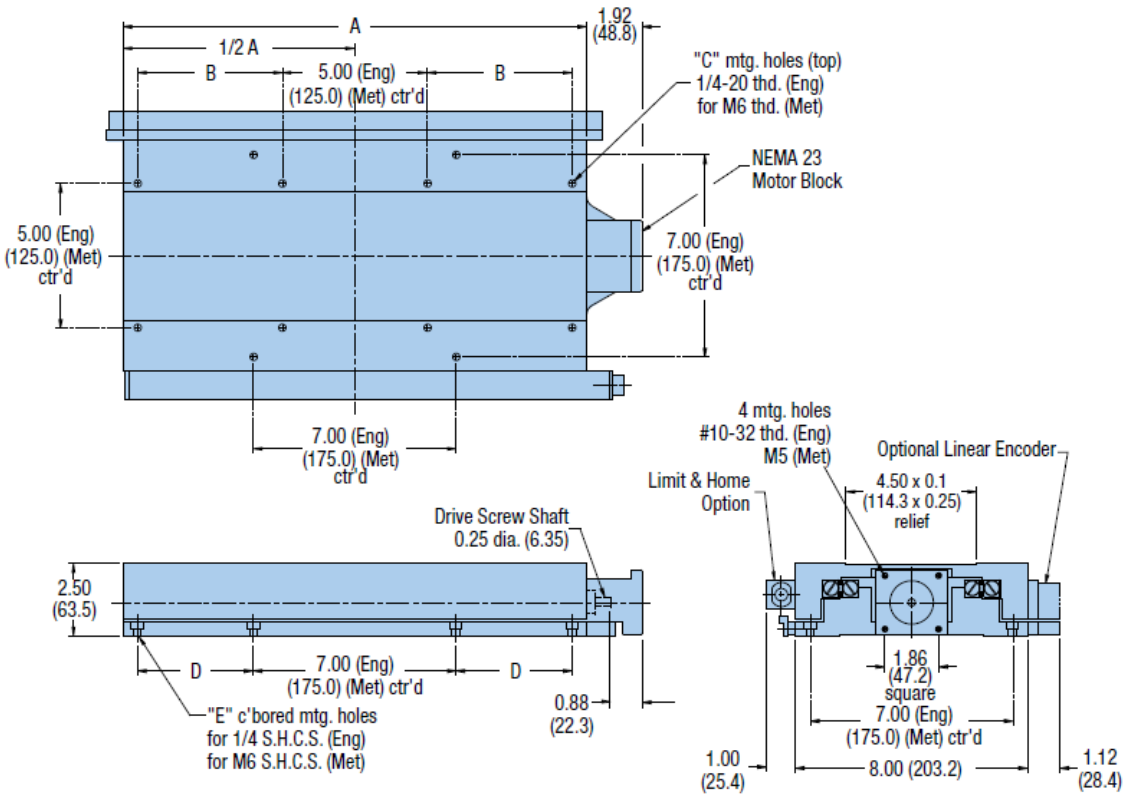

Figure 42: Parker Daeadal 808CT Stage Dimensions

3.6.3 Tip-Tilt Mirror Motion Control

The benefits of a TTM in the camera path were discussed in section 2.7. Only modest ≤ 25 mas on-the-sky motions in each axis of this TTM would be required to center a TT star at the intersection of 4 pixels and the required amount for DAR correcting (section 2.4) is also small (≤ 16 mas).

As shown in the mechanical design section the fold mirror just prior to the camera dewar could be replaced with a TTM. The fold mirror is located ~160 mm from the image plane and ~115 mm from the pupil plane.

In order to produce a 1" image motion the fold mirror would need to tilt by arctan(1" * 0.797 mm/" / 160 mm) / 2 = 0.143°. This same tilt would shift the pupil image by 1" * 0.797 mm *115/160 = 0.57 mm. The pupil mask diameter to pass the full 10.949 m pupil is 15 mm. If a 1% pupil motion is acceptable then the maximum image motion that could be accommodated is 1" * 0.15/0.57 = 0.26". Since we would want to control the image motion to < 5 mas then the positioning accuracy would need to be better than 0.005/1 * 0.143° = 2.6" on the mirror.

The mechanical model presented in section 3.1 includes the Optics in Motion OIM102.3 elliptical fast steering mirror shown in Figure 43. The standard gold coated 2.1x3 inch fused silica elliptical mirror has a rms wavefront quality of 158 nm. The angular range of the mirror, ±1.5°, far exceeds our requirements. The angular resolution of < 2 μrads on the mirror corresponds to 2E-6 rad * 2 * 160 mm / 0.727 mm/arcsec = 0.9 mas at the focal plane, which meets our 5 mas requirement assuming the angular resolution is closely related to the positioning accuracy for small angular moves. A built-in high precision optical sensor monitors the angle.

Prior to implementing motorized motion control we intend to use a 3 inch diameter mirror mount with Newport AJS100-02H manual adjustment screws. These screws have a 6 mm range with 0.7 μm sensitivity. If mounted on a 3 inch radius a 0.7 μm sensitivity corresponds to 0.0007/75 * 2 * 160 mm / 0.727 mm/arcsec = 4 mas and the 6 mm range corresponds to 34 arcsec on the sky.

Figure 43: OIM102.3 elliptical fast steering mirror

4. NIR TTS Camera

We will use the already procured Teledyne H2RG serial number GBA222 detector (18 μm/pixel). This detector uses the latest 2.5 μm cut-off HgCdTe recipe exhibiting low noise; 10.5 e- for correlated double sampling readout. Experiments with a very similar device (H2RG GBA220) indicate that multiple sampling will deliver substantial noise reduction. TT stars can be used anywhere on the detector with object selection performed by identifying one or more simultaneous regions of interest (ROI). Sequential windowed non-destructive readout will be employed with sample averaging to reduce readout noise with each ROI being sampled at the appropriate rate for the TT in that ROI, while also delivering the necessary frame rate.

4.1 Camera Mechanical Design

Elements of the camera dewar design are based on the TTS dewar design developed for the NGAO preliminary design (KAON 730). During the preliminary design the dewar design was changed to incorporate most of the reimaging optics (except for the field lens and fold mirror) and a filter change

mechanism. This project will still provide an opportunity to prototype some of the elements of the future NGAO TTS system.

The Polycold Compact Cryocooler (PCC) has been selected to cool the cryostat but the operating temperature, and hence the gas, is still to be determined based on the dark current characteristics of the HW2RG detector that we have procured (see section 4.4). The cryostat design, as discussed below, has been developed assuming a cold enough temperature to make the dark current negligible, which will allow it to support a range of temperatures down to this minimum.

The TRICK cryostat provides a vacuum insulated environment to maintain the HW2RG detector at a stable temperature below 90 K. The cryostat will also maintain the temperature of all optical elements from the filter and pupil mask to the detector surface at a temperature below 150 K while shielding the optical path from stray light.

The cryostat insulates the cold detector and optical and detector components from conduction, convection, and radiation heat transfer. The high vacuum environment prevents heat transfer from the environment to the cold sections of the dewar by means of gas molecules. The vacuum environment after pumping and cool down is expected to be less than 10^{-6} torr and the heat transfer due to residual gas molecules colliding with the internal cryostat surfaces is assumed to be negligible. The quality of the vacuum environment will decrease due to out gassing of surface contaminants inside the cryostat and permeation of gas molecules through the cryostat seals after initial vacuum pumping. An ion pump will be connected to the cryostat vacuum housing to continually remove gas molecules that enter the evacuated area in order to maintain the vacuum insulation quality over time. Shields are included in the cryostat to reduce the rate of radiation. The cold surfaces, shields, and internal cryostat walls will be polished, electroless nickel coated, post polished, and gold coated in order to lower the emissivity below 0.05. Maintaining the emissivity of internal surfaces will significantly reduce the radiation heat transfer to the cold surfaces. The heat transfer to the cold components by means of thermal conduction will be reduced by supporting the structures using a low thermal conductivity material with a small cross sectional area and a long conduction path. The low thermal conductivity material used to support both the radiation shield and the cold plate will be cryogenic G10 fiberglass that has a thermal conductivity less than 0.6 watts/m-K. The heat transfer from thermal conductivity will also be reduced by mounting the 90 K detector on top of the 150 K cold plate with insulating mounts. The 150 K cold plate will be mounted to the radiation shield with insulating mounts. Finally the radiation shield will be mounted to the cryostat wall using insulating mounts. The wires from the detector and thermal control elements provide an additional thermal conduction path to the detector and cold plate. The heat conduction through the wires will be minimized by using a long section of printed copper traces on a Kapton substrate to connect the detector to the cryostat electrical feed through.

The Teledyne detector package is mounted to a Molybdenum 364 substrate. The detector will be mounted inside the cryostat to a base made of the same to Molybdenum 364 alloy in order to match the thermal expansion/contraction properties. As seen in Figure 44 the mounting base will have some stress relieving flexures machined at the interface to the three detector mounting points in order to further minimize the possibility of damage to the detector from thermal deformations.

The temperature stability of the detector will be controlled using a Lakeshore model 340 temperature controller. This controller is capable of providing temperature stability better than the required ±0.1 K (TBC). The Lakeshore model 340 is already widely used at WMKO. The detector temperature will be measured using a Lakeshore PT-103-AM platinum RTD sensor. The controller will maintain the set temperature by supplying current to two 50 ohm cartridge heaters connected in parallel (see Figure 45). A NTE 8065 or a Microtemp G4A01072C thermal cutoff switch will be wired in series with the cartridge heaters to provide an additional level of over temperature protection for the detector. The NTE8065 will shut of the heater at 66 °C, 72 °C for the G4A01072C, if the LAKESHORE 340 failsafe features fail to operate. The Lakeshore 340 will be outfitted with an 8-channel scanner card for RTD sensors so that additional 103-AM platinum RTD sensors can be monitored. The additional sensors will be placed at the cold tip of the PCC cold head, the cryostat cold plate, and the radiation shield. All of the thermal management components will get wired to a separate connector mounted to a single thermal control block so that the wiring can be done easily external to the cryostat. Subsequently a cable from the vacuum feed through will be connected to the connector. A 25 conductor micro D connector has been selected for this

connector to minimize space taken up inside the dewar. This connector is available with solder cups, prewired pigtails, and right angle PC board mounts. The connections to the sensors, and heaters could be done with a prewired pigtail connector or solder cup connector. The connection to the vacuum feed through can be done using a flexible printed circuit on a Kapton substrate with a right angle PC board connector on each end.

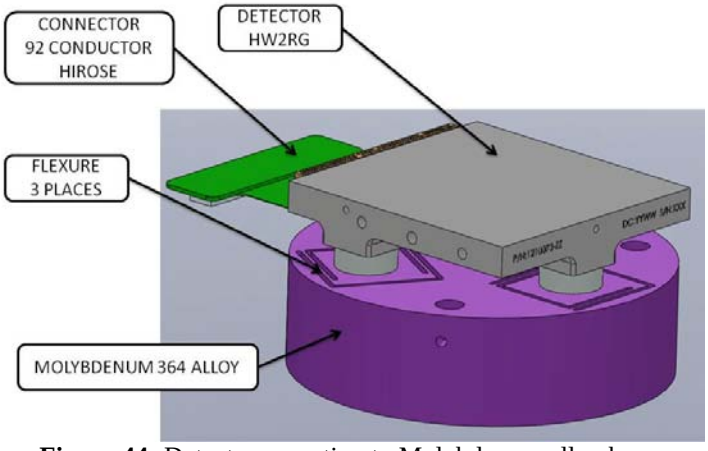

Figure 44: Detector mounting to Molybdenum alloy base

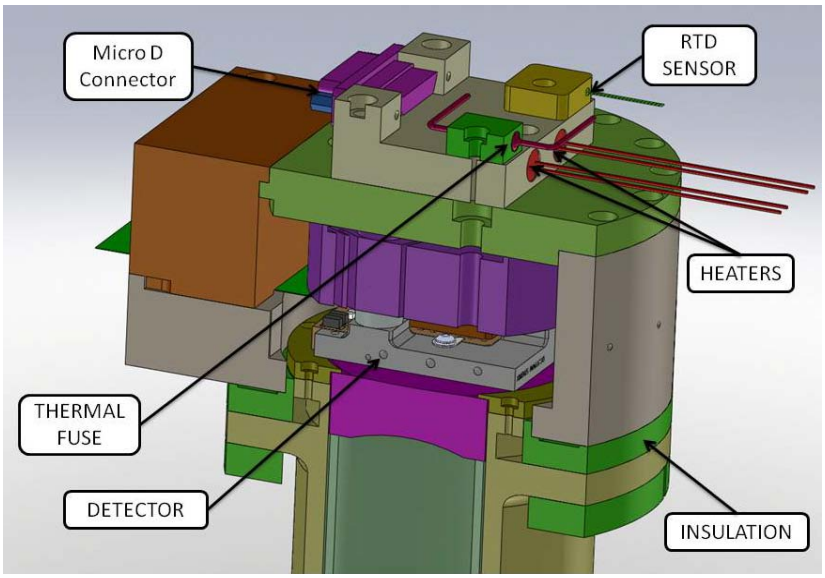

Figure 45: Detector temperature control mechanics

The optical elements in front of the detector will be mounted inside a lens tube as shown in Figure 46. Sufficient radial clearance will be supplied so that the optics will not be compressed in the radial direction when the lens tube cools. The optics will be spring preloaded in the axial direction so that the optic positions are metered to the ends of the lens tube while permitting the tube and optical elements to expand and contract in the axial direction without significant changes in axial clamping loads.

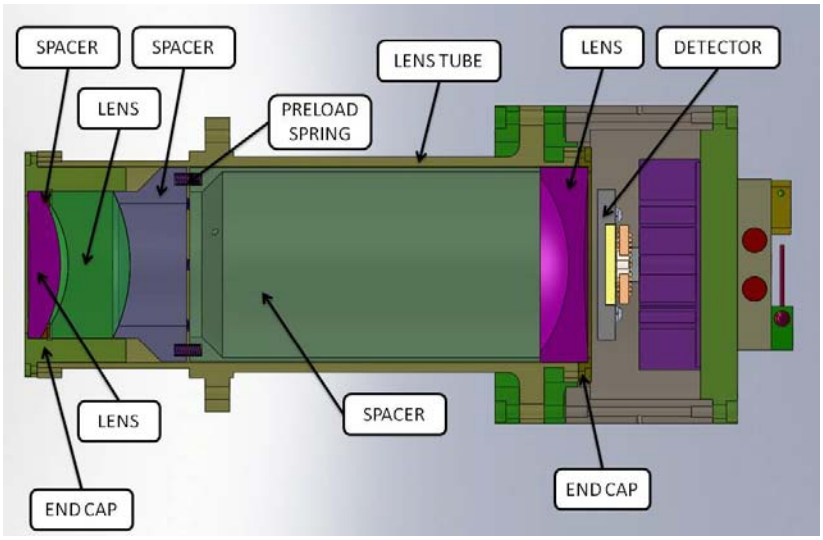

Figure 46: Lens tube in front of the detector

The filters, with pupil mask, are placed within the cells of the filter wheel as shown in Figure 47. Sufficient radial clearance will be provided so that the filter wheel cells will maintain clearance during temperature cycling. The filter/pupil mask will be retained with a compliant sheet metal retainer. The lens after the filter wheel is mounted to the filter wheel cover. Radial clearance will be provided around the lens cell to maintain clearance during temperature cycling. The lens will be kept in place with a spring load retainer to permit axial expansion and contraction of the lens without large changes in clamping force. The vacuum chamber window will be mounted in a counter bored hole at the input to the cryostat. The window will seal against an o-ring in an o-ring grove. The window is retained with a wave spring and retainer clamp. The clamping force to seal the o-ring will mainly be provided by the atmospheric pressure after vacuum is applied to the cryostat.

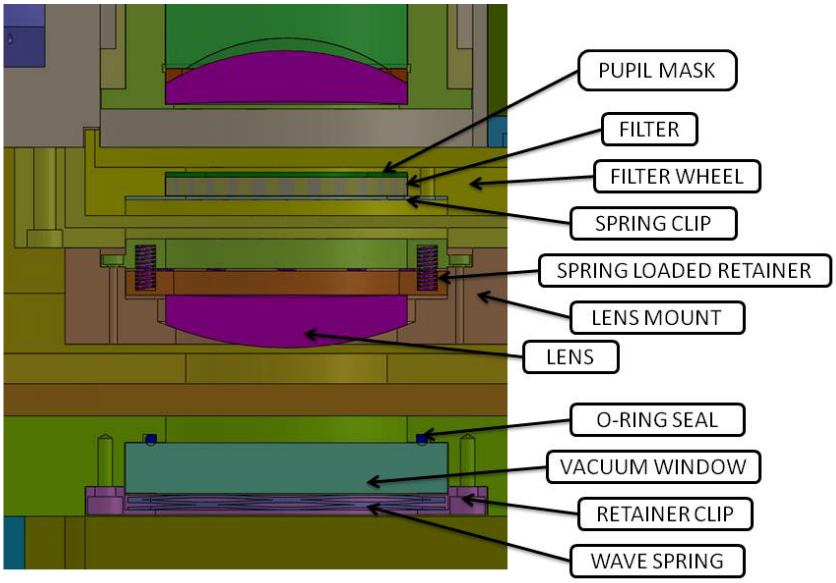

Figure 47: Filter wheel and cryostat optics before the filter wheel

There will be two selectable band pass filters with their associated pupil masks located in the filter wheel (see section 4.2). A third filter wheel positions will have an opaque blank that will permit the calibration of the detector dark current. The filter wheel will also have three additional cells for future expansion. Initially these cells will have blanks installed.

The filter, or rather pupil, positioning tolerance is discussed in section 4.3.3. The radial position accuracy and repeatability of the pupil mask will be maintained within the required tolerance by the filter wheel bearing as shown in Figure 48. The bearing will be a preloaded duplex pair of angular contact bearings with ABEC 7 tolerance configured back to back. The bearing will have 440C races with a physical vapor deposited molybdenum disulfide (MoS2) coating to serve as a solid lubricant. The bearing will have ceramic Si_3N_4 balls and molybdenum disulfide impregnated Teflon retainers. The solid lubricant and ceramic balls are required for reliable operation because bearing temperature will be between 80 and 150 K. The low temperature operation of this bearing requires that the bearing shaft and housing be made of 440C stainless steel so that the shaft and housing expand and contract at the same rate as the bearing as the temperature changes. The duplex pair preload will be applied with a compliant spring elements so that the preload force remains approximately constant over the temperature range that the bearing will experience. The bearing resistance torque is expected to be less than 1 inch-pound.

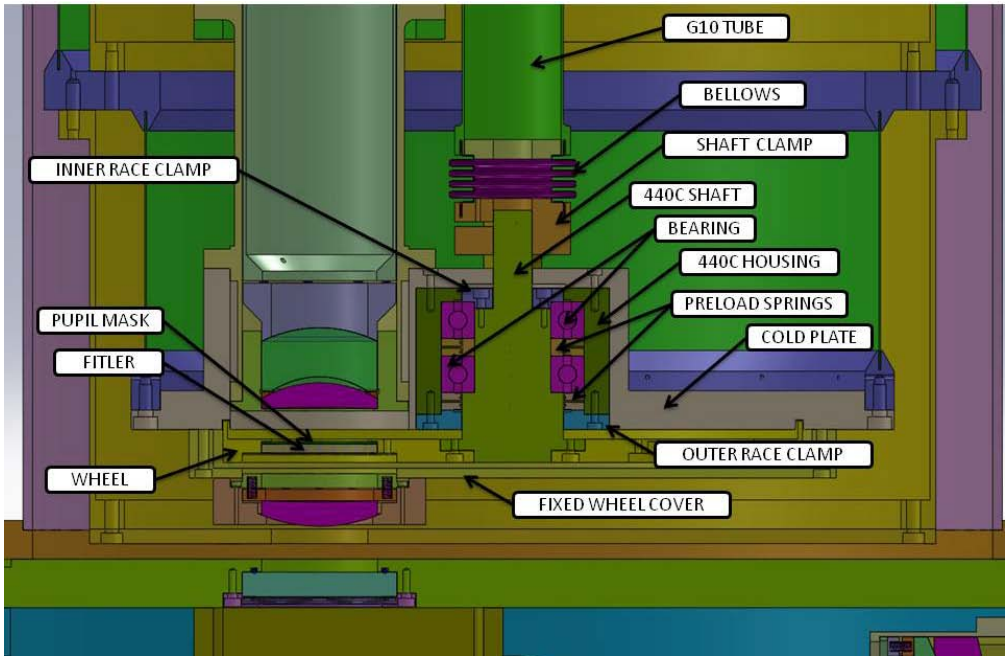

Figure 48: Filter wheel details

The tangential positioning accuracy / and repeatability of the pupil mask will be achieved using a geared servo-motor and encoders as shown in Figure 49. The servo motor and gearbox will be located external to the cryostat to provide easy access for maintenance and to avoid the complexities associated with cryogenic and vacuum rated motors, gearboxes, and sensors. The rotary position of the wheel will be transferred through the vacuum chamber wall using a Rigaku ferrofluidic rotary motion feed through. The vacuum side of the ferrofluidic rotary feed through will be coupled to the filter wheel with a custom shaft coupling that consists of shaft clamps and stainless steel bellows at each end and a section of cryogenic G10 tubing between the bellows. The G10 tube will thermally isolate the filter wheel from the rotary feed through while providing high torsion stiffness. The air side of the rotary feed through will be attached to 160:1 harmonic drive gearbox. The input of the harmonic drive gearbox is coupled to a Quicksilver Controls Inc. QCI-A17H-3-6T smart motor. This motor is a stepper motor that has an 8000 count per revolution incremental encoder. The stepper motor is connected to QCI's D2-IGB motor controller. The D2-IGB controller operates the stepper motor in closed loop control as a brushless DC motor. There are 1280000 (160 X 8000) motor encoder counts per filter wheel revolution. One motor encoder count corresponds to 0.3 μm of tangential pupil mask motion since the filters cells are located at a radius of 63.5 mm from the bearing. The use of an incremental encoder with the controller requires a home position signal to establish the absolute position for the encoder. A MicroE Systems Mercury II 6000 sensor and 63.5 mm OD / 8192 line glass scale will be attached to the output of the harmonic gearbox. The glass scale has a

home position line that activates once per revolution of the filter wheel. The Quicksilver Controls Inc. D2-IGB controller is capable of being configured to use this encoder to close the position loop and the motor encoder to close the velocity and acceleration loops. If the Mercury II 6000 sensor is configured for 400X interpolation of the glass scale lines the tangential resolution of the pupil mask will be 0.122 μm. The rotational velocity of the filter will need to be limited to less than 3.5 RPM so that the maximum encoder input speed of the QCI controller is not exceeded.

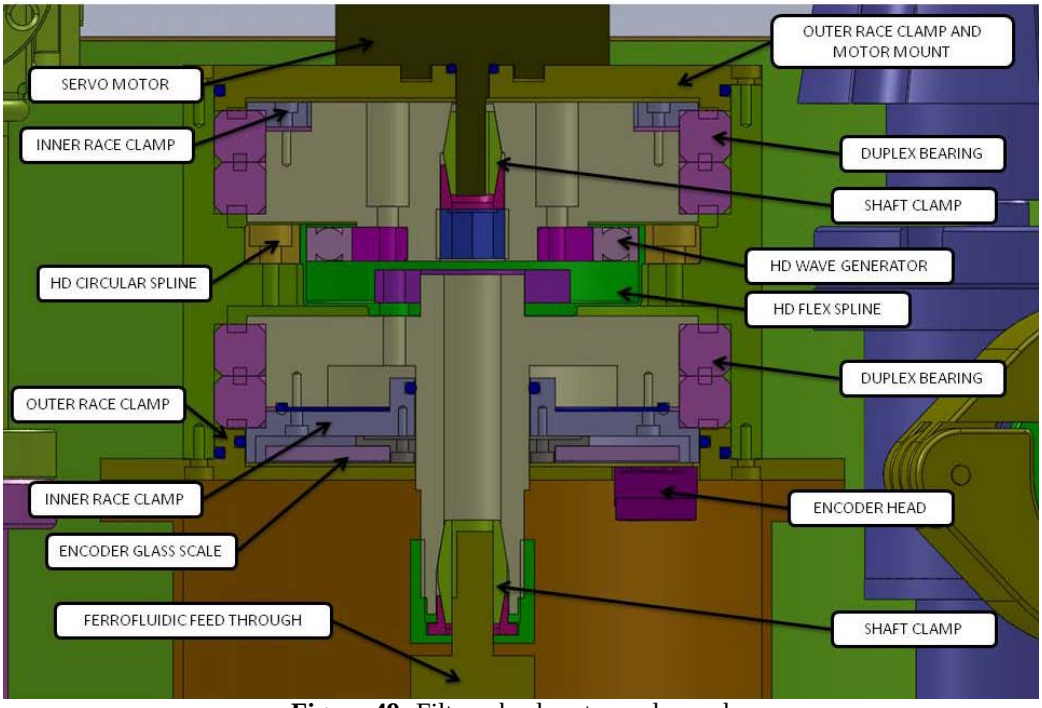

Figure 49: Filter wheel motor and encoder

The use of the MicroE encoder home position sensor external to the cryostat avoids the difficulties of implementing an internal cryogenic home position sensor. Cryogenic sensors are more expensive, frequently have reliability issues due to thermal cycling, require signal conditioning, and require an electrical feed through out of the vacuum environment. The use of an external home position sensor does create a problem in establishing a link between the physical position of the filter wheel cells and the home position line. This problem is solved by placing a retractable alignment pin inside the cryostat that is bolted to the cold plate. The pin slides in a close tolerance slip fit bore. A radial slot that has a close tolerance fit with the pin is placed in the filter wheel. The filter wheel is rotated and alignment pin inserted in the radial slot prior to the final drive train clamping of the filter wheel to the motor / gearbox / encoder assembly. The motor is subsequently commanded to the home position of the encoder and the final drive train clamping connections made. The home position is now physically referenced to a filter wheel cell position without using a cryogenic sensor. The alignment pin is retracted following the final clamping of the drive train. Access ports are included in the cryostat design to permit insertion and retraction of the alignment pin and to clamp the shaft coupling to the vacuum side of the ferrofluidic feed through.

The motor has a rated stall torque of 43 oz –inch. The motor's optimal speed is 2700 RPM. At this speed the available motor torque is 30 oz-in. With the 160:1 gear ratio the output speed would be 16.875 RPM. This is faster than what is permitted by using the Mercury II encoder in combination with the D2-IGB controller. Hence the available output motor torque will be between 30 oz-in and 43 oz-in or a gearbox output torque between 300 in-lbf and 430 in-lbf. The gearbox has a rated torque of 248 in-lbf, and a limited peak torque of 566 in-lbf. The expected torque required to turn the filter wheel is less than 1 inch-lbf so there is plenty of torque margin. This gearbox is being used for its high stiffness, high gear ratio for precision, zero backlash, and large back drive torque properties. The back driving torque is between 17.7in-

lbf to 58.4 in-lbf. The gear box stiffness at low load is 97358 in-lbf/rad. A 1 in-lbf load corresponds to 1E-5 rad of windup or 0.7 microns of pupil mask motion.

The electrical cables from both the detector and the thermal control assembly need to pass through the vacuum chamber wall. A flexible printed circuit board will be fabricated for each cable on a thin kapton substrate. A 92 conductor surface mount connector will be placed on the ends of each side of the flexible circuit for the detector cable and a 25 pin microD connector PC board connector will be placed on each of the thermal management cable. The cables will be potted into a slotted vacuum flange using low permeability epoxy to form the cable feed through. The use of potted flexible circuits will minimize the labor required to produce feed through wiring, minimize the wire mess inside the cryostat, and minimize the likelihood of wiring errors from had wiring.

The cables outside the cryostat have to be routed to their interface electronics. The cable from the detector will be connected directly to the ARC control box located on the AO bench cover near the cryostat. The cables from the thermal control assembly will connect to an extension cable that will be routed 12 m to a rack in the AO electronics room where the cable will interface with the Lakeshore 340 temperature controller. The cables from the QCI servo motor and Micro-E encoder head cable will be routed 12 m to a rack in the AO electronics room where the cables will interface with the Quicksilver Controls D2-IGB motor controller. The cable from the Gamma Vacuum 3S ion pump will be routed 12 m to a rack in the electronics room where the cable will interface with the small ion pump controller. The pair of cooling gas hoses to and from the cryo-cooler will also be routed to the AO electronics control room.

The PCC cold head is mounted to the end flange of the cryostat. The tip of the cold head is cantilevered from the interface flange on the end of the coiled thin walled gas tubes. The tip of the cold tip needs to be restrained laterally from vibrating during transport so that the thin walled gas tubes do not fail due to fatigue. The lateral restraint needs to permit the expansion and contraction of the cold head along the axial direction during cool down and warm up. A pin will be placed at the end of the cold tip. This pin will fit concentrically inside a hole in a post mounted to the cold plate. This arrangement will restrain the lateral motion of the cold tip to the radial clearance between the hole and pin (~80 μm). Flexible sheet metal strips will also be attached to the tip of the cold head to conduct heat from the detector and the cold plate. The design of the flexible sheets is such that screws can be tightened through and access port on the cryostat end plate. The access port is also used as the vacuum feed through for the electronic cables. The conduction paths between the detector and cold head is designed to have a temperature difference of a few degrees K while the conduction path between the cold tip and the cold plate is designed to have a temperature drop of approximately 75 K. The thermal resistance of the conduction paths will be adjusted as required during testing to achieve the nominal target temperatures.

The light enters the camera through a field lens pair located outside the vacuum environment. The light is subsequently folded 90° through the cryostat window by means of a flat mirror oriented 45° to the incident beam. The mirror is located in the converging beam after the field lens pair. The field lens pair is mounted in a 102 mm diameter lens tube that is supported by a large tube concentric to the cryostat chamber. The field lens pair is separated from each other with a spacer. The lenses are held in the lens tube with a spring loaded retainer to permit the axial expansion and contraction of the lenses within the lens tube. The fold mirror will be mounted in the same concentric ring as the field lens. This ring will be indexed to the bottom of the cryostat and to the tip-tilt stage with dowel pins so that the ring position can be removed and installed to a repeatable position that preserves the alignment. Eventually the fold mirror will be an actively controlled mirror. The base line mirror tip-tilt mechanism is Optics in Motion OIM102.3 elliptical fast steering mirror. Due to project cost constraints the mirror provided with the cryostat will be mounted to a kinematic mirror mount with manual adjusters that permits an upgrade to an actively controlled tip/tilt mechanism in the future.

The entire cryostat can be aligned in tip/tilt about a kinematic point located on the optic axis just behind the field lens. Tip-tilt about this point is guaranteed by using a spherical bearing surface that has its center at this point. The tip tilt adjustments are made using manual adjustment screws. Locking bolts are provided to lock the cryostat in place following the alignment.

Figure 50 and Figure 51 provide a cross-sectional and top view of the camera, respectively.

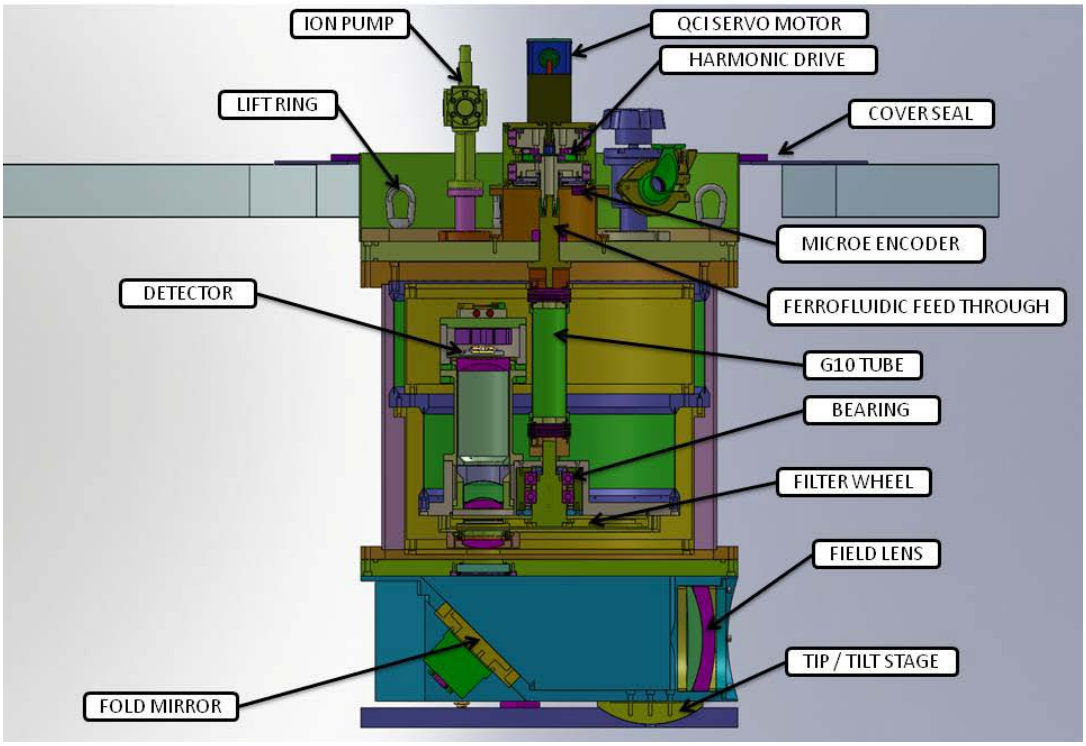

Figure 50: Cross-sectional view of the NIR TTS camera

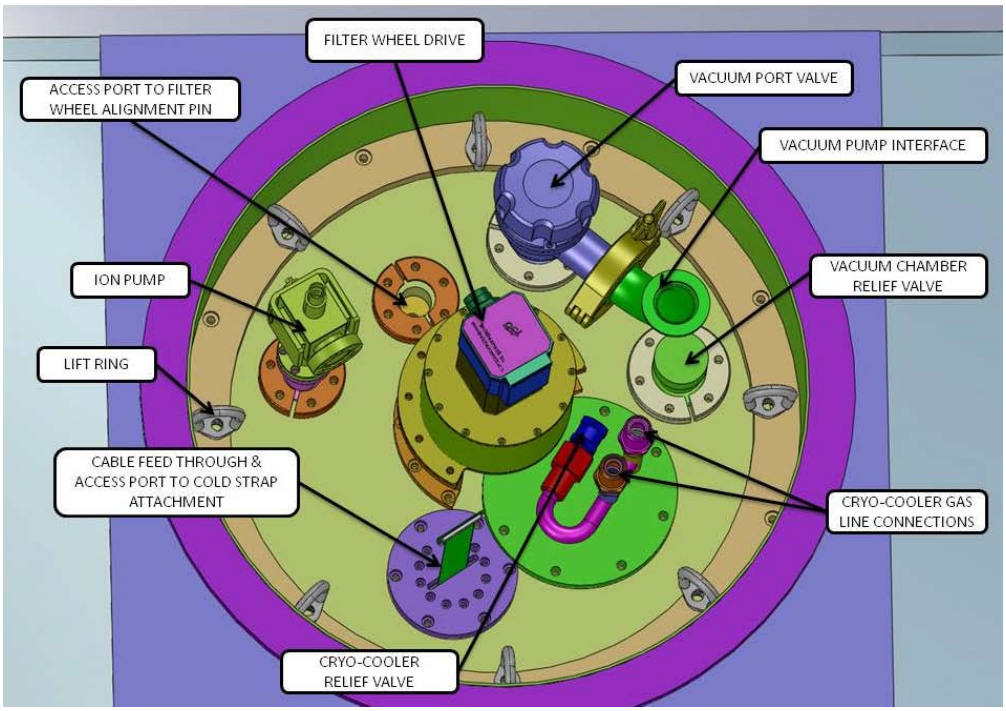

Figure 51: Top view of camera dewar

Consideration was given to operational safety of the cryostat. A relief valve was installed on the end plate of the cryostat to prevent the vacuum chamber from being pressurized from cryo-cooler gas leaking into the vacuum chamber due to structural failure of the cooler internal gas tubing. A relief valve comes on the

back side of the cryocooler cold head that will vent the working fluid gas if the gas from the compressor exceeds the allowable pressure inside the cooling lines or cold head. A 368 mm diameter tube is bolted to the endplate of the cryostat to make sure that any and all gas that may be released from the cryo-cooler system is vented to the room and not into the AO bench enclosure.

The cryostat that needs to be installed onto the AO bench could weigh on the order of 45 kg. Lifting attachment points will be provided on the top plate of the cryostat ensure that the cryostat can be lifted into place safely with the aid of lifting hardware (see KAON 855).

4.2 Cryocooler Heat Load Estimate

The radiation heat transfer and conduction heat transfer equations are solved in an excel spreadsheet. The total heat load on the cryocooler for an emissivity of 0.05 was computed to be 3.3 W assuming the detector and cold plate are at 85 K to be conservative. In order to maintain some margin we will assume a 5 W heat load.

The following mechanisms contribute to the heat load:

- Radiation from the cold to the shield and then from the shield to the vacuum chamber (2.3 W).
- Radiation from the detector to the room through the entrance window (0.40 W).
- G10 cold plate conduction to the shield and hence to the chamber (0.15 W).
- Wire conduction to the shield and hence to the chamber (0.33 W).
- Kapton substrate conduction to the shield and hence to the chamber (0.002 W).
- G10 shaft coupling conduction (0.11 W).

The assumptions that go into this calculation include:

- Cold plate and camera surface area = 0.32 m^2, at 85 K (to be conservative).
- Heat shield surface area = 0.45 m^2, at 249.5 K.
- Vacuum chamber wall surface area = 0.52 m^2, at 293 K (for lab operation; colder at telescope).
- Emissivity = 0.05 for cold plate, camera, heat shield and vacuum chamber wall.
- G10 cold plate cross-sectional area to shield = 0.0004 m^2 with length = 0.072 m. Cross-sectional area and length to chamber = 0.0005 m^2 and 0.083 m, respectively. Conductivity = 0.6 W/m K.
- Electrical traces area = 9.7E-7 m^2 with 0.15 m to shield and 0.05 m to chamber wall, and a conductivity of 401 W/m K.
- Kapton substrate area = 1.45E-5 m^2 with 0.15 m to shield and 0.05 m to chamber wall, and a conductivity of 0.2 W/m K.
- G10 shaft coupling area = 7.8E-5 m^2 with a 0.093 m length.

The big effect and also source of uncertainty is what emissivity can be obtained on a weighted average basis. The plan is to polish and gold coat surfaces as much as possible. With a reasonable polish and gold coat a 0.02 emissivity is possible. However, this will not be obtainable when a weighted average is done on all surfaces since there will be gaps in the shields where cables, the rotational shaft and cryocooler go through. These gap areas will have an emissivity of 1 (i.e., 0.031 m^2 of polished gold with an emissivity of 0.02 is equivalent to 0.00063 m^2 of gap). There will also be areas that will not be gold coated with varying emissivity. For this reason the assumed 0.05 emissivity is based on polishing the majority of areas to try and obtain 0.02. During detailed design we will want to seal or baffle the feed through areas on the heat shield to help minimize the risk of not obtaining the 0.05 weighted average emissivity goal.

4.3 Filters and Pupil Stops

4.3.1 Filter Options

Two filters, H and Ks, will be housed near or at a pupil within the camera dewar. We have reviewed the filter choices with reference to the NIRC2 filters (http://www.keck.hawaii.edu/realpublic/inst/nirc2/filters.html). Ks or Kp would be preferred for the K-

band filter due to their shorter cutoff and hence lower background contribution. We have opted to go with the 2MASS H and Ks filters (http://www.ipac.caltech.edu/2mass/releases/allsky/doc/sec3_1b1.html#s6) since this will enable a good match with the 2MASS catalog which we will be using to identify TT stars.

A third position of the filter mechanism is required to block the beam so that dark current can be measured, as well as for diagnostic purposes such as verifying read noise performance. Additional positions could prove useful for example to test focus sensing by introducing some astigmatism.

Note that filters are required in addition to the pickoff dichroics since cold filters are needed to reject the thermal background; the dichroics are also unlikely to be able to be built to match the filter profiles.

4.3.2 Pupil Stop

A circumscribed pupil (for maximum resolution and throughput), with an equivalent outer radius of 11.0 m, will be combined with the H-band filter. An inscribed pupil for better thermal background rejection, with an outer radius of 10 m, will be used with the Ks-band filter. In both cases a central obscuration of 2.65 m will be used. These diameters are shown versus the Keck telescope pupil in Figure 52.

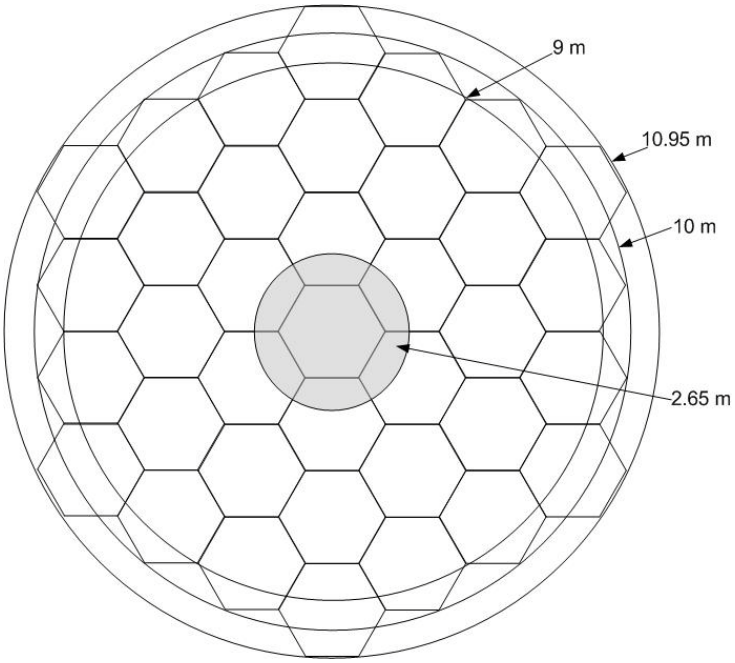

Figure 52: Keck telescope overlaid with different size pupil masks

4.3.3 Filter Exchange Mechanism Positioning Tolerance

The filter positioning accuracy, or more critically repeatability, is set by the pupil masks on the filters. In particular, the tightest constraint is on the Ks filter pupil mask since it is undersized to minimize thermal background. Our selected accuracy requirement is ±0.5% of the pupil mask diameter. For a 20 mm diameter pupil mask this corresponds to ±0.1 mm.

4.4 CryoCooler

The Brooks Polycold PCC compact cooler selected for the NGAO tip-tilt sensor requires a flammable gas mixture to reach the optimal operating temperature. For safety reasons we re-evaluated this choice for the NIR TTS during the preliminary design.

The detector temperature must be low enough for dark current to be less than the background flux. The cold head needs to be ~5K below the required detector temperature so that active temperature control can be provided. Also, it may be possible to get lower read noise by pushing the detector reverse bias to higher

than normal levels. However, this produces elevated dark current and particularly hot pixels. An additional 10K of margin would provide space for operation at high reverse bias.

From Table 15 the H and Ks backgrounds are 545 and 745 electrons/second/pixel, respectively (from the total background row when the integration time is changed to 1 second and the number of pixels is reduced to 1).

Teledyne's data for the H2RG-222 detector that we have procured indicates a median dark current of 0.003 electrons/sec/pixel at 77K with hot pixels extending to 0.03 electrons/sec/pixel. The detector acceptance report shows 68064 pixels high with respect to the in-range dark current or 1.6%. The probably of not having a hot pixel in an ROI is therefore $(1\text{-}0.016)^{16}$ = 77% for one 4x4 pixel ROI or 46% for three. It is therefore highly desirable to cool based on the hot pixel dark current.

Figure 53 is a plot of dark current versus temperature. Several different curves are shown. The median dark current from the Teledyne promotional materials for the 2.5 μm cutoff detector that we have is shown as the orange curve. The two black curves above this are the measured median dark current, multiplied by a factor of 10 for hot pixels, for the 4 detectors in ESO's HAWK-I instrument. The purple curve above this is the theoretical dark current scaled from the measured hot pixels for our detector. Assuming that we need to cool the detector so that the worst case measured hot pixels match the H-band background then we would need to cool to 130K; actually to 125K if we allow a 5° margin for active temperature control.

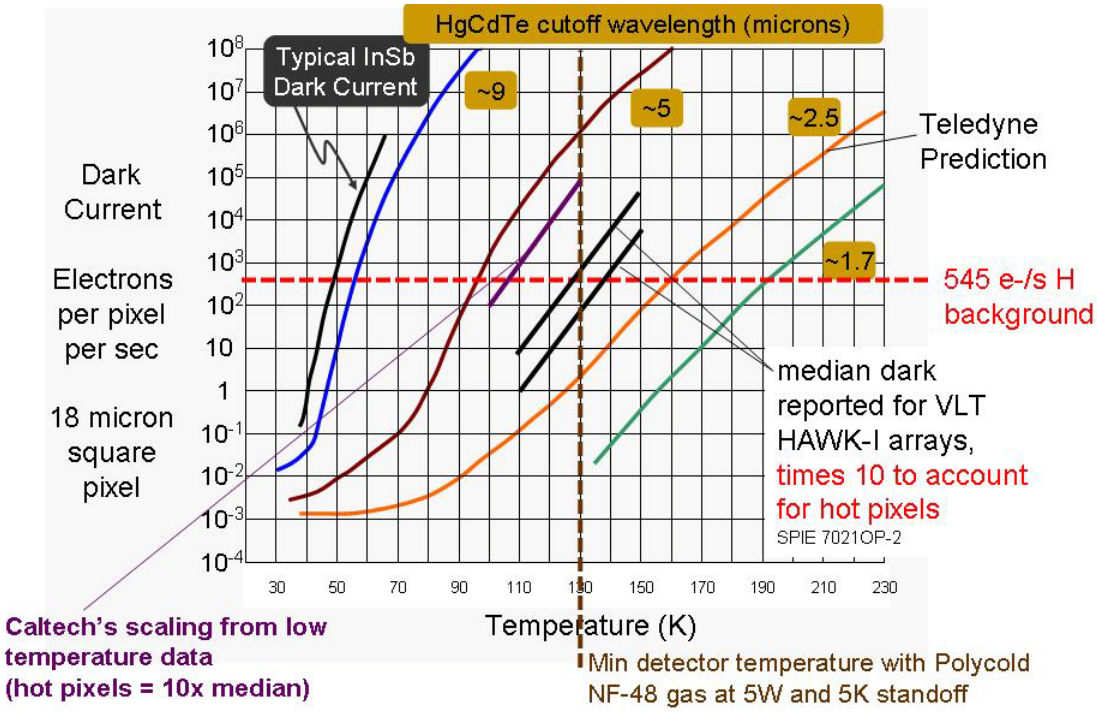

Figure 53: Dark current versus temperature

The refrigeration systems listed in Table 6 were evaluated for their suitability for the NIR TTS. The vibration requirement is < 5 mas, which is 1/10th of a pixel or 1.8 μm; the lowest vibration systems were therefore strongly favored. From these low vibration systems the liquid nitrogen system was excluded primarily for operational reasons and the ARS-ORCA size made it much less desirable (especially since NGAO will long term require 3 of these tip-tilt sensors). This returned us to the Polycold cryotiger and the choice of flammable or non-flammable gas. The Polycold force versus frequency plot versus other types of coolers is shown in Figure 54.

Table 6: Potential refrigeration systems

Model	Type	Gas	T(K)	Flammable?	Vibration	Length(mm)
Polycold	Joule-Thompson	PT13	<90	Moderate	Lowest	175
Polycold		NF48	125	No		175
ARS-ORCA		Mix	<90			325
Cryomech	Pulse Tube	Helium	<70		1lb at 2.4Hz	Several parts
Thales			<70		Medium	Integrated compressor
Thales	Stirling	No hoses	80		High	
Sunpower			70		High	250
Cryomech	Gifford-Mc	Helium	<70		Highest	250
Cryogen	Autofill	Nitrogen	77		Lowest	100

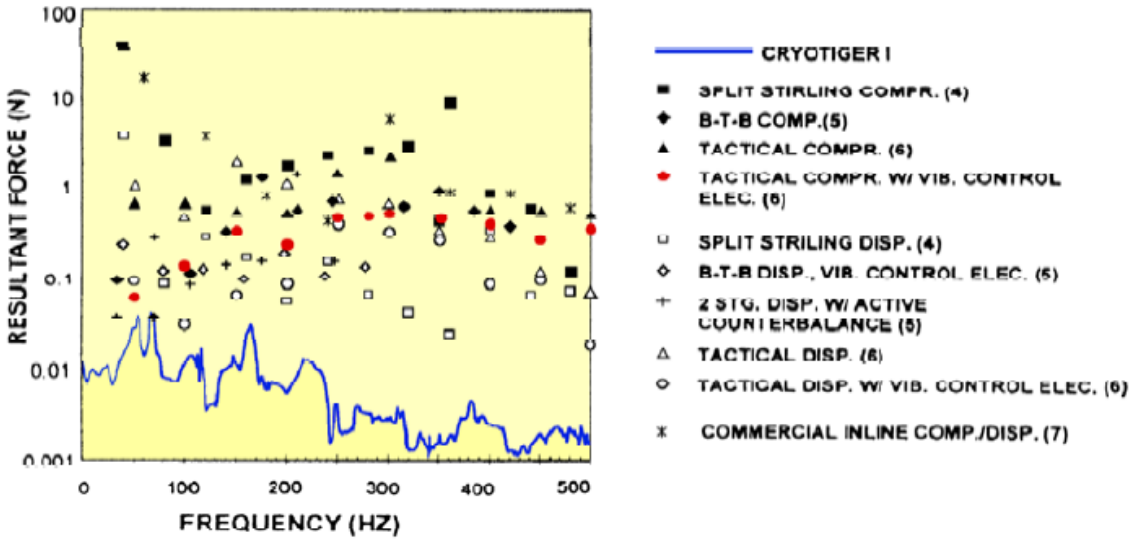

Figure 54: Cryotiger vibration performance versus other coolers (from Dennis Hill, Throttle Cycle Cooler Vibration Characterization, 1996)

The cooling curves for the Polycold gases are shown in Figure 55. The NF-48 just makes the 125k cooling requirement from Figure 53 including a 5K margin for active temperature control. We may have a better detector than the worst case in Figure 53 however there is no margin for errors in our thermal load or thermal background estimates, for growth in hot pixel intensity over time (currently a major worry for JWST) or for high reverse bias operation. Although we will endeavor to make use of the NF-48 gas mixture if practical we must also be prepared to use a PT gas if necessary.

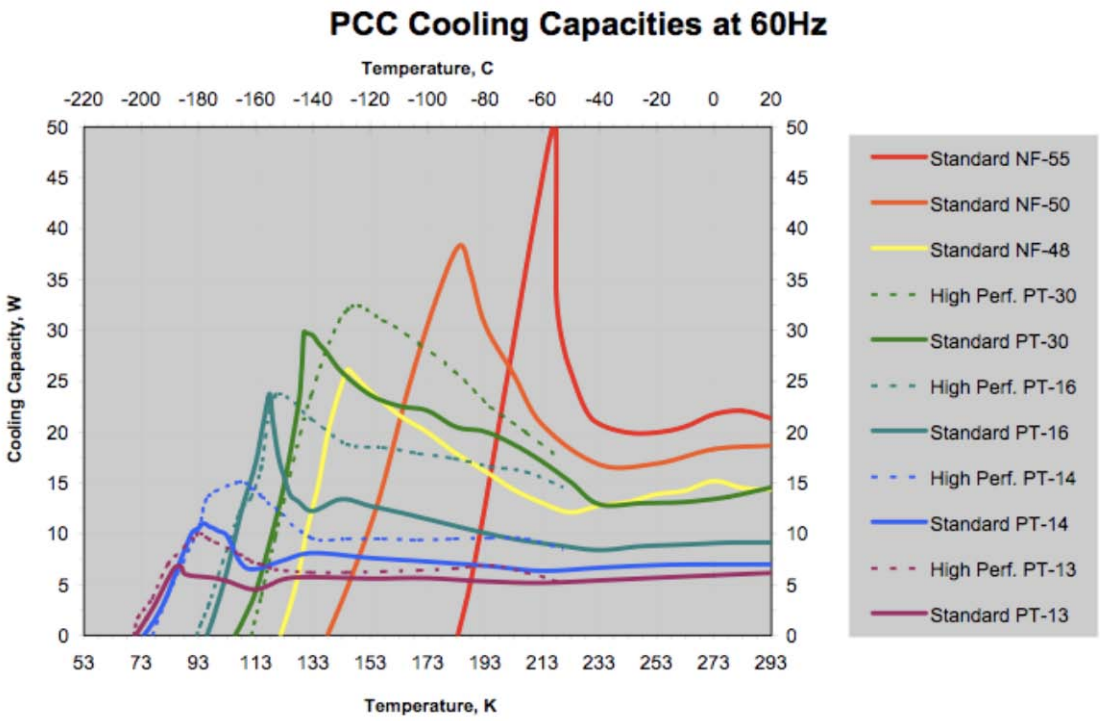

Figure 55: Polycold compact cooler cooling capacities versus gas type

The PT gas mix ratio is proprietary but consists of neon, nitrogen, argon, methane, ethane and propane. All of these gases have boiling points well below the dome ambient temperatures so none could condense on optics in the event of a leak. The NF gas is a combination of hydro fluorocarbons and inert gases, and condensation is also not an issue for this mixture.

The Brooks Polycold Compact Cooler operating manual provides a minimum room size requirement for the PT gases calculated according to ANSI/ASHRAE 15 standards. This minimum room size represents a gas concentration corresponding to 25% of the lower flammability limit (the minimum concentration capable of propagating a flame). For the PT13 gas with 50 feet of flexible line and an external absorber this minimum room size is 9.0 m^3. With the derating for altitude, 1/(1-7.94e-5*h) = 1.50 where h = 4200 m, the minimum room volume becomes 13.5 m^3.

We have chosen to locate the Polycold compressor in the AO electronics vault in order to minimize the gas volume. The lines to reach the NIR TTS camera could then be less than 50 feet in length. The electronics room volume is ~23 m^3 and the AO enclosure is 85 m^3. Both of these volumes exceed the 13.5 m^3 minimum volume calculated above. The electronics room also meets the compressor's operation temperature range of 50°F to 95°F. Figure 56 shows the compressor (top right) and its proposed location in the AO electronics room. The compressor will be suspended from the ceiling in a manner to minimize the transmission of vibrations.

If flammable gas is necessary then we will need to include a gas monitor in the AO electronics room. It may also be necessary to interlock any potential ignition sources (such as the white light source) in the event of a leak. This additional safety features would be reviewed as part of the engineering change and safety review.

Baffling will be provided between the back end of the camera dewar, where a pressure relief valve will be located, and the AO bench top cover, in order to ensure that any cryo-gas leak does not flow onto the AO bench.

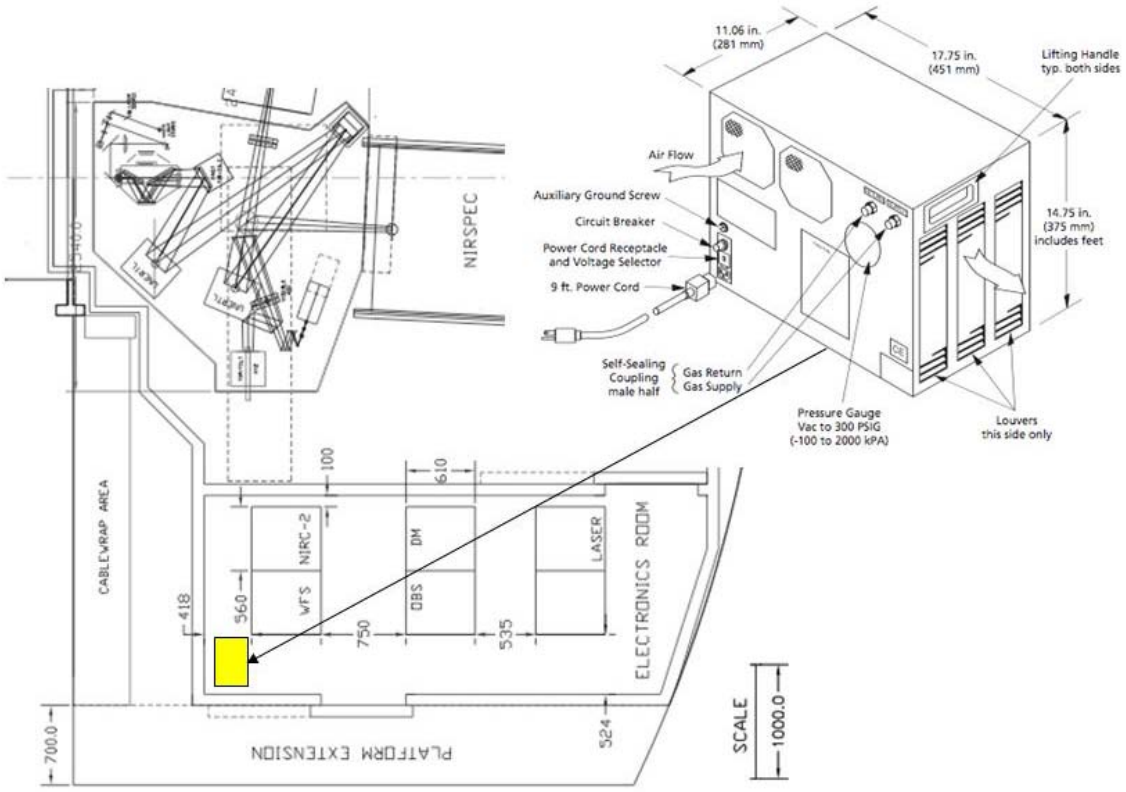

Figure 56: Polycold compressor (top right) and proposed location in the AO electronics room

4.5 Detector Readout Scheme

4.5.1 Overview

The purpose of this section is to describe the readout modes and timing for the Keck NIR Tip Tilt Sensor, the commands to set the readout parameters, and resulting data packet format on the video link to the RTC.

4.5.1.1 Detector Readout Modes and Noise Performance

The detector is read out non-destructively in window mode, through a single channel. The window coordinates are updated prior to each window scan by programming the four window corners into internal registers of the H2RG multiplexer over a high-speed serial line. The time required to update the window coordinates is approximately ~5 µs, allowing the readout of multiple windows at any location during any given exposure. This flexibility can be utilized to accommodate some combination of multiple guide stars (when available with sufficient brightness).

Conventional readout algorithms employing multiple sampling to beat down the read noise suffer a >50% duty cycle penalty at high frame rates. We overcome this limitation by using a readout mode already tested at the California Institute of Technology (CIT) in which the detector is only reset when the integrated signal level approaches saturation as shown in Figure 57, typically every 100 to 1000 exposures for guide stars faint enough to be impacted by read noise. The “exposures” are then synthesized by using the group of samples representing the end of one exposure as the “zero level” for the next exposure to obtain duty cycles of > 99%. When reset becomes necessary there will be a gap in the data stream that will be small compared to the update rate.

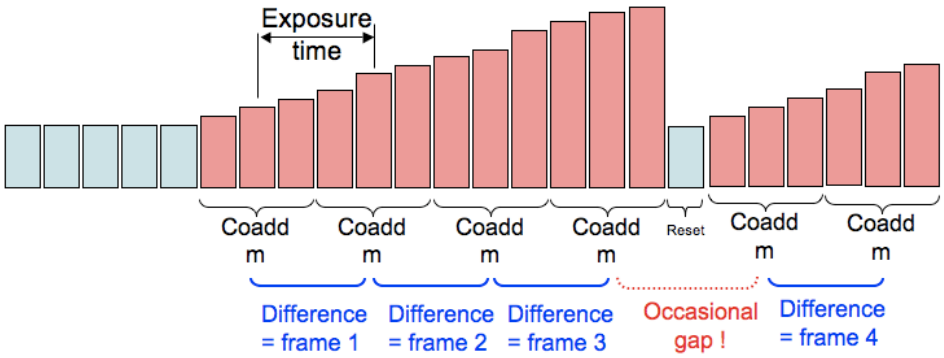

Figure 57: In "Differential Multi-Accumulate" readout mode the detector is reset only when necessary to avoid saturation to obtain ~100% duty cycle. Reset typically occurs every 100 to 1000 frame scans. Non destructive reads are averaged and exposures are synthesized by differencing averaged frames.

For an N pixel square window, the frame scan time, $t_s = 5.16N^2 + 10.32N + 5.28$ µs = 143 µs for a 4x4 pixel window, or 47 µs for a 2x2 window.

A representative low noise 2.5 µm cut-off H2RG tested at CIT, exhibited the following noise components added in quadrature: 11 e- of white noise, which scales as the inverse of the square root number of samples per exposure, 0.06 e- of dark noise which scales with the square root number of samples per exposure and a 2.4 e- floor due to 1/f noise. The total noise as a function of exposure rate and number of pixels per frame is shown in Figure 58.

Full field readout can be used for confirmation of guide star positions, reading out through 32 channels to keep read time down to ~1 second. With the speed improvements discussed above, a 14x14 pixel (0.7" square) region centered on the TT star can be read out at 1 kHz, but elevated read noise (12 e-), to provide initial guiding until the TT loop is closed. As the spot position is stabilized by the TT feedback, the window size will typically be reduced to 2x2 or 4x4 pixels, while in some cases it may be larger with commensurate frame rate penalty.

The pixel readout rate will always be fixed (nominally at 6 micro-seconds per pixel).

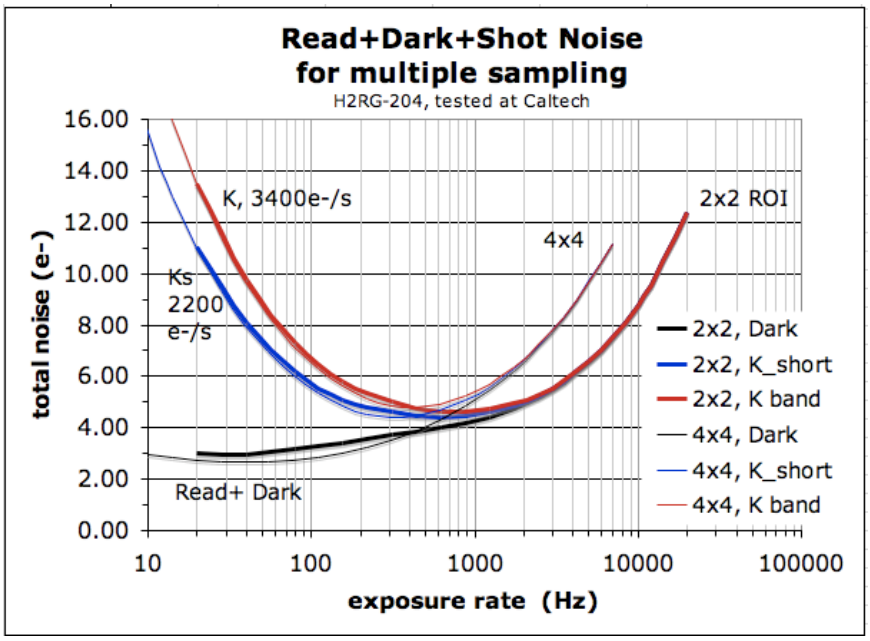

Figure 58: Laboratory noise measurements after coadding non-destructive reads for a low noise 2.5 µm cutoff H2RG in the dark and with projected background (sky, telescope and AO) noise added.

4.5.1.2 Pros and Cons of Multiple Regions of Interest

At this time, multiple ROIs are a goal and not a requirement. Nonetheless, we discuss here the plan to implement multiple ROIs, and present some of their advantages and disadvantages. Subsequent sections will assume that multiple ROIs will be used.

Benefits of multiple ROIs:

- Measurement of tilt anisoplanatism. The correct tip-tilt for the science object can be inferred by interpolating between several off axis guide stars.
- Signal-to-noise. Combining the signals from several guide stars when there is no dominant source near the science target may enhance signal to noise.
- Centroiding errors due to non-ideal pixel behavior tend to be averaged away. Possible sources of systematic centroiding errors (generally quite small) are intrapixel response variation, sub-pixel sized particulates on the detector surface, spatial variation in interpixel capacitance, non-linearity, reciprocity failure, and image persistence. Stochastic errors due to abnormally high dark current or read noise are also mitigated of course.

Disadvantages of multiple ROIs:

- Complexity in the AO Supervisory Controller, waveform generator, data format and processing. For this reason, the readout of multiple regions of interest (ROIs) is only goal and not a requirement, but the following camera sections are based on the presumption that the added complexity is not a serious cost driver, is worth the investment, and is likely to be required in the long run anyway.
- Readout noise: The read noise is reduced as the square root of the number of non-destructive reads combined, until either the detector 1/f noise (~2e-) or shot noise in the background dominates. Spreading the available time for multiple sampling among more pixels (bigger or more ROIs) does not affect the noise per read but it does reduce the number of coadds and thus degrades the final noise after coadding.

4.5.1.3 Self Heating

Repeated addressing of the same pixels in a ROI causes a "self-heating" of that region of the detector. Over time this heated region reaches a quasi-equilibrium state. From an arbitrary state to a selected 4x4 pixel region, settling time is approximately 3000 frames (approximately 387 msec). The concern is that a sudden, small (1 or 2 pixel) shift in the ROI position from a heated region in quasi-equilibrium to a region which includes relatively cooler (previously unaddressed) pixels could result in an erroneous centroid calculation. Measurements indicate that after such a 1 pixel shift there is a settling period of about 200 frames (approximately 26 msec). However, the amplitude of this self-heating effect is comparable to the noise and is likely negligible.

4.5.2 Detector Readout Scheme

Readout of multiple ROIs will be supported. Since 3 or 4 are likely the maximum number needed, we will set the maximum number of allowable ROIs to 8. This is a somewhat arbitrary choice which exceeds are foreseeable needs.

The relative frequency of sampling for each ROI will be adjustable so that a larger fraction of the sampling time can be allocated to averaging sources that are fainter and thus more susceptible to read noise.

The AO Supervisory Controller (SC) will be responsible for determining the position, size and visitation rate for the various ROIs, within the constraints of a readout scheme encoded in the format of Table 7, and explained below.

ROIs are read sequentially thorough a single output channel on the H2RG detector. Four coordinates describing the corners of the ROI are transmitted from the detector control electronics (AKA ARC or Leach Controller) to the H2RG as a serial bit stream. The time to transmit one word over this serial interface is approximately 2.5 μseconds; hence it takes about 10 μseconds to position an ROI on the H2RG.

A raster scan of the requested size is digitized at that location, and then a command is issued to reprogram the next region.

To optimize the reduction of low frequency noise components by sample averaging, the samples must be maximally separated (thus evenly distributed) in time. For example, regions A, B and C, if sampled at three different frequencies must be ordered:

A B A B A B A B C A B A B A B A B C ...
not A A A A B B B B C A A A A B B B B C ...

A readout table, shown schematically in Table 7, describes this scheme. Each row of the table describes a unique ROI. The ROIs are accessed in the same order as listed in the table and a row of the table is written into a volatile memory on the ARC Timing Board using a single command. The periodicity (or decimator) parameter describes the rate at which the ROI is sampled. Periodicity of 0 indicates that ROI is not sampled and marks the end of the table (for fewer than eight ROIs). For iteration *i*, an ROI will be sampled when

i modulo P = 0,

where P is the periodicity parameter for the ROI in question.

PERIODICITY	DELAY	START COL	START ROW	# OF COLS	# OF ROWS
P1	T1	X1	Y1	ΔX1	ΔY1
P2	T2	X2	Y2	ΔX2	ΔY2
P3	T3	X3	Y3	ΔX3	ΔY3
P4	T4	X4	Y4	ΔX4	ΔY4
P5	T5	X5	Y5	ΔX5	ΔY5
0	--	--	--	--	--
--	--	--	--	--	--
--	--	--	--	--	--

Table 7: Data structure defining the multiple ROI readout algorithms. Each line corresponds to one ROI (up to a maximum of 8) with the order in the table specifying the ROI access order. A value of 0 for the periodicity parameter will mark an early end of the table (for fewer than 8 ROIs).

The multiple ROI readout will be generated as follows, where ROIn is the index into Table 7 (i.e. row number). NUM_ROI is calculated in the DSP as the number of rows before Pn=0 (which would be =5 for the example of Table 7:). CYCLES_PER_RESET will be programmed using a separate command.

```
While video=off, then idle;

While video=on {
        Select full frame;
        Set detector's global reset;
        Send Configuration packet to video link;
        Clear global reset;
        For i = 1 to CYCLES_PER_RESET {
                For ROIn = 1 to NUM_ROI {
                        If i/P(ROIn)=integer,
                                Send coordinates for ROIn to H2RG;
                                Read ROI;
                                Delay for T(ROIn);
                        };
                };
        };
```

At some stage in this loop the processor must check for a received command. It is TBD where this check will occur, but it will occur at only one point in the loop, for example, at every reset. Simply checking for the presence of a command will take TBC nanoseconds. If a command is received it can take from TBC to TBC additional nano/μ seconds to then process it.

What this does is to reset all pixels on the detector, then scan through the ROI specifications executing each region once every P times through the loop, where P can have different value for each ROI.

The time delay after reading any given ROI allows the overall looping rate and spacing of each ROI within the loop to be adjusted if required. Typically this time delay will be zero, so the detector will be readout continuously. The 24 bit delay parameter is specified in 40 ns clock cycles so that the maximum delay will be 0.671s which safely exceeds requirements.

Example: Consider the case of two regions, where one contains a bright star and the other a faint star, such that the star at (1100,900) is surrounded by a 4x4 region and is read 9 times more often than another at (200,300) surrounded by a 4x6 region. It is determined that the bright star needs to be reset every 1 sec or so. The readout definition table might look like that shown in Table 8.

Periodicity	Delay	X start	Y start	X size	Y size
1	0	1098	898	4	4
9	0	198	297	4	6
0					

Table 8: Example ROI readout table definition, shown in base-10 notation

The first ROI is read out every time while the second ROI is read every 9th time through the readout loop. For our pixel time = 6 μs, then (neglecting line and frame overheads) the mean loop execution time will be

$$6\ \mu s * (4*4/1 + 4*6/9) = 112\ \mu s,$$

so in order to have ~ 1s between resets, we will have

$$1s / 112\ \mu s = 8928 \text{ cycles per reset.}$$

In this example, the fastest exposure that can be synthesized for the ROI with the brighter star is

$$9 * 112\ \mu s = 1.008 \text{ ms.}$$

4.5.3 Packet Protocol on Video Data Link

4.5.3.1 Special Character Codes

Each packet of information transmitted on the second fiber optic channel is identified by a Special Character Control Code (K code) supported by the HOTLink Transmitter/Receiver device. The Special Character Byte Name shall be K.29.7 ($0A). Presence of this Special Character indicates that the following word(s) contain some sort of flag or configuration information, rather than pixel data from the detector. In the diagrams and discussion that follows, this special K.29.7 character code will be denoted simply as “K”. Note that the implementation of fiber optic receiver in the Microgate RTC will need to recognize this Special Character Code and deal with it accordingly.

4.5.3.2 Header Words

A 16-bit header word will immediately follow the K code. Valid header word values are shown in Table 9. Reception of any other value not shown in the table should indicate an error condition.

header value		meaning
decimal	hexadecimal	
0	00	ROI configuration table follows
1	01	data for ROI#1
2	02	data for ROI#2
3	03	data for ROI#3
4	04	data for ROI#4
5	05	data for ROI#5
6	06	data for ROI#6
7	07	data for ROI#7
8	08	data for ROI#8
82	52	a RESET has occurred

Table 9: Valid header words which can be the first word following a Special Character K.29.7 Code

Configuration Table

When the header word following a K code is $00 then the next 16 bit word is a counter, which will increment when any line in the configuration table has changed. Subsequent words will be the configuration table itself, as depicted in Table 8. Only the rows of the table will be transmitted, six words per row. The end of a table will not be specially marked. If this is undesirable then we could first transmit the number of rows (i.e. number of ROIs) after the $00 header and before the first table row is sent.

The configuration table could be sent only when it has changed but it is our intention to also send it every time the array is reset, since this is dead time anyway. However, the presence of the configuration table is not to be used as an indicator of a reset.

The 16 bit incremental counter that is transmitted with the configuration table can be used to indicate a change in the configuration. When a change is made to the ROI configuration table (using the ROI command in §4.5.5) the detector controller will increment this counter. The receiver (i.e. the RTC) can compare the transmitted counter value with the previously received value. A change in value indicates a change in configuration; no change in value indicates the configuration has not changed. When the counter reaches $FF it will wrap around to $00. The counter will start at $00 upon power-up or initialization.

Reset

When the header word following a K code is $52 then a global reset has occurred. All pixels in all ROIs will be reset at the same time. There will be no selective resetting of any given ROI.

Packet Examples

In the following examples, each white box represents a 16-bit word in the data stream to the RTC.

Example #1: Transmission of a configuration packet.

K	00	CC	P1	T1	X1	Y1	DX1	DY1	P2	T2	X2	Y2	DX2	RY2	Pn	…

where the CC is the configuration counter and Pn, Tn, Xn, etc. use the nomenclature of Table 7:.

Example #2: Transmission of data.

K	01	pp	pp	pp	pp	K	01	pp	pp	pp	pp	K	02	pp	…

where pp indicates a 16 bit pixel value. This example represents data from two ROIs, the first one being 2x2 with a periodicity=1 and the second ROI having a periodicity=2.

4.5.4 Error Detection on Video Data Link

When the video data link is functioning normally, the bit error rate on the relatively short fiber between the Detector Controller and RTC should be very low under normal circumstances, and probably will be much lower than the cosmic ray rate (about one per hour in a 4x4 pixel ROI), therefore no mechanism such as a check sum will be provided to detect data corruption. The RTC may employ some sort of outlier rejection on centroids (for example) to make the system robust against cosmic rays or noise spikes.

A more likely scenario is a hardware or software malfunction leading to the complete absence of data or the loss of packet synchronization (too many or too few bytes). The absence of data will have to be detected by a time-out in the RTC. The incorrect number of bytes in a packet will be detected by reception of a data value when a K code is expected or vice versa. An error should be flagged by the RTC, which should attempt to recover packet synchronization by looking for the next K code. Recovery should be a matter of waiting for a K code and then acting on the header word which immediately follows (see Table 9).

Of order ten thousand packets per second are typically flowing on the video link, so it is unwise to generate a message for every error, in case that error is persistent. A practical solution is for the RTC to set an error flag or (better) to increment a counter, which is polled at a lower rate.

4.5.5 Detector Controller Commands

The ARC Detector controller utilizes "3-letter commands" that can have up to four 24-bit parameters. Commands will reply with an ASCII 'DON' (0x444F4E) on success or an ASCII 'ERR' (0x455454) on error.

ROI – Region Of Interest

Programs the Region Of Interest data structure as shown in Table 7 and described above.

Usage: `ROI <ROIn> <A1> <A2> <A3>`

where <ROIn> is the Region of Interest number (1-8)
and <An> are 24-bit arguments, packed as follows:

<A1> bits 0-11	<Pn>	Periodicity factor (0-TBD)
<A1> bits 12-23	<Tn>	Time delay (0-TBD)
<A2> bits 0-11	<Xn>	Start column (1-2048)
<A2> bits 12-23	<Yn>	Start row (1-2048)
<A3> bits 0-11	<DXn>	Number of columns (1-2048)
<A3> bits 12-23	<DYn>	Number of rows (1-2048)

Each given line of the ROI table is programmed by the ROI command once. ROIs can be programmed in any order and a single ROI definition can be overwritten without altering its neighbors. Although the ROIs can be reprogrammed "on the fly" (that is, while video mode is on and data is currently streaming), changing the length of the ROI configuration table will be prohibited while video mode is enabled. (TBD) That is, the number of ROIs cannot be changed without first disabling video mode. Note that a 0 must be written for the Periodicity factor following the last ROI, as depicted in Table 7. The number of ROIs will be internally calculated using the presence of this 0 to mark the early end of the table (the 0 is not required when all eight ROIs are used).

Examples: (1) to program for ROI#1 a 4x4 window starting at row=512, column=768 with Periodicity=1 and time delay=0:

```
ROI 0x000001 0x000001 0x200300 0x004004
```

(2) to write a 0 to the Periodicity factor for ROI#2, enforcing only one ROI:

```
ROI 0x000002 0x000000
```

(3) to write the ROI table as depicted in Table 8 (note that three separate commands are required):

```
ROI 0x1 0x1 0x38244A 0x4004
ROI 0x2 0x9 0x1290C6 0x6004
ROI 0x3 0x0
```

CPR – Cycles Per Reset

Set the number of read cycles before a RESET occurs.

Usage: `CPR <n>`

where <n> is the number of cycles to read before a reset will occur (1-TBD).

VON – Video ON

Enable the video mode and begin streaming data out the secondary fiber transmitter. The detector will be reset and read according to the ROI table (see Table 7 and the ROI controller command).

Usage: `VON`

VOF – Video OFf

Disable the video mode and stop streaming data out the secondary fiber transmitter.

Usage: `VOF`

SWG – Set Window Geometry

Enable 1 channel window mode and set the geometry for that window.

Usage: `SWG <X> <Y> <DX> <DY>`

where
<X> is the starting column (1-2048)
<Y> is the starting row (1-2048)
<DX> is the number of columns (1-2048)
<DY> is the number of rows (1-2048)

After enabling window mode with this command, subsequent expose (SEX) commands will reset and read this specified window only.

SSS – Set Subarray Size

Set the size for a subarray and enable 32 channel output mode. Passing 0 for <DX> will enable full-frame mode. This command should be used in conjunction with SSP except when using full-frame mode (for which SSP has no effect).

Usage: `SSS <DX> <DY>`

where

<DX> is the number of columns in the subarray (1-2048)
<DY> is the number of rows in the subarray (1-2048)

SSP – Set Subarray Position

Set the position for the subarray configured by the SSS command (section 0). Rather than using the H2RG window mode output and programming the registers, the dimensions passed to this command are used to skip over rows and columns.

Usage: `SSP <X> <Y>`

where
<X> is the number of columns to skip (1-2047)
<Y> is the number of rows to skip (1-2047)

FSM – Film Strip Mode

Enable/disable and configure the filmstrip mode.

Usage: `FSM <E> <N>`

where
<E> is the filmstrip enable state, 1=on, 0=off
<N> is the number of frames in the filmstrip (1-TBD) [TBD to be determined by available memory]

A single FITS file will be produced with dimensions of <DX> columns x (<N> * <DY>) rows where <DX> and <DY> have been previously set by either the SWG or SSS command. The filmstrip mode will operate in either 1 channel window mode (when preceded by SWG) or in 32 channel mode (when preceded by SSS).

SEX – Start EXposure

Start a single-frame or filmstrip exposure (I.E. non-video).

Usage: `SEX`

PON – Power ON

Turn on all camera biases and clocks

Usage: `PON`

POF – Power OFf

Turn +/- 15V power supplies off

Usage: `POF`

SBN – Set Bias Number

Set a particular DAC number, for setting DC bias voltages on the ARC-32 clock driver board and ARC-46 IR video board.

Usage: `SBN <#> <DAC> <BOARD> <VOLTAGE>`

where
<#> is the board ID number (0-15)
<DAC> is the DAC number (0-7)
<BOARD> is the string name of the board; 'CLK' or 'VID'
<VOLTAGE> is the voltage to set (0-4095)

SMX – Set MuX

Specify which of the clock driver outputs to present to the two auxiliary SMB coaxial output connectors on the ARC-32 clock driver board. These outputs are connected to a set of six multiplexers that same the clock driver outputs.

Usage: `SMX <#> <MUX1> <MUX2>`

where
<#> is the board ID number (0-15)
<MUX1> is the clock driver output to go to the first SMB connector
<MUX2> is the clock driver output to go to the second SMB connector

SET – Set Exposure Time

Set the exposure time for single-frame images.

Usage: `SET <T>`

where <T> is the exposure delay in milliseconds.

SVO – Set Video Offset

Set the ARC-46 video board offsets

Usage: `SVO <#> <DAC> <OFFSET>`

where
<#> is the board ID number (0-15)
<DAC> is the DAC number (0-7)
<OFFSET) is the offset voltage (0-4095)

RET – Read Exposure Time

Read the elapsed exposure time while an exposure is in progress.

Usage: `RET`

This command returns the number of milliseconds elapsed, or 0 if no exposure is in progress.

AEX – Abort Exposure

Stop the exposure timer. This will not abort readout in progress, only the exposure timer before readout starts.

Usage: `AEX`

SER – SERial command

Transmit a serial register command to the H2RG.

Usage: `SER <COMMAND>`

where <COMMAND> is a 16 bit register command.

RIR – Reset Internal Registers

Assert MAINRESETB to clear all internal H2RG registers to default settings.

Usage: `RIR`

INI – INItialize array

Initialize the internal H2RG registers to TRICK-default settings.

Usage: `INI`

4.6 Camera Host Computer and Servers

The camera host computer will depend on two essential requirements: It must be supported by the WMKO computer systems group and it must support the ARC PCI interface board and driver. At this point, the brand and model of the computer is TBD.

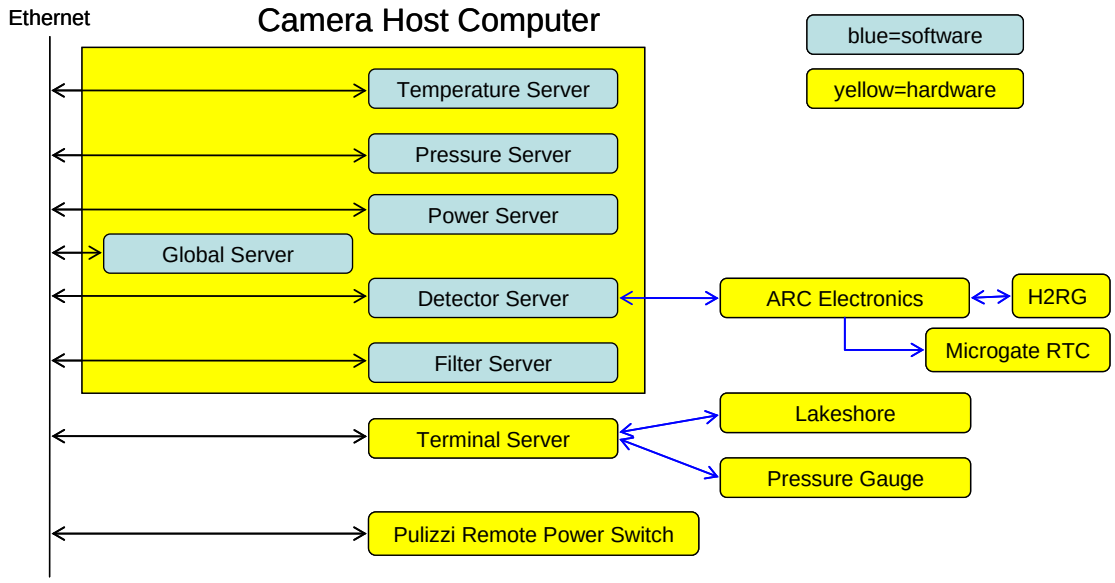

Figure 59: Keyword servers

The host software subsystem will consist of six servers – six instances of the same server with different application libraries – which will be used to control and monitor the TRICK hardware subsystems: detector, temperature, pressure, power and a filter wheel. The sixth instance is the global server which provides, among other things, a single point of contact to clients on the network. The basic server code, written by Keck software engineer, Allan Honey, uses remote procedure calls (RPCs) to implement the Keck Tasking Library (KTL) keyword, network interface for communicating among Keck clients and servers. Figure 59 shows the interfaces for the camera system. Each server, shown in blue, consists of the base code plus a dynamically-loaded library that is application specific. Each library is created from three

source files, a keyword interface module, a top-layer applications module and a hardware-level module. These libraries already exist for all servers except for the filter server.

4.6.1 Global Server

Each of the servers can communicate keywords directly or through the Global Server. The Global Server is designed to provide a single contact point for external clients. The Global Server software will use code ported from MOSFIRE/OSIRIS and customized for this application. The Global keywords will be mapped to sub-server keywords. The Global Server will also create the proper header for FITS files created by the system including the specified DCS and AO keywords.

4.6.2 Detector Server

The detector server will be based on the application code written for OSIRIS, MOSFIRE and NIRES. It will offer keyword control and readback of the detector's exposure modes and parameters, sub-frame ROIs and their parameters and FITS file, frame and path naming, as well as the ARC electronics DSP code and parameters. It will offer two main operating modes: the production of FITS files for field acquisition, dark and flat-field calibration images and "filmstrip" files for video-mode debugging without the real-time hardware; and video mode, which will cause a continuous stream of pixel data to be sent on an auxiliary fiber channel of up to eight detector regions of interest. Although the existing detector servers provide most of the functionality required by the NIR TTS detector server -- including the interface to the ARC electronics -- some customization will be necessary. Keywords and their associated functionality, that are necessary to select and configure ROIs and turn on and off video mode will need to be added.

4.6.3 Temperature Server

The temperature server will be based on work done for MOSFIRE. The server offers temperature control (set points, ramp and PID control-loop parameters) as well as monitoring of up to eight additional temperature sensors for a total of ten. Temperature sensors can be labeled through keyword control. Outputs to the heaters, as a percentage of total power, can also be monitored. The only anticipated changes to the MOSFIRE temperature server are in the number of channels to be monitored and the values of the control parameters. For the MOSFIRE camera, we have found that the Lake Shore 340 "autotune" control mode provides excellent temperature control.

4.6.4 Pressure Server

The pressure server will be based on code written for MOSFIRE. The server offers monitoring of the camera dewar pressure as well as configuration of the pressure-gauge electronics. It is likely that the pressure monitoring hardware selected for the NIR TTS will be different from that used by MOSFIRE so a new hardware layer will need to be written. No other changes are anticipated.

4.6.5 Power Server

The power server will be based on work done for MOSFIRE. It offers on-off control of power outlets as well as outlet status monitoring. The outlets can be accessed by name or number. Outlet names can be set by keyword control. The only change anticipated for this server is the number of outlets to be controlled.

4.6.6 Filter Wheel Server

The filter-wheel server will be based on work done for MOSFIRE but will use only the skeleton outline of the server. The server will offer complete control of the filter wheel's motion, the ability to set position, displacement, acceleration, speed, deceleration as well as controller-specific parameters (for example, continuous and peak current, hold power and power-up and power-down time). An encoded system is anticipated. The server will be able to select filters by name or by position number. Limit and home switches will be supported if necessary. Very few changes are anticipated for the application and keyword-interface modules of the server. The hardware module will have to be customized to the communications and protocol requirements of the TBD motion controller.

4.7 Detector Controller

Two options were considered for the readout electronics: the SIDECAR ASIC used for MOSFIRE and the Astronomical Research Cameras (ARC) SDSU-III readout electronics used for OSIRIS. The SDSU-III

readout electronics, shown in Figure 60, was selected for a combination of reasons including superior noise performance, controller cost, ease of implementation, cost of interfacing, and schedule and budget risk. The primary factor was the hands-on experience of the Caltech team that will develop the camera with the ARC readout electronics and the demonstrated performance by this team with these electronics.

The ARC detector controller layout is shown in Figure 60. The boards are all standard ARC products with the exception of the ARC-22 timing board which has been modified to include a 2nd fiber transmitter to send video data to the RTC, and a modified PAL and some additional wiring to allow for the use of special characters.

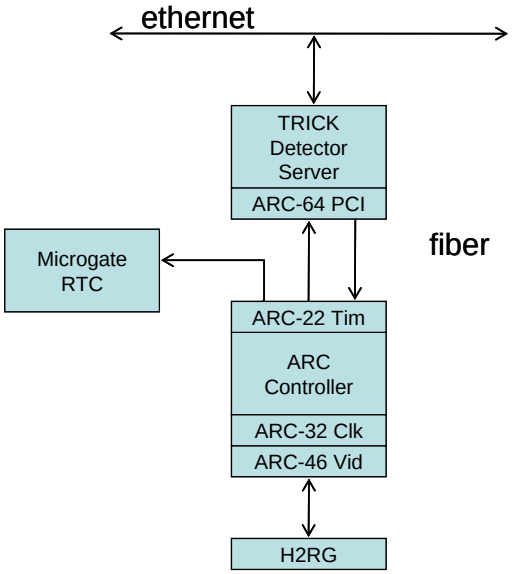

Figure 60: ARC Detector Controller. *All electronics for the array are external to the cryostat. The flex cable from the array is extended through the back cover to interface boards external to the cryostat. These interface boards then lead to the ARC readout electronics (the clock and video boards).*

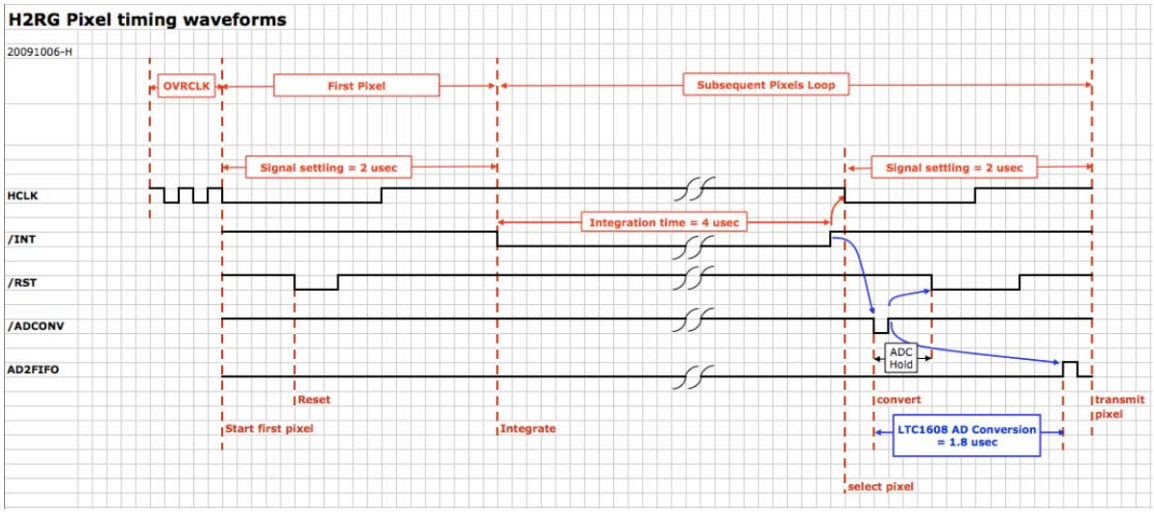

Figure 61: Optimized waveform timing

Multichannel readout (16 or 32 channels) will be supported for rapid full field imaging during acquisition, while only single channel readout in window mode will be used for TT sensing. A FITS file is produced in single-frame image mode reading for: 1) field acquisition (32 channel readout); 2) dark and flat field calibration in single channel readout to match the channel(s) used for video (window) readout; and 3) film-strip readout for video mode diagnostics without the RTC present. In video mode a continuous stream of pixels will be provided to the RTC.

The pixel timing waveform is shown in Figure 61. The typical waveform produces ~ 10 μsec pixels. We will use the optimized 6 μsec pixels developed during the TMT study for the best speed versus noise. Most of the clocking has been nested into the settling period, which cannot be further reduced.

4.8 Camera Hardware Locations

The camera itself will mount on the NIR TTS focus stage via an interface plate. The camera will mount kinematically to this interface plate. The readout electronics must be within ~1.5 m of the camera. These electronics will therefore reside in an air cooled, thermally insulated enclosure on top of the AO bench cover; the air cooling will be provided by a hose to the existing air-to-glycol heat exchange in the AO room. The ARC controller power supply will reside in the AO electronics room. The camera host computer will reside in an electronics rack in the AO electronics room (another option which could be considered would be to locate the host computer in the computer room next to the control room).

The location of the cryocooler compressor was discussed in section 4.4. The Lakeshore Temperature controller and ion pump controller will be located in the AO electronics room.

4.9 Camera System Electronics

4.9.1 Overview

4.9.1.1 System Components

A block diagram of the system electronics components and their connections is shown in Figure 62.

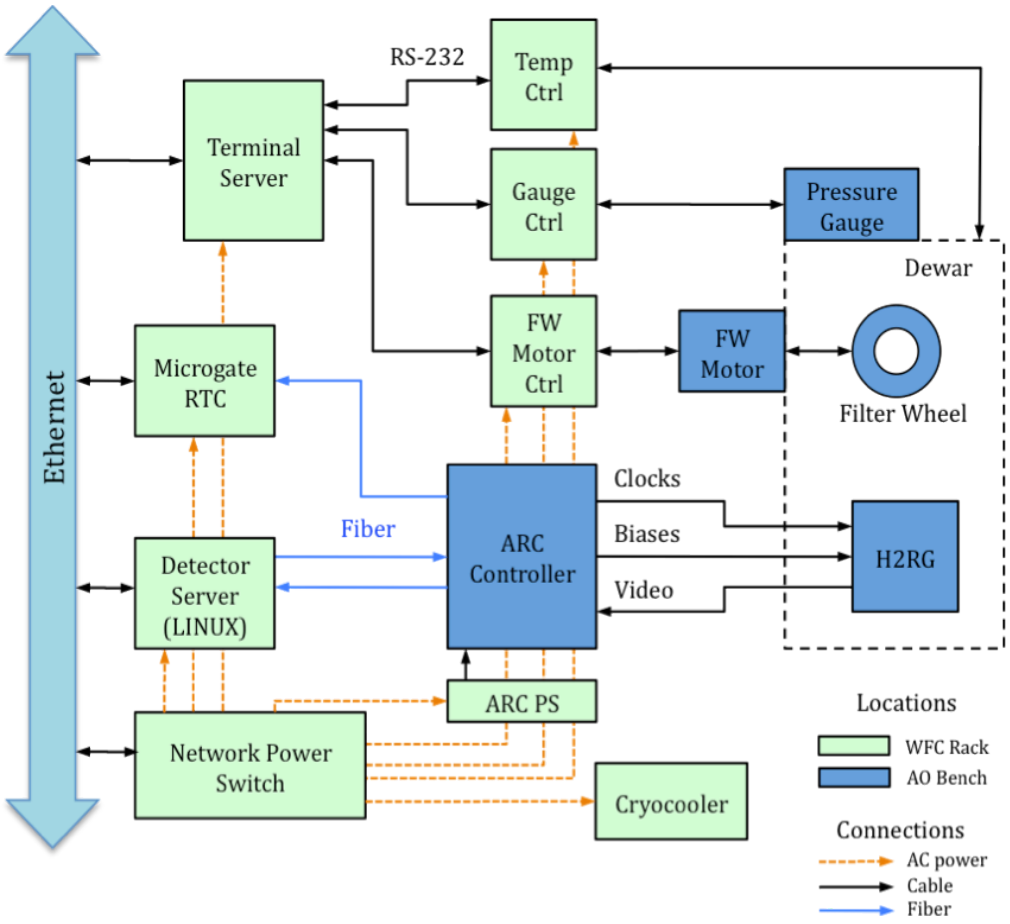

Figure 62: Block diagram showing the electronics modules and the control connections

The main components of the camera system electronics are:

- NIR camera dewar, containing the NIR detector (Teledyne's Hawaii-2RG) and the filter wheel.
- Detector controller from Astronomical Research, Inc (ARC).
- Filter wheel motor and controller, from Quicksilver Controls, Inc.
- Pressure gauge and controller.
- Temperature controller from Lakeshore Cryotronics, Inc.
- Cryocooler, from Polycold.
- Terminal Server
- Detector Host computer
- Network power switch

4.9.1.2 Monitoring and Control Interfaces

Control and status monitoring is via the Ethernet connection to the Detector Server, which is connected to the ARC Detector Controller via a fiberoptic link (pair of fibers, bidirectional); the ARC Controller sends a continuous "video" data stream to the Microgate RTC via a single fiber (unidirectional) or returns single frames or bursts of video data to the Detector Server, whose length is limited by buffer memory

The auxiliary modules (temperature, pressure and filter wheel motor controllers) will be connected via RS-232/485 interfaces to a terminal server to allow access via Ethernet.

The cryocooler does not provide remote access.

4.9.1.3 Power Inputs

The ARC detector controller has its own power supply module (ARC-80), connected through a custom cable. The power supply module requires 150 W of 120 V AC power.

The temperature controller is connected directly to 120 V AC power.

The pressure gauge controller requires TBD.

The filter changer motor controller requires +12 VDC to +48 VDC, maximum of 4 Amps.

AC power is provided via a Network Power Switch (Pulizzi IPC3401) so that power to any or all of the subsystems listed above can be remotely switched.

4.9.2 Detector Mount Wiring

The "detector mount" is the mechanical module which supports the H2RG detector, keeping it close to focal surface (Z direction) and maintains its position (XY) across thermal cycles, while minimizing stress due to thermal contraction and providing accurate thermal stabilization at the required cryogenic temperature.

The mount accommodates the installation of a flexible circuit to connect the detector with the external controller electronics while providing sufficiently low thermal conduction.

The mount will have embedded heater resistors and a cryogenic temperature sensor to control the temperature of the detector. The control loop will be provided by the Lakeshore temperature controller. The temperature sensor will be a calibrated Resistive Thermal Device (RTD) to avoid the possibility of noise rectification seen in conventional diode sensors.

A thermal fuse will be connected in series to the resistors to prevent overheating in the event of malfunction.

4.9.3 Detector Controller Electronics

The detector electronics will be a standard controller from Astronomical Research Cameras, Inc. (ARC), configured for IR detector operation. The controller consists of the following boards:

- A PCI Interface Board (ARC-64) which provides the interface to the Microgate RTC.
- A Timing Board (ARC-22) which provides the communication between the controller and the host computer, generates timing waveforms and provides overall controller supervision.
- A Clock Driver Board (ARC-32) which translates digital input clock signals into analog output signals.
- Four 8-channel IR Video Boards (ARC-46), each containing eight identical video processors for 32 channel operation (maximum H2RG video channel count).
- A standard ARC 6-slot controller housing (ARC-70).
- Standard power supply (ARC-80).

The ideal location of the detector controller module is as close to the detector as possible, to minimize the wiring length of the video signals coming form the detector. Long lines increase the risk of crosstalk and noise. Mounting the controller directly to the dewar is highly desirable since it protects the expensive detector against ESD (Electrostatic Discharge) when handling the assembly, and has the additional advantage that a cable is eliminated.

In our current design the controller is separated from the dewar by a short cable to permit thermal insulation of the controller and to facilitate easier handling. Beyond ~1.5 m cable length a 32-channel preamplifier module and local buffering should be considered primarily to isolate the detector from ESD, but with the secondary advantage that a longer cable can be driven.

The detector controller electronics will be housed in a thermally insulated enclosure, supplied by WMKO. Warm air extracted though a hose to a remote heat exchanger will be replaced by ambient air. The controller will continue to use its internal recirculation fan as installed by the manufacturer. A temperature sensor will be mounted within the Detector Controller to remotely monitor its internal temperature. This sensor will be connected to one of the inputs of the Lakeshore temperature controller.

A standard ARC Large Power Supply (ARC-80) will provide the DC voltages required by the detector electronics. Its enclosure is made of machined aluminum panels. Its size is 12.25 x 8.25 x 5.25 inches and it weighs 16 lbs. Its design allows for a power cable of up to 16.5 feet long without the need of compensation for voltage drop due to cable resistance. The power supply is to be located in a rack in the AO electronics room 30 feet away, and thus will probably require special adjustment.

The main ground star point is the only point where analog ground, digital ground and chassis ground are physically connected. This will be located on the controller backplane. A diagram of the grounding scheme is shown in Figure 63.

Each of the regulators in the power supply box are separately transformer-isolated and will float relative to each other until connected to the controller since this is the only place where analog and digital grounds are tied together.

Continuous Faraday shielding is provided by the dewar, the detector controller enclosure, braided shields around cables and the power supply enclosure. The screwed joints between panels provide for shield continuity and the alodine coating on the Detector Controller panels assures continuity in that enclosure. Electrical continuity to the braid around cables is established by passing this connection through pin(s) in the connector and does not rely on continuity with the connector backshell or a connection from backshell to mating connector and its panel.

Electrical safety codes require that the metallic enclosures, which serve as RFI shield, be grounded through the earth pin of the AC socket. We do not intend to isolate all other connections to the shield, which typically occur where the dewar contacts the surrounding structure and may occur through motor drivers

and pressure gauge, or ion pump. In our experience, the ground loops created thus are benign, even for much longer exposures than contemplated in this application, since the loop current flows only in the shield. We find that keeping impedances in the shield path low is a more robust approach than relying heavily on strict isolation which is easily bridged by accident. Isolation helps of course and remains a worthy goal. If difficulties arise at high frequencies an RF choke can be added to the earthing wire to open the loop.

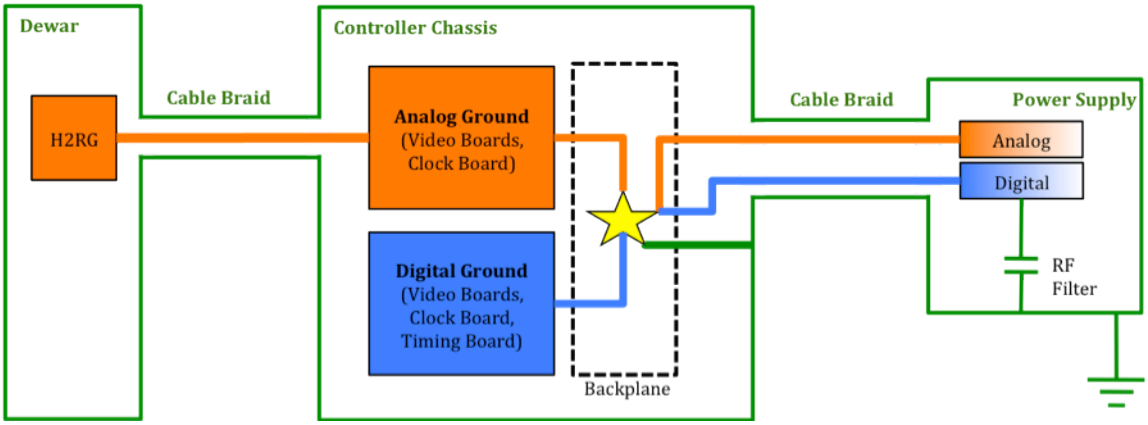

Figure 63: Grounding scheme for the camera electronics. Orange is analog ground, blue is digital ground, and green is chassis/earth ground.

4.9.4 Temperature Controller

The temperature controller will be a Lakeshore Cryotronics, Inc. model 340 controller, configured with an 8-channel sensor card for a total of 10 sensor inputs (the model 340 has two standard inputs). The controller provides two independent control loops, one with a maximum heater output of 100 W and the other with a maximum output of 1 W.

The 1 W control loop will be used on the detector mount. Resolution is 1 mK. Long and short term stability requirements for the system are relatively lax compared to the capabilities of the Lakeshore controller due to the high frame rate. We use it primarily to standardize on equipment, but it has the added benefit of providing sufficient stability to operate the detector in long exposure mode so that its performance can be benchmarked using conventional science readout schemes.

The 100 W loop will be used for controlled warm up for the dewar cold surface. While not absolutely required, this will pay for itself by facilitating debug and maintenance by reducing the warm up time. For minimal stress induced by differential thermal expansion, constant slew rate will be maintained. For safety the warm up will stabilize at room temperature without human intervention and a Microtemp thermal fuse will provide protection against malfunction. Power resistors will be chosen so that the maximum voltage available at the Lakeshore output cannot produce an unsafe temperature slew rate. Power resistors will be potted into structures whose temperature is monitored and to which the thermal fuse is attached so the heaters cannot lose thermal contact (which would cause catastrophic failure). In addition they will be located so that there is no line of sight for condensates from the power resistors and detector.

During warm up, the detector thermal servo is also driven to maintain the detector at a fixed offset above the cold head so that cryopumping onto the detector will not occur. Since the detector is enclosed this is a relatively low risk anyway.

The following is a list of the temperature sensor locations to be monitored with the Lakeshore controller:

- Detector mount (servo controlled)
- Cold finger (servo controlled)
- Radiation shield.
- Dewar wall.

- Detector electronics enclosure.

The detector mount sensor, which requires high stability and immunity to interference, will be a 4-wire RTD Lakeshore Cernox sensor (model CX-1030-CU). All other sensors will be uncalibrated Silicon diodes (1N 914) which are inexpensive but quite adequate when an absolute accuracy of ±2 K is sufficient and errors due to rectification of interference (e.g. from clocks) is thus not a concern

5. Real-Time Controller

The existing real-time control (RTC) system (Johansson et al., SPIE Proc. 7015-121, 2008) must be upgraded to interface to the TTS readout electronics and to use the information provided by the TTS. We have contracted with Microgate, the fabricator of this control system, to provide a hardware interface for the TT data and additional processing power for the tip-tilt computations (see KAON 824 for the statement of work; note that Microgate was selected due to their expertise with the existing systems and our past very positive experience with this vendor). The resultant system will be able to utilize data from both the existing visible TT sensor and the NIR TTS, including up to one visible TT star and three NIR TT stars. We have an operational spare real-time control system in a lab at WMKO headquarters that will be used to fully test the system prior to telescope integration.

The PDR level RTC design developed by Microgate is documented in KAON 862. This KAON is an update to the existing as built RTC document with the revised sections noted in the revision history. There are only minor updates to the following RTC sections since the SDR.

5.1 Top Level Schematics

The main components of the real-time controller are shown in Figure 64. The down-link tip-tilt (DTT) mirror is controlled by the DTT controller which uses either the wavefront sensor (WFS) camera or the STRAP tip-tilt sensor for its tip-tilt information. Both STRAP and the DTT controller are part of the Microgate controller as seen in Figure 65. The WFS camera interfaces to the Microgate controller over an AIA port.

From the RTC perspective the only parts of Figure 64 that are potentially affected by integration of the NIR TTS will be the WIF, WFP and TRS. No changes are required to the wavefront sensor camera or STRAP. No changes are required to the DM, DTT or UTT controllers.

The mechanical layout of the front panel of the VME crate in which the Microgate AO system (MGAOS) real-time controller resides is shown in Figure 66 (from the Microgate Detailed Design Review document). There are spare slots in the VME portion and also within the MGAOS system (which has its own non VME bus internally). Either the existing BCU board would need to be modified to accept an interface from the NIR TTS readout electronics or a new BCU board would need to be added to accommodate this interface.

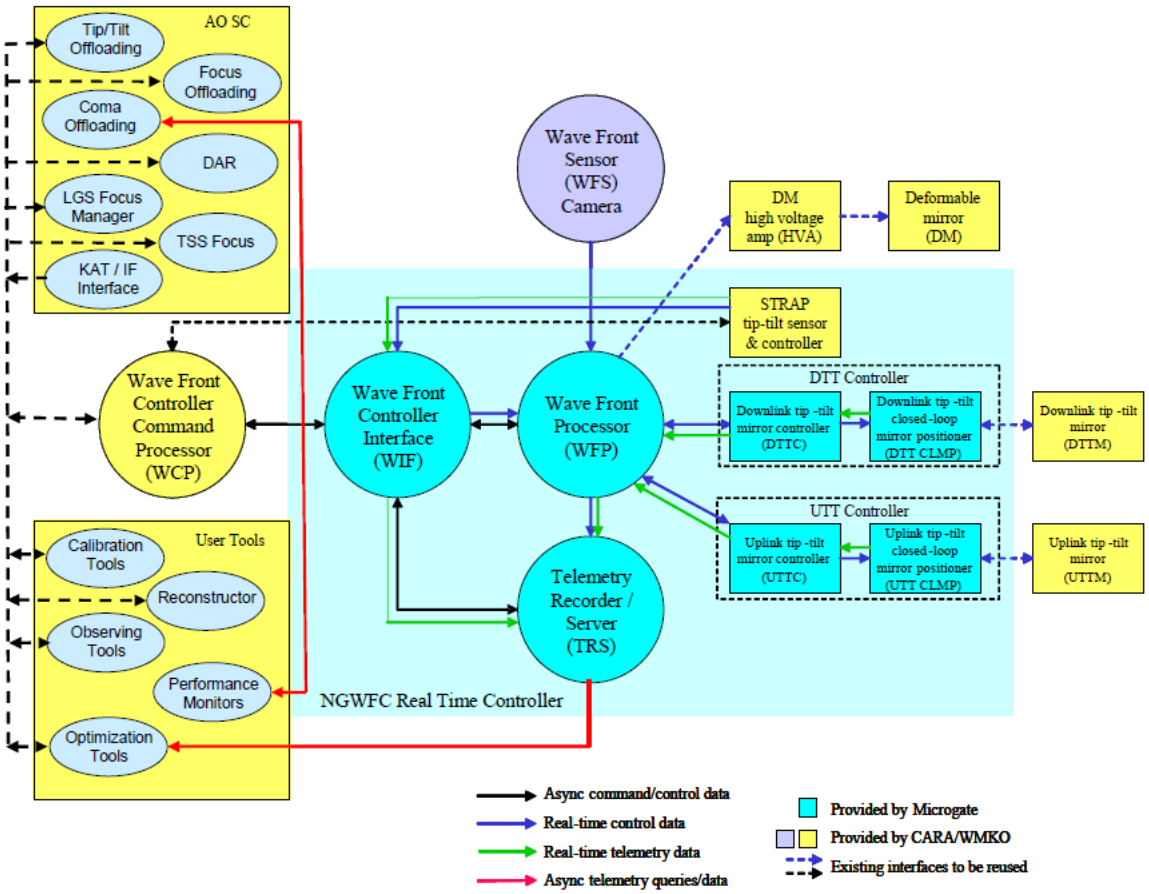

Figure 64: The main components of the real-time controller

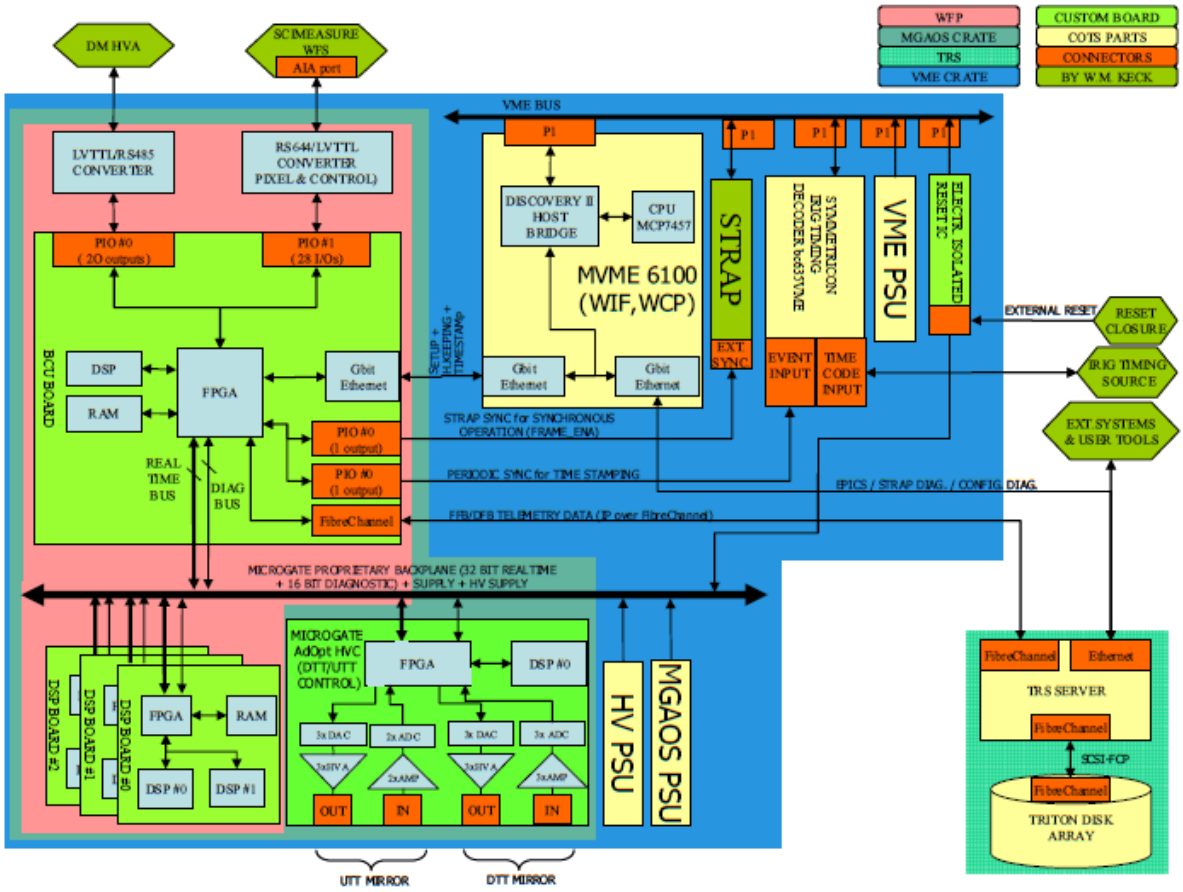

Figure 65: A block diagram of the Microgate real-time controller system

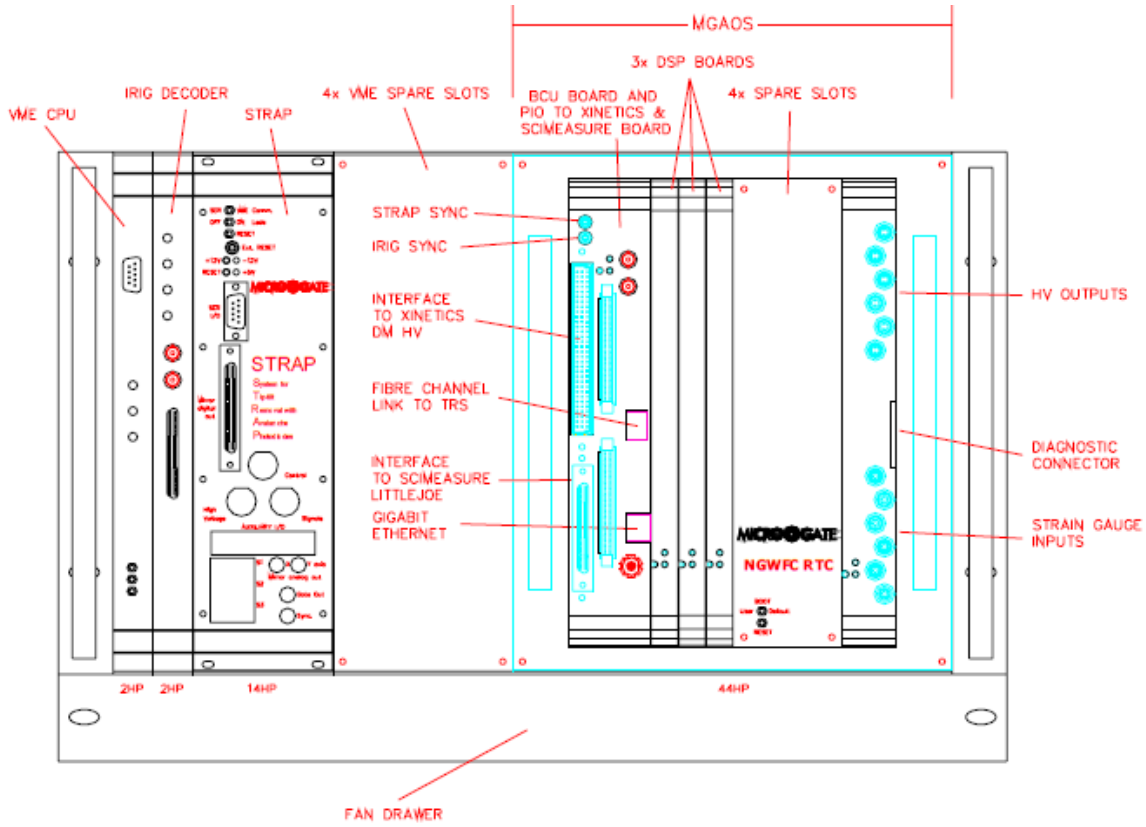

Figure 66: VME and Microgate real-time controller crate mechanical layout

5.2 Camera to Real-Time Controller Interface

Figure 67 provides a schematic of the major elements of the NIR TTS system. This camera is also referred to by the acronym TRICK for Tilt Removal with Ir Compensation at Keck. The TRICK camera controller (AKA Leach) will interface to the NGWFC RTC through a new interface to the WIF. The raw camera pixel data will be provided to the Microgate controller via a unidirectional fiber optic interface from the ARC timing board, providing a continuous data stream along with configuration information. No path exists on this fiberlink to send command or status information from the Microgate system back to the Leach controller.

Data packets from the camera to RTC should map to a single ROI. Since ROIs can be quite small the header which identifies the origin of the data needs to be very short, to minimize overheads. It is proposed that data be transmitted in packets whose format and purpose are identified by a single 16 bit header word.

Special characters will be used to identify the packet header word. This would be based on the special characters (K28.x) made available by the 8-10 bit encoding technique used by the Hotlink transceivers. The special characters will identify the header word, leaving the entire 16 bit (65536 codes) word value for packet type definition.

An ARC timing board was procured in November 2010 with a modification to provide two fiber transmitters to allow communication to both the host computer and the real-time controller. This board was successfully tested to ensure that the two fiber interface approach functions properly and also to test whether special characters can be used to identify the packet header word.

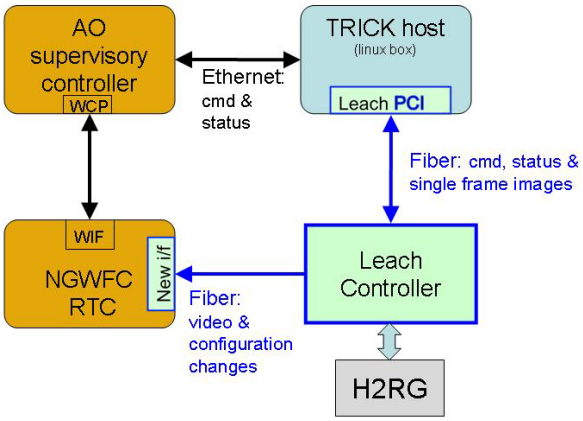

Figure 67: Top-level interface schematic

Data and configuration changes are provided over a fiber optic link from the NIR TTS camera readout electronics to the Microgate RTC. Commands to the Microgate RTC are provided over the existing interface between the AO system and the Microgate RTC.

5.3 Real-Time Controller Software

The Microgate controller will need to perform the following data processing steps in real-time on the data received from the camera:

- coadd multiple samples for each pixel for noise reduction.
- subtract the preceding co-added packet to obtain the difference (or "frame" value shown in Figure 57) for that pixel.
- subtract sky frames and
- scale by a flat field.

The equation describing this process is

$$i_c[k,t] = i_f[k](i[k,t]-i[k,t-1] - i_b[k])$$

where i[k,t] is the coadd of m frames of incident flux at pixel k, i[k,t-1] is the coadd of the previous m frames at pixel k, $i_b[k]$ is the background level at pixel k, $i_f[k]$ is the normalized flat-field gain response for pixel k, and $i_c[k]$ is the resulting compensated pixel. A pixel gain map file will be provided to the Microgate controller by the AO control system whenever the controller is restarted. The processed pixel values will need to be thresholded.

The real-time controller (RTC) will be capable of performing either a 4x4 pixel centroid or a correlation algorithm on the data from each ROI. The centroiding process is the same as that described in KAON 517.

The correlation algorithm is that presented by Poyneer (Appl. Opt. 42, 5807 (2003)). The correlation, C, between the reference image, r[i,j], and the subimage from each ROI, s[i,j], is calculated either directly or using FFTs (whichever way is faster). The reference image will be determined offline and will be provided to the Microgate controller. The direct implementation is

$$C[m,n]=\sum_i \sum_j r[i-m, j-n]s[i,j]$$

And the Fourier transform implementation is

$$C[m,n]=F^{-1}\left[F^{*}\{r\}\cdot F\{s\}\right]$$

Given the discrete maximum, (Δ_x,Δ_y), the sub-pixel shift is found using parabolic interpolation in one direction at a time:

$$\hat{x} = \Delta_x + \frac{0.5(C_{-1} + C_1)}{C_{-1} + C_1 - 2C_0} \quad \text{and} \quad \hat{y} = \Delta_y + \frac{0.5(C_{-1} + C_1)}{C_{-1} + C_1 - 2C_0}$$

Note that the star images used for the tip-tilt measurement will not normally be located at the intersection of 4 pixels. In addition, the star image will move on the detector during the course of a science exposure due to such effects as differential atmospheric refraction. The position of the centroid offset position to which the tip-tilt mirror should drive the star image and the location of the ROI will therefore need to be periodically updated. These updated positions will be provided to the wavefront controller.

The TT RTC control loop is illustrated schematically in Figure 68. The STRAP controller processing is unchanged. The NIR TTS camera (TRICK) controller processing is similar with two exceptions: the initial processing to coadd samples and then to subtract the previous packet, and the choice of using a centroid or correlation algorithm. The TT errors calculated for each ROI and the STRAP TT error are then averaged together after applying multiplicative scaling factors. The scaling factors are a function of the SNR for each TT star and their positions with respect to the science object.

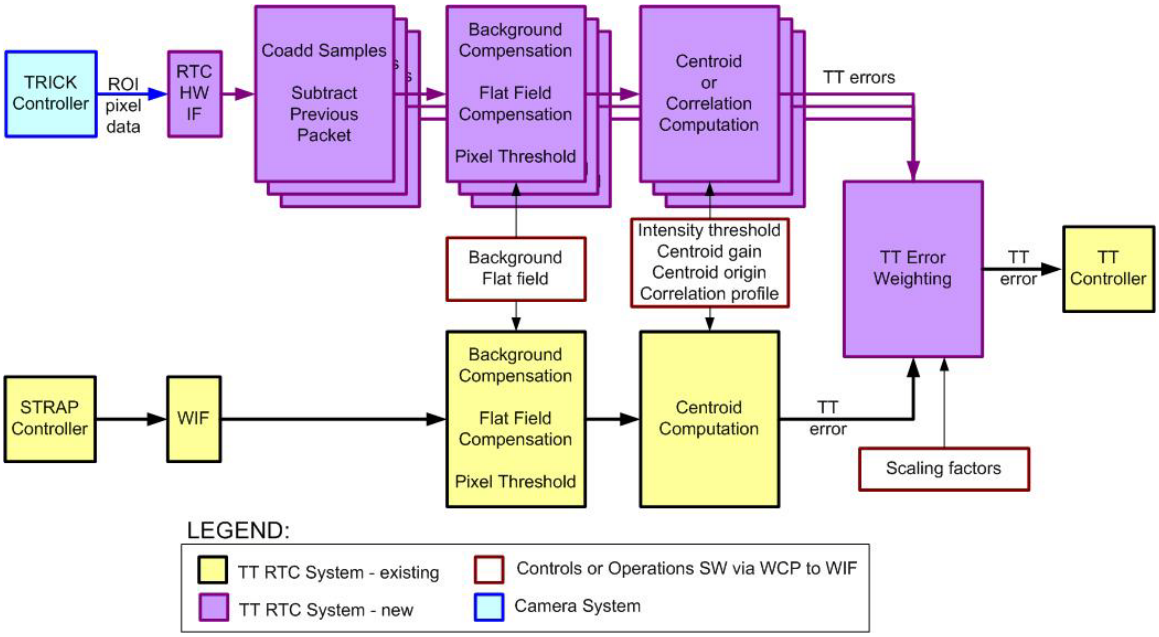

Figure 68: TT RTC Control Loop

The controller must also be capable of calculating focus from an astigmatic image. This focus value is only planned to be used for calibration (see section 2.6) and for experimental purposes (e.g. astigmatism could be introduced by the deformable mirror in order to test the on-sky utility of that approach to focus measurement).

5.4 Estimating Tip-Tilt from Multiple Stars

The purpose of this section is to review approaches to estimating tip-tilt from multiple TT stars.

Given a set of guide stars with known locations we can make measurements of the variation in position caused by atmosphere turbulence. In principle this information can be used to infer the instantaneous position of an object located in different average position on the sky. Let us call this vector deviation in direction $\boldsymbol{\Theta}_{sc}$ representing the instantaneous motion for the science direction,

$$\Theta_{sc} = \begin{bmatrix} \theta_{SCx} \\ \theta_{SCy} \end{bmatrix}. \qquad (1)$$

The subscripts x and y denote motion along two arbitrary orthogonal axes. The deviation in position for each measured guide star, Θ_i, is given by a measurement vector

$$\Theta_i = \begin{bmatrix} \theta_{ix} \\ \theta_{iy} \end{bmatrix}. \qquad (2)$$

The measurement of all n (typically 2-3) guide stars can be combined into a single measurement vector Θ_{gs} of greater dimension, given by

$$\Theta_{gs} = \begin{bmatrix} \theta_1 \\ \vdots \\ \theta_n \end{bmatrix}. \qquad (3)$$

The general minimum variance estimator is given on page 87 of Luenberger (1969). Applying this general estimator to the this problem for tip tilt in the science direction, the result is

$$\widehat{\Theta}_{SC} = \left\langle \Theta_{SC} \Theta_{gs}^T \right\rangle \left\langle \Theta_{gs} \Theta_{gs}^T \right\rangle^{-1} \Theta_{gs}. \qquad (4)$$

The notation $\langle\ \rangle$ is used to denote expectation values, superscript T is the vector transpose operation and superscript minus 1 is the matrix inverse, which is assumed to exist. An equivalent method was suggested by Don Gavel for tip tilt and low order mode estimation for the Keck NGAO project (see KAON 695 equation 46; a slightly different notation is used).

The expectation values needed to evaluate equation 4 are the covariance matrices between tip and tilt in the various directions. These can be evaluated by measurements, simulations or from theoretical considerations (the final results are given as integrals over the turbulence profile). The first covariance matrix involves the covariance between the measurements and the observation (science object) directions; this matrix can be calculated from theory or estimated from the data possibly aided by the measured turbulence profile. The second covariance matrix involves only directly measured quantities. As such it could be taken directly from measurements made at the start of an observation and updated from telemetry as the observation proceeds, to compensate for changing conditions.

An alternative to the above formalism is the modal estimation technique used by Marcos Van Dam in KAON 826. This technique uses 3 NGS tip tilt measurements, identical to the vector in equation (3) above. These measurements are then used to estimate 5 atmospheric modes. These modes are global tip and tilt in the science direction and 3 tilt anisoplanatism modes. These last 3 modes can be visualized as focus (1 mode) and astigmatism (2 modes) located above the telescope at an altitude consistent with the anticipated atmospheric turbulence profile. These three modes are used to fit the differential motion of the three NGS. This provides a better solution than just fitting global tip and tilt alone. The values of the 3 tilt anisoplanatism modes are not used in the control of the AO system.

Based on the results discussed in section 2.5.3 the estimator proposed for NGAO, a minimum variance estimator appears to work better then the modal estimator discussed in the previous paragraph. The minimum variance estimator also generalize for the case of 2 stars from the 2 star case much better than the modal estimator, which did not really work for the 2 star case at all. Using 2 stars appears to provide a large jump in performance compared to a single star.

5.5 Tip-Tilt Mirror Controller

The existing control algorithms are discussed in KAON 517. The tip-tilt mirror controller dataflow diagram is shown in Figure 69.

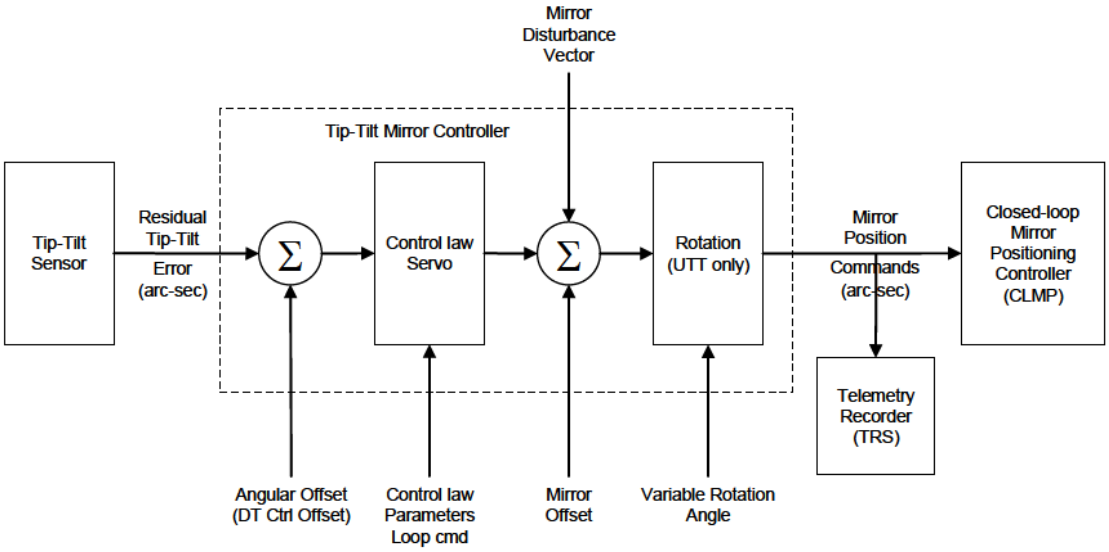

Figure 69: A dataflow diagram of the tip-tilt mirror controller

The residual tip-tilt error is received from the appropriate tip-tilt sensor via the WFP as an input *xy* pair, (C_{ix}, C_{iy}), already scaled appropriately to be in units of arcsec. When STRAP is selected as the tip-tilt sensor, the real-time APD quad-cell flux values are used in a centroid computation, without flat field compensation, and the resulting centroids are multiplied by the STRAP system matrix to convert from quad-cell units to arcsec and to convert for any rotational difference between the STRAP sensor and the (*x*, *y*) coordinate system of the tip-tilt controller:

$$\begin{bmatrix} C_{ix} \\ C_{iy} \end{bmatrix} = \begin{bmatrix} a_{11} & a_{21} \\ a_{12} & a_{22} \end{bmatrix} \begin{bmatrix} C_{Sx} \\ C_{Sy} \end{bmatrix}$$

where (C_{Sx}, C_{Sy}) are the STRAP centroids. The STRAP system matrix values are determined offline using an IDL calibration tool.

We need to modify the WFP to process the raw NIR TTS data into a residual tip-tilt error in arcsec (i.e., the left hand input shown in Figure 69). The Microgate telemetry recorder/server (TRS) will need to be modified to write NIR TTS data to disk.

6. Control Loops Overview

Prior to discussing the controls and operations software it is useful to provide an overall schematic of the control loops between the multiple subsystems. Such an overview is provided in Figure 70. The components of each of the five major systems are indicated using the color scheme shown in the legend of Figure 70, as are the relevant existing hardware components and the light path between these components.

Observations of a new target are begun by loading the pre-planned star list which includes the TT and LBWFS guide stars. An acquisition image is taken with the existing acquisition camera to center up the science target. The ROIs are located based on the star list. A TRICK camera image is taken to confirm the TT stars are appropriate and to provide the total seeing-limited flux for each TT star. The operator selects which ROIs are to be used, whether or not STRAP will also be used and what algorithm (centroid or correlation) will be used by the RTC. The camera reset time is set by the magnitude of the brightest star.

When the TT loop is closed the data from each ROI and from STRAP are sent to the RTC in order to determine the TT to be sent to the TTM. The existing offload control loop offloads the TTM to telescope pointing (and in the future we might add rotator control based on any rotation seen in the 3 TT star images).

The DAR loop is acting continuously to provide centroid origin offsets to the RTC and to reposition the STRAP x,y stage and ROI positions as appropriate. The focus control loop adjusts the position of the

STRAP and camera focus stages as a function of OSIRIS plate scale and TRICK camera wavelength. The wavelength control loop selects the appropriate dichroic and TRICK camera filter as a function of the OSIRIS science filter.

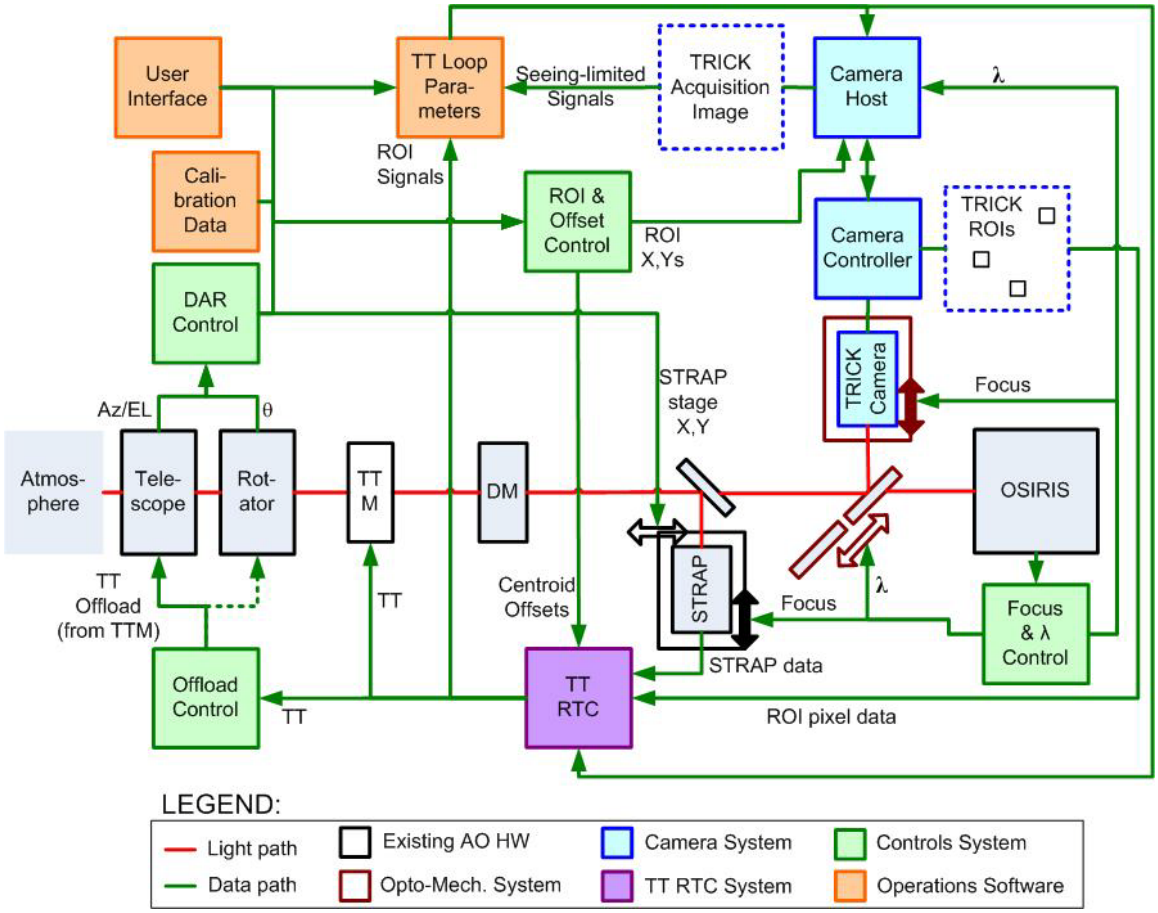

Figure 70: Control Loops Overview

Dithering is not shown explicitly in Figure 70 but in this case the TT loop is automatically opened, the ROI positions and centroid offsets, and STRAP x,y position are changed, and the TT loop is re-closed. The high order DM control loop is kept closed during this operation.

7. Controls

The controls system includes modifications to the existing AO optics bench subsystem (OBS) and supervisory controller (SC; see the SC box on the left side of Figure 64). The motion and device control listed below fall into the OBS category while the other software changes fall into the SC category.

We will present keyword interfaces throughout this section. The configuration controlled keyword list is maintained in KAON 857, which should be used as the primary keyword reference.

7.1 Motion Control

The motion control for the NIR TTS camera detector requires control of three separate 1-DoF (Degree of Freedom) devices namely:

- a stage to change between H and K band filters in the camera dewar. The filter motion control, likely a stepper motor with limit switches and a stepper controller, will be provided by the camera subsystem. Control and status of this filter wheel will be provided through keywords.
- a stage to move the desired optical pickoff into or out of the beam. It will be sufficient to position the optical pickoff and filter to the ~ 1 mm level since they are moving parallel to their optical surfaces. Note that 1 mm is small compared to the ~ 22 mm point source beam size on the optical pickoff.
- a focus stage for the relay optics and camera detector assembly to match the TTS focus to that of the science instrument OSIRIS. The focus stage should be capable of being positioned accurately enough not to significantly enlarge the diffraction-limited core (34 mas or 25 μm at H-band). From the geometric perspective if we only allowed a 5 μm blur due to defocus then this would correspond to a defocus of 13.66 x 5 μm = 68 μm, where 13.66 is the f/# input to the TTS. A positioning accuracy of ± 0.05 mm is therefore sufficient for the focus stage.

The optical pickoff (dichroic) and focus stage are identified to be 1-DoF linear position control devices. The control for these devices is provided through PMAC motion control hardware and the associated EPCOM infrastructure. The existing PMAC controller in the OBS crate has two spare channels that will be used to connect these devices. The interfaces for these devices follow the familiar 1-DoF command and feedback functionality, as well as the sequencing and state control provided by the PMAC Sequencer. EPICS channel access is used as the primary communication protocol for all devices and control loops. Keyword Task Library (KTL) instances will be defined for common user commands and feedback. These keywords will be added to the appropriate configuration files and will be made available across the Keck network.

At the device level these channels and keywords are generic and follow the standard EPCOM templates. As the PMAC controller is in the existing OBS crate, the OBS software will be modified to include 1-DoF control for these devices. The engineering DM screen for OBS will be updated to include the controls for operating these devices.

The keywords interface to control the optical pickoff is tabulated below:

Channel	Description	Type
OBTDINIT	Initialization-command-for-TTD	BOO
OBTDHALT	Halt-command-for-TTD	BOO
OBTDSTBY	Standby-command-for-TTD	BOO
OBTDNEED	Subsystem-needed-for-TTD	BOO
OBTDERRS	Error-string-for-TTD	STR
OBTDERVL	Error-status-value-for-TTD	INT
OBTDSTAT	State-of-TTD	ENUM
OBTDSTST	State-of-TTD-as-string	STR
OBTDNAME	Named-position-control-for-TTD	STR
OBTDNMCP	Named-position-use-current-position-for-TTD	BOO
OBTDNMDF	Named-position-name-to-define-for-TTD	STR
OBTDNMGO	Named-position-define-name-for-TTD	BOO
OBTDRA	Raw-value-of-TTD	INT
OBTD	User-value-of-TTD	M
OBTDRL	Relative-value-of-TTD	M

The keywords interface to control the focus stage is tabulated below:

Channel	Description	Type
OBTDRL	Relative-value-of-TTD	BOO
OBTFINIT	Initialization-command-for-TTF	BOO
OBTFHALT	Halt-command-for-TTF	BOO
OBTFSTBY	Standby-command-for-TTF	BOO
OBTFNEED	Subsystem-needed-for-TTF	STR

OBTFERRS	Error-string-for-TTF	INT
OBTFERVL	Error-status-value-for-TTF	ENUM
OBTFSTAT	State-of-TTF	STR
OBTFSTST	State-of-TTF-as-string	STR
OBTFNTFE	Named-position-control-for-TTF	BOO
OBTFNMCP	Named-position-use-current-position-for-TTF	STR
OBTFNMDF	Named-position-name-to-define-for-TTF	BOO
OBTFNMGO	Named-position-define-name-for-TTF	INT
OBTFRA	Raw-value-of-TTF	M
OBTF	User-value-of-TTF	M

7.2 Device Control

Device control software allows for controlling the camera and associated assemblies remotely so as to coordinate the operation of the instrument with the rest of the system. This includes the power supply for the detector electronics, startup and shutdown sequences, filter wheel change and dewar temperature control. In addition, parameters for image sampling and detector readout are also controlled.

The remote operation for the device control is from the Keck AO SC exchanging commands and statuses with the Camera host computer global server via keyword interface. The global server connects to device servers that contain the device specific library containing hardware module, application layer and keyword interface. A detailed description of the Camera host computer services is provided in section 4.5 of this manual.

The following sections describe the functionality in detail.

7.2.1 Power Supply Control

The SC must be able to control the on/off modes of the power supply to the combination of the camera device and associated electronics. The device must go to standby mode in the case where the power is ON for an extended period of time with no load from the device.

Fault information should be captured for troubleshooting purposes and indicated as such It can be over voltage, over current or any fault leading to the shut down of the power supply.

It is required to be able to cycle power to the power supply remotely via a remote controlled switch device (e.g., Pulizzi).

Keywords:

Channel	Description	Type
TRKPSCMD	Command PS_On/Off	ENUM (ON,OFF)
TRKPSSTS	Power supply status	ENUM (ON,OFF)

7.2.2 Startup and Shutdown

The appropriate startup sequence necessary for safe and correct operation of the device must be implemented. This includes initialization of the device control elements like the temperature setting, default filter position (blocked position in filter wheel). Upon completion of the startup sequence, the device must go to Standby state where it is ready for operation.

Device Status: should represent the current status of the camera device. Standby means it’s ready for operation. If the device is operating properly, it should indicate normal status. A fault condition of the device is to be reported in the status as such. It is desired to have a second level of detail for fault information such as device failed, or communications to host computer ie., fiber link faulty (timeout for example), or communications problem to the RTC and report any other issues with protocol like unknown command requested. A reasonable level of information exchange to satisfy safe and correct operation of the device and electronics will be defined during detailed design phase.

Shutdown of the device must incorporate the necessary sequence to shut the device down in the safe and correct manner.

Both the startup and shutdown sequences will be typically initiated by operator scripts.

Keywords:

Channel	Description	Type
TRKINIT	Initialize, reset and power up controller	INT
TRKRESET	Reset controller	INT
TRKSTAT	Status of the detector	ENUM (INIT, STANDBY, HALT, FAULT)
TRKFAULT	Detector fault status	ENUM (NO_FAULT, FAULT)

7.2.3 Filter Wheel Control

A three position filter mechanism is housed near the pupil within the camera dewar. It is necessary to have the ability to command a filter change request as per science observation, calibration or startup/shutdown demands. Interface to the filter wheel motion controller must be provided so that it can be commanded to switch positions between H, K and blocked position. The status of the filter wheel controller and the current position must be available to read.

Keywords:

Channel	Description	Type
TRFWPREQ	Filter wheel position request	ENUM (H, K, BLOCK)
TRFWCUPS	Current filter wheel position	ENUM (H, K, BLOCK)
TRFWSTAT	Status of the filter wheel controller	ENUM (NO_FAULT, FAULT)

7.2.4 Temperature Control

The NIR TTS camera detector and dewar will need to be maintained at the proper operating temperature. A Lakeshore temperature controller will be in place to accomplish the temperature control. This temperature controller will be remotely controlled from the AO SC via keywords.

Keywords:

Channel	Description	Type
TRKTCCMD	Temperature control command	ENUM (ENABLE, DISABLE)
TRKTCSTS	Temperature control status	ENUM (OK, FAULT)
TRKTCFLT	Temperature controller fault status	ENUM (NO_FAULT, FAULT)
TRKTCSV	Setpoint value for temperature controller	DBL
TRKTCTMP	Temperature reading from the controller	DBL

7.2.5 Detector Readout Control

The image transfer from the camera device occurs in two separate ways:

a) full frame image request from the AO acquisition tool in the observing software to the Camera host computer and image data served back from the Camera host computer to the AO acquisition software

b) uni-directional subframe (ROI) image transfer from Leach controller electronics to RTC

As the image data transfer to RTC is uni-directional, the SC will provide the parameters necessary to define the image to the host computer. The host computer must communicate this to the Detector controller so that it sends the appropriate image data to the RTC.

A detailed description of the detector readout scheme is provided in section X.Y in this manual.

The list of parameters involved in the image processing request and transfer is listed in the TRICK keywords.xls document (KAON 857).

Keywords:

Channel	Description	Type
TRKFRMMD	full frame mode or sub frame mode for image data transfer	ENUM (FULLFRAME_32CH, FULLFRAME_1CH, VIDEO)
TRKOBNM	Object name	STR
TRKOBTYP	Object type	STR
NUMOFROI	number of ROIs	INT
ROI1X	x pixel address corresponding to bottom left corner of ROI1	INT
ROI1Y	y pixel address corresponding to bottom left corner of ROI1	INT
ROI1SX	size in X pixels of ROI1	INT
ROI1SY	size in Y pixels of ROI1	INT
ROI1P	Periodicity of ROI1	INT
ROI1DL	Delay for ROI1	INT
ROI2X	x pixel address corresponding to bottom left corner of ROI2	INT
ROI2Y	y pixel address corresponding to bottom left corner of ROI2	INT
ROI2SX	size in X pixels of ROI2	INT
ROI2SY	size in Y pixels of ROI2	INT
ROI2P	Periodicity of ROI2	INT
ROI2DL	Delay for ROI2	INT
ROI3X	x pixel address corresponding to bottom left corner of ROI3	INT
ROI3Y	y pixel address corresponding to bottom left corner of ROI3	INT
ROI3SX	size in X pixels of ROI3	INT
ROI3SY	size in Y pixels of ROI3	INT
ROI3P	Periodicity of ROI3	INT
ROI3DL	Delay for ROI3	INT
ROIBX	x pixel address corresponding to bottom left corner of background ROI	INT
ROIBY	y pixel address corresponding to bottom left corner of background ROI	INT
ROIBSX	size in X pixels of background ROI	INT
ROIBSY	size in Y pixels of background ROI	INT
ROIBP	Periodicity of background ROI	INT
ROIBDL	Delay for background ROI	INT
ROICPR	Cycles per Reset for ROI	INT
TRKRESTIM	# of samples between resets (determined by the magnitude of the brightest star) same for all ROIs	INT
TRKSAMMD	sampling mode	ENUM (UTR, Pseudo CDS, Fowler)
TRKITIME	time between reads or integration time	DBL
TRKNUMSM	Number of samples/reads	INT
TRKNUMFM	Number of co-added frames	INT
TRKCODN	Completed frames in current coaddition sequence	INT
TRKABEXP	abort exposure	ENUM (IMMEDIATELY, AFTER READ, AFTER COADD)

TRKEXPNG	Flag to indicate exposure is in progress	ENUM (NOT EXPOSING, EXPOSING)
TRKSTSX	start a saved exposure	INT
TRKSTTX	start a test exposure	INT
TRKEXPTIM	AO-NIRTTS-take-exposure	INT
TRKCOL	Number of columns of detector	INT
TRKROW	Number of rows of detector	INT
TRKIMGTY	Type of image written to disk	ENUM (ABORTED TEST, ABORTED DATA, DATA IMAGE, TEST IMAGE)
TRKLOGCM	Comment for logging/frame header?	STR
TRKFNM	File name for saved data image	STR
TRKSVDIR	Directory to which saved files are written	STR
TRKSVRX	Save more recent test exposure	INT
TRKTSDIR	Directory to which test files are written	STR
TRKTSFN	Name of data file for test exposure	STR
TRKWREX	write each read of exposure to disk	INT
TRKIMGDN	set to 1 when image writing to disk is done	INT

7.3 Real-time controller interface

The existing real time controller for NGWFC will be modified for hardware and software changes for adding the NIR TTS. The hardware change is to the BCU board to include an interface to the camera controller via a fiber link. A continuous stream of unprocessed sub frame pixel data from the NIR TTS camera controller is sent over to the RTC via the fiber link. The data sent over to the RTC from the camera controller is not via keywords rather as byte stream over the fiber link. The table below shows the data content. The exact format of the byte stream is identified in xxx section.

Description of data	Data type
Raw pixel data packet for ROI1	Byte array
Raw pixel data packet for ROI2	Byte array
Raw pixel data packet for ROI3	Byte array
Raw pixel data packet for ROI4	Byte array
ROI1 location (bottom left x pixel address)	Byte array
ROI1 location (bottom left y pixel address)	Byte array
ROI2 location (bottom left x pixel address)	Byte array
ROI2 location (bottom left y pixel address)	Byte array
ROI3 location (bottom left x pixel address)	Byte array
ROI3 location (bottom left y pixel address)	Byte array
ROIB location (bottom left x pixel address)	Byte array
ROIB location (bottom left y pixel address)	Byte array
ROI1 X size in pixels	Byte array
ROI1 Y size in pixels	Byte array
ROI2 X size in pixels	Byte array
ROI2 Y size in pixels	Byte array
ROI3 X size in pixels	Byte array
ROI3 Y size in pixels	Byte array
ROIB X size in pixels	Byte array
ROIB Y size in pixels	Byte array
ROI1 Periodicity	Byte array
ROI2 Periodicity	Byte array
ROI3 Periodicity	Byte array
ROIB Periodicity	Byte array

ROI1 Delay in 40ns clock cycle	Byte array
ROI2 Delay in 40ns clock cycle	Byte array
ROI3 Delay in 40ns clock cycle	Byte array
ROIB Delay in 40ns clock cycle	Byte array
Reset Packet	Byte array

The RTC software is modified for processing the raw pixel data, calculating centroid estimate and using the centroid to control the existing down link tip-tilt mirror. The software to be implemented is described in KAON 824 Statement of Work for Microgate.

In addition to the image data processing, the interface between the RTC and AO SC will be modified to exchange data for user tools, control loop parameters and optimization parameters. The interface between the NGWFC RTC and the AO SC and User Tools is through the Wavefront Controller Command Processor (WCP) on the AO side and the Wavefront Controller Interface (WIF) on the NGWFC RTC side. These will be modified to process additional commands required for the NIR TTS project. The details are discussed below by functionality. Note that the set of functionality that already exists for the WFS and STRAP that remains unchanged is not described here.

7.3.1 Measurement Selection

Currently, the source of the measurement for the tip-tilt control changes depending on the operating mode of the science observation. This function will be extended to include the choice of measurement based on user selection and includes NIR TTS measurement as well as a parallel operation of STRAP and NIR TTS. The table below shows the current functionality and the new additions (last two rows in the table)

Operating Mode / User selection	**Measurement used for DTT Mirror control**
NGS	WFS
LGS	STRAP
Dual NGS	STRAP
LGS + NIR TTS	NIR TTS
Dual NGS + NIR TTS	NIR TTS
LGS + STRAP + NIR TTS	STRAP + NIR TTS

The keyword that allows this already exists and it is listed below.

Keywords:

Channel	Description	Type
DTSENSOR	Select WFS, STRAP, NIRTTS or STRAP+NIRTTS	ENUM (WFS, STRAP, NIRTTS, STRAP_NIRTTS)

7.3.2 Number of Samples to Co-Add

The number of samples to coadd is a function of the brightness of the star. Fainter stars need more samples to be coadded as opposed to bright stars. While the logic for determining the optimal number of samples to be coadded for a guide star is implemented in the observing user software and maintained in a set of keywords, these parameters must be communicated to the RTC for processing the raw pixel data via the WIF command set.

Keywords:

Channel	Description	Type
TRKNMAD1	Number of samples to coadd for ROI1	INT
TRKNMAD2	Number of samples to coadd for ROI2	INT
TRKNMAD3	Number of samples to coadd for ROI3	INT
TRKNMADB	Number of samples to coadd for background ROI	INT

The WIF command set is SET/GET NUMBER OF COADDS.

7.3.3 Intensity Threshold

Upon processing the pixel data for an ROI, the value of the processed pixels is checked against a threshold number that is predetermined by the user. If the pixel intensity exceeds the threshold value, then the pixel data should not be used. This threshold value is maintained in a keyword and communicated to RTC via the WIF command set.

Keywords:

Channel	Description	Type
TRKINTH	intensity threshold for NIR TTS	DBL

The WIF command set is SET/GET INTENSITY THRESHOLD.

7.3.4 Sky Background

To reduce the effects of the sky background it's measurement will be maintained as an array in a set of keywords and communicated to the RTC via WIF commands.

Keywords:

Channel	Description	Type
TRKRO1BG	background for ROI1	DBL Array
TRKRO2BG	background for ROI2	DBL Array
TRKRO3BG	background for ROI3	DBL Array

The WIF command set is SET/GET BACKGROUND.

7.3.5 Flat Field

Flat fields in the H and K band configurations for photometric and gain responses will be calibrated by calibration routines in the observing user software. These flat field gains must be used by the RTC as scaling factors as part of data processing. The flat field gain responses will be maintained in a set of keywords and communicated to the RTC via WIF command set.

Keywords:

Channel	Description	Type
TRKRO1FF	flat field for ROI1	DBL Array
TRKRO2FF	flat field for ROI2	DBL Array
TRKRO3FF	flat field for ROI3	DBL Array

The WIF command set is SET/GET FLAT FIELD.

7.3.6 Algorithm Type

A script in the observing software will determine the type of algorithm to be used, maintained in a keyword set that will be communicated to the RTC via WIF command set.

Keywords:

Channel	Description	Type
TRKRO1AL	Type of algorithm Centroid/Correlation	BOO
TRKRO2AL	Type of algorithm Centroid/Correlation	BOO
TRKRO3AL	Type of algorithm Centroid/Correlation	BOO

The WIF command set is SET/GET ALGORITHM TYPE.

7.3.7 Reference Image

To implement the correlation algorithm, a reference image is required. The reference image is determined offline and maintained in keywords to be sent to the RTC via WIF command set.

Keywords:

Channel	Description	Type
TRKRO1RI	reference image r[i,,j] for ROI1	DBL Array
TRKRO2RI	reference image r[i,,j] for ROI2	DBL Array
TRKRO3RI	reference image r[i,,j] for ROI3	DBL Array

The WIF command set is SET/GET REFERENCE IMAGE.

7.3.8 Centroid Gain

The centroid gain to be used on each ROI is an optimization parameter that will be maintained in keywords to be sent to RTC via WIF command set.

Keywords:

Channel	Description	Type
TRKRO1CG	Centroid gain for ROI1	DBL
TRKRO2CG	Centroid gain for ROI2	DBL
TRKRO3CG	Centroid gain for ROI3	DBL

The WIF command set is SET/GET CENTROID GAIN.

7.3.9 Weighting Factor

Combining centroid data from multiple ROIs and STRAP begs the need for weighting factors to apply on the centroids. The weighting factors depend on magnitudes of the tip-tilt stars, their off-axis distance and the relative performance of NIR TTS versus STRAP. These weighting factors are determined in the observing software and maintained in keywords to be sent to RTC via WIF command set.

Keywords:

Channel	Description	Type
TRKROIWT	weighting factor to be applied to TT error for combining centroids	2D DBL Array

The WIF command set is SET/GET WEIGHTING FACTORS.

7.3.10 Centroid Offset

The dynamic offset correction from differential atmospheric refraction and non-sidereal tracking moves the star image on the detector during the course of science exposure. The position of the centroid offset to which the tip-tilt mirror should drive the star image and the location of the ROI will be periodically updated. The updated centroid offset will be sent to the RTC via WIF command set.

Keywords:

Channel	Description	Type
TRKRO1CO	centroid offset to be applied for ROI1	DBL Array
TRKRO2CO	centroid offset to be applied for ROI2	DBL Array
TRKRO3CO	centroid offset to be applied for ROI3	DBL Array
TRKROBCO	centroid offset to be applied for background ROI	DBL Array

The WIF command set is SET/GET CENTROID OFFSET.

7.3.11 Interaction Matrix

To account for flips/orientation and rotation between the DTT mirror actuator and the NIR TTS image, an interaction matrix is used. This is determined at the time of initial optics alignment and maintained in keyword to be communicated to RTC via WIF command set.

Keywords:

Channel	Description	Type
TRKINTMT	Interaction matrix to address flips/orientation/rotations between DTT mirror actuator and NIR TTS	DBL Array

The WIF command set is SET/GET INTERACTION MATRIX.

Note that in the operating mode with NIR TTS and STRAP in parallel, the interaction matrix for NIR TTS will be applied to the NIR TTS data and the interaction matrix for STRAP will be applied to STRAP data before combining the two data sets.

7.3.12 ROI Location Change

If the dynamic offset from DAR and non-sidereal calculations were to put the centroid location outside the current ROI boundary, then a flag is issued to the RTC to notify of the ROI location change along with the new centroid offset value. Upon reading this flag, RTC will maintain the centroid offset in a buffer and will wait to read the change in the ROI location in the next data packet for when this centroid offset is to be applied.

Keywords:

Channel	Description	Type
TRKRO1CH	Flag to indicate change in ROI location for ROI1	BOO
TRKRO2CH	Flag to indicate change in ROI location for ROI2	BOO
TRKRO3CH	Flag to indicate change in ROI location for ROI3	BOO
TRKROBCH	Flag to indicate change in ROI location for background ROI	BOO

The WIF command set is SET/GET ROI CHANGE.

7.3.13 Focus Conversion

A focus conversion parameter for each ROI is determined offline in the observing software and maintained in keywords to be communicated to the RTC via WIF command set.

Keywords:

Channel	Description	Type
TRKFOC1C	Focus conversion parameter for ROI1	DBL
TRKFOC2C	Focus conversion parameter for ROI2	DBL
TRKFOC3C	Focus conversion parameter for ROI3	DBL

The WIF command set is SET/GET FOCUS CONVERSION.

7.3.14 Correlation Metric

The effectiveness of the correlation algorithm is computed in the RTC and maintained as an average number. This is for diagnostic purposes to determine if the correlation algorithm is working and/or if atmospheric condition changes demands a new reference image to be sent to the RTC. This is read back from the RTC via WIF command into keywords to be used by the observing software.

Keywords:

Channel	Description	Type
TRKRO1CM	average metric for effectiveness of correlation algorithm for roi1	DBL
TRKRO2CM	average metric for effectiveness of correlation algorithm for roi2	DBL
TRKRO3CM	average metric for effectiveness of correlation algorithm for roi3	DBL

The WIF command set is GET CORRELATION COEFFICIENT.

7.3.15 Focus

Focus error is measured in the RTC for each ROI. This is read back from the RTC via WIF command into keywords to be used by the observing software and focus control in the AO Supervisory Controller.

Keywords:

Channel	Description	Type
TRKFOC1	Focus value calculated by RTC for ROI1	DBL
TRKFOC2	Focus value calculated by RTC for ROI2	DBL
TRKFOC3	Focus value calculated by RTC for ROI3	DBL

The WIF command set is GET FOCUS.

7.3.16 Centroid

Centroid calculated by RTC for each ROI is communicated via WIF command to keywords used by the observing software.

Keywords:

Channel	Description	Type
TRKRO1CE	centroid value calculated by RTC for ROI1	DBL
TRKRO2CE	centroid value calculated by RTC for ROI2	DBL
TRKRO3CE	centroid value calculated by RTC for ROI3	DBL

The WIF command set is GET CENTROID.

7.3.17 Pixel Intensity

The average pixel intensity or flux for each ROI is calculated by RTC and communicated via WIF command to keywords used by the observing software.

Keywords:

Channel	Description	Type
TRKRO1PI	pixel intensity for ROI1 (average)	DBL
TRKRO2PI	pixel intensity for ROI2 (average)	DBL
TRKRO3PI	pixel intensity for ROI3 (average)	DBL
TRKROBPI	pixel intensity for background ROI (average)	DBL

The WIF command set is GET AVG PIXEL INTENSITY.

7.3.18 Error Counter

An error detection and recovery scheme is in place to identify loss of packet synchronization between the camera controller and RTC. In the event that a word is dropped or header word is corrupted during transmission over the fiber link, a counter is incremented in the RTC.

Keywords:

Channel	Description	Type
TRKERCNT	error counter incremented upon wrong data from camera	INT

The WIF command set is GET ERROR STATS.

7.4 Telemetry

7.4.1 Full Data Telemetry

A new table similar to the existing STRAP table is needed to log following NIR TTS related data variables. This will allow for optimization during observations, offline analysis and data retrieval. The new table will be called NIRTTS and will log the data at the full NIR TTS read rate that may or may not be synchronous with the WFS frame rate.

Variable	**Data type**
PIXEL INTENSITY IN EACH ROI (SET OF 3 + background)	FLOAT ARRAY
FOCUS VALUE FOR EACH ROI (SET OF 3)	FLOAT
METRIC FOR EFFECTIVENESS OF CORRELATION ALGORITHM FOR EACH ROI (SET OF 3)	FLOAT

The current “dttcentroids” field in the STRAP database table will contain the combined centroid TT error when the DTSENSOR is configured for LGS, Dual NGS, NIRTTS, STRAP+NIRTTS modes.

7.4.2 Averaged Telemetry Variables

The current implementation of averaged telemetry computation that includes *continuous telemetry* data and *on demand* data stream will be expanded to include NIR TTS related data variables.

Continuous data stream accumulates samples for the defined variables until a user defined period has expired, then calculates the average and saves the result to be read by WIF. The following NIR TTS variables will be added to the existing variable list.

Configuration Parameter	Data type
PIXEL INTENSITY FOR EACH ROI (SET OF 3 + background)	FLOAT
CENTROID VECTOR FOR EACH ROI (SET OF 3)	FLOAT ARRAY
FOCUS FOR EACH ROI (SET OF 3)	FLOAT
METRIC FOR EFFECTIVENESS OF CORRELATION ALGORITHM FOR EACH ROI (SET OF 3)	FLOAT

On demand data stream is computed similar to continuous data stream with the exception that accumulation is initiated by a WIF command. A single accumulation and average computation is performed until a new request arrives. At the moment, no changes are foreseen in this implementation.

7.4.3 Configuration Parameters

The database table for configuration parameters (paramidtypes) will be updated to include NIR TTS related configuration parameters. The configuration parameters table primarily contains key system configuration parameters and is not stored in real time at the data frame rate rather once at system startup and thereafter whenever any specific parameter changes. The parameter save is combined with the unique configuration ID value as a means to keep track of when the configuration parameters were saved. This archiving of the configuration parameters is useful in interpreting diagnostic data and reconstructing the system history for exact operating mode/configuration for each data frame during post processing. The following NIR TTS related configuration parameters will be added to this table.

Configuration Parameter	Data type
BACKGROUND FOR EACH ROI (SET OF 3)	FLOAT ARRAY
FLAT FIELD FOR EACH ROI (SET OF 3)	FLOAT ARRAY
TYPE OF ALGORITHM (CENTROID/CORRELATION) (SET OF 3)	INT
REFERENCE IMAGE FOR EACH ROI (SET OF 3)	FLOAT ARRAY
INTERACTION MATRIX	FLOAT ARRAY
CENTROID GAIN FOR EACH ROI (SET OF 3)	FLOAT ARRAY
WEIGHTING FACTOR TO BE APPLIED TO TT ERROR FOR COMBINING CENTROID ERRORS FROM ROIS AND STRAP	FLOAT 2D ARRAY
FOCUS CONVERSION PARAMETER FOR EACH ROI (SET OF 3)	FLOAT
PIXEL INTENSITY THRESHOLD	FLOAT
NUMBER OF SAMPLES TO COADD (SET OF 3 + background)	INT
PIXEL NUMBER FOR ROI X POSITION (SET OF 3 + background)	INT
PIXEL NUMBER FOR ROI Y POSITION (SET OF 3 + background)	INT
ROI SIZE X (SET OF 3 + background)	INT
ROI SIZE Y (SET OF 3 + background)	INT
ROI SIZE Periodicity (SET OF 3 + background)	INT
ROI SIZE Delay (SET OF 3 + background)	INT
ROI SIZE Cycles Per Reset	INT

Note: the current configuration parameter for saving DTSENSOR will include the appropriate enumeration value for NIRTTS and STRAP+NIRTTS in addition to the currently defined NGS, LGS and Dual NGS values.

7.5 ROI location and Centroid Offset Computation

The acquisition tool along with the AO guide star tool has the location of the science target and guide stars in RA/Dec units of the telescope. When the target guide star is selected, the acquisition software sends the RA/Dec, equinox, epoch information directly to the telescope pointing subsystem. The pointing subsystem converts the target positions and position angle to azimuth and elevation mount coordinates as well as physical rotator angles. The pointing subsystem produces the azimuth and elevation demands to drive the telescope to the desired mount position and to track the desired object on the sky. The pointing subsystem coordinates the slewing of the telescope position with the auto-guider subsystem. Since this offset is handled exclusively by the telescope control system and the necessary infrastructure is currently in place, no changes are anticipated for the NIR TTS sensor implementation. The only addition is the change to the existing acquisition script to compute the ROI locations and populate the keywords reserved for them.

The SC will also send the ROI locations and sizes to the NIR TTS host computer. The keywords of interest for the NIR TTS from the acquisition process are listed below:

Channel	Description	Type
TRKRO1X	X pixel address corresponding to bottom left corner of ROI1	INT
TRKRO1Y	Y pixel address corresponding to bottom left corner of ROI1	INT
TRKRO1SX	Size of ROI1 in X pixels	INT
TRKRO1SY	Size of ROI1 in Y pixels	INT
TRKRO2X	X pixel address corresponding to bottom left corner of ROI2	INT
TRKRO2Y	Y pixel address corresponding to bottom left corner of ROI2	INT
TRKRO2SX	Size of ROI2 in X pixels	INT
TRKRO2SY	Size of ROI2 in Y pixels	INT
TRKRO3X	X pixel address corresponding to bottom left corner of ROI3	INT
TRKRO3Y	Y pixel address corresponding to bottom left corner of ROI3	INT
TRKRO3SX	Size of ROI3 in X pixels	INT
TRKRO3SY	Size of ROI3 in Y pixels	INT
TRKROBX	X pixel address corresponding to bottom left corner of background ROI	INT
TRKROBY	Y pixel address corresponding to bottom left corner of background ROI	INT
TRKROBSX	Size of background ROI in X pixels	INT
TRKROBSY	Size of background ROI in Y pixels	INT

7.5.1 Image Shift from Pickoff

The ROI locations can be influenced by the pickoff optic used in the NIR TTS since the pickoffs are likely to have slightly different tilts. The result of the tilt is an image shift. The K type pickoff will be used as the reference and image shift for the other pickoffs will be calibrated in Xim,Yim coordinate units and stored as pickoff shift parameter in k1aoScNIRTTSPickoff.par file. When the pickoff is changed, the corresponding image shift is read in the observing script code to account for the offset in the ROI locations of the guide stars. This is read once at the beginning of the observing setup as it is constant per the configuration of observing.

Keywords:

Channel	Description	Type
AOTRPKPX	Offset to X position in NIR TTS Xim/Yim coordinates for the current pickoff selected	INT
AOTRPKPY	Offset to Y position in NIR TTS Xim/Yim coordinates for the current pickoff selected	INT

7.5.2 Image Shift from Plate Scale of Science Instrument (OSIRIS)

A change in the plate scale in the science instrument will also change the image position on the science instrument. OSIRIS supports four different plate scales (0.02, 0.035, 0.05, 0.1 arcsec per pixel) for the spectrograph and a 0.02 plate scale for the imager. A change in the plate scale configuration necessitates an offset to be accounted for in the ROI locations of the guide stars. The offset in NIR TTS Xim/Yim coordinate units is maintained for each of the plate scale configurations in k1aoScNIRTTSOsiris.par file. This is read in the IDL script code during the observing setup procedures.

Keywords:

Channel	Description	Type
AOTROSPX	Offset to X position in NIR TTS Xim/Yim coordinates for the current OSIRIS plate scale	INT
AOTROSPY	Offset to Y position in NIR TTS Xim/Yim coordinates for the current OSIRIS plate scale	INT

7.5.3 Image Shift from Distortion and Field Curvature in Either OSIRIS or NIR TTS

The field curvature in OSIRIS spectrograph and the imager as well as NIR TTS causes image moves from the optical axis. Image shift also occurs from distortion. These will be pre-calibrated for OSIRIS and the NIR TTS combined together and accounted for as offset to the location of the guide stars. As the instrument is not currently available and the effects of the distortion map unknown at this point, provision is made for accommodating the distortion map in the form of a look up table or a polynomial curve fit. Either way, the offsets are position dependent and different regions on the detector will have a set of x,y offsets expressed in NIR TTS Xim,Yim coordinate units. Each ROI will pick the x,y offsets corresponding to the region. The field curvature and distortion offsets are applied as part of ROI calculation in the acquisition software during the day time preparation for the observation.

Keywords:

Channel	Description	Type
AOTROSSX	Offset to X position in NIR TTS Xim/Yim coordinates from distortion map	INT
AOTROSSY	Offset to Y position in NIR TTS Xim/Yim coordinates from distortion map	INT

7.5.4 User Requested Offset (including dither and nod requests)

The user requested offset is generally known as the hand paddle offset that directly interfaces with the telescope controls. The user offset is currently entered via an operator GUI in RA/Dec units as RA/Dec offsets (keywords RAOFF, DECOFF) and these are processed by the pointing subsystem to slew the telescope to the desired target position.

Dither correction adds prescribed offsets according to a dither pattern defined in a script with the offsets defined in RA/Dec units. This is similar to the user requested offset. Nod is an offset position defined by the user in RA/Dec units also.

Therefore the user offset, dither and nod are all treated the same way. A sequence of events occurs with interaction between the AO and telescope controls as shown in the Figure 71 flowchart.

The resume positions provided by the telescope control system are processed in the AO Supervisory Controller for the FSM and TSS. These same positions are converted to NIR TTS Xim/Yim coordinates to relocate the ROI and compute the new centroid offsets to be sent to the RTC. If the ROI location changes, these must be sent to the NIR TTS Host computer.

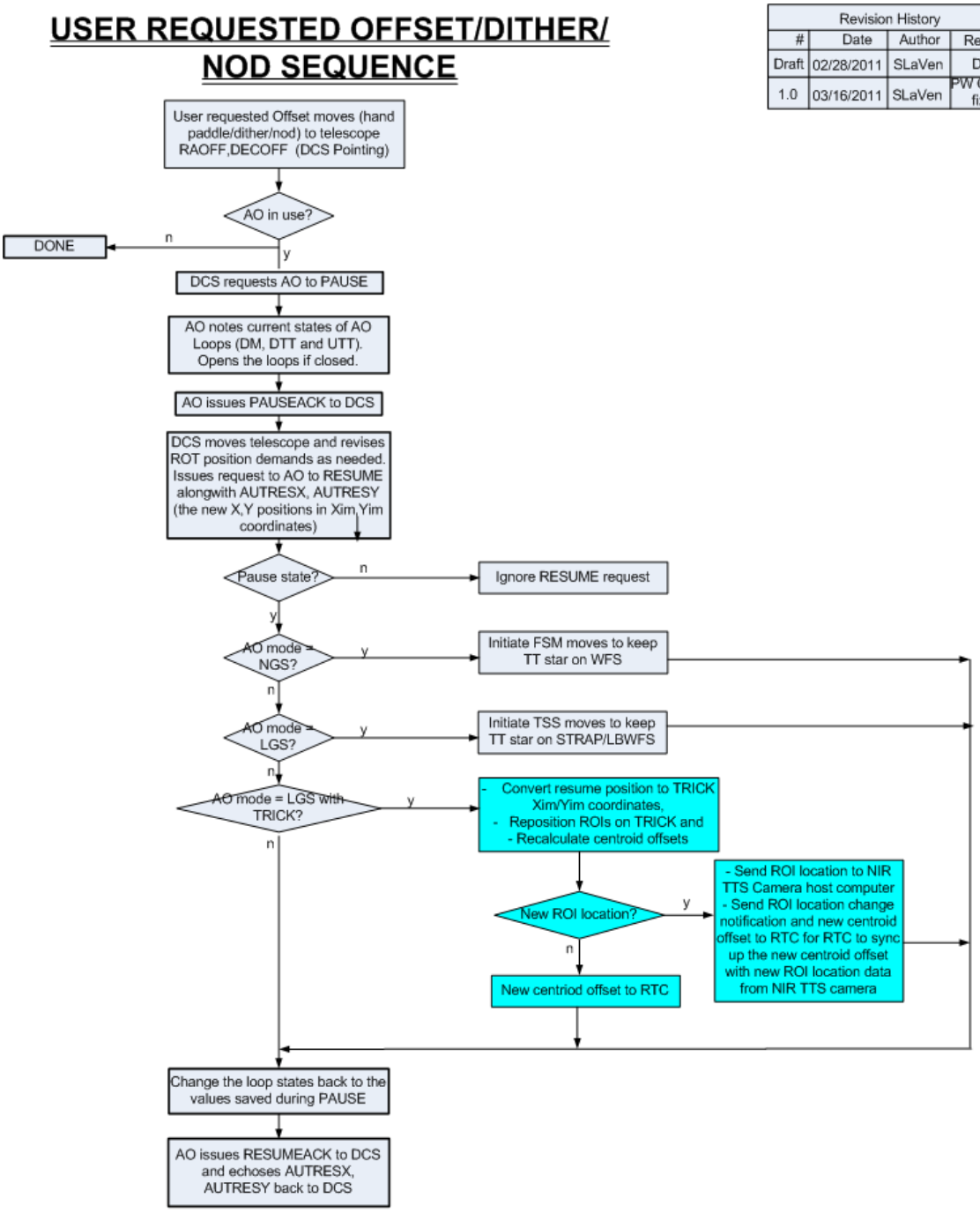

Figure 71: User requested offset/dither/nod sequence

Keywords:

Channel	Description	Type
AUTRESX	Resume X position from telescope to AO controls for user requested offset including dither and nod	INT
AUTRESY	Resume Y position from telescope to AO controls for user requested offset including dither and nod	INT

7.5.5 Differential Atmospheric Refraction Compensation

The DAR offset controller is responsible for calculating and compensating for the affects of DAR in order to keep the science object fixed on the science instrument. DAR is a relative calculation based on the difference in wavelength between the science instrument and the sensor measuring TT. The effective wavelengths of the science instrument and TTS are functions of their relative filters and of colors of the science object and TT object, respectively. The amount of DAR changes with telescope elevation and its orientation is in the direction of the vertical angle on the AO bench.

The OSIRIS side of DAR is already in place. The TTS side of the code is already in place for NGS AO mode when the NGS WFS is used for TT tracking and for LGS mode when STRAP is used for TT tracking. The code should be in updated to use the NIR TTS for LGS and NGS AO.

A second DAR will be implemented for the center wavelength of the NIR TTS. The wavelength will change between usage of the H-band and K-band filters in the NIR TTS camera. DAR tracking is automatically turned on whenever the TT loop is closed and the detector for NIR TTS is selected. DAR can also be enabled during acquisition by the user. The DAR offset in NIR TTS Xim,Yim coordinates will be summed in the final summation block discussed in section 7.5.7.

Keywords:

Channel	Description	Type
TRKDARX	DAR controller offset for NIR TTS in NIR TTS Xim/Yim coordinate for X position	INT
TRKDARY	DAR controller offset for NIR TTS in NIR TTS Xim/Yim coordinate for Y position	INT
TRKDAREN	Enable DAR	BOO

7.5.6 Non-Sidereal Tracking

A goal is to support non-sidereal tracking. This mode is already supported by STRAP so it is not a high priority. This mode will be feasible with the NIR TTS since the centroid offset can be constantly updated and the ROI can be changed between exposures. The goal of maintaining the science object position to 10 mas for a 50 arcsec per hour non-sidereal object would require changing the centroid offset by 5 mas every 0.36 seconds and changing the ROI by 1 pixel (50 mas) every 3.6 seconds. Currently we plan to consider this mode during the design phase but will not implement it at least initially.

The non-sidereal tracking offset to move the guide star at the velocity and in the opposite direction to the moving science object so as to keep the science object on the science instrument has already been implemented via IDL scripts. The script updates the non-sidereal offset correction in RA/DEC arcsec units and sends the correction directly to the telescope pointing system. The script also updates the incremental changes to the tip-tilt stage position via keywords AOTSDX and AOTSDY. These keywords must be read, converted to NIR TTS camera coordinates and added to the final summation block discussed in section 7.5.7.

Keywords:

Channel	Description	Type
AOTSDX	Non-sidereal correction in AO bench Xim/Yim coordinate for X position	INT
AOTSDY	Non-sidereal correction in AO bench Xim/Yim coordinate for Y position	INT

7.5.7 Region of Interest and Centroid Offset Determination

This section describes the determination of the offsets to be sent to the RTC and the NIR TTS host computer.

The fixed and dynamic offsets are summed together as shown in Figure 72. The non-sidereal offset correction is converted to Xim,Yim coordinates before being added in the summing block.

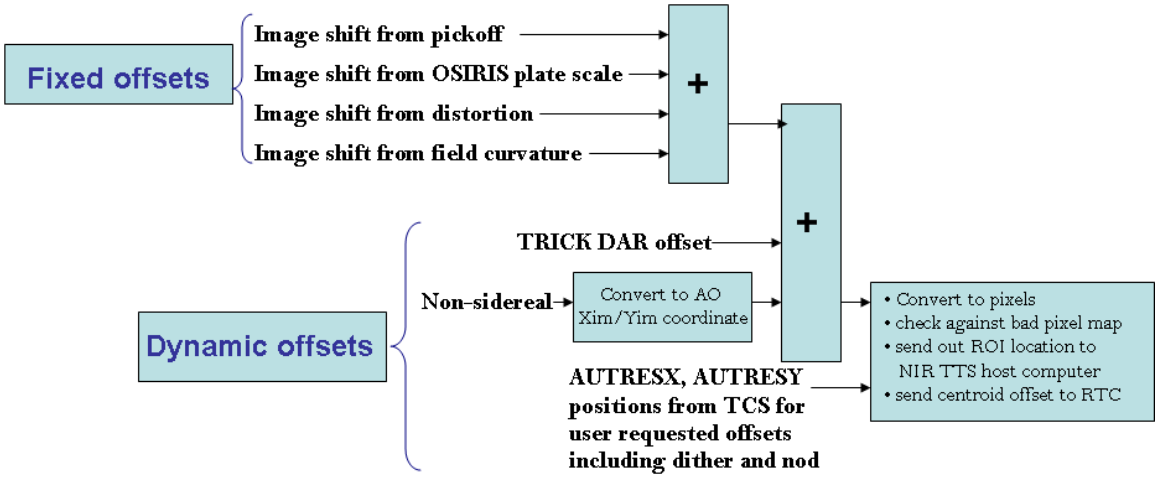

Figure 72: ROI offset and centroid offset calculation

The output of the summation block is converted to NIR TTS pixel units. The new offset is added to the previous centroid offset. The closest integer number of pixels in each axis is added to the previous ROI location to determine the new ROI location to be communicated to the NIR TTS camera host computer. The remainder is the new centroid offset to be communicated to the RTC along with a ROI location change notification. The RTC will wait to read the next data packet with the corresponding ROI change to apply the new centroid offset.

Keywords:

Channel	Description	Type
TRKRO1CO	Centroid offset to be applied to ROI1	INT (array)
TRKRO2CO	Centroid offset to be applied to ROI2	INT (array)
TRKRO3CO	Centroid offset to be applied to ROI3	INT (array)
TRKROBCO	Centroid offset to be applied to background ROI	INT (array)

If the ROI location is changed it must be checked against the bad pixel map to ensure that the ROI doesn't include any bad pixels. Should the new ROI location include bad pixels, a warning must be issued to the operator to intervene.

7.6 Focus Compensation Control

In the current system the focus position of the NGS WFS or LBWFS/STRAP are automatically adjusted when the science instrument configuration (e.g. plate scales, filters, IFU or imager) is changed. The same correction will need to be applied to the NIR TTS focus stage when the NIR TTS is being used.

The field curvature for the NIR TTS must be measured as a calibration. A focus algorithm has to be developed once the field curvature measurement is made. The algorithm should account for the field curvature of OSIRIS as well. The focus controls will be implemented to control the NIR TTS focus stage.

Keywords:

Channel	Description	Type
TRKFOCLP	Focus control loop enable/disable	BOO
TRKFOCGN	Focus control parameters	DBL (array)
AOFCC0TR	NIR TTS specific C0 parameter	DBL
AOFOCERR	Focus error	DBL

7.7 Sodium Altitude Correction

Currently the LBWFS focus measurement is used to adjust the calculated altitude of the sodium layer which is in turn used to adjust the position of the WFS focus stage in order to keep the WFS conjugate to the sodium layer (a zero LBWFS focus measurement means that the WFS is conjugate to the sodium layer). The NIR TTS offsets the potential of a higher bandwidth focus measurement. This is currently a goal for the NIR TTS. The RTC is being designed to provide a focus measurement from each ROI.

Keywords:

Channel	Description	Type
TRKFOC1C	Focus conversion parameter for ROI1 to RTC	DBL
TRKFOC2C	Focus conversion parameter for ROI2 to RTC	DBL
TRKFOC3C	Focus conversion parameter for ROI3 to RTC	DBL
TRKFOC1	Average focus error measured by RTC for ROI1	DBL
TRKFOC2	Average focus error measured by RTC for ROI2	DBL
TRKFOC3	Average focus error measured by RTC for ROI3	DBL
TRKFCROI	Select which ROI to be used for focus control	INT

7.8 Rotator Control

Three stars on the NIR TTS would provide enough information to tell you whether the AO rotator was tracking properly. We are not currently planning to use this information to correct the rotator position or tracking rate. However if the rotator did not track adequately then we would find that the off-axis TT stars were giving a radial dependent TT error in the direction of the rotation error. If we discover this to be the case then we will need to add a future upgrade to provide a feedback control loop to the rotator to hold the TT star positions.

8. Operations Software

The Keck I LGS AO operations software (the items shown in the User Tools box in Figure 64 plus some pre-observing tools) will need to be modified and added to in order to integrate the TTS system.

8.1 Pre-Observing Software

8.1.1 AO Guide Star Selection Tool

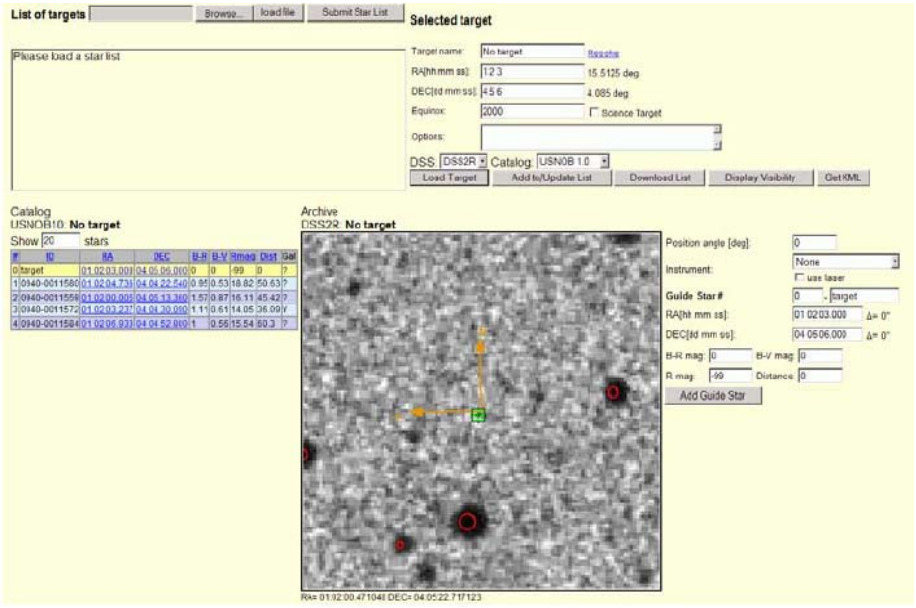

Figure 73: Existing AO Guide Star Tool Web Page

The selection of natural guide stars (NGS) is a crucial factor in determining the feasibility of any mode of AO observations. For the current Keck II AO system, the need to select NGS in proximity to astronomical targets is done using the AO Guide Star Tool (see Figure 73). This tool queries the USNO, 2MASS, and the Hubble Guide Star Catalogs (GSC). It also displays images from the Digitized Sky Survey (source of GSC catalog) with overlays representing the instrument field of view and AO field of regard (also known as technical field of view). The guide star tool is used to generate a star list that is compatible with the Keck format. The star list is the main interface between the telescope acquisition software and the AO user tools (aoacq.pro specifically). This interface ensures that the intended science target is observed with minimal overhead.

It is anticipated that the NIR TTS system will use from one to three IR tip-tilt stars. In addition, the observer might also want to consider using the current STRAP sensor which has peak sensitivity in the visible (R band) on some targets instead. In either case, the observer will still need to select a visible band star for the LBWFS which helps to compensate for changes in the sodium layer structure and range. Another consideration is that the NIR TTS system will use dichroics to select which part of the NIR bands is sent to the NIR TTS sensor and OSIRIS. An observer will have to evaluate which of several possible dichroic choices is optimal.

The main interface between the AO guide star selection tool and the AO setup software is the star list file. Currently the star list is a text file. It must conform to certain formatting conventions (see the current Keck Star List format). New flags will be needed for the star list to make it compatible with both visible and NIR tip-tilt stars. Details of the new format are included in a later section. The proposed AO guide star selection tool for the NIR TTS is to modify the current web based tool to work with additional catalogs and more complex guide star configurations. The anticipated changes and the rationale for them are detailed in the following sections.

8.1.1.1 New Star Catalogs

The NIR sensor will use stars as faint as K~16 for tip-tilt correction. This is fainter than the completeness limit of the current standard NIR all sky star survey 2MASS. With the current version of the guide star selection tool it is possible to use the following catalogs: USNO B, Sloan Digital Sky Survey (SDSS), 2MASS point source, and GSC-2. Currently the ability to select SDSS has been disabled because it did not cover the full sky. It is recommended that SDSS be put back into service for the NIR TTS project. Lack of full sky coverage is not an issue for AO guide star selection. In particular, the SDSS covers the north galactic pole where the guide star density is low so having that catalog to cover those areas is desirable. In general, the SDSS survey gives superior photometric and astrometric information than surveys based on photographic plates such as USNO and GSC-2.

In the case of catalogs such as SDSS or GSC-2 that do not include measurements in the NIR, conversions can be made using several of the cataloged bands and the proper formula. Because of its anticipated use with JWST, several studies have been performed on the conversion of GSC-2 and SDSS magnitudes to near infrared magnitudes:

1. Kriss and Stys, “The Suitability of Guide Star Catalog 2 (GSC-2) as a Source for JWST Guide Stars”, STScI-JWST-R-2002-0002, 2003.
2. Nelan, et al., “Operational Work-Around for Meeting the 95% Guide Star Acquisition Rate for JWST”, STScI-JWST-R-2003-0001A, 2003.
3. Chayer and Nelan, “Algorithms for Transforming GSC-II Magnitudes into the NIR”, JWST-STScI-001410, April 14, 2008.
4. Hutchings, et al., “Faint Objects at High Galactic Latitude in the Sloan Digital Sky Survey”, PASP 119, 2007.
5. Bilir, et al., “Transformations between 2MASS, SDSS and BVRI Photometric Systems: Bridging the Near Infrared and Optical”, MNR, 384, pp. 1178-1188, 2008.

Kriss and Stys find that GSC-2 is complete to magnitudes slightly fainter than J = 17, which is similar to the NIR TTS magnitude limit of K~16 assuming a late spectral type for the average field star. The AO guide star selection tool would be modified to perform the magnitude conversion to NIR bands as needed

on queries made from visible band catalogs such as GCS 2.3 or the SDSS. At present, this same technique will be used for JWST, as they do not plan to issue future electronic versions of the GSC merged with 2MASS or SDSS catalogs. The AO guide star selection tool currently converts 2MASS magnitudes to R band for STRAP.

Future visible and IR catalogs will provide fainter NIR guide stars than the current 2MASS catalog. Examples of such upcoming surveys include UKIDSS, WISE, and Pan STARRS. Most current and new catalogs have adopted a format that makes for easy web based queries. However it is not clear if all future catalogs will support the Virtual Observatory (VO) standard format. Future catalogs will need to be dealt with on a case-by-case basis as they become available, as updates to the AO guide star selection tool.

8.1.1.2 Cross Reference Star Catalogs

With the NIR TTS system the user will need to select both infrared and visible band stars. At present, for a selected science target, the guide star tool can display a list of possible NGS guide stars from one of several catalogs. The displayed lists often have the same star from several catalogs; the user is left to cross reference and cross check these lists manually. Although a single cross check list is highly desirable, it appears difficult to produce a consistently high quality final listing. The catalogs currently available are not based on the same methodology, have different limiting magnitudes, and different errors in star positions. A related issue is the user wait time when many catalogs are queried at the same time and then merged. Cross checking a guide star between catalogs will remain the responsibility of the user.

The listing of possible guide stars from catalog queries should display the following information in a standard layout:

> Index Number, Catalog ID, RA, Dec, Bmag, Vmag, Rmag, Hmag, Kmag, Distance from science target (arcseconds)

The final set of reported magnitudes either directly from the catalog or calculated by Keck would be B, V, R, H, and K replacing the current fields, R, B-V, and B-R. The full list is need to be compatible with the color indices used for the AO setup tool (aoacqu.pro) and differential atmospheric refraction (DAR) compensation.

8.1.1.3 Star Catalog Image Overlays

In addition to displays from the photographic DSS Blue, Red and NIR bands, the guide star tool should also provide options to display images from the 2MASS catalog over the full sky and the SDSS in regions of the sky where it is available. These catalogs can currently be searched and images displayed suitable for "finder charts"; see the NASA/IPAC Infrared Science Archive (IRSA) Finder Chart tool. There is already a script that converts Keck star lists to the IRSA finder charts table format for batch processing. It is located at /home/kics/instr/bin/keck2irsa on the Keck software development system.

8.1.1.4 Overlays for the NIR TTS Field of Regard, Tip-tilt Sensor Stage and OSIRIS

The current guide selection star tool will need a means to indicate that it is for the AO system on Keck I as opposed to Keck II. The current guide star tool includes an overlay for the OSIRIS instrument. These will be updated to reflect the new position or pointing origins on the Keck I AO system. The Tip-tilt Sensor Stage (TSS) overlay should also be updated to reflect the orientation on the Keck I telescope and vignetting. These tasks should be performed as part of implementing LGS AO and OSIRIS on Keck I.

The NIR TTS full image or field of regard should reflect its orientation and possible vignetting as an overlay on the guide star selection tool. A means of displaying both the TSS vignetting and the NIR TTS field of view at the same time is desirable. In general, it is a good practice to not select stars too close to the edge of the field so as not to preclude dithering. As a goal, an appropriate size box for the observer's desired dither size will be superposed on the selected stars to help this assessment.

8.1.1.5 New Star List Flags to indicate NIR TTS Guide Star Setups

It is anticipated that an additional flag will need to be added to the Keck star list to designate the tip-tilt stars to be used with a given LGS science target. At present the flag **lgs=1** is used to designate an LGS AO mode target and **lgs=0** is used to designate a NGS AO mode target. The NGS used for tip-tilt correction are placed on the lines immediately after the LGS science target and have no lgs identifier. The current Keck star list format for all instruments is being updated as part of the Telescope Control System Upgrade project. The new format will support a new opmode = value flag. The opmode flag can include almost anything to indicate the observing mode for all instruments (not just AO) for that science target, possibilities include: lgs, ngs, imaging, spectroscopy, polarimetry, etc. The opsmode keyword is reserved for science targets only. New star list tools will be backwards compatible with the current method of LGS target designation.

The NIR TTS project will need a means to distinguish science targets from tip-tilt stars. We propose to add additional flags to the star list to indicate whether the NGS tip-tilt star is a NIR or visible NGS or both. Guide stars would be labeled as either visible band **vistt=#**, or near infrared band **irtt=#**, the number will be used to group the various guide stars into setups for each science target. In addition the final star list would be populated with the appropriate NIR magnitude bands or R band magnitudes. A short example is shown below to help clarify the proposed changes. Lines that start with the hash sign (#) are comments for explanation of the different guide star setups. This symbol would not be parsed correctly by the various tools that read the star list at Keck and these lines must be removed from the final star list actually used. Also note that magnitudes, color indices, position angles are not complete on all line below, the list is for illustration purposes and is not intended as a formal statement of the final interface.

Current star list file for galactic center:

```
#
#   Galactic Center with USNO field stars for STRAP/LBWFS
#
Sag A*          17 45 40.041 -29 00 28.12 2000.0 lgs=1
0609-0602733    17 45 40.713 -29 00 11.18 2000.0 rmag=14.0 sep=19.3 b-v=0.83 b-r=1.65 pa=45
0609-0602749    17 45 42.287 -29 00 36.80 2000.0 rmag=13.5 sep=31.2 b-v=0.68 b-r=1.40
#
```

Proposed list for same target with NIR TTS:

```
#
#   Galactic Center with IRS 7 on NIR TTS and Vis star for LBWFS
#
Sag A*          17 45 40.041 -29 00 28.12 2000.0 opsmode=lgs
IRS7            17 45 39.987 -29 00 22.24 2000.0 irtt=1  kmag=6.5 sep=5.0 b-v=2.76 b-r=1.0 pa=45
0609-0602733    17 45 40.713 -29 00 11.18 2000.0 vistt=1 rmag=14.0 sep=19.3 b-r=1.65 pa=45
#
#   second GC setup if IR7 not suitable
#
IRS16NW         17 45 40.045 -29 00 26.87 2000.0 irtt=2  kmag 10.03 sep=2.0 …
 609-0602733    17 45 40.713 -29 00 11.18 2000.0 vistt=2 rmag=14.0 sep=19.3 …

#
#   third GC setup three NIR stars
#
IRS16NW         17 45 40.0454 -29 00 26.874 2000.0 irtt=3 kmag 10.03 sep=2.0
IRS15SW         17 45 39.9224 -29 00 18.035 2000.0 irtt=3 kmag 10.39 sep=10.0
  IRS1W         17 45 40.443  -29 00 27.55  2000.0 irtt=3 kmag 12.00 sep=1.0
0609-0602733    17 45 40.713  -29 00 11.18 2000.0 vistt=3 rmag=14.0 sep=19.3
#
#  default to VIS setup if all IR setups not suitable
#
#
0609-0602733    17 45 40.713 -29 00 11.18 2000.0 vistt=4 rmag=14.0 sep=19.3
0609-0602749    17 45 42.287 -29 00 36.80 2000.0 vistt=4 rmag=13.5 sep=31.2
#
```

In addition to the AO guide star selection tool, the observatory software group supports a Finder Chart tool for seeing limited instruments. The software group plans to merge the AO guide star selection tool and the

Finder Chart tool at some point in the future. The new Finder Chart star selection tool will allow "grouping" targets in some manner and moving targets forward or backward in the star list that it produces. The grouping feature is not requested by NIR TTS but would be a useful feature.

8.1.2 Performance Estimation Tool

The observer needs to determine if a particular target is observable for both observing proposal and observing planning purposes. The availability of natural guide stars is a crucial factor in determining the feasibility of any mode of AO observations. The NIR TTS project is required to provide a tool that predicts AO performance. This should allow an observer to determine what AO performance can be expected for a set of possible guide stars.

In addition, the tool can be used while observing to determine if expected performance is actually being achieved. This could be a useful diagnostic for problems and would allow the astronomer to adapt to the observing conditions. For example, on a given target they might be able to use brighter stars further off-axis if the high altitude turbulence was weaker that night or they might modify their observing plan to concentrate on targets with convenient NGS if the conditions are poor. The tool will not be part of the operational software and will not be built to AO operational standards. In any case the AO system could still observe without it. However, it should be the same tool the astronomer used for planning but with an automatic (or manual) input of the existing conditions.

After observations the tool would provide a check on the expected quality of the data. The validity of the tool would be updated using AO telemetry and science data as a basis for comparison. These periodic updates would improve the tools ability to predict performance in varying conditions.

It is anticipated that the NIR TTS system will use from one to three IR tip-tilt stars. In addition, the observer might also want to consider using the current STRAP sensor which has peak sensitivity in the visible (R band). In either case, the observer will still need to select a visible band star for the AO Low Bandwidth Wavefront Sensor (LBWFS) which helps to compensate for changes in the sodium layer structure and range. Ideally, the performance estimation tool would be tightly interfaced to the future AO guide star selection tool. It would provide the capabilities to evaluate which of several guide star scenarios would provide the best AO performance. Another consideration is that the NIR TTS system will use an optical pickoff (dichroic or annular mirror) to send part of the NIR bands to both the NIR TTS sensor and the science instrument. An observer will have to evaluate which of several possible pickoff choices is optimal.

For the current Keck I and II AO systems, this need to find natural guide stars in close proximity to an astronomical target is met by the AO guide star tool. The current NIR TTS design calls for a modified star list format that will be used as the interface between an updated AO guide star selection tool and the AO performance Tool. The user will use the AO guide star tool to configure the guide stars for the particular scenario and then save that star list to disk. The AO performance estimation tool will need to be able to read this file.

The output of the performance tool would be predictions for Strehl and ensquared energy, and possibly a point spread function image. The user-provided inputs to this tool would include:

- **Star list**: text file produced by user or by AO guide star selection tool
- **Seeing conditions:** several default conditions (i.e., median, good and poor seeing); also allow inputs from the Mauna Kea MASS/DIMM during observations and from its data archive. User can enter seeing values by hand from, for example, the value reported at night by the AO system
- **Telescope elevation:** input or calculated from object position, date, and time; possibly provided automatically at the telescope from DCS/TCS keywords
- **NIR TTS observation wavelength**: Include option for NIR TTS pickoff setting; possibly provided automatically at the telescope from AO keywords or input by user

- **Science instrument setup**: including relevant parameters for science instrument. Including among others, the OSIRIS imager plate scale and filter or IFU plate scale and appropriate wavelength range for spectroscopy; possibly provided automatically at the telescope from DCS/TCS keywords

8.1.3 Performance Estimation Requirements

The following are the relevant requirements placed on the performance estimation software from KAON 835. The abbreviation SR-## is used to indicate the unique identification number for each system requirement.

> **SR-47**: The NIR TTS system shall provide the needed tools to support science observation planning.
>
> **SR-65**: The NIR TTS system shall be provided with the documentation required to support science operations planning. This should include at least 3 months of performance characterization data after the system has begun being used for shared-risk science.
>
> **SR-66**: Goal: The NIR TTS shall be provided with a performance estimation tool for both pre-observing planning and observing. This would be even more useful with a PSF simulator attached to it.

8.1.4 Possible Performance Estimation Tool Methodologies

At least three techniques could be used to develop a prediction capability; these are listed in order of increasing complexity:

Report: A list or table of the performance either as measured during commissioning of the instrument or from a series of models or simulation runs. This method documents the performance but doesn't allow the user to easily configure the tool to match the observing scenario.

Scaling Law Tool: The simple AO performance rules of thumb or scaling laws (see for example Hardy, 1998) are simple analytical formulae that are often used to scale or predict AO performance based on perturbations to a measured or known performance point. For an idealized AO system, the scaling laws should be able to predict performance from first principles. However, in practice this usually proves unsatisfactory unless allowances are made for the non-ideal nature of some AO components. A possible way to design this tool would be to use the measured or simulated performance as a starting point. It would then use scaling laws to interpolate or extrapolate the results to match the actual observing setup and atmospheric conditions. This technique combines the relative simplicity of method one (report) but allows the results to be adapted to the actual conditions and setups that an observer would be using.

Monte-Carlo Simulations: The best prediction of the performance on an AO system can be done by detailed computer simulation that use the Monte Carlo technique to model the behavior of the AO system. In the past, these codes were complicated and took long periods of time to run. As high computer performance continues to get cheaper, some of these obstacles can be removed. As an example: Matthew Britton (while at Caltech) provided a web interface to several of his AO simulation codes. The user submitted a request using a form on a web page. An input file was prepared from this web form and a computer simulation was added to a batch queue on the dedicated AO simulation computer at Caltech. When the computations were completed, the results could be retrieved by the user. Another advantage of this tool is that it can be easily configured to provide the observer with a PSF image if desired.
At present, it appears that the scaling law method provides the best path forward. It can be tailored to the observing setup and can provide rapid return of information. The Monte Carlo tool is appealing because it would simulate the exact observing scenario but it is likely to require more resources than are available at this time.

8.1.5 Performance Estimation Software Organization

At present, we assume that the combination of reported performance plus Scaling Law method is the basis for the future performance estimation tool design. Further, we assume that the main interface to the performance tool will be an upgraded version of the AO star list.

The processing steps on the graphical user interface (GUI) would be arranged as follows:

i. User selects targets and AO guide stars configuration from Keck star list file. This configures the tracking mode (STRAP, NIR TTS, both, etc.).

ii. User configures date and checks elevation (air mass) and telescope limits (K1 for NIR TTS).

iii. User configures science instrument (pull down list or separate popup window).

iv. User selects AO atmospheric conditions. Choice of one of several default conditions (i.e., median, good and poor seeing); also allow inputs from the Mauna Kea MASS/DIMM during observations and from its data archive. GUI should show summary statistics (r0, Greenwood frequency) as well as the turbulence profile.

v. User selects a button to start computation of AO performance. GUI lets observer compare performance with different guide star configurations and to compare performance with different IR tracking modes, number of targets and compensation mode. GUI would return Strehl, ensquared energy and possibly an option to download a PSF model.

vi. User can modify the star list with NGS targets based on results from above steps.

vii. User can save the modified star list and AO performance results.

These steps would be selected from the main GUI and the user could vary his selections and recompute results as needed. Default inputs would be provided except for loading a science target and a set of NGS guide stars.

8.1.6 Performance Estimation Tool Software Interfaces

The performance estimation tool will need to be interfaced to the following software; exact details are to be determined:

- Keck Star List: Format for these target lists will need to be modified as discussed in section 8.1.1 to indicate NIR targets, pickoff selection, and tracking mode.
- Mauna Kea MASS/DIMM profile information.

8.1.7 Performance Estimation Tool Software Realizations

We anticipate that the software languages used to develop the AO performance tool will have the following features:

- Not critical for astronomical observations with the Keck I AO and OSIRIS. Therefore it does not need to be constructed to comply with all levels of the Keck operational software standards.
- Should be easy to modify by AO engineers or support astronomers. This allows the tool to reflect the current performance of the AO system in a timely manner without extensive software rewrites. While the needed changes would be confined as much as possible to a configuration file that is read by the tool at startup, some parts of the code such as parametric fits to existing data might need to be modified inside some code sections. Personnel at the observatory will need to periodically update the tool.
- Should be written in a language that allows easy interfaces to plotting and other graphical visualization tools. The language should provide an easy means to interface with computational libraries for data fitting, Fourier transforms, and other mathematical functions.
- Should have an interface that can he used by the average AO observer.

- Should be useable by the average astronomer at their home institution.

Based on this list of desirable features, we would select IDL or possibly Python as the software language for the AO performance tool. Keck AO has used both Python and IDL to produce tools for the AO system in the past and either could be used for the AO performance tool. At present IDL, would be preferred as it is more familiar to the astronomical community, the Keck support astronomers, and the AO development team.

The development of this software will be tracked with a version control system, using the Keck cvs software standard. It is TBD if the master version of the software would be kept on the summit K1 AO server or at the Waimea headquarters. An executable version of the software plus user documentation would be distributed from the Keck public website for use by outside astronomers. A nighttime version would be hosted on an appropriate AO or instrument workstation.

A high level flow chart of the processing steps is shown in Figure 74. A prototype user interface is shown in Figure 75.

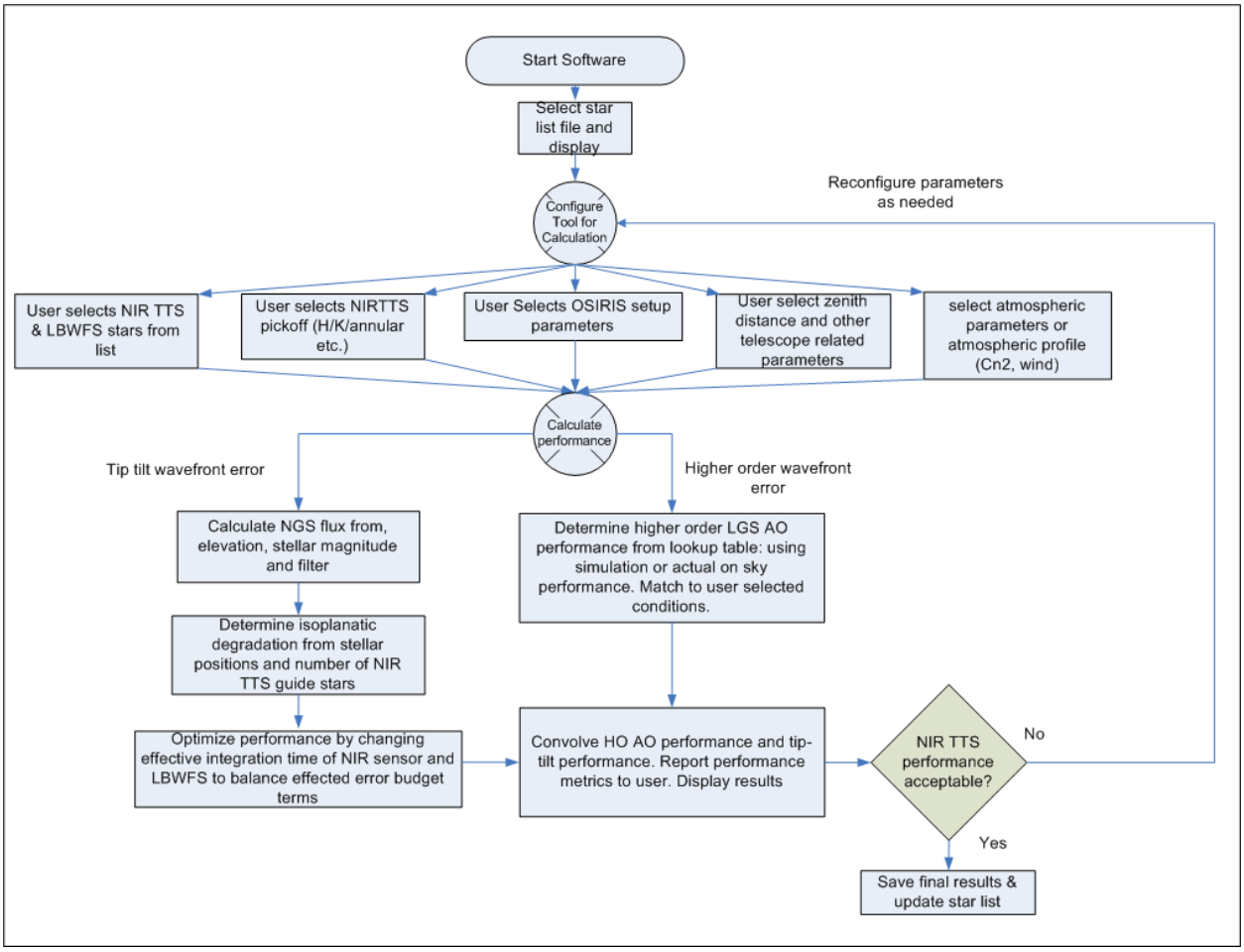

Figure 74: A simplified flow chart of the AO prediction tool

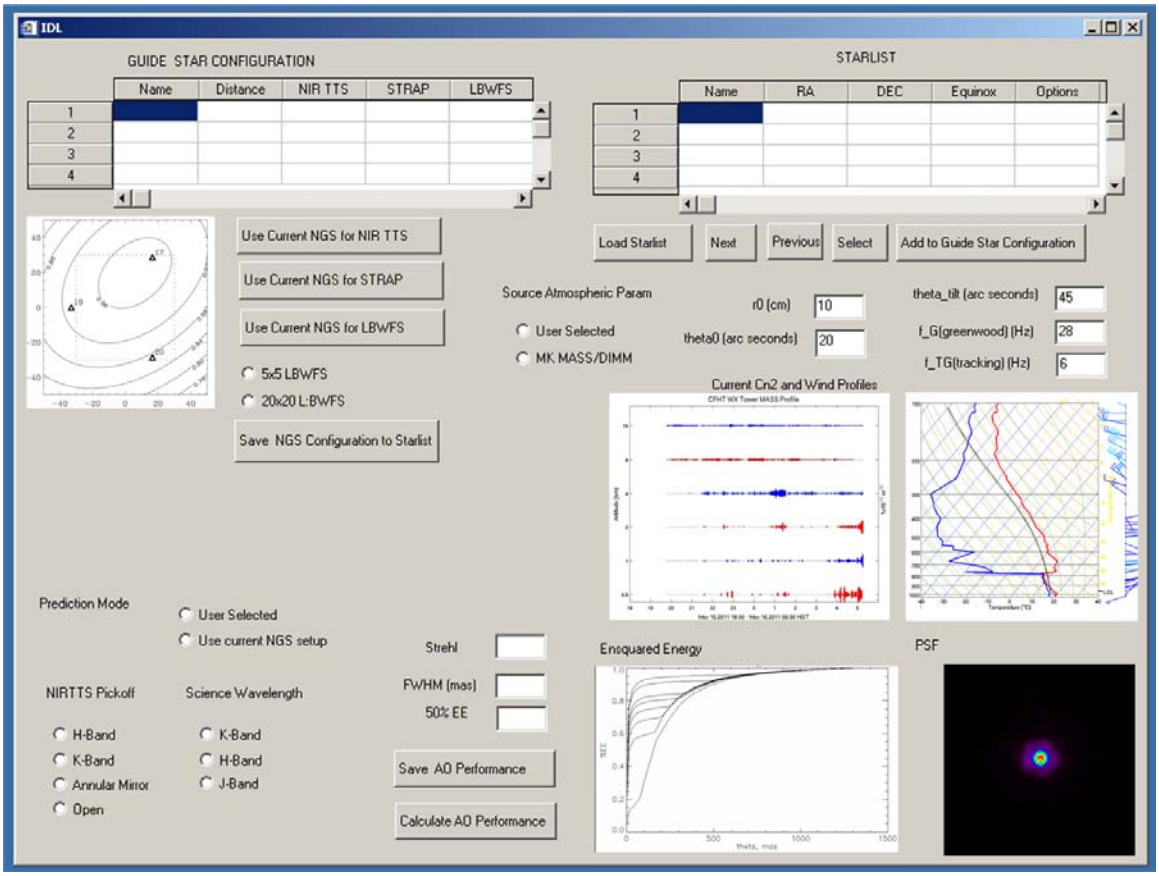

Figure 75: A prototype GUI for the AO prediction tool. Top portion of the GUI display the user star list. The user can select guide stars and add them to the current guide star configuration. Setups can be configured for STRAP, NIR TTS (1-3 stars) and the LBWFS. The user is also able to select the atmospheric and wind profiles using the middle right section of the GUI. The bottom section displays the estimated performance. This GUI is only a "sketch" the final GUI will likely look much different but incorporate some of the same functionality.

8.2 Observation Setup

The observation setup will be done via the AO acquisition tool. This is where the various observing modes (NGS, NGS with STRAP, LGS) are currently selected. Additional LGS modes will need to be made available to support NIR TTS usage.

The observer or operator will need to be able to select between multiple tip-tilt sensor options in order to setup the AO bench. The impact of each of these options, listed below, on the NIR TTS setup is discussed in the sub-bullets:

- WFS (for NGS AO observing only)
  - The NIR TTS pickoff mechanism should be in the open position.
- STRAP
  - The NIR TTS pickoff mechanism should be in the open position.
- NIR TTS in H-band
  - The NIR TTS pickoff mechanism should be in the H-band reflective dichroic position.
  - The NIR TTS focus stage should be at the H-band focus position corresponding to the current instrument configuration.
  - The NIR TTS filter positioner should be in the H filter position.
- NIR TTS in Ks-band
  - K-band reflective dichroic position.
  - Ks-band focus position corresponding to the current instrument configuration.

    - Ks-band filter.
- NIR TTS with annular mirror (if this option exists)
    - Annular mirror position.
    - Ks-band focus position corresponding to the current instrument configuration plus Ks-band filter or H-band focus position plus H-band filter.
- NIR TTS and STRAP
    - Both sensors are configured appropriately.

For the NIR TTS the following parameters need to be selected and communicated to the real-time control system:

- Choice of TTS (NIR TTS or NIR TTS + STRAP)
- Number, location and size of ROIs. This could initially come from the target list coordinates of the TT stars. The ROI locations will be regularly updated due to DAR; the actual locations could come from the camera controller.
- Number of samples to be taken between resets – could come from camera
- The pixel read rate (this will always be the same but may need to be set)
- Algorithm to be used (centroid or correlation)
- Background to be subtracted from each ROI
- Flat field for each ROI for scaling
- Weight to be applied to each ROI for determining the TT to be applied to the TTM
- What telemetry is to be recorded by the telemetry recorder system
- Initial centroid offset to be used (this will be regularly updated)

For the NIR TTS the following parameters need to be selected and communicated to the NIR TTS camera controller when it is in TT tracking mode (a separate mode exists for acquisition):

- Number, location and size of ROIs
- Number of samples to be taken between resets
- The pixel read rate (this will always be the same but may need to be set)

8.3 Calibrations

The calibrations discussed in this section are divided into three categories: camera, coordinate transformations, focus, and distortion and rotation mapping.

8.3.1 Camera Calibrations

The following camera calibrations will be required:

1. Flat fields in the H and K-band configurations for photometric and gain calibration purposes. Dome flats can be taken before or after observing. Dome flats are successfully used for NIRC2 and OSIRIS. These could be taken in parallel with the OSIRIS dome flats. Dome flats for NIRC2 are extremely stable and are available as a library. We could have a similar library of flats for the NIR TTS.
2. Dark frames for characterization purposes. The filter mechanism will provide a blocked position.
3. A bad pixel map for ROI selection purposes. This can be obtained from the dome flats.
4. An on-sky photometric calibration in both H and K-band. This would be obtained by observing photometric standards. It would be advantageous to have the NIR TTS filters match those used for the 2MASS catalog if that will be our primary source for identifying TT stars. Once calibrated the camera could be used to update the magnitudes of stars being used for TT sensing and these could be written to the science image FITS header or recorded by the observer for future observations.

8.3.1.1 Dome Flats

The NIRC2 dome flats procedure can be found at http://www2.keck.hawaii.edu/inst/nirc2/DomeFlats.html. The dome flat lamps designed for the optical instruments are used. The exposure time to reach ~8000 DN is

1.2 seconds for the H filter and 4.5 seconds for the Ks filter when using the NIRC2 wide field camera. Given that the wide field camera has 40 mas pixels the exposure times would need to be reduced by a factor of $(40/50)^2 = 0.64$ for the NIR TTS.

The procedure for NIRC2 dome flats is:

1. In any waikoko xterm type 'configAOforFlats' and answer Y to the prompt (if you have checked beforehand with your support astronomer).

2. Bring up the dome lamp control gui found under 'interface subcomponents' on the pulldown.

3. Turn on the SPEC lamps and confirm that you see flux on the AO WFS (and that OFF results in very little flux on the AO WFS). If this check doesn't work out, check the light path (e.g., OFM in SC gui, Tertiary position, etc.). Note that there are two flat field lamps so if you only see ½ of the expected flux there may be a burned out light.

4. Manually take the flats using the recommended times, or run a script (e.g., /home/nirc2eng/vis/arc/flat_examples/makeFlats).

The DCS keywords for lamp control = flimagin and flspectr (e.g., to turn both off "modify –s dcs flimagin=0 flspectr=0").
Since the NIR TTS camera will not (at least initially) be used as a science camera the purpose of the dome flat will only be to determine the relative gains of pixels. This relative gain information would be used by the optimization tools to produce a reconstruction matrix for the RTC. This is expected to be relatively stable and would be infrequently required. If the NIR TTS is used as a science camera then the NIRC2-type procedure discussed above may need to be run on a nightly basis.

8.3.1.2 Dark Frames

Dark frames are obtained with the NIR TTS camera shutter closed. It is not clear that these will be needed for other than diagnostic or characterization purposes. Dark frames will be useful if we wish to scale the background which would allow changing the integration time on the fly with no telescope offset required (alternatively we could measure the sky difference from a sky ROI). If the NIR TTS camera is to be used as a science camera in the future then longer integration dark frames would be required by the observer. Dark frames are needed to identify saturated or high pixels as discussed in the next section.

8.3.1.3 Bad Pixel Map

This bad pixel map should be a FITS image. The bad pixel map would only need to be produced infrequently. This data could be used to determine what ROI locations should be used. Generally it is appropriate to remove three types of bad pixels: those that are always dead or low, those that are always saturated or high and those with non-linear responses. The always dead/low pixels are found from flats, the always saturated/high pixels are found from darks and the non-linear response pixels are found by taking longer exposure flats.

The approach to identify the dead/low pixels is to take a few NIR TTS full frame images with the flat field lamps on. For each frame identify potentially bad pixels. Use those bad pixels common between the images to produce a low/dead pixel map.

8.3.1.4 Photometric Calibration

We need to first distinguish between absolute and relative photometric calibration. Absolute photometric calibration would be required to determine the system throughput and/or the true magnitude of TT stars. Relative photometry is a simpler task that would allow us to measure the uniformity and linearity of response across the detector. The dome flats discussed above will be used to measure the relative photometry. The remainder of this section refers to absolute photometry.

A link to several near-infrared photometric standard catalogs can be found at http://www2.keck.hawaii.edu/inst/nirc/stds.html. These include Eric Persson's HST JHK standards, Elias JHKL standards, UKIRT faint standards, MSSSO southern JHKL standards and IRTF bright standards, as

well as a link to Mauna Kea summit extinction values. An alternate Mauna Kea atmospheric transmission tool is linked from the OSIRIS page to http://www2.keck.hawaii.edu/cgi-bin/ion-p?page=mktrans.ion.

The photometric calibration involves taking sufficiently long integrations on the NIR TTS to get good a good SNR. The night must be photometric and the integration time and zenith angle need to be recorded. To reduce the dependence on zenith angle it would be best to take images within 30° of zenith. The photometric calibration can be performed off-line using the saved images.

The photometric calibration will be useful for validating our throughput calculations.

Using the photometric calibration to determine the true magnitudes of TT stars is more challenging. A similar tool is not available for the acquisition camera or for MAGIQ in general. An off-line tool is available for doing photometric measurements with the star stacking camera which is good to the 10% flux level. Doing real-time photometry is currently only a goal.

8.3.2 Camera Coordinate System Transformations

8.3.2.1 Camera Coordinate System Transformation to the Pointing Origin

The NIR TTS camera must be put into the existing AO coordinate system in order to use it as an acquisition camera. The existing acquisition camera provides the pointing origin reference. Two keywords must be set for the NIR TTS camera: TVANGL and TVFLIP. These are the pointing origin to camera angle and y-flip, respectively, with respect to the acquisition camera.

The following pointing origin names and positions will need to be set in the OSIRIS configuration file (we have used pointing origin #4 here which is used by NIRC2 on k2):

```
# pointing origin #4
group {
   string  k1:dcs:poName     = "REF-T";
   double  k1:dcs:poXpos     = -0.22 mm;
   double  k1:dcs:poYpos     =  0.72 mm;
   int          k1:dcs:poPreset   = 1;
}
```

The coordinates (poXpos,poYpos) are the location of the center of the NIR TTS detector with respect to the center of the acquisition camera (pixels 512,512). These coordinates will need to be calibrated. A separate calibration is periodically performed to determine the optical axis with respect to the center of the acquisition camera.

8.3.2.2 Camera Coordinate System Transformation to the Tip-Tilt Mirror

A calibration is needed between the camera detector pixels and the tip-tilt mirror controller axes. The existing IDL toolbox has a calibration to provide this transformation for the STRAP system; it converts from STRAP centroids (Cx,Cy) to arcsec (x,y) of the tip-tilt controller inside the RTC hardware.

8.3.3 Focus Calibration and Field Curvature

The NIR TTS needs to be kept conjugate to the science instrument. During the day a fiber at the input to the AO system is used to position the NGS WFS, LBWFS and STRAP at a focus conjugate to the science instrument. Offsets for different science instrument plate scales or filters are also calibrated.

A simple IDL-type calibration tool will be developed to support the NIR TTS focusing as defined in Table 10. The best focus will be measured routinely for the Ks filter and K-reflective dichroic. It may be desirable to perform this procedure at least once per observing run.

The best focus for other configurations will be determined infrequently and focus offset keywords for these configurations will be set. For example, a focus offset will need to be determined for when the annular mirror is inserted or when the H-band reflective dichroic and H-band filter pair is used.

Where to position the NIR TTS stage would depend on the TT star off-axis position if there is significant field curvature. The field curvature should be measured as a calibration. This calibration procedure would only need to be done once or after a major change to the system. The calibration procedure would be the same as the focus calibration procedure listed above but would need to be performed with the SFP at multiple field points. If there is a significant field curvature then this field curvature could be used by the focus algorithm to best position the NIR TTS focus stage as a function of the location of the TT star(s).

Table 10: Focus calibration tool

Category	Details
User Interface	New button on WFCIDL.pro calibration gui Button pops up focus calibration gui
Algorithm	1. Check configuration and reposition if necessary. Rotator at 45°, DFB & ISM out of beam, TT & DM loops open, K-band reflective dichroic in beam, Ks filter for NIR TTS, SFP on rotator axis at pre-determined best focus for default OSIRIS configuration (there will be delta focus terms with respect to this default position), fiber source on with appropriate SND. • The operator could manually change the NIR TTS pickoff & filter and/or the ROI and SFP positions if a non-standard focus measurement is desired (e.g., to measure the field curvature or to measure the offset for the H-reflective dichroic and H-filter pair). 2. Measure focus. Adds 45° astigmatism to deformable mirror. Closes TT loop on NIR TTS ROI with no centroid offset. RTC measures & reports focus. 3. Adjust focus. Moves NIR TTS focus stage to zero focus within a tolerance. Reports focus.
Keywords	OBS and RTC keywords to control devices Focus measurement from RTC and a focus zero-point for the NIR TTS focus stage
Telemetry	None

8.3.4 Distortion and Rotation Mapping

The extent to which positions are known on the NIR TTS will impact how well the science object can be positioned on the science instrument. A field distortion measurement will need to be made at least once, or after any major changes to the system. The position angle (PA) will also need to be measured on the NIR TTS.

A sufficient distortion map and PA measurement on the NIR TTS are needed to ensure that he relevant repositioning requirement is met, namely the nodding and positioning requirement of ≤ 120 mas (3-sigma) for moves ≤ 60 arcsec and ≤ 70 mas for moves ≤ 5 arcsec.

The repositioning requirement is on OSIRIS. The OSIRIS distortion and rotation must therefore also be known and we assume that these measurements will have already been performed and will be available.

The distortion map is an input to the repositioning algorithm.

8.3.4.1 Optical Model Distortion Map

The Zemax optical model, which includes the telescope and AO system as well as the NIR TTS, will produce a distortion map (see section 3.4.1). This can be used as our initial distortion map pending a more accurate measurement.

8.3.4.2 Daytime Distortion and Position Angle Calibration, plus Vignetting Map

A distortion map could be made by moving the AO input fiber (SFP stage) around the field and recording the corresponding position on the NIR TTS. The fiber stage only has a motor encoder so its positioning accuracy is limited to ~ 10 μm or 14 mas. The tip-tilt sensor stage (TSS) on which STRAP is mounted has a Heidenhain optical load encoder which offers an accuracy of at least 5 μm, and perhaps as good as 2 μm, if it could be used to measure the fiber source position.

Some level of distortion mapping and PA determination should have already been performed for STRAP and the TSS stage since it will be the initial TT sensor used with OSIRIS. If we can use STRAP/TSS to measure the fiber position then we could reference the NIR TTS measurements to the STRAP/TSS distortion and PA measurements. Note that STRAP and the NIR TTS are on the same side of the rotator, therefore any rotator effects are removed.

How do you accurately measure the fiber source position on the NIR TTS? From section 2.5 we see that centroid measurements at least can be biased by the Strehl and background; the correlation algorithm should be more robust. Although this may not be necessary, for maximum confidence in the fiber source position the source should be driven to the intersection of 4 pixels. An approach to do this would be to close the TT loop on the NIR TTS with the appropriate ROI. The TTS stage then could be moved to zero the TT signal on STRAP, and the TTS encoders could then provide an accurate measure of the fiber source position. Unfortunately this approach requires that TT measurements can be made with STRAP while the NIR TTS sensor loop is closed, which may not be an available option.

Taking the above considerations into account, including that simultaneous STRAP and NIR TTS measurements may not be available, we will use the following procedure as a baseline:

- Setup: AO bench configured for single mode fiber (SFP) on-axis, rotator (ROT) at 45° (which produces no rotation), sodium dichroic (SOD) in beam and NIR TTS K-band reflective dichroic in beam. TT loop closure driven by STRAP. Start with the fiber on the rotator optical axis at the best focus for OSIRIS, and with the appropriate neutral density (SND) for the fiber. Verify the correct exposure time on the NIR TTS.
- Move the SFP by 5" steps in x and y to fill in a grid of 120"x120". This is a total of 576 measurements. Move the TSS by the same amount.
- At each point close the STRAP loop and record the TSS x,y encoder position. If the flux drops below a defined limit identify this point as vignetted. In the vignetted case we will only use the NIR TTS image to determine if there is also vignetting on the NIR TTS.
- At each point take a NIR TTS full frame image.
- In post-processing for each NIR TTS image determine the x,y coordinates of the image using the same correlation algorithm as used by the RTC.
- Also, for each NIR TTS image determine if there is vignetting.
- Take a difference between the TSS x,y coordinates and the NIR TTS image x,y coordinated to produce a distortion map.
- Use the vignetting information to produce a vignetting map for the NIR TTS (as well as for STRAP). Finer SFP/TSS motions can be used to better define the vignetting boundaries.

The above algorithm would be done most efficiently if it were implemented in a separate IDL or Python tool. The tool would need to be able to take and save full frame images.

8.3.4.3 On-sky Distortion Calibration

A more accurate distortion map could be obtained on the sky, if necessary, by observing a cluster with known astrometry. Such a field has been used for distortion mapping on NIRC2. The relevant NIRC2 astrometry documentation can be found at http://www2.keck.hawaii.edu/inst/nirc2/forReDoc/post_observing/dewarp/.

M92 ($17^h15.6^m$, +43°12') was used by Yelda et al. (ApJ 725, 331, 2010) to produce a geometric optical distortion model for NIRC2. A procedure also exists for using M15 ($21^h27.6^m$, +11°57').

The on-sky distortion calibration procedure is currently only planned as a backup procedure. It would also be necessary if we decided to use the NIR TTS as a science imager (this is currently only a longer term goal).

8.3.4.4 On-sky Position Angle Calibration

A PA calibration check should be performed on sky. This can be done simply with the following procedure:

- Setup: Rotator in PA mode with North nominally vertical on the NIR TTS. Higher order DM loop closed on the laser.
- Position a star near the center of the NIR TTS with the TT loop closed and no centroid offset (so the star is centered on the intersection of 4 pixels).
- Move the telescope by 40 arcsec North and move the ROI by the same amount. Close the tip-tilt loop with the NIR TTS with telescope offloading off and record the TT error in x and y.
- Repeat the previous step with an 80 arcsec South move.
- Use the x errors to compute the required correction to the PA offset for the NIR TTS, make this correction, and repeat the test.

An alternate PA (and distortion) check is to pick a pair of stars with a known PA (and separation) and simply take a full field NIR TTS image of this pair. The image can be processed off-line to measure the PA (and separation).

8.4 User Interfaces

The current Keck I AO system GUI will be modified to operate with the NIR TTS. The user interface will be integrated into the existing interface which features tools written in IDL, so called "widgets" and the scripting language Python. Current design decisions call for all NIRTTS tools to written in IDL. Configuration management will be done with cvs using the current repository used for the existing IDL tools. One exception to the use of IDL is the AO guide star selection tool, the existing tool is a web based tool written in the PHP scripting language.

The modified user interfaces for the NIR TTS are described in the remainder of this section. Prototype GUIs for the guide star selection and AO prediction tools were already discussed in sections 8.1.1 and 8.1.7, respectively. Engineering GUIs will also be developed to control the camera and motion control devices.

8.4.1 NIR TTS "Widget" Planning Tool

The proposed planning tool for position angles, dither sizes, and pointing offsets is shown in Figure 76. The tool is a modification of the current TSS widget used for LGS observation with the Keck II system. The tool duplicates some of the functionality of the current AO guide star selection tool, but allows the observer to test dither sizes and some other observing sequence functionality not available in the AO guide star selection tool. Also because it is installed on the summit, this tool will have access to DCS and AO keywords for pointing and rotator position angle. As such it can be used to identify targets on ACAM or the NIR TTS in full frame mode. The modified version will include ROI display (green boxes) and the updated position of the OSIRIS instrument (magenta boxes).

8.4.2 ACAM and NIR Camera Tool

The tasks of field identification and full frame operation of the NIR TTS camera will be done from the GUI shown in Figure 77. The GUI will allow the user to operate ACAM and the NIR camera. The selected guide stars for LBWFS or STRAP will be shown as square boxes on the ACAM display. The NIR camera display will have boxes around the selected guide stars and a "zoom" window for each ROI in the bottom edge of the display. The display shown in Figure 77 has only 2 active ROIs displayed of the 4 possible ROI windows supported by the software.

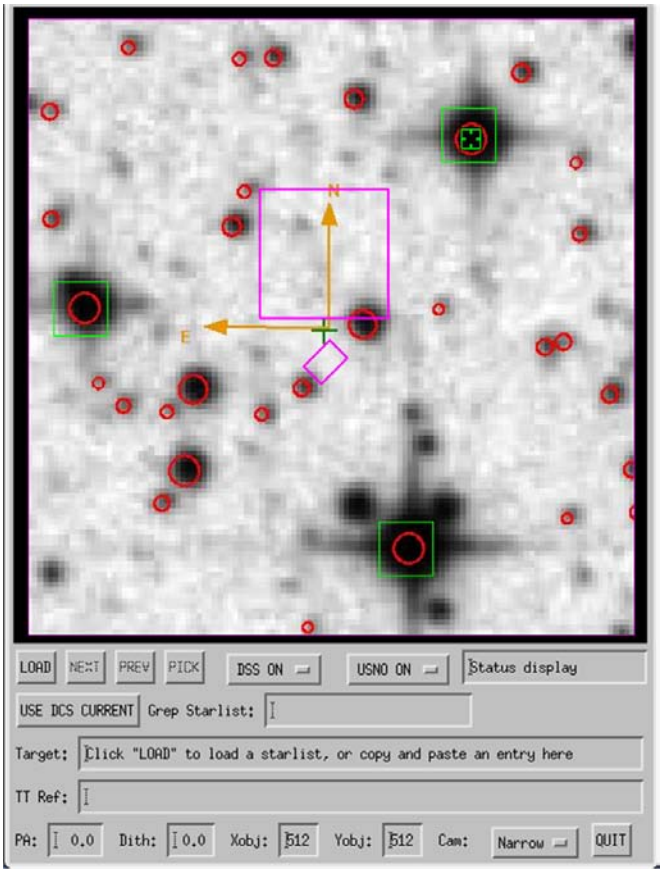

Figure 76: Updated TSS widget to include NIR TTS ROI display

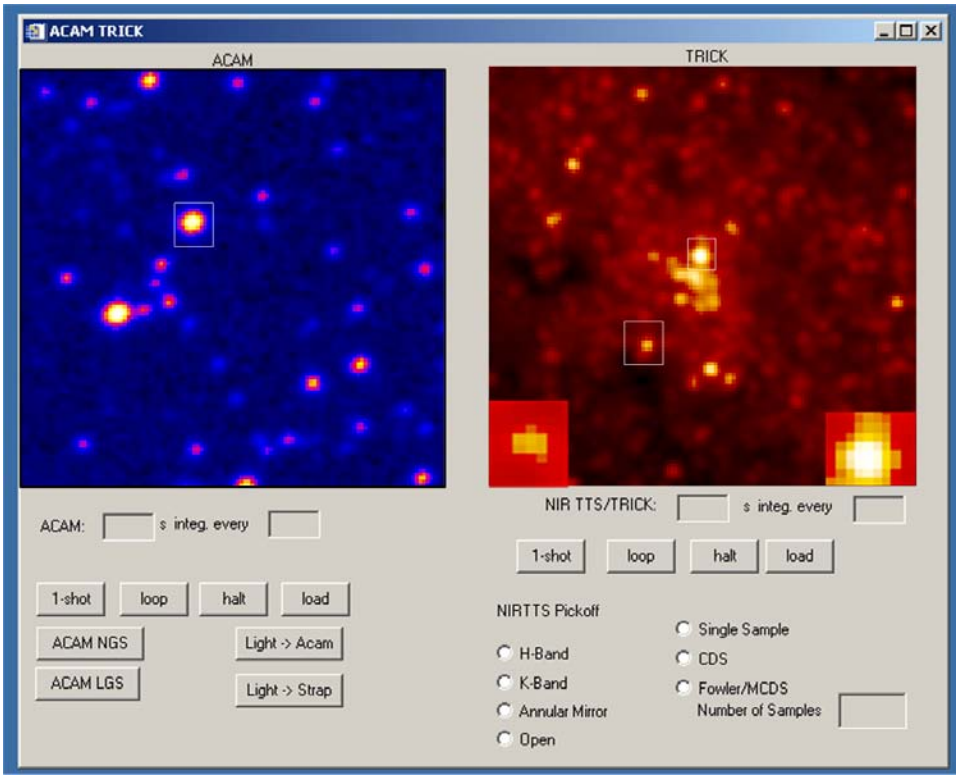

Figure 77: A combined ACAM and NIR camera display for field identification

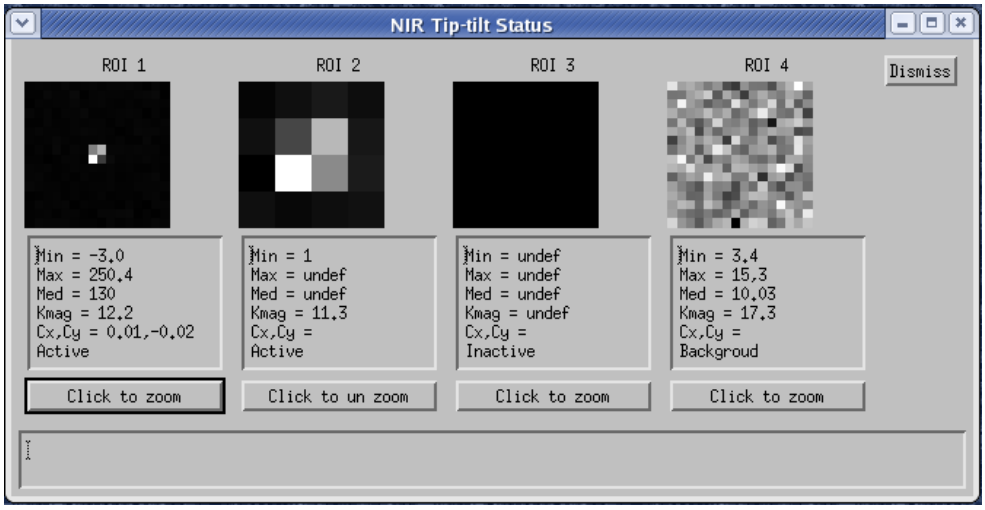

Figure 78: NIR TTS tip tilt status GUI

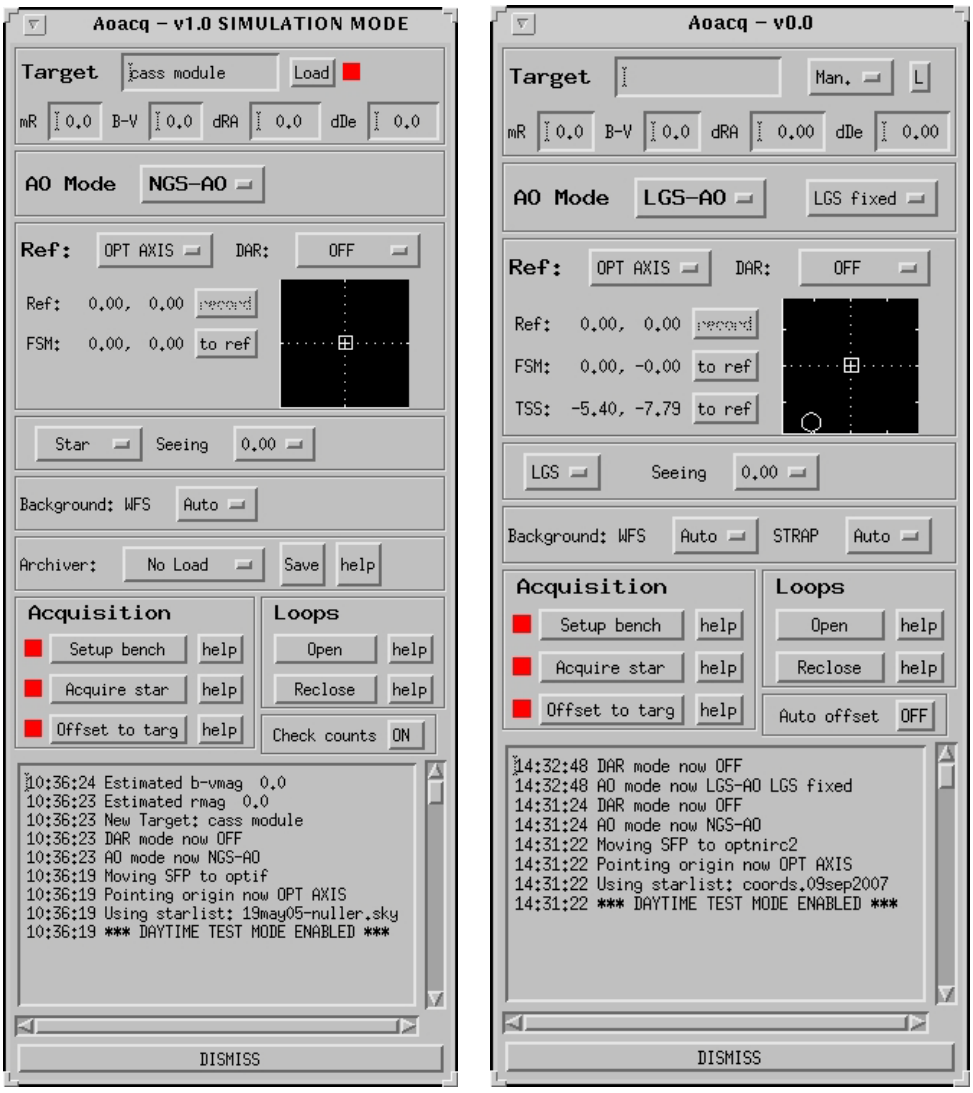

Figure 79: Current AO Acquisition GUIs for NGS (left) and LGS (right). These will be modified to support multiple NIR guide stars

8.4.3 Tip-Tilt Status Display

The status of the NIR TTS when it is used with the RTC will be monitored by the GUI shown in Figure 78. The ROIs used for tip-tilt correction will be displayed along with statistics and status information. In the GUI ROI 4 is used for background estimation and ROI 3 is inactive. The final GUI will likely include the option of displaying a strip chart showing the total signal in each ROI over that past few minutes as this has proven to be a good system diagnostic with the STRAP sensor.

8.4.4 AO Acquisition GUIs

The current AO acquisition GUIs will be modified to work with multiple NGS as required for the NIR TSS project. The current GUIs are shown in Figure 79.

8.4.5 AO Calibration GUI

The current calibration widget will be modified to include calibration for the NIR TTS system. The current calibration GUI is shown in Figure 80.

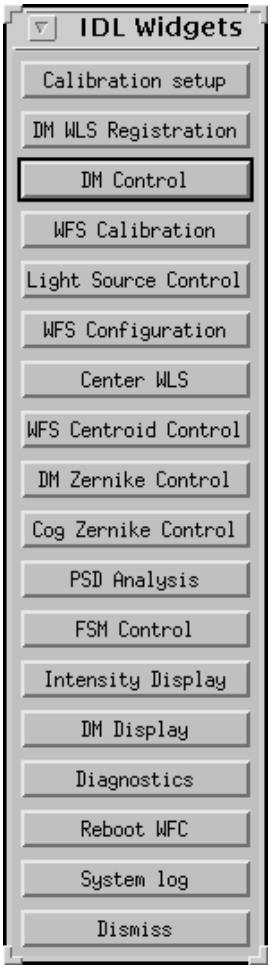

Figure 80: The current IDL calibration GUI

8.5 Observing Tools and Sequences

8.5.1 Acquisition

Acquisition will be performed by a full frame readout mode of the TTS detector. The locations of up to three stars will be selected for ROI readout.

Pre-observing software will be provided for the astronomer to pre-select targets for TTS operation. Taking an acquisition frame will be the final step in determining the appropriateness of a target for TT sensing and its precise position for the ROI.

The acquisition steps include the following:

1. Next target selected and telescope slew begins.
2. NIR TTS software calculates desired TT star locations on the NIR TTS and NIR TTS setting.
    - The TT star locations should be identified in the observer's target list along with their H and K magnitudes.
    - The observer selects the science instrument configuration: science wavelength, science mode (IFU or imaging) and plate scale for IFU science.
    - The observer or operator selects the NIR TTS wavelength (H or K).
    - The desired TT star locations on the NIR TTS are calculated, including the effects of differential atmospheric refraction. This calculation is performed continuously to account for DAR and for changes in the system configuration.
    - The frame reset time is calculated based on the magnitude of the brightest TT star.
3. Observing assistant identifies and centers the brightest TT star on ACAM once the slew has been completed and closes loops.
    - We may move to using the NIR TTS for this acquisition longer term if it improves observing efficiency. The TT stars could automatically be identified by searching around the expected target coordinates.
    - Guiding with ACAM (i.e. MAGIQ) is left on.
    - If STRAP is also to be used then its TT loop could be closed at this point and the ACAM guiding could be turned off.
    - Laser propagated.
    - DM loop closed.
4. NIR TTS software centers the field on the NIR TTS and closes the tip-tilt loop.
    - A telescope offset is made to nominally center the science object.
    - An image is taken on the NIR TTS.
    - The centroids for each TT star are determined.
    - A difference is taken with the desired positions. If the difference is below a threshold then the TT loop is closed with the largest region of interest required. Otherwise a telescope offset is made to move the TT stars to the desired positions and the TT loop is closed.
    - Guiding with ACAM should be stopped just before closing the NIR TTS TT loop.
    - The region of interest is automatically reduced to the desired region of interest as the centroid errors are reduced below a threshold.
5. Science image taken, if sufficiently short, to verify centering. An offset can be made if needed.

We intend to modify the existing WMKO MAGIQ acquisition software for NIR TTS acquisition. For MAGIQ use the camera interface must provide: full frame images for field identification and sub frame images for centroiding needed for pointing adjustments and offsetting. Images are best delivered in binary format directly via an application programming interface (API). FITS images could be used instead however this would add 1 to 2 seconds of overhead per frame. Camera exposure time and binning control should be available so they can be integrated into the MAGIQ GUI. A camera definition file will be needed to be used by MAGIQ. MAGIQ is also capable of saving a FITS image.

8.5.2 Tip-Tilt Loop Parameter Optimization

A high level tool is needed to provide the tip-tilt loop parameters used by the RTC. These include weighting factors to be used for each sensor and ROI, as well as the tip-tilt loop gain and bandwidth. These parameters will be dependent on such factors as the tip-tilt star positions, magnitudes, and the seeing conditions.

Setting up the NIR TTS system involves a number of potential tradeoffs among these are the following:

- Sensor type: visible or NIR

- NIR TTS wavelength: H or Ks-band
- Isoplanatic angle
- Positions of available tip-tilt stars
- Number of tip-tilt stars: 1-3
- Level of AO correction at the locations of the off-axis guide stars

The simulation results of section 2.5.3 highlight some of these tradeoffs. The complex nature of this parameter space was a motivation for including a performance estimation tool in the AO pre-observing planning software, see section 8.1.2. One key aspect of the proposed tool is the ability to use information from the current AO system configuration and atmospheric data from the Mauna Kea facility MASS/DIMM. The tool can be used to give a preliminary optimization of the relevant AO parameters and what sensor (STRAP or NIR TTS) is best to use given a set of AO guide stars and expected atmospheric conditions.

The exact level of AO correction will have an impact on which tip-tilt estimation algorithm (correlation or centroid) will give the best performance. As demonstrated in Figure 15 and Figure 16, as the level of AO correction of the off-axis tip-tilt star degrades the instantaneous image will transform from one with a single diffraction-limited core to one with several bright speckles. The correlation algorithm will essentially track the location of the brightest of these speckles. The optimization software will need to periodically analyze the NIR images from the telemetry stream to verify that only one significant correlation peak is present, multiple peaks would indicated that the AO correction is degrading and several speckles are likely present. If other peaks are present then the software would suggest to the user that the centroid algorithm may perform better on this guide star. On the other hand when the centroid algorithm is being used the optimization software could perform a correlation offline on images from the telemetry date to determine if the correlation algorithm would give better performance and suggest the appropriate change. The Strehl and seeing disk measurements suggested in sections 8.5.5and 8.5.4 are also a method that can be used to aid in optimizing the algorithm choice for tip-tilt estimation. For example, a lower estimated Strehl would indicate the possibility of several speckles providing an indication that the centroid algorithm is a better choice. In extreme cases the user may elect to switch from the NIR TTS to STRAP. As demonstrated in Figure 18, for guide stars at large off-axis angles STRAP is predicted to give slightly better performance than the NIR TTS.

When the natural guide star asterism is changed the optimization tool will need to load a new tip-tilt tomography reconstruction matrix into the RTC. This tool would function similarly to the current reconstruction matrix tool that loads the reconstruction matrix for use with the Shack-Hartmann wavefront sensor and deformable mirror. The tip-tilt reconstructor tool would monitor keywords that indicate the configuration of the NIR TTS system. Changes would trigger the appropriate computations and loading of results as the new tip-tilt reconstruction matrix. Based on the latest simulation results of van Dam discussed in section 2.5.3 (FWN 17), the minimum variance estimator gives superior performance over the modal estimator used during the system design phase of this project. These reconstructors are also favored because they generalize easily for 2 or 3 stars.

In order to have the best performance the NIR TTS system will need some level of automation for setting the various parameters for the operation of the tip/tilt loop. The necessary modifications would need to be made to the current AO acquisition tools and the control loop gain optimization tools. Information about the current AO acquisition tool (aoacq.pro) is found at http://www2.keck.hawaii.edu/optics/ao/ngwfc/aoacq.html. Information about the control loop optimization tool (bw_widget.pro) is found at http://www2.keck.hawaii.edu/optics/ao/optimizer/index.html.

The acquisition tool currently sets the exposure time of the various sensors based on the natural guide stars catalog magnitude. Next, based on the available detector counts it adjusts the exposure time to be as short as possible but with sufficient SNR; this allows the system to adapt to changes in elevation and atmospheric transparency for example. The AO acquisition tool would be extended to work with the NIR TTS. The control parameters (integrator leak factor and control loop gain) are set by the acquisition tool based on a detector exposure time and a lookup table of previously determined control loop gain settings found to be optimal for that exposure time during “typical” conditions. These values can be refined by using the

optimization tool (bw_widget.pro). This tool analyzes the AO telemetry to determine the control loop gain that would result in the smallest reported residual error in the AO diagnostics. The user has the option of changing the gain to this value. The user can run this feature of the optimization tool iteratively to refine the AO loop performance. A similar procedure would be run using suitable noise statistics from 1 to 3 NIR TT stars. This option will need to be added to the current optimization tool and it will need to use information from 1 to 3 stars to optimize the overall TT loop performance.

Exposure time is an interesting question given that up to 3 TT stars of different magnitudes will be used on the same detector. The NIR TTS detector non-destructive read pixel sampling rate will be constant, although different ROI will be visited at different rates. The "exposure time" will be set by the time when the array needs to be reset to avoid saturation as discussed in section 4.5. The reset rate will be set by the brightest star being used. Given the detector well depth of ~100,000 electrons there is still sufficient well depth between the brightest and faintest stars that could usefully be used together.

The other control loop parameter of importance for NIR TTS optimization is the so called "centroid gain" this is the conversion factor from centroid to input tilt. The current design proposes to use a seeing disk background measurement (section 8.5.4) to reduce the sensitivity to the centroid gain and a calculated NGS star Strehl (section 8.5.5) to estimate the centroid gain factor. Alternatives to this technique include the following two methods, which appear appropriate for the case of a single NGS star but will likely need to be modified for the 2 and 3 guide star cases.

The first is dithering the TTM by a known amount at a known frequency. Using synchronous detection techniques it is possible to recover the error signal at the dither frequency. If the current "centroid gain" is correct then the dither amplitude from the tilt measurement should equal the input dither amplitude. This method requires accurate calibration of the TTM amplitude and good knowledge of system loop transfer functions, and must avoid vibration contributions.

The second method is used in the current AO system. It uses the prior knowledge that noise in the TT diagnostics is white and therefore the signal's power spectral density should be flat from about 100 Hz to 500 Hz. Assuming that the control loop transfer function is known then the loop gain and centroid gain are merged into one factor. By estimating the centroid gain that satisfies the flatness of the high frequency spectrum one can determine the centroid gain.

A decision has not yet been made about the ultimate optimization algorithms. Laboratory and on-sky testing could be used to determine the best methods and these could be developed into the final operational software.

8.5.3 Image Repositioning (nodding, dithering and micro-dithering)

Astronomical observations must overcome two main obstacles. The first is that the sky background is continuously changing because of atmospheric OH emission line variability (J, H, and K bands) and temperature changes (K band). In addition, IR arrays have more pixel response variability and greater non-linearity compared to CCDs. To deal with these issues a number of specialized observing techniques have been developed.

Dithering refers to a technique where several exposures are made of the same object with the telescope slightly displaced from the field center. The moves are usually repeated in a so called "dithering sequence". Depending on the exact effect to be overcome, pixel to pixel response variations or sky background changes, the dither pattern and size of moves will be varied accordingly but it is typically only a few pixels in a regular pattern.

Typically, nodding refers to techniques that move the science object a large part of or completely off of the science detector to measure the sky background. This technique is used when the science object is known to contain extended emission over the full or large part of the field of view. The two techniques, nodding and dithering, are often used together. For example, a 4 move dithering sequence on the science object followed by a move to blank sky, "nod off source", followed by the same 4 move dithering sequence to

measure the background then a move back to the science object, "nod on source" to repeat the full set of dithering and nodding again.

System Requirement SR-23 states that "the NIR TTS system shall support normal science observing modes such as dithering, nodding and offsetting" and makes the following definitions:

1) Micro-dithering is performed to finely position a science object on the science detector.
2) Dithering is performed to move a science object around the science detector.
3) Offsetting is performed to mosaic an image, to obtain a measurement of the sky background, or to perform a blind offset from a reference star to the science target when the science target is not visible on the detector. Nodding is considered to be the same as offsetting.

SR-24 states that "The NIR TTS system shall be able to position an object on the science instrument to an accuracy of ≤ 120 mas (3-sigma) for moves ≤ 60 arcsec (i.e., an offset or nod) and ≤ 70 mas for moves ≤ 5 arcsec (i.e., a dither), assuming the tip-tilt star stays within the NIR TTS field of view."

The SR-24 requirements will be met by moving the telescope and adjusting the ROI locations and centroid offsets using the approach outlined in section 7.5.4. Given the 50 mas pixel resolution on the NIR TTS camera these requirements should easily be met.

SR-25 states that "The NIR TTS system shall be able to reposition an object on the science instrument to a relative accuracy of ≤ 5 mas for moves ≤ 20 mas (i.e., a micro dither), assuming the NIR TTS system tip-tilt loop was already closed."

The SR-25 requirement requires a tenth of a pixel repositioning accuracy which should be achievable for such small moves. This requirement will be met by changing the NIR TTS camera centroid offset, and when appropriate the ROI location, as part of the user requested input to the ROI and centroid offset calculation (section 7.5), without requesting a telescope move and hence without opening the AO loops. A similar functionality is currently provided by the "Slit Nod Widget" for NIRSPEC. The software checks the move size and does not reposition the telescope directly but instead move the AO field steering mirror if the requested move is smaller than 0.25". We will need a similar software check for OSIRIS requested moves; and will set the threshold higher than the 20 mas threshold in SR-25 (100 mas would seem reasonable). Note that the LGS wavefront sensor and the LBWFS will initially see the resultant offset on the down TT mirror until the TT offloading moves this to the telescope.

The approaches to repositioning the image can be briefly summarized as follows:

Nodding, offsetting or dithering (moves > 100 mas):

1. Open TT loop.
2. Offset telescope by desired amount.
3. Calculate new TT star position(s) on the NIR TTS.
4. Close TT loop on the calculated TT star positions after the telescope offset is complete.
    - Note that TT offloading and DAR tracking should start as soon as the TT loop is closed.

Micro-dithering (moves ≤ 100 mas):

1. Calculate new TT star position(s) on the NIR TTS and implement these new positions.

8.5.4 Seeing Disk Background Measurement

The following steps define a potential process for seeing disk background measurement:

1. With the LGS and TT loops closed take an 8x8 pixel image around each TT star.
2. Use the pixels outside the central 4x4 pixel to measure the seeing disk.
3. Extrapolate the seeing disk measurement into a seeing disk flux for each pixel in the central 4x4 pixels.

The nested windows arrangement proposed for the TMT could be used to make this measurement. The outer window will be sampled less often and would therefore be noisier.

Proper subtraction of the seeing disk is one means of making the TT sensor gain insensitive to the Strehl ratio. This measured background could be subtracted as part of the RTC system data processing.

8.5.5 Strehl Ratio Determination

If the Strehl ratio is known in each ROI then the optimal TT gain can be determined. A method for determining the Strehl is to first measure the total signal for each TT star in the acquisition image. To first order the Strehl ratio is then simply the signal in the 2x2 pixel region around the star (especially if the seeing disk has already been subtracted) divided by the total signal measured in the acquisition image. This Strehl ratio would feed back into the TT loop parameter optimization in section 8.5.2 and would also be a useful diagnostic to publish for the observer or operator.

8.5.6 Sky Background Measurement

STRAP requires a background measurement for stars dimmer than about 12^{th} magnitude. This background is recorded during acquisition by nodding the telescope 30" and is usually sufficient for the duration of the science observation (up to several hours). Occasionally, due to changing backgrounds due to the moon or even a very thin layer of cirrus, a new background may be beneficial, especially for the dimmest TT stars. A new background requires observations to stop such that the AO operator can move the telescope off to the sky. Operationally, one STRAP background per acquisition is the standard.

The NIR TT sensor will be able to change exposure time/coadds and take an exposure via keywords. For STRAP and the WFS, backgrounds are recorded by executing an IDL script that sets all the relevant keywords. These background scripts are run by the acquisition script or when the AO operator prompts the system to record a new background. We will match this functionality with the NIR TT sensor.

We anticipate that the background for the NIR TT sensor will change more rapidly than for either STRAP or the WFS. As such, we may require an ability to update the background. The brute force method would be to suspend operations and move off target to record another sky frame. Unfortunately, how the IR background changes differs from band to band, night to night, or even within a night; therefore, there may be no set time after which a new background is needed. A more robust solution would allow the periodic measurement of the background without interrupting science.

The NIR TT sensor is required to support 1 to 3 regions of interest (ROI) that correspond to the locations of 1 to 3 TT stars. The background measurement is subtracted from each ROI before the TT correction is calculated. We have added a requirement for the NIR TTS to support a fourth ROI for the purpose of making background measurements. The current median value of the background ROI will be compared to the median value of the original measurement. Once the two measurements deviate by a threshold, the backgrounds for the other ROIs will be scaled to the new background measurement. We select the median value as it is more robust to cosmic rays and bad pixels than a mean. The location of the dedicated ROI in the focal plane will be selected by the AO operator. Figure 78 shows the NIR TTS status mock up with a dedicated background ROI.

Three other options for an on-the-fly background measurement were considered but rejected in favor of the fourth ROI approach discussed above. These included: an interleaved full or partial frame readout from which to select a background area, a larger ROI size to get the background (this would likely include the seeing disk) and the nodding of one of multiple ROIs periodically to get a background ROI.

8.5.7 Science Image FITS Header

In order to facilitate analysis and to maintain the system configuration used during the observation, additional data will be available to be placed inside the science instrument FITS header. The needed parameters will be available as keywords so that they can be easily written to the FITS header. The NIR TTS will employ the current mechanism of a keywords configuration file that contains which AO keywords will be written to the FITS headers for the science instrument. The software that writes the FITS files read these configuration text files to determine which keywords to put into the headers. This allows greater flexibility in deciding what keywords are written to the science headers. Changes can be made by editing the configuration file to include the needed new NIRTSS keywords. A sample list of science instrument

FITS header keywords in shown in Table 11, this is only a preliminary list to illustrate the type of keywords to place into science camera FITS headers.

Table 11: Sample NIR TTS system keywords to append to the OSIRIS FITS headers

Comments	Keyword	Description
Track Sensor Type	DTSENSOR	Select-WFS-or-STRAP-or-TRICK-or-STRAP+TRICK
Tip-tilt loop gain	DTGAIN	Set-TT-loop-gain
Centroid or Correlation	TRKRO1AL	Type of algorithm Centroid/Correlation
	TRKRO2AL	Type of algorithm Centroid/Correlation
	TRKRO3AL	Type of algorithm Centroid/Correlation
# samples ROI mode	TRKRO1IE	# of samples to use (integration time) for co-add for ROI1
	TRKRO2IE	# of samples to use (integration time) for co-add for ROI2
	TRKRO3IE	# of samples to use (integration time) for co-add for ROI3
# ROI	NUMOFROI	number of ROIs
ROI #1 info	ROI1X	x pixel address corresponding to top left corner of ROI1
	ROI1Y	y pixel address corresponding to top left corner of ROI1
	ROI1SZ	size in pixels of ROI1
ROI #2 info	ROI2X	x pixel address corresponding to top left corner of ROI2
	ROI2Y	y pixel address corresponding to top left corner of ROI2
	ROI2SZ	size in pixels of ROI2
ROI #3 info	ROI3X	x pixel address corresponding to top left corner of ROI3
	ROI3Y	y pixel address corresponding to top left corner of ROI3
	ROI3SZ	size in pixels of ROI3
Centroid gain for NIRTTS sensor	TRKRO1CG	Centroid gain for ROI1
	TRKRO2CG	Centroid gain for ROI2
	TRKRO3CG	Centroid gain for ROI3
Weight factor	TRKRO1WT	weighting factor to be applied to TT error for ROI1
	TRKRO2WT	weighting factor to be applied to TT error for ROI2
	TRKRO3WT	weighting factor to be applied to TT error for ROI3
Focus Keyword	TRKFOCRO	which ROI to use for Focus control
Pickoff position	OBTDNAME	Named-position-control-for-TTD
	OBTDNMCP	Named-position-use-current-position-for-TTD
	OBTD	User-value-of-TTD
Focus stage position	OBTFNTFE	Named-position-control-for-TTF
	OBTFNMCP	Named-position-use-current-position-for-TTF
	OBTF	User-value-of-TTF
Camera filter name	FWPOSREQ	filter wheel position request
	FWCURPOS	filter wheel position readback
TRICK Temp	TRKTCSV	temperature setpoint for control
	TRKTCTMP	temperature reading
	TRKDTGN	Detector gain in electrons per ADU/pixel?

8.5.8 NIR TTS Camera Image FITS Header

When NIR TTS camera is not sending data to the NGWFC it functions in a mode similar to the current AO acquisition camera and standalone science imagers. To facilitate calibration of this camera and to use it as an auxiliary acquisition camera it will have the ability to save data in FITS file format when requested by the astronomer, observing assistant or other users. The NIR TTS sensor will have software on its camera host server for writing FITS files and will be able to populate the header with DCS, AO and NIR TTS camera keywords as requested using a similar keyword configuration file as the science instruments. A sample list of NIR TTS camera FITS header keywords in shown in Table XYZ, this is only a preliminary list to illustrate the type of keywords to place into NIRTTS camera FITS headers.

Table 12: Sample DCS, AO and NIR TTS keywords to append to the NIR TTS camera FITS header

Comments	Keyword	Description
Standard DCS	UT_Date	
	UT_Time	
	TARGNAME	
	OBJECT	
	AIRMASS	
	AZ	
	EL	
	TELFOCUS	
	ROTDEST	
	ROTMODE	
Standard AO	AODMSTAT	DM loop status
	AODTSTAT	DT loop status
	DMGAIN	DM loop gain
	DTGAIN	DT loop gain
	WSFRRT	WFS frame rate
AO OBS Pickoff position	OBTDNAME	Named-position-control-for-TTD
	OBTDNMCP	Named-position-use-current-position-for-TTD
	OBTD	User-value-of-TTD
AO OBSFocus stage position	OBTFNTFE	Named-position-control-for-TTF
	OBTFNMCP	Named-position-use-current-position-for-TTF
	OBTF	User-value-of-TTF
TRICK camera filter	FWPOSREQ	filter wheel position request
	FWCURPOS	filter wheel position readback
TRICK Temp	TRKTCSV	temperature setpoint for control
	TRKTCTMP	temperature reading
TRICK full frame readout	TRKDTGN	Detector gain in electrons per ADU/pixel?
	TRKFRMMD	full frame mode or sub frame mode?
	TRKSAMMD	sampling mode
	TRKITIME	time between reads or integration time
	TRKNUMSM	Number of samples/reads
	TRKNUMFM	Number of co-added frames
	TRKCODN	Completed frames in current coaddition sequence
	TRKCOL	Number of columns of detector
	TRKROW	Number of rows of detector
	TRKNOIFN	file name containing read noise frame
	TRKBADPX	file name containing bad pixel map
	TRKLINCO	file name with linearization coefficients
	TRKSATLV	Saturation level of detector
	TRKDTGN	Detector gain in electrons per ADU/pixel?

8.5.9 Telemetry Recorder System

A command to the real-time control system will determine what real-time data will be recorded by the telemetry recording system. It will also be desirable to record some control system parameters along with the telemetry. These items are TBD.

9. Predicted Performance

9.1 Throughput and Emissivity

A spreadsheet tool has been developed to calculate the throughput and emissivity to the NIR TTS detector (this is based on a tool developed for NGAO, KAON 723). This spreadsheet will be updated as the throughput is better understood for each of the components. The calculation includes sky, telescope, AO system and NIR TTS throughput and includes a degradation term for aging of the optics. Each component is also assigned a temperature that is used for the emissivity calculation.

The percent throughput is shown in Table 13. At the center of the Ks band the throughput of the AO system to the dichroic pickoff feeding the NIR TTS is calculated to be 69%, including the impact of dust and aging (71% in H-band). The throughput of the NIR TTS optics including the K-band reflective dichroic is 75%. The overall throughput is 47%.

The emissivity in units of photons/(m^2-sec-nm-arcsec^2) is given in Table 14. The background contribution of the AO and NIR TTS optics is 1.7 times that of the sky + telescope at 2.1 μm. The final percentages in Table 14 are for the degraded case.

Table 13: Percent Throughput

			One-year	Wavelength		Kp		
Optic	**Coating**	**Temp C**	**Degradation**	**1.9**	**2**	**2.1**	**2.2**	**2.3**
Kmirror, surf 1	CoatingData!Keck_Al	2.0	2.0%	97.3%	97.3%	97.3%	97.3%	97.3%
Kmirror, surf 2	CoatingData!FSS99_106_45	2.0	1.0%	98.0%	97.8%	97.6%	97.4%	97.3%
Kmirror, surf 3	CoatingData!Keck_Al	2.0	1.0%	97.3%	97.3%	97.3%	97.3%	97.3%
TT mirror	CoatingData!FSS99_106_45	2.0	2.0%	98.0%	97.8%	97.6%	97.4%	97.3%
OAP1	CoatingData!FSS99_106_45	2.0	2.0%	98.0%	97.8%	97.6%	97.4%	97.3%
DM1	CoatingData!FSS99_500_0	2.0	2.0%	97.6%	97.6%	97.6%	97.6%	97.6%
OAP2	CoatingData!FSS99_106_45	2.0	2.0%	98.0%	97.8%	97.6%	97.4%	97.3%
IR/Vis Dichroic IR Path	CoatingData!None	2.0	1.0%	95.0%	95.0%	95.0%	95.0%	95.0%
IR/Vis Dichroic IR Path	CoatingData!None	2.0	1.0%	99.5%	99.5%	99.5%	99.5%	99.5%
TRICK Dichroic, surf 1	CoatingData!None	2.0	1.0%	97.0%	97.0%	97.0%	97.0%	97.0%
TRICK field lens, surf 1	CoatingData!FSS99_500_0	2.0	1.0%	97.6%	97.6%	97.6%	97.6%	97.6%
TRICK field lens, surf 2	CoatingData!FSS99_500_0	2.0	1.0%	97.6%	97.6%	97.6%	97.6%	97.6%
TRICK mirror	CoatingData!FSS99_500_0	2.0	1.0%	97.6%	97.6%	97.6%	97.6%	97.6%
TRICK window, surf 1	CoatingData!None	2.0	1.0%	99.0%	99.0%	99.0%	99.0%	99.0%
TRICK window, surf 2	CoatingData!None	-40.0	0.5%	99.0%	99.0%	99.0%	99.0%	99.0%
TRICK dewar optics	CoatingData!None	-40.0	0.5%	90.0%	90.0%	90.0%	90.0%	90.0%
AO System				80.5%	79.9%	79.2%	78.7%	78.4%
AO System, Degraded				69.6%	69.2%	**68.6%**	68.1%	67.8%
TRICK Optics				79.5%	79.5%	79.5%	79.5%	79.5%
TRICK Optics, Degraded				74.7%	74.7%	**74.7%**	74.7%	74.7%
AO System + TRICK, Degraded				52.0%	51.7%	**51.2%**	50.9%	50.7%
AO + TRICK, Degraded + Sky + Telescope				4.6%	30.3%	**46.9%**	43.9%	43.7%

Table 14: Emissivity

Optic	**Coating**	**Temp C**	**1.9**	**2**	**2.1**	**2.2**	**2.3**
Kmirror, surf 1	CoatingData!Keck_Al	2.0	3.05E-02	9.68E-02	2.74E-01	7.02E-01	1.65E+00
Kmirror, surf 2	CoatingData!FSS99_106_45	2.0	2.03E-02	6.91E-02	2.09E-01	5.62E-01	1.35E+00
Kmirror, surf 3	CoatingData!Keck_Al	2.0	2.57E-02	8.15E-02	2.31E-01	5.93E-01	1.39E+00
TT mirror	CoatingData!FSS99_106_45	2.0	2.92E-02	9.82E-02	2.93E-01	7.81E-01	1.87E+00
OAP1	CoatingData!FSS99_106_45	2.0	3.04E-02	1.03E-01	3.07E-01	8.19E-01	1.96E+00
DM1	CoatingData!FSS99_500_0	2.0	3.48E-02	1.12E-01	3.20E-01	8.24E-01	1.94E+00
OAP2	CoatingData!FSS99_106_45	2.0	3.32E-02	1.12E-01	3.36E-01	8.98E-01	2.15E+00
IR/Vis Dichroic IR Path	CoatingData!None	2.0	5.25E-02	1.70E-01	4.85E-01	1.25E+00	2.94E+00
IR/Vis Dichroic IR Path	CoatingData!None	2.0	1.33E-02	4.30E-02	1.23E-01	3.17E-01	7.46E-01
TRICK Dichroic, surf 1	CoatingData!None	2.0	3.70E-02	1.20E-01	3.42E-01	8.80E-01	2.07E+00
TRICK field lens, surf 1	CoatingData!FSS99_500_0	2.0	3.27E-02	1.06E-01	3.02E-01	7.78E-01	1.83E+00
TRICK field lens, surf 2	CoatingData!FSS99_500_0	2.0	3.39E-02	1.09E-01	3.12E-01	8.05E-01	1.90E+00
TRICK mirror	CoatingData!FSS99_500_0	2.0	3.51E-02	1.13E-01	3.24E-01	8.33E-01	1.96E+00
TRICK window, surf 1	CoatingData!None	2.0	2.10E-02	6.77E-02	1.93E-01	4.98E-01	1.17E+00
TRICK window, surf 2	CoatingData!None	-40.0	1.12E-04	4.61E-04	1.65E-03	5.22E-03	1.48E-02
TRICK dewar optics	CoatingData!None	-40.0	7.81E-04	3.23E-03	1.16E-02	3.65E-02	1.04E-01
AO System, Degraded			0.27	0.88	2.58	6.74	15.99
TRICK Optics, Degraded			0.16	0.52	1.49	3.84	9.05
AO System + TRICK, Degraded			0.43	1.40	4.06	10.58	25.04
Sky + Telescope			2.02	2.99	2.40	8.96	9.01
Degraded AO System + TRICK + Sky + Telescope			2.45	4.39	6.47	19.54	34.05
AO System + TRICK as % of Sky + Telescope			21%	47%	169%	118%	278%

9.2 Signal-to-Noise Ratio

A spreadsheet tool has been developed to determine the signal-to-noise ratio (SNR) for the NIR TTS. The spreadsheet is shown in Table 15. The throughput numbers are from Table 13 and the Strehl numbers are from the performance of the current Keck II LGS AO system (these values will be improved with the Keck I laser and center launch system). The signal is then calculated for the indicated magnitude star at the indicated zenith angle and off-axis distance. The thermal background noise is calculated from the measured background for NIRC2 (which should be quite similar to those for the NIR TTS) and the read + dark noise is from Figure 58.

Table 15: SNR calculation spreadsheet

The case shown is 45° zenith angle, 45" off-axis, K=14 TT star with 100 Hz sampling using 4x4 pixels.

Quantity	Units	H-band	Ks-band	Notes
Telescope throughput		0.92	0.92	
AO system throughput to TRICK		0.50	0.51	
Detector QE		0.75	0.84	Measured H2RG median QE
Telescope + AO Throughput		***34.4%***	***39.7%***	
Strehl at zenith		0.12	0.30	LGS web page
Zenith angle		45	45	
Strehl at zenith angle		0.08	0.21	LGS web page: SR(K')=0.24 for R=17 & median seeing
Tip-Tilt star off-axis distance	arcsec	30	45	
Isokinetic angle	arcsec	55	70	LGS web page: 64, 73 & 95" measured
Tip-Tilt Star Strehl		***6%***	***13%***	
Wavelength	nm	1633	2124	NIRC2 Kp filter
Filter Bandwidth	nm	300	336	NIRC2 Kp filter
log f (in W/cm2/um) at zero mag		-13	-13.4	K-band (Allen, p. 202)
Telescope diameter	cm	1000	1000	
Flux (above atmosphere for 0 mag)	W	2.36E-08	1.05E-08	
Photon energy	J/photon	1.22E-19	9.35E-20	(Allen, p. 15)
Flux (above atmosphere for 0 mag)	photon/sec	1.94E+11	1.12E+11	
Magnitude		14.5	14.0	H-K = 0.5 assumed
Flux (above atmosphere for mag)	photon/sec	3.07E+05	2.82E+05	
Atmospheric Transmission		0.989	0.989	(Allen, p.126 - 0.6 air mass at zenith)
Photons on telescope	photon/sec	3.04E+05	2.79E+05	
Integration time	s	0.01	0.01	
Total signal in AO-corrected core	**electron**	***60***	***146***	
Background (sky + thermal)	mag/arcsec^2	13.6	12.56	K'-band background measured on NIRC2
Zero point magnitude		25.44	24.74	NIRC2 sensitivity manual
Number of pixels		16	16	
Arcsec/pixel		0.05	0.05	
Total background	***electron***	87	119	
Background noise	**electron**	**9**	**11**	
Seeing disk photon noise	**electron**	**12**	**12**	Assumes 15% of total seeing disk energy in 4x4 pixels
Readout + dark noise	**electron**	**3.5**	**3.5**	Lab noise measurements
Photon noise	**electron**	**8**	**12**	
Noise	**electrons**	**22**	**25**	
SNR		***2.7***	***5.9***	

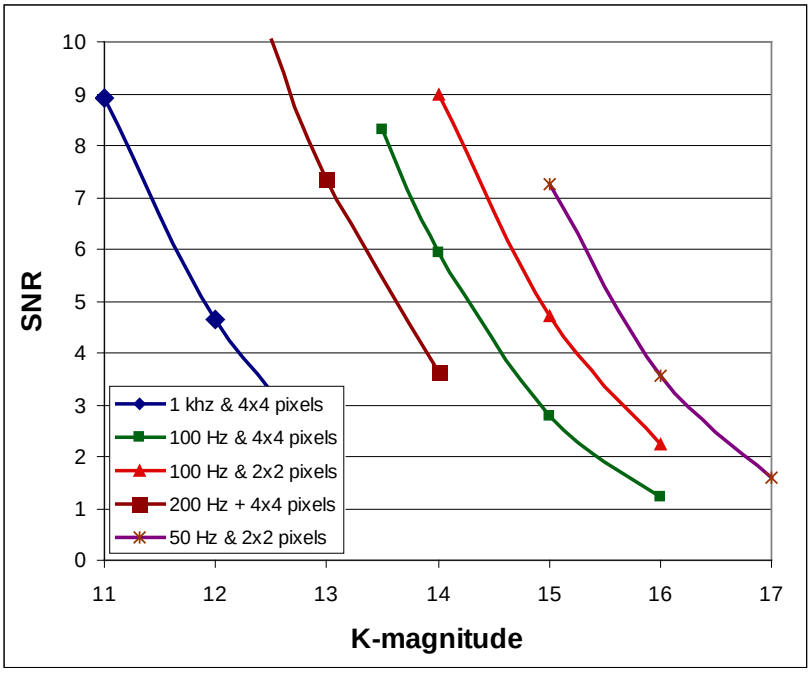

Figure 81: SNR versus K-magnitude (median seeing, 45° zenith angle, 45" off-axis and 5 electrons/pixel noise assumed in all cases).

A plot of SNR versus K-magnitude is shown in Figure 81 for a range of conditions; for the brightest stars (at left) the NIR TTS is run at 1 kHz using 4x4 pixels, while the rate is reduced to 50 Hz with 2x2 pixels for the faintest stars. This plot indicates a limiting magnitude of K ~ 16 for these conditions. The average star is redder than M0 (for a M0 star R-K = 2.4) so this limiting K magnitude corresponds to a limiting magnitude of R > 18.4 star. STRAP and the LBWFS are limited to R ~ 19 so the limiting magnitudes are comparable.

9.3 Performance Trades

KAON 823 summarizes some performance trades studied during the system design, in particular analysis to support the choice of the pickoff optics options by evaluating the relative performance of H and Ks-band TT sensing. This analysis assumes the Keck I LGS AO system with a center launched 30W mode-locked CW laser. The NGAO galaxy assembly science case was evaluated which assumes median seeing conditions, 60° galactic latitude, 30° zenith angle and an integration time of 1800 seconds.

The residual 1-D RMS TT error for H and Ks-band tip-tilt sensing (TRICK), and for the existing STRAP sensor are shown in Figure 82. The advantage of Ks-band sensing for large sky fraction is very clear. H-band sensing has an advantage over STRAP for the low sky coverage case but the H-band Strehl is simply too low when moving far off-axis as required for high sky coverage.

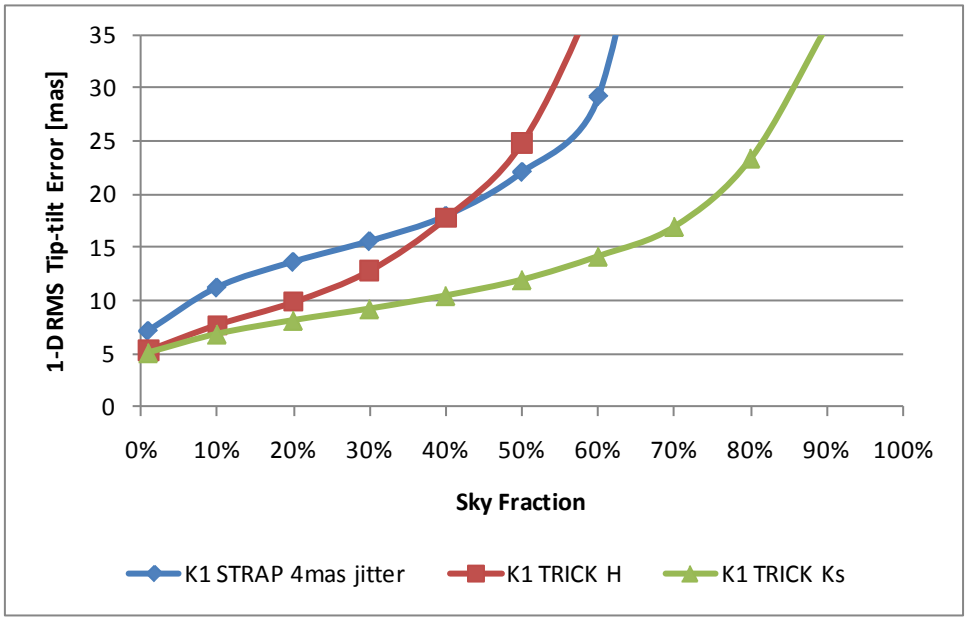

Figure 82: Residual 1-D RMS TT error for the NIR TTS at H and Ks, and for STRAP

The K-band science Strehl ratio and ensquared energy (EE) within a 50 mas spaxel, corresponding to the cases in Figure 82, are shown in Figure 83 and Figure 84, respectively. For 50% sky coverage Ks-band sensing results in a Strehl of 36% versus 18% for H-band sensing.

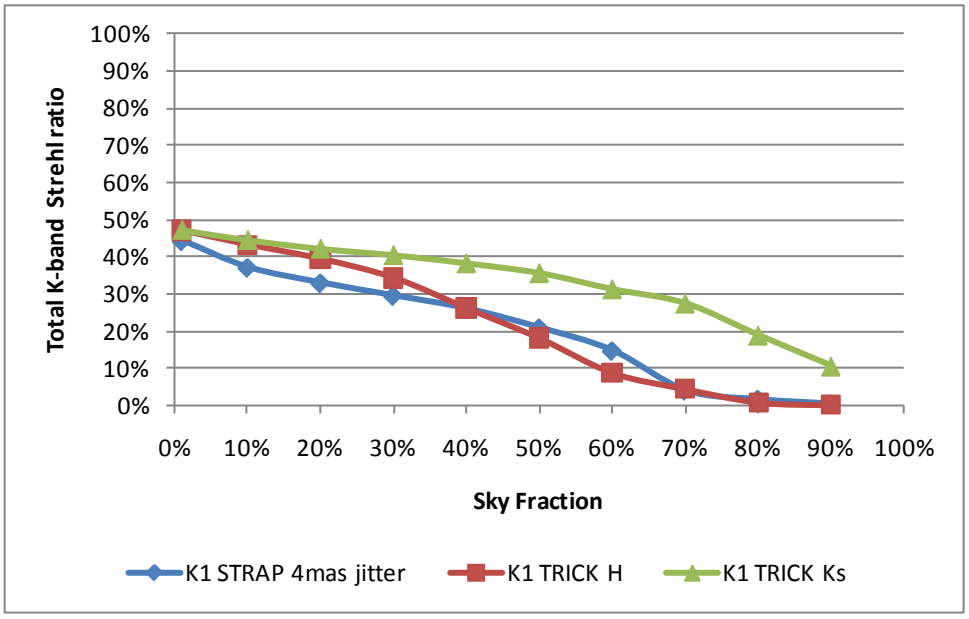

Figure 83: Strehl performance for the galaxy assembly science case

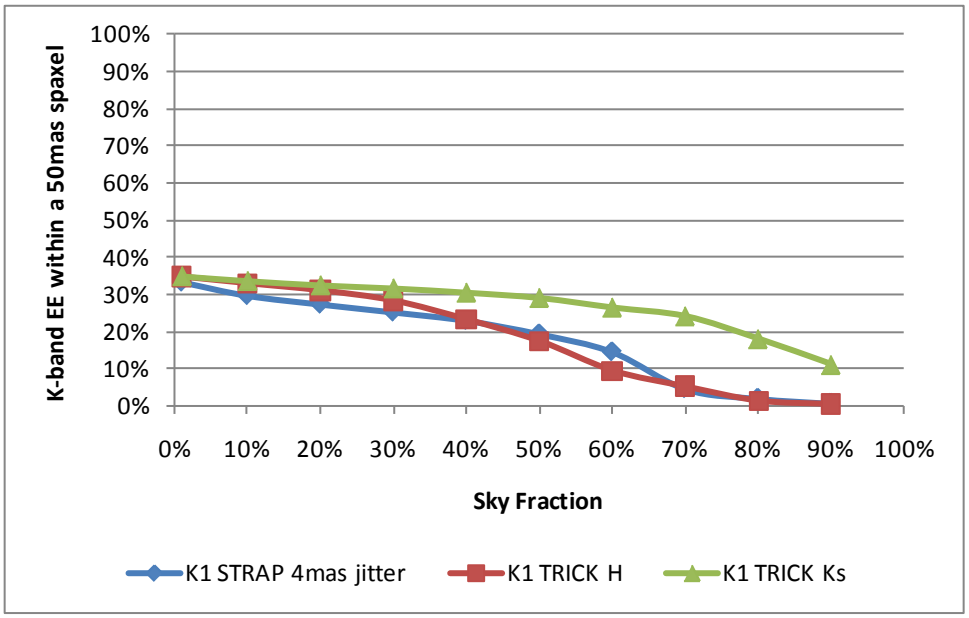

Figure 84: Ensquared energy performance for the galaxy assembly case

TT performance depends on TT star color as shown in Figure 85. STRAP outperforms NIR TT sensing for stars of G spectral type or earlier. The vast majority of main sequence stars are however M spectral class for which the NIR TTS performance, in Ks and H, significantly outperforms STRAP. As can be seen from this plot the performance predictions are very dependent on star color. During the preliminary design we intend to check our color and star frequency assumptions given this critical dependence.

The performance versus zenith angle is plotted in Figure 86. Both H and Ks-band performance degrades rapidly once a particular zenith angle is reached due to the breakdown of off-axis AO correction.

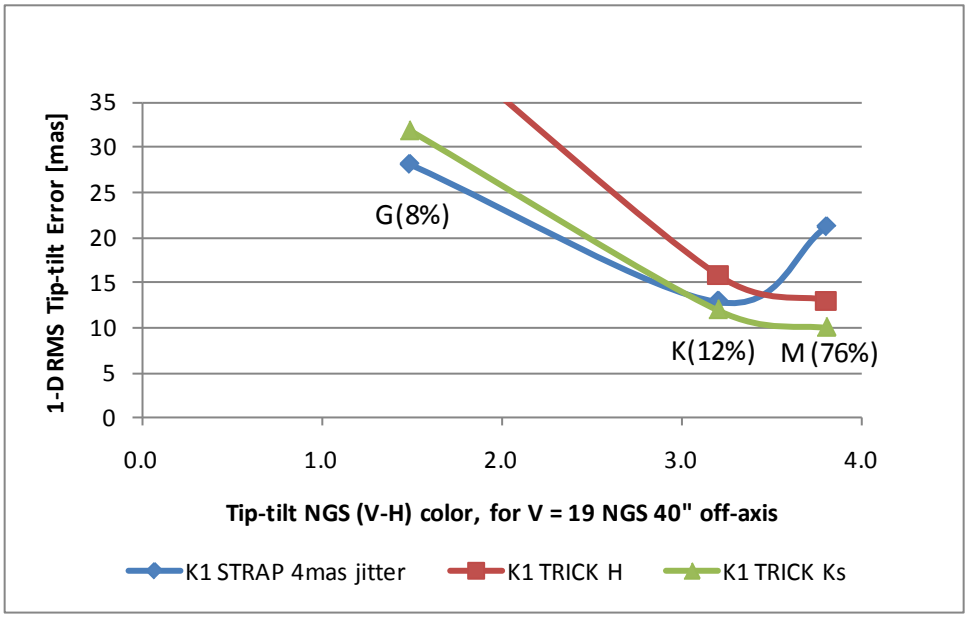

Figure 85: TT performance for a V = 19 NGS located 40" off-axis, assuming different spectral type stars. The number in parentheses is the fraction of all main sequence stars of that type (from LeDrew, 2001).

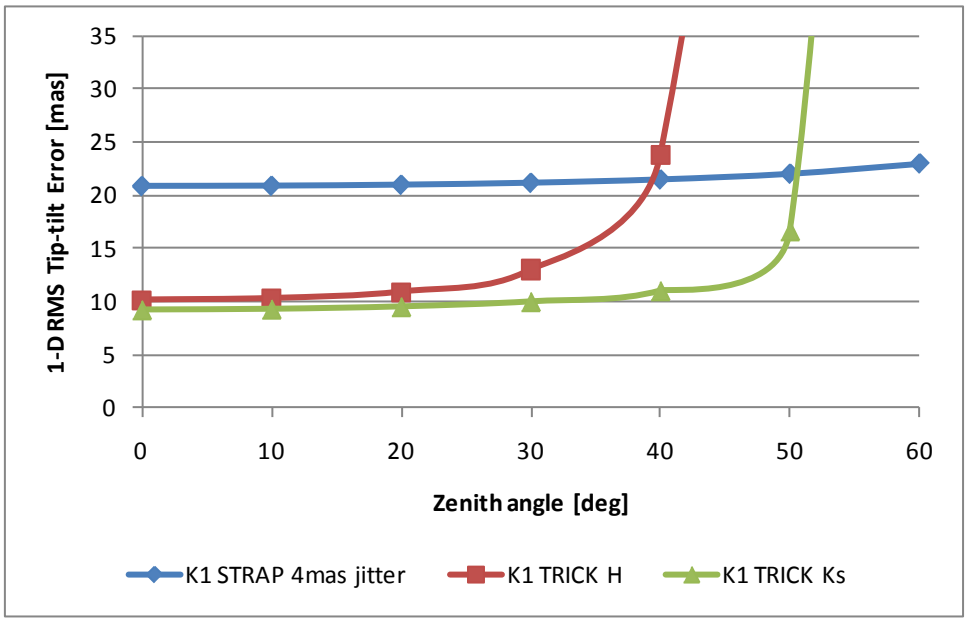

Figure 86: TT performance for the galaxy assembly science case as a function of zenith angle

These analyses influenced our optical pickoff choices. In addition to the originally planned K-band dichroic we concluded that it was worthwhile to have an H-band dichroic to allow us to do improved K-band science for the low sky coverage cases. The significantly higher Ks-band for the high sky coverage case also implied that an annular mirror, that passed the K-band science light while allowing us to use Ks-band sensing for off-axis TT stars, would also be valuable.

9.4 Error Budget

The analysis in this section was prepared for the proposal and has not been revisited during the system design. We will update this analysis during the preliminary design.

An extensive spreadsheet based error budget tool has been developed for WMKO and Palomar, with anchors to AO simulations and on-sky results. This tool has been used to generate the error budgets listed in Table 16 for observations of high redshifts galaxies at a zenith angle of 30° assuming a Spagna 2001 star density model. The predictions for the current Keck II LGS AO system are a K-band Strehl of 20% for imaging and an ensquared energy of 18% for 0.05" spaxel IFU observations. This is consistent with observations. For example, Wright et al. (2009) report Strehl ratios of between 22 and 30% for six z ~1.6 galaxy observations with OSIRIS using relatively bright TT stars (V-band 14.5 to 16.8); fainter TT stars are assumed for this higher sky coverage case. The Strehl is predicted to improve to 26% with a planned higher power laser on Keck I, and then to 41% with the implementation of the proposed TTS.

The predicted ensquared energies for Keck I as a function of the seeing parameter, r_0, is shown in Figure 87 for the case of high redshift galaxies. Three scenarios are shown, the existing STRAP TTS (green), a NIR TTS operating at J/H-band (blue) and a NIR TTS operating at K-band (red). For the proposed K-band NIR TTS, the reduction in the rms tilt error (dashed line) from 20 to 10 mas under median seeing conditions (r_0 =16 cm) results in an increase in the ensquared energy (solid line) from 23 to 32% in a 50 mas spaxel.

Error Term	High-Redshift Galaxies (r0 = 14.7 cm @ 30° zenith angle; wind 9.5 m/s)		
	K2 2009	K1 2010	K1 2013 (w/ new TTS)
Atmospheric Fitting	126	126	126
Telescope Fitting	66	66	66
Science Camera	30	30	30
DM Bandwidth	108	55	55
DM Measurement	146	71	71
Tip-tilt Bandwidth	145	145	89
Tip-tilt Measurement	191	192	95
Tip-tilt Anisoplanatism	190	190	111
LGS Focus Error	34	34	34
Focal Anisoplanatism	187	187	187
LGS High Order Error	50	50	50
Calibration Errors	29	29	29
Miscellaneous	90	36	101
Total Wavefront Error	442	405	329
Science Wavelength	2.2 μm		
Strehl Ratio	20%	26%	41%
Ensquared Energy (50 mas)	18%	23%	32%

Table 16: Keck LGS AO wavefront error budgets (in nm rms) for the high redshift galaxies science case at 30° zenith angle as performance is improved: current 2009 Keck II LGS AO system performance, predicted Keck I LGS AO system with the new laser in 2010, and the Keck I LGS AO system with the proposed TTS.

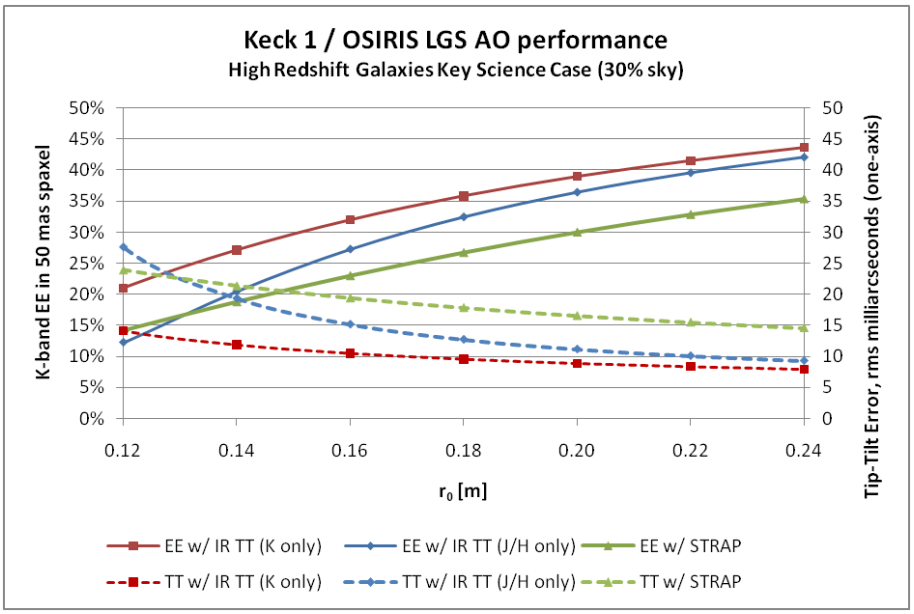

Figure 87: Predicted performance for the case of high redshift galaxies

A ~40% improvement in ensquared energy (~55% in Strehl) with the proposed NIR TTS would produce significant high-redshift galaxy science gains. A corresponding increase in signal-to-noise ratio (SNR) can be expected for AO observations of point sources for both photon-limited or background limited observations (or a Strehl-squared reduction in integration time to reach the same SNR). For LGS studies of extended sources or faint sources next to bright sources, the contrast is the key science metric and will be increased by Strehl/(1–Strehl).

10. Documentation

The documentation to be provided with the operational NIR TTS system will include the required documentation to support the astronomer, the operator and engineering personnel.

Observer/astronomer documentation will include the following items available from the public website:

- Performance data
- Observing preparation and observing guidelines/procedures

Operator documentation will include the following items available from the Keck intranet website:

- An operations guide
- Any maintenance procedures
- Any troubleshooting procedures

Engineering documentation will include the following items available from the AO folder in KeckShare:

- Design, implementation and performance documents (documented as KAONs)
- Vendor manuals & results

11. Acceptance, Integration and Test

The acceptance, integration and test plan is documented in KAON 855.

12. System Requirements Compliance

The system requirements are defined in KAON 823 and managed in a spreadsheet, KAON 835, along with their compliance. All requirement changes are tracked on the “Changes” sheet of this spreadsheet. The compliance choices are either: yes, no or DD (to be determined during the detailed design). The system requirements and there compliance are provided in Table 17.

Table 17: System Requirements

#	Overall Requirements	Compliance
1	Provide a NIR TTS system for the Keck I LGS AO system and OSIRIS.	Yes
2	The NIR TTS system shall be capable of operating as an integrated part of the Keck I LGS AO control system.	Yes
3	When the NIR TTS system is not in use it shall allow the current science modes of the AO system and science instruments to be used with no reduction in performance.	Yes
4	Provide improved tip-tilt correction and improved sky coverage for LGS AO science operations. Specifically, the NIR TTS system shall achieve the performance improvements predicted in Table 1 under the conditions indicated. The performance is allowed to degrade with respect to Table 1 as the conditions worsen. *See "WFE Budget" tab.*	Yes
5	Goal: Provide TBD improved focus correction and reduce the overhead for focus measurements by TBD during LGS AO science operations.	No (future option)
6	The NIR TTS system shall be operable, with performance consistent with system requirement #4, over a range of seeing conditions up to the 80^{th} percentile seeing. The goal is 90^{th} percentile seeing.	Yes
7	The NIR TTS system shall be operable, with performance consistent with system requirement #4, over the telescope zenith angle range from 0.5° to 65°.	Yes
8	The NIR TTS system shall come equipped with a means of identifying the location of tip-tilt stars on the camera. For example, the NIR TTS could have its own acquisition mode or the existing acquisition camera should be capable of adequately positioning stars on the NIR TTS.	Yes
9	Goal: The NIR TTS system shall be capable of using up to three tip-tilt stars as input to the real-time controller tip-tilt determination, plus a single readout area for sky background measurements.	Yes
10	The NIR TTS system shall be capable of using non-point sources ≤ 0.1" in diameter, with performance consistent with system requirement #4.	Yes
11	Goal: The NIR TTS system shall be capable of using non-point sources ≤ 1" in diameter, with performance consistent with system requirement #4.	0.8" max
12	Goal: The NIR TTS system shall be capable of operating in parallel with the existing visible TTS (STRAP) for improved tip-tilt correction. Both sets of data shall be capable of being used together by the real-time controller to calculate the tip-tilt to be applied to the tip-tilt mirror.	No (future option)
13	The NIR TTS system shall be capable of using stars as faint as K = 16 mag over its entire field of view.	Yes
14	The NIR TTS system shall be capable of using stars as faint as H = 16 mag over its entire field of view.	Yes
15	When the NIR TTS system is used the science field of view of interest shall be unvignetted. Depending on the science case the science field of view of interest may include just the OSIRIS IFU or both the IFU and imager. Options shall be provided to allow both the IFU and imager fields of view to be passed when the NIR TTS is operated in H or K-band.	Yes
16	The NIR TTS shall be positioned to be parfocal with the science instrument focal plane. This will require that the NIR TTS be able to refocus for different observing modes.	Yes
17	The time required for any routine daytime calibrations of the NIR TTS system shall not exceed 20 minutes.	DD
18	The time required for any routine nighttime start of night calibrations of the NIR TTS system shall not exceed 10 minutes.	DD

19	The time required to initialize (assumes power up and loading of software has been performed as part of startup) the NIR TTS system shall not exceed 10 minutes. This initialization refers to the associated computer systems, software and motion control devices. The NIR TTS camera is assumed to be at operating temperature.	DD
20	The NIR TTS system shall not increase the typical LGS AO acquisition time by more than 15 seconds.	DD
21	Other than acquisition time, the NIR TTS system shall not reduce the observing efficiency of the current LGS AO system. Observing efficiency includes the time to perform such tasks as nodding, dithering and offsetting.	Yes
22	The NIR TTS system shall support differential atmospheric refraction corrections between the TTS and the science instrument for a ≤ 20 minute science exposure for zenith angles ≤ 60°, with performance consistent with system requirement #4.	Yes
23	The NIR TTS system shall support normal science observing modes such as dithering, nodding and offsetting. Definitions: 1) Micro-dithering is performed to finely position a science object on the science detector. 2) Dithering is performed to move a science object around the science detector. 3) Offsetting is performed to mosaic an image, to obtain a measurement of the sky background, or to perform a blind offset from a reference star to the science target when the science target is not visible on the detector. Nodding is considered to be the same as offsetting. The amplitudes and accuracy of these moves are defined in SR-24 and SR-25.	Yes
24	The NIR TTS system shall be able to position an object on the science instrument to an accuracy of ≤ 120 mas (3-sigma) for moves ≤ 60 arcsec (i.e., an offset or nod) and ≤ 70 mas for moves ≤ 5 arcsec (i.e., a dither), assuming the tip-tilt star stays within the NIR TTS field of view.	Yes
25	The NIR TTS system shall be able to reposition an object on the science instrument to a relative accuracy of ≤ 5 mas for moves ≤ 20 mas (i.e., a micro dither), assuming the NIR TTS system tip-tilt loop was already closed.	Yes
26	The stability of the NIR TTS with respect to the AO bench shall be ≤ 5 mas over a 1 hour exposure, assuming a temperature change of ≤ 1° C.	DD
27	The NIR TTS system shall be able to reposition an object on the science instrument to ≤ 10 mas after an intermediate move of ≤ 10 arcsec, in support of dithering.	Yes
28	The NIR TTS system is not expected to support non-sidereal tracking; this mode will continue to be supported by STRAP. As a goal, the NIR TTS system shall be able to maintain the position of a non-sidereal object on the science instrument to ≤ 5 mas for a non-sidereal object with a deviation rate of 50 arcseconds per hour or less, assuming the tip-tilt star stays within the NIR TTS field of view.	No (future option)
29	As a goal the NIR TTS shall support fixed pupil mode. In this mode the NIR TTS shall be able to maintain the position of science object on the science instrument to ≤ 5 mas for an off-axis tip-tilt star that remains on the NIR TTS throughout the observation. This mode need only be supported during meridian transiting ≥ 5° (TBC) from the zenith.	No (future option)
30	As a goal the NIR TTS should provide some measure of performance. Desired quantities include a Strehl measurement and a measure of the seeing disk profile (a two component Gaussian fit has been suggested) plus a relative photometry measurement for each tip-tilt star.	Yes
31	The NIR TTS system shall meet all of its performance requirements in the operating environment conditions given in Table 2.	Yes
32	Provide the ability to operate the NIR TTS with the high order NGS WFS in "dual NGS" mode to support development & testing.	Yes

#	Optical Requirements	Compliance
33	The unvignetted field of view of the NIR TTS shall be at least a 100" diameter circle with a goal of a 120" diameter circle.	Yes
34	The operational wavelengths of the NIR TTS shall be the short wavelength end of K-band (e.g. Ks or K') and H-band. Only one of these bands will be used at any given time.	Yes
35	When the NIR TTS system is used the transmission in the science wavelength shall not be reduced by more than 5%. The goal is 3%.	DD
36	When the NIR TTS system is used the emissivity in the science wavelength shall not be increased by more than 5% averaged over the science band. The goal is 3%.	DD
	Mechanical Requirements	
37	The NIR TTS system shall not introduce vibrations into the LGS AO system that would impact science performance. This requirement is already covered by requirement 4 but is included here to draw specific attention to the importance of minimizing vibrations.	DD
38	The NIR TTS system shall not mechanically interfere with the components already on the AO bench, unless these components can be and are appropriately modified to support the integration of the NIR TTS system.	Yes
39	The NIR TTS system mounted on the AO bench shall not exceed a total mass of 70 kg (TBC).	DD
40	The associated NIR TTS system equipment not on the AO bench shall not exceed a TBD envelope.	DD
	Electronic/Electrical Requirements	
41	The NIR TTS system shall use less than or equal to TBD of electrical power.	DD
42	The NIR TTS system on the AO bench shall not exceed a one-hour average heat dissipation of 5 Watts into the AO bench environment.	DD
43	The associated NIR TTS system equipment not on the AO bench shall not exceed a one-hour average heat dissipation of 10 Watts into the AO clean room.	DD
44	If practical the NIR TTS system electronics shall be located in a rack in the AO electronics room and cables must be of appropriate length to reach these locations. If cable lengths are required to be shorter, then the cables shall be at least long enough to allow placing this equipment outside of the enclosure directly around the AO bench.	DD
	Safety Requirements	
45	The NIR TTS system shall be able to withstand the acceleration profile (to be provided) without damage or severe misalignment. Restraints should be provided to prevent hardware from damaging itself or other hardware during an earthquake.	DD
	Software Requirements	
46	The NIR TTS system shall provide the needed operational tools to support its daytime calibration.	Yes
47	The NIR TTS system shall provide the needed tools to support science observation planning.	Yes
48	The NIR TTS system shall provide the needed operational tools to support nighttime science operations.	Yes
	Interface / Logging Requirements	
49	The NIR TTS system must support an interface to the Observatory standard KTL keywords. For example, command and status communications between the NIR TTS	Yes

	camera system and the optics bench, supervisory controller and operations software shall be via keywords.	
50	All telemetry from the NIR TTS shall be provided to the existing telemetry server.	Yes
51	The NIR TTS system shall be capable of saving images in FITS format.	Yes
	Spares Requirements	
52	The spare NGWFC electronics hardware setup currently available in WMKO HQ shall be updated to match the final hardware configuration that will be designed for the NIR TTS project.	Yes
	Reliability Requirements	
53	The NIR TTS system shall meet all of its performance requirements without repair after shipment to Keck headquarters and to the telescope.	Yes
54	The NIR TTS system shall have a lifetime of ≥ 10 years.	Yes
55	The NIR TTS system shall be capable of operating on ≥ 200 nights per year.	DD
56	The NIR TTS system shall lose no more than 5% of its total observing time to faults.	DD
57	The NIR TTS system shall have a median time between faults that result in ≥ 10 minutes of lost observing time, of ≥ 10 nights of operation.	DD
58	The time to restart the NIR TTS system shall not exceed 10 minutes.	DD
59	The NIR TTS system shall meet all of its performance requirements without repair or realignment after being subjected to any number of cycles of any of the non-operating environmental conditions shown in Table 3.	DD
60	The NIR TTS system shall be able to withstand a total and sudden loss of electrical power or a transient power event, without suffering damage.	DD
61	The NIR TTS system shall be able to operate without telemetry logging in the event that the Telemetry Recorder System (TRS) is non-operational.	DD
	Service and Maintenance Requirements	
62	AO system unavailability or downtime to install and integrate the NIR TTS system shall not exceed 2 weeks.	DD
63	Routine maintenance on the NIR TTS shall not require more than 1 technician for 4 hours every 4 months.	DD
	Documentation Requirements	
64	The NIR TTS system shall be provided with the documentation required to understand and document its as-built design, and to maintain and operate it.	Yes
65	The NIR TTS system shall be provided with the documentation required to support science operations planning. This should include at least 3 months of performance characterization data after the system has begun being used for shared-risk science.	Yes
66	Goal: The NIR TTS system shall be provided with a performance estimation tool for both pre-observing planning and observing. This would be even more useful with a PSF simulator attached to it.	Yes
67	The NIR TTS system shall successfully complete a handover review, with TBD success criteria, before being transferred to the responsibility of the AO operations group.	Yes

	Configuration Management Requirements	
68	All code changes and documentation updates shall be managed according to existing WMKO configuration management practices.	Yes
69	All software releases on the operational system shall be revertible to an on-sky demonstrated software release within 15 (TBC) minutes.	DD
70	The NIR TTS system shall receive approval from the AO configuration control board prior to implementation into the Keck I LGS AO system.	Yes

13. Functional Requirements Compliance

The functional requirements, which are flowed down from the system requirements to subsystems, have been developed for four subsystems: camera system, opto-mechanics, controls and observing software. The RTC functional requirements have been defined and are included in the Microgate SOW (KAON 824). The non-RTC functional requirements are maintained in the KAON 835 requirements spreadsheet. All subsystems must meet the system requirements, although in some cases the system requirements are not applicable to a particular subsystem. A summary of which system requirements are applicable to each subsystem can be found in KAON 835. The subsystem functional requirements, excluding the RTC requirements, are shown in Table 18, Table 19, Table 20 and Table 21, along with their compliance status. The flowdown column references the system requirements (SR) number from which a particular functional requirement flows.

Table 18: Camera system functional requirements

#	Overall Requirements	Flowdown	Compliance
1	The camera system shall include a cryogenic dewar containing reimaging optics, a filter changer mechanism with H and K' filters and motion control, and an H2RG detector; the camera control electronics and host computer, and the associated cryo and vacuum systems.	SR-1	Yes
2	The camera system shall interface to the opto-mechanical system as defined in KAON 836.	SR-1,2,38	Yes
3	The camera system shall interface to the controls and observing software systems as defined in KAON 836.	SR-1,2	Yes
4	The camera system shall interface to the Microgate RTC system as defined in KAON 824.	SR-1,2,9	Yes
5	The camera system shall deliver a read + dark noise of < 5 electrons total for one region of interest up to 4x4 sampling at 1 kHz.	SR-4	Yes
6	The camera shall have a full frame readout mode that writes images in FITS format. As a goal the images should also be available in binary format via API.	SR-8	Yes
7	The camera shall provide H and Ks filters and a remote means of switching between these two filters.	SR-13,14	Yes
8	Goal: The camera shall provide a blocked position to allow dark measurements.	SR-46	Yes
9	The time to read out a full frame image shall be ≤ 5 sec.	SR-8,20	Yes
10	The time required to initialize the camera system shall not exceed 5 minutes.	SR-19	DD
	Optical Requirements		
11	The camera shall have a plate scale of 50 mas/pixel.	SR-4	Yes
12	The camera system shall have a wavefront quality ≤ TBD nm rms.	SR-4	DD
13	The camera system shall have a throughput of ≥ TBD % including the detector QE at Ks.	SR-13	DD

14	The camera system shall have a throughput of ≥ TBD % including the detector QE at H.	SR-14	DD
15	Optical distortions within the camera system shall be ≤ 10 mas for any two points separated by ≤ 60".	SR-24,25	DD
	Mechanical Requirements		
16	The stability of the camera system with respect to its mounting surface shall be ≤ 3 mas over a 1 hour exposure, assuming a temperature change of ≤ 1° C.	SR-26	DD
17	The camera system shall mount to the AO bench within an envelope defined in the camera ICD (KAON 836). The camera system shall not mechanically interfere with the components already on the AO bench, unless these components can be and are appropriately modified to support the integration of the NIR TTS system.	SR-38	Yes
18	The camera system mounted on the AO bench shall not exceed a total mass of 50 kg.	SR-39	DD
19	The associated camera system equipment not on the AO bench shall not exceed a TBD envelope.	SR-40	DD
	Electronic/Electrical Requirements		
20	Each opto-mechanical stage shall be provided with an appropriate servo motor and encoder to ensure that the positioning requirements can be met. The filter exchanger positioning requirement is ≤ 1 mm.	SR-1,2,4	Yes
21	The camera system shall use less than or equal to TBD of electrical power, in excess of the current system.	SR-41	DD
22	The camera system on the AO bench shall not exceed a heat dissipation of 3 Watts into the AO bench environment.	SR-42	DD
23	The associated camera system equipment not on the AO bench shall not exceed a heat dissipation of 7 Watts into the AO clean room.	SR-43	DD
24	The associated camera system equipment not on the AO bench shall be capable of being placed at least TBD m from the NIR TTS system location on the AO bench.	SR-44	DD
	Reliability Requirements		
25	The camera system shall lose no more than 3% of its total observing time to faults.	SR-56	DD
26	The camera system shall have a median time between faults of ≥ 20 nights of operation.	SR-57	DD
27	The time to restart the camera system in the event of a fault shall not exceed 5 minutes.	SR-58	DD
	Service and Maintenance Requirements		
28	Routine maintenance on the camera system shall not require more than 1 technician for 2 hours every 4 months.	SR-63	DD
29	The camera shall be operable in a stand-alone mode to support both development and diagnostics once installed	SR-63	Yes
30	The camera hardware shall be serviceable while in position or shall be removable for service such that no realignment is required after reinstallation.	SR-63	Yes
	Documentation Requirements		
31	Procedures must be provided for any required calibrations.	SR-17,18	DD

Table 19: Opto-mechanical system functional requirements

#	Overall Requirements	Flowdown	Compliance

1	The opto-mechanical system shall include a the opto-mechanics to fold the beam to the NIR TTS camera, the opto-mechanics for the NIR TTS that are outside of the camera dewar and any associated motors and encoders, as well as any required modifications to the AO bench to support this hardware.	SR-1	Yes
2	The opto-mechanical system shall provide an interface plate to mount the camera as defined in KAON 836.	SR-1,2	Yes
3	Each opto-mechanical stage shall interface to the controls via a TBD connector.	SR-1,2	Yes
4	The opto-mechanical system shall provide a means of sending H or K'-band light to the camera system while transmitting the other science bands to OSIRIS. Two options are required: an H-band reflective dichroic and a K-band reflective dichroic. A goal is to leave a position for a future annular mirror that will transmit the IFU science field.	SR-15	Yes
5	The opto-mechanical system shall provide a focus stage.	SR-16	Yes
6	The time to re-position a stage via the control system shall not exceed 10 seconds.	SR-17,18,20,21	Yes
7	The time required to initialize the opto-mechanical system via the control system shall not exceed 5 minutes.	SR-19	Yes
8	Goal: The fold mirror shall be replaceable with a tip-tilt mirror used to maintain a star image at the center of a ROI (to correct small offsets, <~25 mas, & DAR without producing a significant impact on the pupil position).	SR-5,22,25,27	Goal
	Optical Requirements		
9	The opto-mechanical system shall have a wavefront quality ≤ TBD nm rms to the camera system.	SR-4	DD
10	The opto-mechanical system shall have a wavefront quality ≤ TBD nm rms to OSIRIS.	SR-4	DD
11	The opto-mechanical system shall have a throughput of ≥ TBD % at K' to the camera system.	SR-13	DD
12	The opto-mechanical system shall have a throughput of ≥ TBD % at H to the camera system.	SR-14	DD
13	Optical distortions within the opto-mechanical system shall be ≤ 10 mas for any two points separated by ≤ 60".	SR-24,25	DD
	Mechanical Requirements		
14	The reflected beam off each fold optic must be co-linear and repeatable to the following tolerances: the image shift shall be ≤ 0.1" and the pupil shift shall be ≤ 5% of the full pupil. The goal is ¼ of these numbers.	SR-21	DD
15	The stability of the output optical beam shall be ≤ 3 mas over a 1 hour exposure.	SR-26	DD
16	The opto-mechanical system shall mount to the AO bench within a TBD envelope. The opto-mechanical system shall not mechanically interfere with the components already on the AO bench, unless these components can be and are appropriately modified to support the integration of the NIR TTS system. Any required modifications are the responsibility of the opto-mechanical system.	SR-38	Yes
17	The opto-mechanical system mounted on the AO bench shall not exceed a total mass of 10 kg (TBC).	SR-39	No
	Electronic/Electrical Requirements		

17	Each opto-mechanical stage shall be provided with an appropriate servo motor and encoder to ensure that the positioning requirements can be met. The dichroic exchanger positioning requirement is ≤ 1 mm. The focus stage positioning requirement is ≤ 0.05 mm.	SR-1,2,4	Yes
18	The opto-mechanical system shall use less than or equal to TBD of electrical power, in excess of the current system.	SR-41	DD
19	The opto-mechanical system on the AO bench shall not exceed a heat dissipation of 2 Watts into the AO bench environment.	SR-42	Yes
	Reliability Requirements		
20	The opto-mechanical system shall lose no more than 1% of its total observing time to faults.	SR-56	Yes
21	The opto-mechanical system shall have a median time between faults of ≥ 100 nights of operation.	SR-57	DD
22	The time to restart the opto-mechanical system in the event of a fault shall not exceed 5 minutes.	SR-58	Yes
	Service and Maintenance Requirements		
23	Routine maintenance on the opto-mechanical system shall not require more than 1 technician for 2 hours every 12 months.	SR-63	Yes
24	The camera hardware shall be serviceable while in position or shall be removable for service such that no realignment is required after reinstallation.	SR-63	Yes

Table 20: Controls system functional requirements

#	Overall Requirements	Flowdown	Compliance
1	The controls system shall include the motion control required for the opto-mechanical system, the device control required for the camera system and real-time control system, and any other software residing at the optics bench (OBS) or supervisory control (SC) level. This subsystem shall include any required modifications to the AO electronics to support this functionality.	SR-1	Yes
2	The opto-mechanical system stages shall interface to the controls via a TBD connector.	SR-1,2	Yes
3	The controls shall interface to the camera system as defined in KAON 836.	SR-1,2	Yes
4	The controls system shall position the opto-mechanical focus stage to be conjugate to the science instrument focal plane.	SR-16	Yes
5	The time to re-position a camera system or opto-mechanical system stage via the control system shall not exceed 10 seconds.	SR-17,18,20,21	Yes
6	The time required to initialize the opto-mechanical or camera systems via the control system shall not exceed 5 minutes.	SR-19	Yes
7	The controls shall support differential atmospheric refraction corrections between the TTS and the science instrument.	SR-22	Yes
8	The controls shall support normal science observing modes such as dithering, nodding and offsetting.	SR-23	Yes
9	Potential goal only: the controls system shall support non-sidereal tracking.	SR-28	Goal
10	Goal: The controls system shall be able to support a tip-tilt mirror used to maintain a star image at the center of a ROI.	SR-4,22,25,27	Goal
11	Goal: The controls system shall be able to use focus information from the RTC to update the sodium altitude information, instead of or in addition to LBWFS focus information.	SR-5	Goal

12	Goal: The controls system shall be able to use the tip-tilt information from 3 stars to compute and correct the rotation error in the AO rotator.	SR-9	Goal
	Software Requirements		
13	The controls system shall provide the needed operational tools to support its daytime calibration.	SR-46	Yes
14	The controls system shall provide the needed operational tools to support nighttime science operations.	SR-47	Yes
	Reliability Requirements		
15	The controls system shall lose no more than 2% of its total observing time to faults.	SR-56	Yes
16	The NIR TTS shall have a median time between faults of ≥ 30 nights of operation.	SR-57	DD
17	The time to restart the controls system in the event of a fault shall not exceed 5 minutes.	SR-58	Yes
	Service and Maintenance Requirements		
18	Routine maintenance on the controls system shall not require more than 1 technician for 4 hours every 8 months.	SR-63	Yes

Table 21: Operations software system functional requirements

#	Overall Requirements	Flowdown	Compliance
1	The observing software system shall provide the high-level software to plan science observations, prepare the system for observations and to carry out the observations.	SR-1	Yes
2	The observing software system shall interface to the camera, real-time control and controls systems via ethernet using keywords.	SR-1,2,49	Yes
3	The observing software system shall identify the location of tip-tilt stars on the camera.	SR-8	Yes
4	Goal: The NIR TTS system shall coordinate operating in parallel with the existing visible TTS (STRAP) for improved tip-tilt correction.	SR-12	Yes
5	The time required to initialize the observing software system shall not exceed 3 minutes.	SR-19	DD
6	The observing software system shall support normal science observing modes such as dithering, nodding and offsetting.	SR-23	Yes
7	As a goal the observing software should provide some measure of performance (for example, a Strehl measurement).	SR-30	Yes
	Software Requirements		
8	The observing software system shall provide the needed operational tools to support its daytime calibration.	SR-46	Yes
9	The observing software system shall provide the needed tools to support science observation planning.	SR-47	Yes
10	The observing software system shall provide the needed operational tools to support nighttime science operations.	SR-48	Yes
	Interface / Logging Requirements		
11	The observing software system shall be capable of retrieving telemetry from the telemetry server.	SR-30,50	Yes
12	The NIR TTS system shall be capable of saving images in FITS format.	SR-8,51	Yes
	Reliability Requirements		

13	The observing software system shall lose no more than 2% of its total observing time to faults.	SR-56	DD
14	The observing software system shall have a median time between faults of ≥ 30 nights of operation.	SR-57	DD
15	The time to restart the observing software system in the event of a fault shall not exceed 5 minutes.	SR-58	DD
	Service and Maintenance Requirements		
16	Routine maintenance on the observing software system shall not require more than 1 software engineer for 4 hours every 12 months.	SR-63	DD
	Documentation Requirements		
17	Goal: The observing software system shall provided a performance estimation tool. This would be even more useful with a PSF simulator attached to it.	SR-66	Yes